UNIVERSIDAD COMPLUTENSE DE MADRID

FACULTAD DE FARMACIA


# TESIS DOCTORAL

Transglutaminase 2 Conformation as a New Target to Treat Vascular Dysfunction in Aging and Diabetes

MEMORIA PARA OPTAR AL GRADO DE DOCTOR

PRESENTADA POR

Estéfano Pinilla Pérez

DIRECTORES

Luis Rivera de los Arcos
Ulf Simonsen

# UNIVERSIDAD COMPLUTENSE DE MADRID

FACULTAD DE FARMACIA


# TESIS DOCTORAL

TRANSGLUTAMINASE 2 CONFOTMATION AS A NEW TARGET TO TREAT VASCULAR DYSFUNCTION IN AGING AND DIABETES

MEMORIA PARA OPTAR AL GRADO DE DOCTOR

PRESENTADA POR

Estéfano Pinilla Pérez

DIRECTOR

Luis Rivera de los Arcos
Ulf Simonsen


# Transglutaminase 2 Conformation as a New Target to Treat Vascular Dysfunction in Aging and Diabetes

Tesis doctoral de

D. Estéfano Pinilla Pérez

Madrid
2020

## I. PREFACE

The present PhD thesis is the result of a joint programme between Aarhus University and Complutense University of Madrid, and it is based on the work carried out between 08/2016 and 04/2020. Science is a collective endeavor and the completion of this thesis would not have been possible without the participation of many people.

I would like to thank first my main supervisor from Aarhus University, Professor Ulf Simonsen for welcoming me in his group, first as an Erasmus student and later as PhD candidate, giving me the independence that I was craving as a recent graduate, and encouraging me to initiate my PhD studies in his group; without his continuous support, trust and guidance, this project would not have been possible. I also owe a great deal of gratitude to my supervisor from Complutense University of Madrid, Professor Luis Rivera de los Arcos, who is without any doubt the best teacher I had during my undergraduate years as a pharmacy student. In his classes he knew how to convey his fascination for physiology. He welcomed me in his lab and introduced me to cardiovascular research, and without his support, knowledge of the field, and guidance as I worked on this project, I would not had been able to complete my PhD studies. I would also like to extend my gratitude to my other supervisors, Associate Professor Vladimir Matchkov and post-doctoral student Simón G. Comerma-Steffensen. To Vladimir, for his support, expertise, and assistance particularly in the electrophysiological studies of this thesis. To Simón, for his expertise with *in vivo* models and his continuous support and friendship, first as a colleague PhD student and later as my supervisor; we have spent a lot of late hours in the lab that allowed me to learn a great deal from him and to develop a lot of respect for him and the work he does.

I am very thankful to all the collaborators from both Denmark and Spain, as well as to the co-authors of the studies presented in this thesis. To Associate Professor Niels Henrik Buus for his expertise in nephrology, for the fruitful discussions and for his collaboration in the study with human arteries. To all my colleagues and collaborators from the Department of Physiology in the Faculty of Pharmacy at Complutense University of Madrid, to name a few: Professor Dolores Prieto, and Dr. Belén Climent, Dr. Ana Sánchez, Dr. Mercedes Muñoz, Dr. Alejandro Gutierrez, and PhD student Claudia Rodriguez. It is an honor to be part of the department, and they are all an example that excellent scientific work is done in Spanish institutions even when the material conditions are not as good as they should be. There is a worrying narrative in Spanish science suggesting that "the good researchers are the ones that leave the country", forgetting most of the times the excellent ones that stayed. This is a terrible mistake, detrimental to research in Spain.

I am very grateful to all my colleagues in the Department of Biomedicine at Aarhus University, Dr. Junjing Su, Dr. Åsa Lina Alle Madsen, PhD student Lilliana Beck, MSc. Judit Prat, PhD student Asbjørn Petersen and PhD student Frederik Boe Hansen to name a few. I cannot forget either the international students that have visited the laboratory, MSc. Rafael Sobrano Fais, B. Pharm. Gonçalo Esteves, B. Pharm. Diana Feiteira, B. Pharm. Sara Dias, amongst many others. All of them have participated in one way or another to the completion of my PhD. It has been fun

to work with all of them and to share the good and not so good times that scientific research affords us all.

I would also like to thank B. Biotech Susie Mogensen and the laboratory technicians; Heidi Knudsen at the Department of Biomedicine at Aarhus University and Francisco Puente and Manuel Perales at the Department of Physiology in the Faculty of Pharmacy at Complutense University of Madrid, for their excellent technical support.

I have been lucky enough that this project has translational value, and I need to thank the Technology Transfer Office at Aarhus University for their valuable support and excellent guidance in the patent application process as well as in the search for funding. Particularly I would like to express my gratitude to Morten Holmager and Nis Kjær Weibel for working closely with us and giving excellent advice.

It has been inspiring to work with so many great professionals and researchers, I hope to keep cultivating the friendships and collaborations I have made during these years.

I am also very grateful to all the institutions that have supported this project financially.

In addition, I would like to thank Alexandra Danino, Ida Marie Svenningsen and all my friends in Denmark that have given me reasons to get out of the lab and made my time here much more than a working stay. They have made Denmark feel just like home. Special thanks to Alexandra Danino for her English proofreading of the defense.

Finally I would like to express my deep gratitude to my family and friends from Spain. Especially to my friend Félix, whose generosity has given me and my wife a home during my stay in Spain. To my parents Maria de los Ángeles Pérez and Octavio Javier Pinilla and my brother Adriano Pinilla for their continuous love and support, most of the time from a distance. To my grandparents, and in especially to the loving memory of my grandmother Maria de los Ángeles Córdoba, who has not been able to see me complete my PhD studies. More than anything, I would like to thank my wife Beatriz, for her patience and support, for keeping me grounded and believing in me; I would not be able to be here without her love. We started this path together and we have grown as individuals but above all, as a family.

## II. SUPERVISORS

Professor, MD, PhD, Ulf Simonsen (Main supervisor at Aarhus University)
Department of Biomedicine, Aarhus University, Aarhus, Denmark.

Professor, DVM, PhD, Luis Rivera de los Arcos (Main supervisor at Complutense University of Madrid)
Department of Physiology, Faculty of Pharmacy, Complutense University of Madrid, Madrid, Spain.

Associate professor, DMSc, PhD, Vladimir Matchkov
Department of Biomedicine, Aarhus University, Aarhus, Denmark.

Post doc, DVM, MSc, PhD, Simón Gabriel Comerma-Steffensen
Department of Biomedicine, Aarhus University, Aarhus, Denmark.

## III. ASSESMENT COMMITTEE

Professor, PhD, Francisco Pérez Vizcaíno
Department of Pharmacology, Complutense University, Madrid, Spain

Professor, MSc, PhD, Rhian Touyz
Institute of Cardiovascular and Medical Sciences, University of Glasgow, Glasgow, United Kingdom

MD, PhD, Jesper Nørregaard Bech
Department of Clinical Medicine/Clinic for nephrology/hypertension, Aarhus University Hospital, Holstebro, Denmark

## IV. FINANCIAL SUPPORT

The present PhD project has been supported by a full PhD fellowship from Aarhus University Graduate School of Health, and a Proof-of-Concept grant from the Bioinnovation Institute, Copenhagen.

## V. MANUSCRIPTS

The present dissertation is based on the following manuscripts.

I. Estéfano Pinilla, Simon Comerma-Steffensen, Judit Prat-Duran, Luis Rivera, Vladimir Matchkov, Niels Henrik Buus, and Ulf Simonsen. **The transglutaminase 2 inhibitor LDN 27219 age-dependently lowers blood pressure and improves endothelium-dependent vasodilation in resistance arteries.** Submitted for publication.

II. Estéfano Pinilla and Ulf Simonsen. **Acute and chronic treatment with the transglutaminase 2 inhibitor LDN 27219 restores endothelium-dependent vasorelaxation in resistance arteries from diabetic db/db mice.** In submission for publication.

III. Estéfano Pinilla, Ana Sánchez, María P Martínez, Mercedes Muñoz, Albino García-Sacristán, Ralf Köhler, Dolores Prieto, and Luis Rivera. **Endothelial large- and intermediate-conductance $Ca^{2+}$ -activated $K^{+}$ channels mediate rat intrarenal artery endothelium derived hyperpolarization response.** Submitted for publication.

Supplementary material included in the thesis:

IV. Estéfano Pinilla and Ulf Simonsen. **Tissue Transglutaminase Modulators for Medicinal Use.** International PCT patent application number WO2020030648A1. European Patent Office. 13 Feb. 2020.

Additional published articles in which I have contributed during my PhD studies (Not included in the dissertation).

1. Muñoz M, López-Oliva ME, Pinilla E, Martínez MP, Sánchez AB, Rodríguez C, Garcia-Sacristán A, Hernández M, Rivera L, Prieto D. **CYP epoxygenase-derived H2O2 is involved in the endothelium-derived hyperpolarization (EDH) and relaxation of intrarenal arteries.** Free Radical Biology & Medicine, Vol. 106, 2017, p. 168-183.

2. Laursen M, Beck L, Kehler J, Christoffersen CT, Bundgaard C, Mogensen S, Mow TJ, Pinilla E, Knudsen JS, Hedegaard ER, Grunnet M, Simonsen U. **Novel selective PDE type 1 inhibitors cause vasodilatation and lower blood pressure in rats.** British Journal of Pharmacology, Vol. 174, 2017, p. 2563-2575.

## VI. LIST OF ABBREVIATIONS

| | |
|---|---|
| ACh | Acetylcholine |
| AGE | Advanced glycation end-products |
| AMP | Adenosine-5'-monophosphate |
| ANOVA | Analysis of variance |
| AUC | Area under the curve |
| apoE | Apolipoprotein E |
| ATP | Adenosine-5'-triphosphate |
| AT1 | Angiotensin II type 1 receptor |
| $BH_4$ | Tetrahydrobiopterin |
| BPA | 5-(biotinamido)pentylamine |
| BSA | Bovine serum albumin |
| cAMP | 3',5'-cyclic adenosine monophosphate |
| cGMP | 3',5'-cyclic guanosine monophosphate |
| ChTx | Charybdotoxin |
| CKD | Chronic kidney disease |
| COX | Cyclooxygenase |
| COX-2 | Cyclooxygenase 2 |
| CRCs | Concentration-response curves |
| Cys | Cysteine |
| DAPI | 4′,6-diamidino-2-phenylindole |
| DHI | Bromodihydroisoxazole |
| DMSO | Dimethyl sulfoxide |
| DTT | Dithiothreitol |
| EC50 | Half maximal effective concentration |
| ECG | Electrocardiography |
| ECL | Electrochemiluminescence |
| ECM | Extracellular matrix |
| EDH | Endothelium-derived hyperpolarization |
| EDTA | Ethylenediaminetetraacetic acid |
| Em | Membrane potential |
| Emax | Efficacy, maximal effect |
| eNOS | Endothelial nitric oxide synthase |
| ERK1/2 | Extracellular signal-regulated kinases 1 and 2 |
| FLIM | Fluorescence lifetime imaging microscopy |
| FRET | Förster resonance energy transfer |
| $G_h\alpha$ | Transglutaminase 2, tissue transglutaminase, Gh alpha protein |
| GLUT-1 | Glucose transporter 1 |
| GLUT-3 | Glucose transporter 3 |
| GMP | Guanosine-5'-monophosphate |

| | |
|---|---|
| GMP-PCP | Guanosine-5'-[(β,γ)-methyleno]triphosphate |
| GTP | Guanosine-5'-triphosphate |
| GTPγS | Guanosine 5'-O-[gamma-thio]triphosphate |
| HAECs | Human aortic endothelial cells |
| HIF-1 | Hypoxia-induced factor 1 |
| HRP | Horseradish peroxidase |
| HUVECs | Human umbilical vein endothelial cells |
| IbTx | Iberiotoxin |
| IgG | Immunoglobulin G |
| IκB | Nuclear factor of kappa light polypeptide gene enhancer in B-cells inhibitor |
| IP | Intraperitoneally |
| $K_{Ca}1.1$ | Large conductance calcium-activated potassium channel |
| $K_{Ca}2$ | Small conductance calcium-activated potassium channel |
| $K_{Ca}2.3$ | Small conductance calcium-activated potassium channel 3 |
| $K_{Ca}3.1$ | Intermediate conductance calcium-activated potassium channel |
| KPSS | Physiological saline solution with high potassium concentration |
| Kv7 | Voltage-gated potassium channel 7 |
| L-NAME | L-NG-nitroarginine methyl ester |
| L-NOARG | Nω-Nitro-L-arginine |
| MAP | Mean arterial pressure |
| mRNA | Messenger ribonucleic acid |
| NA | Noradrenaline |
| NF-κB | Nuclear factor kappa beta |
| NO | Nitric oxide |
| NOS | Nitric oxide synthase |
| O-GlcNAcylation | O-linked beta-N-acetylglucosamination |
| PAGE | Polyacrylamide gel electrophoresis |
| PB | Sodium phosphate buffer |
| PBS | Phosphate buffer saline |
| PBS-T | Phosphate buffer saline, 0.1% Tween® 20 |
| PCR | Polymerase chain reaction |
| PDI | Protein disulphide isomerase |
| PEG-400 | Polyethylene glycol 400 |
| PET | Positron emission tomography |
| Phe | Phenylephrine |
| PLCδ1 | Phospholipase C delta 1 |
| PSS | Physiological saline solution |
| PVDF | Polyvinylidene fluoride |
| RhoA | Ras homolog family member A |

| | |
|---|---|
| RhoB | Ras homolog family member B |
| RIAEC | Rat intrarenal artery endothelial cell |
| ROS | Reactive oxygen species |
| SBE-b-CD | Sulfobutylether-β-Cyclodextrin |
| SD | Standard deviation |
| SDS-PAGE | Sodium dodecyl sulfate polyacrylamide gel electrophoresis |
| SEM | Standard error of the mean |
| SNP | Sodium nitroprusside |
| TBS-T | Tris-buffered saline, 0.1% Tween® 20 |
| TEA | Tetraethylammonium |
| TG1 | Transglutaminase 1 |
| TG2 | Transglutaminase 2, tissue transglutaminase, Gh alpha protein |
| TG3 | Transglutaminase 3 |
| TG4 | Transglutaminase 4 |
| TG5 | Transglutaminase 5 |
| TG6 | Transglutaminase 6 |
| TG7 | Transglutaminase 7 |
| TGFβ1 | Transforming growth factor beta 1 |
| TNF-α | Tumor necrosis factor alpha |
| VEGF | Vascular endothelial growth factor |
| $VEGF_{165}$ | Vascular endothelial growth factor 165 |
| VEGF A | Vascular endothelial growth factor A |
| Vh | Holding potential |
| VSMC | Vascular smooth muscle cell |
| VWF | Von Willebrand factor |

## TABLE OF CONTENTS

# 1. SUMMARIES

## 1.1 English summary

Endothelial dysfunction is an independent risk factor for cardiovascular complications associated with aging and diabetes. Transglutaminase 2 (TG2) is a ubiquitously expressed enzyme with calcium-dependent transamidase activity; it is overactive in aging and diabetes and has been linked with fibrotic processes in the cardiovascular and renal systems (e.g. stiffening, calcification) as well as with endothelial dysfunction in diabetes and inward remodeling in hypertension. These effects have been ascribed to the open TG2 conformation. On the other hand, the closed conformation of TG2 has GTP-binding activity, acting as a G protein in transmembrane signaling, opening potassium channels in vascular smooth muscle cells (VSMCs) and participating in cell survival. This led to the hypothesis that induction of the closed conformation by pharmacological means would present blood-pressure lowering effects and prevent endothelial dysfunction.

Native electrophoresis in purified human TG2 revealed that the reversible inhibitor LDN 27219 was able to induce the closed conformation of the enzyme *in vitro*. LDN 27219 concentration-dependently relaxed small arteries from rats and humans, mounted in isometric myographs. This direct vasorelaxant effect was endothelium and nitric oxide (NO) dependent. Additionally, incubation with LDN 27219 potentiated acetylcholine-induced relaxation and hyperpolarization by increasing sensitivity to NO through the opening of large conductance calcium-activated potassium channels ($K_{Ca}1.1$). Voltage clamp recordings in freshly isolated VSMCs confirmed that LDN 27219 increased $K_{Ca}1.1$ currents similarly to GTP. Small mesenteric arteries from older rats presented higher levels of transamidase activity and were more sensitive to the potentiation of acetylcholine relaxation by LDN 27219 compared to arteries from younger animals. Accordingly, infusion of LDN 27219 decreased blood pressure more effectively in 35-week than in 12-week-old anesthetized rats. Contrarily, induction of the open conformation of TG2 with irreversible inhibitors such as VA5 and Z-DON had no effect on vascular tone or blood pressure, but reduced acetylcholine vasorelaxation, potassium currents in isolated VSMCs, and prevented the potentiating effect of LDN 27219 on acetylcholine relaxation. These results suggest that arteries from aging animals present higher amount of TG2 in its open conformation and that pharmacological modulation of TG2 to the closed state could potentially restore age-related changes in endothelial function.

The age-dependent vasoprotective effects of the closed TG2 conformation induced by LDN 27219 were also found in small mesenteric arteries from normoglycemic db/+ mice. Additionally, LDN 27219 was shown to partially reverse endothelial dysfunction in arteries from diabetic db/db mice *ex vivo*. Therefore, the effect of three-week treatment with LDN 27219 on the development of endothelial dysfunction in arteries from db/db mice was explored. Long-term treatment with LDN 27219 was more effective in treatment of endothelial dysfunction in small arteries than treatment with an angiotensin II type 1 receptor (AT1) antagonist (candesartan), without affecting blood pressure. This effect seemed to be independent from the arterial sensitivity to NO, suggesting that

other mechanisms related to endothelial cell survival could play a role in the prevention of endothelial dysfunction by TG2 modulation in the long term.

Finally, with the perspective of future application of TG2 modulators to prevent renovascular complications in aging and diabetes, we studied the functional expression of calcium-activated potassium channels in the intrarenal vascular endothelium and their role in the endothelium-derived hyperpolarization. Through voltage clamp studies in isolated endothelial cells and immunohistochemistry, endothelial expression of $K_{Ca}1.1$, intermediate and small conductance calcium-activated potassium channels ($K_{Ca}3.1$ and $K_{Ca}2.3$, respectively) was revealed. Isometric tension recordings on rat intrarenal arteries showed that endothelial $K_{Ca}1.1$ and $K_{Ca}3.1$ channels play a major role in the acetylcholine-induced vasorelaxation of preglomerular vasculature, suggesting that $K_{Ca}1.1$ channel modulation by TG2 could be a potential strategy to improve preglomerular vascular function.

In summary, the findings of the present thesis suggest that TG2 conformation plays an important role in the endothelial function of small arteries, mainly through opening of $K_{Ca}1.1$ channels and increasing endothelial cell survival. Therefore, modulation of TG2 to its closed conformation could be a potential strategy to treat endothelial dysfunction in situations where TG2 is overactive, such as diabetes and aging.

## 1.2 Dansk resumé

Endothelcelle dysfunktion er en selvstændig risikofaktor for kardiovaskulære komplikationer ved aldring og diabetes. Transglutaminase 2 (TG2) er et udbredt enzym med calcium-afhængigt transamidase aktivitet. Enzymet er over-aktiv hos ældre personer samt personer med diabetes, og er set i sammenhæng med fibrotiske processer i det kardiovaskulære system og nyrerne (f.eks. øget stivhed og forkalkning) såvel som ved endothelcelle dysfunktion ved diabetes og forhøjet blodtryk. Disse effekter er blevet tillagt den åbne konformation af TG2. Den lukkede protein konformation af TG2 har GTP-bindende aktivitet og fungerer som G-protein i transmembran-signalering, hvorved der åbnes kaliumkanaler i vaskulære glatte muskelceller (SMCs), og TG2 bevirker også øget celleoverlevelse. Dette har ledt til hypotesen, at induktion af den lukkede konformation vha. farmakologiske metoder vil resultere i blodtryksnedsættende effekter og forebygge endothelcelle dysfunktion.

Nativ electroforese af isoleret human TG2 viste at den reversible hæmmer LDN 27219 var i stand til at fremkalde den lukkede konformation af enzymet *in vitro*. LDN27219 afslappede koncentrations-afhængigt små modstandskar fra rotter og mennesker. Den direkte vasodilaterende effekt var endothelcelle-afhængig og medieret af nitrogenmonoxid (NO). LDN27219 potenserede også acetylkolin-fremkaldt vasodilatation og hyperpolarisering ved at øge følsomheden for NO gennem åbningen af calcium-aktiverede kaliumkanaler med stor konduktans ($K_{Ca}1.1$). Patch clamp studier af isolerede vaskulære glatte muskelceller (VSMCs) bekræftede at LDN 27219 øgede $K_{Ca}1.1$-konduktivitet på samme måde som GTP. Små mesenteriekar fra aldrende rotter udviste højere niveauer af transamidase-aktivitet og var mere følsomme overfor LDN27219 potentiering af acetylkolin-afslapning sammenlignet med arterier fra yngre dyr. Infusion af LDN 27219 formindskede blodtrykket mere effektivt hos 35 uger gamle bedøvede rotter end hos 12 uger gamle rotter. Derimod havde induktion af den åbne konformation af TG2 med irreversible hæmmere såsom VA5 og Z-DON enten ingen effekt på vaskulær tonus eller på blodtryk, men reducerede acetylkolin vasodilatation, kalium-strøm i isolerede VSMCs, og hæmmede den potentierende effekt af LDN 27219. Disse resultater tyder på, at arterier fra aldrende dyr har et højere indhold af den åbne konformation af TG2, og at farmakologisk modulation af TG2 til den lukkede konformation potentielt kan hæmme aldersrelaterede ændringer i endothelcelle-funktion.

De aldersafhængige karbeskyttende effekter af den lukkede TG2-konformation fremkaldt af LDN 27219 blev også fundet i små tarmarterier fra normoglykæmiske db/+ mus. Herudover hæmmede LDN 27219 også endothelcelle dysfunktion i arterier fra diabetiske db/db mus ex vivo. Derfor undersøgte vi også effekten af tre-ugers behandling med LDN 27219 på endothelcelle dysfunktion i arterier fra db/db mus. Langsigtet behandling med LDN 27219 viste sig at være mere effektiv i at forebygge endothelcelle dysfunktion i små arterier end behandling med en angiotensin II type 1 receptor (AT1) antagonist (candesartan), uden at påvirke blodtrykket. Denne effekt ved lang tids behandling med et stof som fremkalder den lukkede konformation af TG2 synes at være uafhængig af den arterielle følsomhed overfor NO, hvilket tyder på at andre mekanismer relateret til endothelcelle overlevelse kan spille en rolle i forebyggelsen af endothelcelle dysfunktion.

Med henblik på fremtidig anvendelse af TG2-modulatorer til at forebygge renovaskulære komplikationer hos ældre patienter samt patienter med diabetes undersøgte vi den funktionelle ekspression af calcium-aktiverede kaliumkanaler i det intrarenale vaskulære endothelium og deres rolle i den endothel-afhængige hyperpolarisering. Ved patch clamp studier af isolerede endothelceller og immunohistokemi påvistes ekspression i endothelceller af $K_{Ca}1.1$, samt mellemstore og små ledende calcium-aktiverede kaliumkanaler med lille og mellemstor konduktans (hhv. $K_{Ca}2.3$ og $K_{Ca}3.1$). Funktionelle isometriske målinger i rotters intrearenale arterier viste at endothelcelle $K_{Ca}1.1$- og $K_{Ca}3.1$-kanaler spiller en stor rolle i acetylkolin-fremkaldt vasodilatation af den præglomerulare vaskulatur, hvilket tyder på at $K_{Ca}1.1$-kanalmodulation af TG2 kunne være en potentiel strategi til at forbedre præglomerular vaskulær funktion.

Sammenfattende tyder resultaterne i denne afhandling på at TG2-konformation spiller en vigtig rolle i endothelcelle-funktionen i små arterier, hovedsageligt igennem åbningen af $K_{Ca}1.1$-kanaler og øget overlevelse af endothelcellerne. Derfor kan modulation af TG2 til dets lukkede konformation være en potentiel strategi til at behandle endothelcelle dysfunktion i situationer hvor TG2 er over-aktiv, såsom ved diabetes og aldring.

## 1.3 Resumen en español

La disfunción endotelial es un factor de riesgo independiente para las complicaciones cardiovasculares asociadas con el envejecimiento y la diabetes. La transglutaminasa 2 (TG2) es una enzima expresada virtualmente en todos los tejidos y que presenta actividad transamidasa dependiente de calcio; esta actividad está incrementada en el envejecimiento y la diabetes, habiendo sido relacionada con procesos fibróticos en los sistemas cardiovascular y renal (p. ej. rigidez, calcificación, etc), así como con disfunción endotelial en diabetes y remodelado vascular interno en hipertensión. Todos estos efectos han sido atribuidos a la conformación abierta de la TG2. Por otro lado, en su conformación cerrada, la TG2 puede unirse con GTP, actuando como proteína G en la señalización transmembrana, abriendo canales de potasio en células musculares lisas vasculares (VSMCs) y promocionando la supervivencia celular. Lo anteriormente expuesto condujo a la hipótesis de que la estabilización de la conformación cerrada por medios farmacológicos podría reducir la presión sanguínea y prevenir la disfunción endotelial.

La electroforesis nativa de TG2 humana reveló que el inhibidor reversible LDN 27219 es capaz de inducir la conformación cerrada de la enzima *in vitro*. El LDN 27219 produjo relajación en arterias pequeñas de ratas y humanos montadas en miógrafos isométricos. Este efecto vasorelajante directo resultó ser dependiente del óxido nítrico (NO). Además, la incubación con LDN 27219 aumentó la sensibilidad del músculo liso arterial al NO por medio de la apertura de canales de potasio activados por calcio de alta conductancia ($K_{Ca}1.1$), potenciando de esa manera la hiperpolarización y vasorelajación inducida por acetilcolina. Registros de patch-clamp con fijación de voltaje en VSMCs aisladas confirmaron que el LDN 27219 incrementa la corriente a través de canales $K_{Ca}1.1$ de manera similar al GTP. Las arterias mesentéricas pequeñas de animales de mayor edad presentaron niveles más elevados de actividad transamidasa y fueron más sensibles a la potenciación causada por el LDN 27219 comparadas con las arterias de animales más jóvenes. Consecuentemente, la infusión de LDN 27219 causó una disminución de la presión arterial más pronunciada en animales de 35 semanas que en animales de 12 semanas de edad. Por el contrario, la inducción de la conformación abierta de la TG2 por inhibidores irreversibles como VA5 y Z-DON no alteraron la tensión vascular *ex vivo* ni la presión arterial *in vivo*, aunque redujeron la vasorelajación inducida por acetilcolina en arterias y las corrientes de potasio en VSMCs aisladas, previniendo los efectos del LDN 27219 *ex vivo*. Estos resultados sugieren que las arterias de animales de mayor edad presentan mayores cantidades de TG2 en su conformación abierta y que la promoción de la conformación cerrada podría restaurar los cambios en la función endotelial causados por la edad.

Estos efectos vasoprotectores dependientes de la edad y provocados por la conformación cerrada de la TG2 inducida por LDN 27219 fueron observados también en arterias de ratones db/+ normoglicémicos. Además, LDN 27219 fue capaz de revertir parcialmente la disfunción endotelial en arterias de ratones db/db diabéticos *ex vivo*. Basándonos en estos resultados, estudiamos los efectos del tratamiento con LDN 27219 durante tres semanas en el desarrollo de la disfunción endotelial en arterias de ratones db/db. El tratamiento con LDN 27219 a largo plazo demostró ser

más efectivo que el tratamiento con candesartan, un antagonista de los receptores tipo 1 de angiotensina II, en la prevención de la disfunción endotelial en arterias pequeñas sin afectar a la presión arterial. Este efecto resultó ser independiente de la sensibilidad arterial al NO, sugiriendo que otros mecanismos relacionados con la supervivencia de las células endoteliales podrían tener un papel en la prevención de la disfunción endotelial modulada por la TG2 a largo plazo.

Finalmente, con la perspectiva de aplicar moduladores de la TG2 en el futuro para prevenir complicaciones renovasculares durante el envejecimiento y la diabetes, estudiamos la expresión funcional de canales de potasio activados por calcio en el endotelio de arterias intrarenales y su papel en la hiperpolarización derivada del endotelio. Utilizando registros de patch clamp en células endoteliales aisladas e inmunohistoquímica, encontramos la expresión de canales $K_{Ca}1.1$ y de canales de potasio activados por calcio de intermedia y pequeña conductancias ($K_{Ca}3.1$ y $K_{Ca}2.3$ respectivamente) en el endotelio de arterias intrarenales. Registros de tensión isométrica revelaron que los canales $K_{Ca}1.1$ y $K_{Ca}3.1$ tienen un papel esencial en la vasorelajación inducida por acetilcolina en la circulación preglomerular, sugiriendo que la modulación de canales $K_{Ca}1.1$ por la TG2 podría ser una estrategia potencial para mejorar la función vascular preglomerular.

En resumen, los hallazgos de la presente tesis sugieren que la conformación de la TG2 juega un papel importante en la función endotelial de las arterias pequeñas, principalmente por medio de la apertura de canales $K_{Ca}1.1$ y del aumento de la supervivencia de las células endoteliales. Por ello, la modulación de TG2 a su conformación cerrada constituye una estrategia prometedora para el tratamiento de la disfunción endotelial en estados que cursan con sobreactivación de la TG2, como son la diabetes y el envejecimiento.

## 2. INTRODUCTION

The endothelium regulates vascular tone in response to hemodynamic and chemical signals, and endothelial dysfunction is an independent predictor of complications in cardiovascular disease and one of the contributors to the increased cardiovascular risk associated with aging and diabetes (1,2). Therefore, further understanding and new approaches to maintain endothelial cell function throughout aging and altered metabolic states are required to prevent development of vascular complications in the elderly and in diabetic population.

Transglutaminase 2 (TG2) is a ubiquitously expressed member of the enzyme family of transglutaminases (TG1-7 and Factor XIIIa). In the presence of calcium, TG2 acquires an open conformation that has transamidase activity, which catalyzes the covalent crosslinking of structural proteins (3). The open conformation of TG2 is thought to be mainly active extracellularly and during local increments of intracellular calcium. On the other hand, the closed conformation of TG2 that is mainly present intracellularly has GTP-binding activity and acts as a G protein ($G_h\alpha$), linking several receptors with their signaling cascades (4).

In the vasculature, TG2 is highly expressed in both the endothelium and the vascular smooth muscle cell (VSMC) layer (5). The transamidase activity of TG2 has been linked with an inward remodeling in hypertension (6–8). Reduced nitric oxide (NO) production leads to externalization and increased TG2 transamidase activity (9,10). This increased transglutaminase activity has been linked to vascular stiffness in aging (9–11). High glucose concentrations increase intracellular calcium and reactive oxygen species (ROS) production leading to upregulation of TG2 transamidase activity in endothelial cells. Inhibition of transamidase activity prevented hyperglycemia-induced endothelial cell apoptosis and endothelial leakage in diabetes (12–14). Besides the detrimental effect of the open conformation promoting vessel stiffness and endothelial dysfunction, our group and others have recently described that TG2 plays a role in the regulation of vascular tone in conductance and resistance arteries (11,15). Additionally, TG2 is recognized as an important target in renal fibrosis and diabetic nephropathy, due to the profibrotic effects of its transamidase activity (16,17).

TG2 was recently discovered to play a role in cell survival and cancer malignancy (18). Therefore, there has been an increasing interest in developing new TG2 irreversible inhibitors that lock the enzyme into its open conformation, inhibiting at the same time the transamidase and GTP binding activities (19–22). On the other hand, there are some reversible TG2 inhibitors, as LDN 27219 (23,24), that seems to be able to stabilize the enzyme in its closed conformation. However the available evidence comes only from “in silico” docking simulations (25). Although we have found a vasorelaxant effect of some TG2 inhibitors in resistance arteries through the opening of potassium channels (15), the role played by the different conformations of TG2 in the regulation of vascular tone remains unexplored.

The main objectives of this thesis are to explore the effects on vascular tone of conformational modulation of TG2 using pharmacological tools. Moreover, we assessed whether the promotion of the closed conformation of TG2 improves endothelial function in aging and diabetes by opening of potassium channels. A future perspective is that TG2 modulators can be used to treat renovascular complications in diabetes. Therefore, we explored the identity of the potassium channels involved in pre-glomerular endothelium-dependent vasorelaxation in the kidney.

# 3. BACKGROUND

## 3.1 The vascular endothelium

The architecture of the arterial wall can be divided in three layers: the outer tunica adventitia, which contains the extracellular matrix (ECM), progenitor cells, and fibroblasts; the middle tunica media is formed by VSMCs, whose contraction level determines the diameter of the vascular lumen; and the inner tunica intima, formed by the endothelium. The endothelium is the cellular monolayer in the interface between the bloodstream and the vascular wall, acting both as a sensor of hemodynamic and metabolic changes, and as an endocrine organ to maintain homeostasis. The most basic function of the endothelium is acting as a semipermeable barrier, controlling the diffusion or active transport of molecules from the blood by different mechanisms (26). Still, it also regulates other processes such as thrombosis, inflammation, generation of new vessels (angiogenesis), and vascular tone (27).

The vascular endothelium can regulate the tone of the underlying VSMCs layer by the release of different vasoactive substances in response to hemodynamic changes and chemical signals. The most well-known of these factors is NO, which is synthetized by endothelial NO synthase (eNOS). The synthesis of NO is constitutive in endothelial cells, and might be enhanced by different compounds such as acetylcholine (ACh). NO diffuses to the VSMCs, where it stimulates soluble guanylate cyclase. The events result in an increased formation of cyclic GMP (cGMP), followed by downstream activations of several pathways leading to vasodilatation. These pathways include the opening of large-conductance calcium-activated potassium channels ($K_{Ca}1.1$), which lead to hyperpolarization of VSMCs and subsequent relaxation (28–30). Endothelial cells also release prostacyclin, which is synthesized by cyclooxygenases (COX) and relaxes the underlying VSMCs through the increase of cyclic AMP (cAMP) by adenylate cyclase activation. Besides these well identified vasodilatory factors, there is the so-called endothelium-derived hyperpolarization (EDH), which is responsible for the remaining endothelium-dependent vasodilatation in conditions of eNOS and COX inhibition. EDH seem particularly important in small arteries and arterioles (31,32). The identity of the factors mediating EDH has been a subject for debate, seeming to be dependent on the context and vascular bed, but several candidates such as epoxyeicosatrienoic acids, C-natriuretic peptide, $H_2O_2$, potassium ions, and direct electrical coupling through myoendothelial gap junctions are currently thought to be of physiological importance (33–36).

The direct spread of hyperpolarization from the endothelium to the VSMCs through myoendothelial gap junctions requires the activation of calcium-activated potassium channels in the endothelium (37). Based on their conductance, these channels can be divided in small, intermediate, and large-conductance calcium-activated potassium-channels ($K_{Ca}2.3$, $K_{Ca}3.1$ and $K_{Ca}1.1$, respectively). The opening of $K_{Ca}2.3$ and $K_{Ca}3.1$ channels is voltage-independent and requires binding of calcium to calmodulin, which is bound to their intracellular terminus. As these channels are present in the vascular endothelium, they are recognized as the main participants responsible for the EDH response (38). On the other hand, $K_{Ca}1.1$ channels opening is triggered by both voltage and calcium, and additionally can be further regulated by associated β-subunits (39). Due to these characteristics and to its expression in the VSMCs of virtually all vascular beds, $K_{Ca}1.1$ channels have been suggested to act as an important negative feedback to limit the magnitude of depolarization and contraction in the VSMCs (40,41). As previously mentioned, $K_{Ca}1.1$ channels also plays a role in the NO-dependent vasodilation mechanism (29,30). Although the expression of $K_{Ca}1.1$ is considered to be limited to the VSMCs in physiological conditions, the channel has also been detected in the endothelium of large porcine renal arteries (42) and murine preglomerular arterioles (43). These findings suggest that $K_{Ca}1.1$ channels may play a role in the EDH response of the renal circulation.

In addition to these vasodilatatory substances, the endothelium is also able to release vasoconstrictors such as endothelin-1 and prostanoids like thromboxane A2 in different situations (44). An adequate balance between endothelium-dependent vasodilation and vasoconstriction is essential for maintaining homeostasis, and the loss of this balance in favor of vasoconstriction is characteristic of endothelial dysfunction.

The assessment of endothelial function in the patient is complicated, and the golden standards are the intra-arterial infusion of endothelium-dependent vasodilators in the forearm or coronary circulation, followed by evaluation of the effects by gauge-strain plethysmography or doppler tipped guidewire respectively. These methods are invasive and time-consuming, limiting their use in a clinical setting. Therefore less invasive measurements of flow-mediated vasodilation in the brachial artery using ultrasound, finger plethysmography and peripheral arterial tonometry have also been used (45). Although there are several circulating markers used to measure endothelial function such as E-selectin, plasminogen activator inhibitor-1 or Von Willebrand factor (VWF), these factors do not reflect the production of NO and should only be used as complementary methods (46). In research animals, the most direct way to assess endothelial function is *ex vivo* examination of vessel reactivity to endothelium-dependent vasodilators.

### 3.2 Endothelial dysfunction

Endothelial dysfunction is characterized by a shift in the actions of the endothelium toward increased vascular permeability and proinflammatory state, reduced vasodilation, and prothrombosis. Cardiovascular risk factors such as smoking, aging, obesity, insulin resistance, and elevated blood pressure can result in increased oxidative stress and reduced NO bioavailability.

Under physiological circumstances and laminar shear stress, eNOS produces NO that maintains the quiescent state of the endothelium by different mechanisms. Still, when uncoupled due to excessive oxidative stress, eNOS participates in the generation of ROS, prolonging the damage and maintaining a proinflammatory environment (28,46). Endothelial dysfunction leads to atherosclerosis, connects multiple risk factors with end-organ damage, and therefore is an independent predictor of cardiovascular events (47,48).

### 3.2.1 Endothelial dysfunction in aging

Advanced age reduces endothelium-dependent vasodilations in both animals and humans (1). Reduction of both NO bioavailability and endothelium-derived hyperpolarizing factors participate in the reduced vasodilation associated with aging (1,28,49). Several reasons have been proposed to explain this reduced NO production, including; increased activity of arginase competing with eNOS for arginine (50), augmented ROS production (51,52), and reduced expression and activity of eNOS, resulting from induction of nuclear factor kappa beta (NF-κB) (53) or reduced bioavailability of tetrahydrobiopterin ($BH_4$), a co-factor required for eNOS activity (54). Finally, endothelial cells undergoing senescence present reduced eNOS activity, suggesting that the process of telomere shortening itself could play a role in the onset of endothelial dysfunction (1). In addition, VSMCs present reduced expression of soluble guanylate cyclase with aging (55). Increased endothelium-dependent contractions caused by prostaglandins seem to be an important part of endothelial dysfunction during aging (28).

### 3.2.2 Endothelial dysfunction in diabetes

Type 2 diabetes is commonly associated with other risk factors such as hypertension, obesity, and dyslipidemia, which can induce damage of the endothelium. Additionally, insulin resistance and chronic exposure to hyperglycemia seem to be independent factors leading to endothelial cell apoptosis and reduced NO bioavailability. In physiological circumstances, insulin stimulates NO production by eNOS phosphorylation. Still, inflammatory cytokines such as tumor necrosis factor-α (TNF-α) can inhibit insulin signaling, reducing eNOS phosphorylation and contributing to insulin resistance (56). The relationship between inflammation and insulin seems bidirectional. Thus, the excess of insulin during hyperinsulinemia leads to the activation of transcription factors such as NF-κB. This results in increased inflammation and monocyte cell adhesion to endothelial cells (57). Hyperglycemia produces metabolic changes in endothelial cells through different mechanisms that lead to increased ROS generation and formation of advanced glycation end-products (AGE), which are protein modifications with deleterious effects in endothelial cells such as NO quenching and inflammation (58). One of these modifications, O-linked β-N-acetylglucosamination (O-GlcNAcylation), has been shown to be of particular importance in the development of cardiovascular complications in diabetes (59,60). Besides reduced endothelium-dependent vasodilation, these processes also increase endothelium-dependent contractions, both through COX overexpression (61) and increased production of endothelin-1 (62,63). Endothelial

dysfunction in diabetes leads to macrovascular and microvascular complications such as atherosclerosis, nephropathy, and retinopathy (64).

### 3.2.3 Endothelial dysfunction in hypertension

Hypertension is thought to have mainly renal and central origins (65). Endothelial dysfunction seems to be, in most cases, a consequence of chronically elevated blood pressure rather than a cause in hypertension (66). However, reduction of endothelium-derived vasodilation and NO bioavailability might aggravate the increase in blood pressure and reduce adequate organ perfusion, resulting in end-organ damage and complications (66). A lot of the mechanisms through which endothelial function is impaired in hypertension are shared with the previously described pathophysiological states, including increased arginase activity, reduced levels of $BH_4$, and mainly increased ROS generation and inflammation levels (1,28). In arteries from some hypertensive animal models, a reduced expression of soluble guanylate cyclase has been found in addition to reduced eNOS expression, which not only suggests a reduced NO production but also decreased NO sensitivity at the VSMC level (67). Endothelium-derived contractile factors are also increased in hypertension of both humans and experimental animal models, particularly vasocontracting prostaglandins play an important role in essential hypertension patients (68). Meanwhile, endothelin-1 seems to play a significant role in hypertension related to kidney disease (69) and pre-eclampsia (70).

### 3.2.4 Endothelial dysfunction in kidney disease

Chronic kidney disease (CKD) results in progressive loss of kidney function and is accompanied by an increased risk of cardiovascular disease, which is a leading cause of mortality in CKD patients (71). Systemic endothelial dysfunction is observed at every stage of CKD, including in children (72), and worsens with the progression of the disease and improves following kidney transplantation (73,74). This evidences that the accumulation of uremic toxins, a consequence of decreased renal clearance, induce endothelial dysfunction as in independent factor (75,76), playing a role in the increased incidence of cardiovascular death among CKD patients.

Endothelial dysfunction in the renal circulation mediates, at least partially, the onset of the most common forms of CKD. In diabetic nephropathy, hyperglycemia induces renal endothelial dysfunction through the mechanisms described above. In brief, these involve endothelial cell apoptosis (77), increased permeability through overactive Vascular Endothelial Growth Factor (VEGF) signaling (78), and glomerular efferent arteriole contraction (79), hence participating in the damage to the glomeruli and reducing kidney function. Moreover, increased ROS generation aggravated by endothelial dysfunction upregulates profibrotic signals such as TGFβ1 in the late stages of the disease, inducing fibrosis (80). Another common form of CKD is the typical presentation of hypertension-induced kidney injury, called arteriolar nephrosclerosis, in which renal pathophysiology endothelial dysfunction is suspected to play an important role (81).

Regulation of vascular tone in the kidney is crucial for its proper function, controlling the glomerular filtration rate and the renal blood flow (82,83). EDH-type relaxation has been shown to be of particular importance for the control of the preglomerular circulation, and therefore, the correct identification of the calcium-activated potassium channels involved in this response in the kidney is key to developing potential renoprotective therapies.

### 3.2.5 Therapeutic approaches to improve endothelial function

Some of the therapies used in the clinic to address cardiovascular risk factors have shown to improve endothelial function until a certain extent, most likely through limiting the damage to the endothelium. Normalization of blood glucose by antidiabetic treatment (insulin, metformin, etc.) have been shown to produce a small improvement in endothelial function (84–86). However, their effects are limited since the damage in the endothelium seems to be persistent for a long time even after blood glucose-lowering (87,88). New generation antidiabetic drugs such as glucagon-like peptide 1 receptor and sodium-glucose cotransporter 2 inhibitors have demonstrated an additional vaso- and renoprotective effect compared to traditional blood glucose-lowering strategies, most likely through their capacity to directly improve endothelial function (89,90). Similarly, limited are the effects on endothelial function of statins and other cholesterol-lowering therapies, as shown by different meta-analyses (91). Antihypertensive treatment with β-blockers or calcium channel antagonists has also shown contradicting efficacy improving endothelial function, particularly in the peripheral vasculature. However, newer β-blockers (e.g., carvedilol) seem to be superior due to an apparent antioxidant effect, also shared by calcium channel antagonists (92). Despite the inhibition of the renin-angiotensin-aldosterone system being considered a cornerstone in the treatment of renal complications in hypertensive or diabetic patients due to its blood pressure-lowering and antiinflammatory effects (81), therapy with angiotensin-converting-enzyme, angiotensin II type 1 receptor (AT1), or renin inhibitors have also shown only limited and context-specific improvement of systemic endothelial function (92).

In conclusion, new approaches are needed to improve endothelial function and lower the risk of cardiovascular complications in aging and diabetic patients. Some new experimental strategies target different pathways, such as endothelial cell senescence in aging (1), AGE generation and its signaling in diabetic patients or the inflammatory component through interleukin inhibition (93). Antioxidant treatments were considered a promising direction to take, but the role of ROS in endothelial dysfunction has demonstrated to be more complicated than initially thought, having protective roles in certain circumstances. Hence, most clinical trials have shown little to no benefit of antioxidant therapy in cardiovascular protection (94). Treatments modulating the opening of potassium channels in the vasculature are also considered a potential path to directly improve endothelium-dependent vasodilation (38), an approach that could be particularly useful in peripheral and intrarenal arteries, where the EDH-type vasodilation seems to be prevalent (32). Moreover, opening of potassium channels could indirectly lead to an increased release of NO (95). However, drugs directly modulating potassium channels can present undesired effects in cardiac conduction and in the central nervous system (96).

### 3.3 TG2: activities, cellular location and regulation

The enzyme family of transglutaminases is composed of transglutaminases 1-7, coagulation factor XIIIa and the catalytically inactive erythrocyte membrane protein band 4.2. All the members of the family except band 4.2 have calcium-dependent transamidase activity. TG2, also known as tissue transglutaminase, is the most widely expressed member of this family and probably the best characterized, being virtually present in most tissue and cell types (3). TG2 is composed of four structural domains: 1) an $NH_2$-terminal β-sandwich (aminoacids 1-140), 2) the catalytic core (aminoacids 141-453) which contains the catalytic triad for transamidase activity (Cys277, His335, and Asp358) and the calcium-binding sites (aminoacids 430-453), 3) a β-barrel (aminoacids 479-586) that contains the specific GTP/GDP binding site not present in most of the other transglutaminases, and 4) a second COOH-terminal β-barrel (aminoacids 587-687) (97,98). The position of these domains can vary depending on the binding of different effectors, being this related to its functions and resulting in the two most common conformational states of TG2: the open and the closed conformations. Essential for this conformational change is the regulatory loop between the catalytic core and the first β-barrel (aminoacids 454-478), which acts as a joint across which the conformation varies (97). Truncated forms of TG2 with shorter COOH-terminus are also found in some cells, such as leukocytes, VSMCs, and endothelial cells (99). These shorter variants of TG2 usually have impaired GTP binding although their relevance in physiology or pathophysiology is yet to be explored.

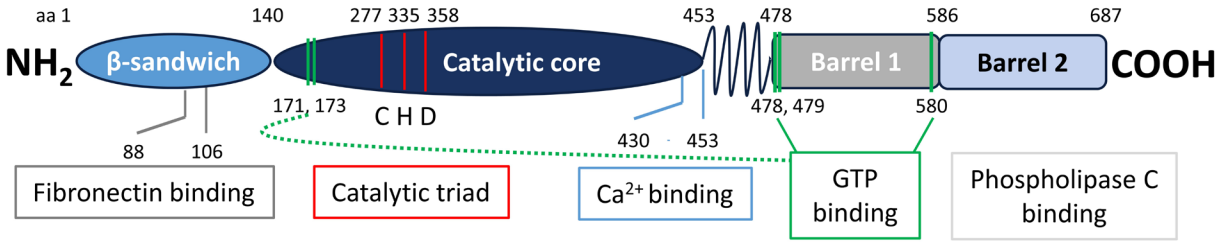


**Figure 1.** Scheme of the structural domains of the TG2 protein and their function. The $NH_2$-terminal β-sandwich domain contains a binding site for fibronectin and is responsible for promoting cell-matrix interactions. In its calcium-induced open conformation, the catalytic core domain of TG2 is responsible for transamidase activity. The β-barrel 1 domain contains a GTP/GDP/ATP-binding site. These nucleotides promote the close conformation of the enzyme that plays an important role in transmembrane signaling. The COOH-terminal β-barrel 2 domain can activate phospholipase C when the enzyme is in the closed conformation.

In the calcium-bound open conformation, the TG2 catalytic triad is exposed and the enzyme has the classical transamidase activity, which results in rapid deamidation of glutamine residues of proteins, polyamine incorporation and ϵ-(γ-glutamyl)lysine isopeptide bond formation between substrate proteins (protein crosslinking). In contrast, when GTP, GDP, or ATP are present, TG2 acquires a closed conformation in which the catalytic triad is inaccessible, therefore lacking transamidase activity (100). In its closed conformation TG2 has been reported to have GTPase and

ATPase activity (101) which allows it to act as a G protein ($G_h\alpha$) in transmembrane signaling mediating phospholipase C δ1 (PLCδ1) activation (102). Only two other members of the transglutaminase family of enzymes, TG3 and TG5, are inhibited by GTP, although they do not seem to have hydrolytic activity (103,104).

In addition to the mutually exclusive transamidase/GTPase activities, several other activities of TG2 have been described. Through *in vitro* experiments, it has been reported that TG2 has protein kinase activity, being dependent on its closed conformation/ATP binding activity and inhibited by calcium. Still, it is unclear whether this activity plays a role in physiology or pathophysiology *in vivo* (98). TG2 has also been shown to directly interact with several proteins as an adhesion/scaffold protein in a way that is variably dependent on its conformation, with some interactions being favored by the closed (105) and others by the open conformation (106,107). TG2 also has protein disulfide isomerase (PDI) activity independently of calcium and nucleotides (108), therefore the role of TG2 conformation in this activity, if any, remains unknown.

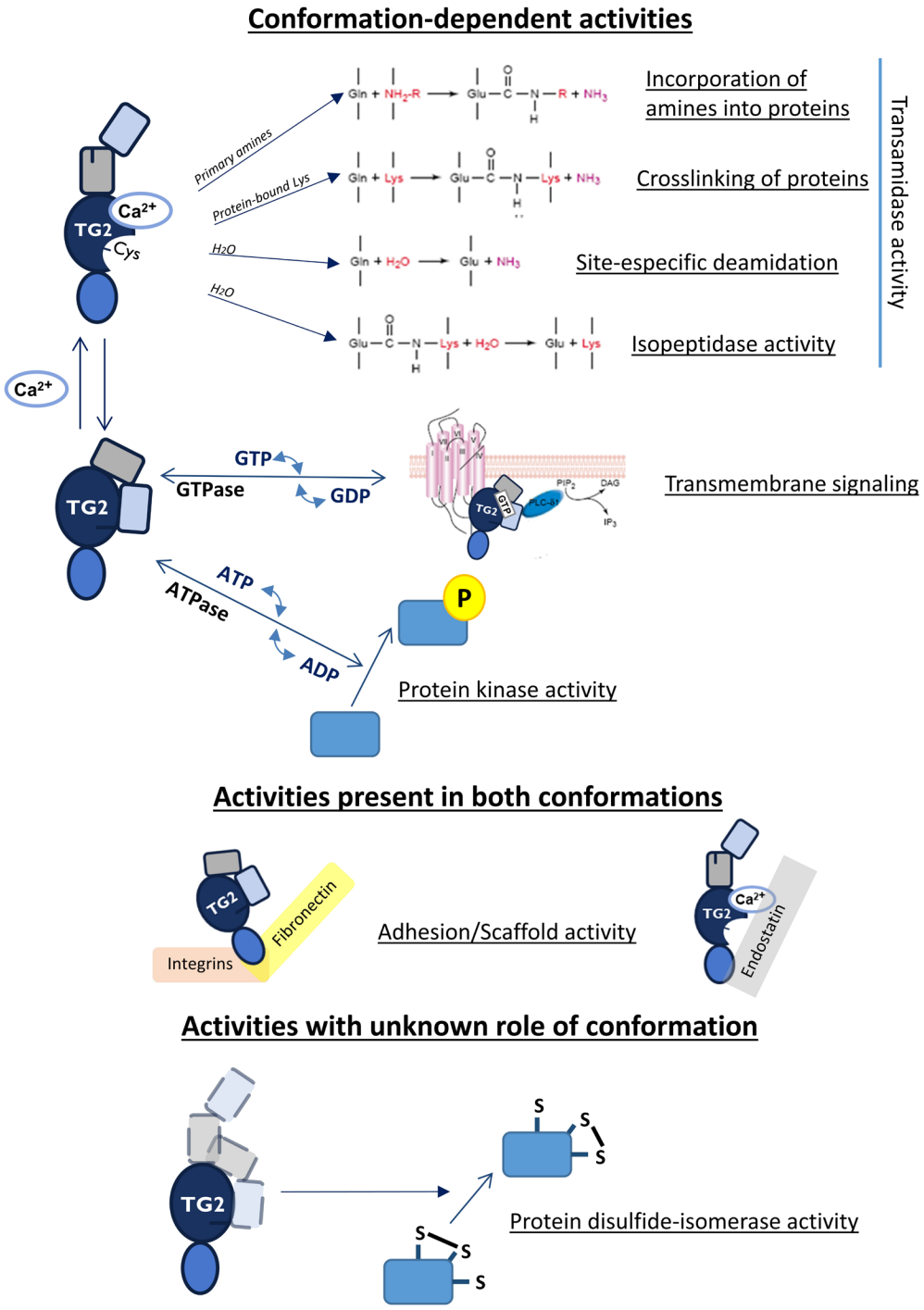


**Figure 2.** Schematic representation of conformation-dependent TG2 activities and TG2 activities in which the effect of enzyme conformation, if any, is not known.

TG2 is present in several subcellular compartments as well as extracellularly, and its functions are going to be dependent on its location and microenvironment. The extracellular space is characterized by low concentrations of nucleotides and high calcium concentration, therefore when localized in the ECM, TG2 is believed to be mainly in its open conformation. Through its

transamidase activity, extracellular TG2 is known to enhance ECM stability by crosslinking fibronectin and collagen fibrils (109,110). Moreover, TG2 participates in post-translational modification of other extracellular proteins usually leading to their stabilization in the cell membrane, such as Transforming Growth Factor β1 (TGFβ1) binding protein (111), VEGF A (112) and AT1 receptors (113). Despite higher concentrations of calcium outside of the cell, TG2 transamidase activity is not continuously active and requires a reductive environment, being inhibited by oxidation (8). Another regulating factor of extracellular transamidase activity is NO, which causes S-nitrosylation of TG2 and inhibits its activity (114). Overactivation of extracellular transglutaminase activity during tissue damage or due to decreased NO bioavailability leads to ECM deposition, playing a role in the onset of fibrotic lesions and increasing cardiovascular stiffness (9,115,116). Besides its transamidase-dependent functions, TG2 also acts as a scaffolding protein in the extracellular surface of the cell membrane, interacting with integrins, fibronectin, and syndecan-4, and promotes cell adhesion, migration, and cell survival (3). Although these particular interactions seem favored by the closed conformation (105), other instances in which TG2 acts as a scaffold protein in the cell membrane depend on the open conformation, like in its interaction with endostatin (106). The mechanisms through which TG2 is externalized are unclear and seem highly context-specific, including passive release through cell damage (117,118), microvesicle shedding (8,119,120), endosomes (120,121) and rapid externalization through pores formed after P2X7 receptor activation in macrophages (122). In the vasculature, S-nitrosylation of TG2 by NO, not only inhibits the transamidase activity but it also reduces TG2 externalization (10).

Most of TG2 is located intracellularly in the cytosol. Due to the low concentration of calcium and high concentration of nucleotides inside of the cell, intracellular TG2 is thought to be mainly in its closed conformation, and measurements of TG2 conformation in cells seems to support this idea (123). TG2 has been shown to act as a G protein, coupled with $\alpha_{1B}$ and $\alpha_{1D}$ adrenoceptors, thromboxane A2, oxytocin, and follicle-stimulating hormone receptors, linking their stimulation with PLCδ1 activation by direct interaction with GTP-bound TG2 (124,125). Via its GTPase activity, TG2 also regulates other pathways participating in the activation of extracellular signal-regulated kinases 1 and 2 (ERK1/2) in cardiomyocytes (126) and inhibiting adenylate cyclase activity in vascular endothelial cells and fibroblasts (127). GTP-bound TG2 has also been shown to positively modulate $K_{Ca}1.1$ channels in the vascular smooth muscle (128). In general, the GTPase activity of intracellular TG2 has been linked with cell survival and protection (18). Intracellular TG2 can acquire an open conformation, activating its transamidase activity during cellular stress, and it is involved in some mechanisms of NF-κB activation and other processes related to inflammation (129,130). Local increases in calcium concentration have also been shown to activate TG2 transamidase activity (8). These local activations could explain the role of TG2 in monoaminylation of cytoplasmic proteins, which seem to be important in modulation of the cytoskeleton and vesicular trafficking, particularly in the vasculature (131–133). The scaffolding activity of TG2, which is independent of its transamidase and GTPase activities, has also been shown to play a role intracellularly activating NF-κB (134).

Besides located intracellularly in the cytosol, TG2 also appears associated with the mitochondrial membrane, inner mitochondrial space, and occasionally to the mitochondrial matrix and inner mitochondrial membrane. However, the mechanisms involved in TG2 mitochondrial trafficking are entirely unknown. Mitochondrial TG2 can activate cell apoptosis through its transamidase activity, and its PDI activity is essential for correct disulfide bond formation in complexes I, II, IV, and V of the electron transport chain (135,136). TG2 is also present in the cell nucleus associated with chromatin, where it has been shown to regulate gene expression through transcription factor and histone transamidation (frequently in processes linked with apoptosis, e.g., hepatic alcohol-induced cell death). Independently of its transamidase activity, TG2 scaffolding capability allows it to act as a transcriptional coactivator (typically in processes related with cytoprotection, e.g., reducing neuronal death during ischemia by interacting with hypoxia-induced factor 1 (HIF-1) signaling) (137). As previously mentioned, TG2 kinase activity might be involved in the phosphorylation of p53, histones H1 and H3, and retinoblastoma protein, but the relevance of this activity *in vivo* is unclear (98).

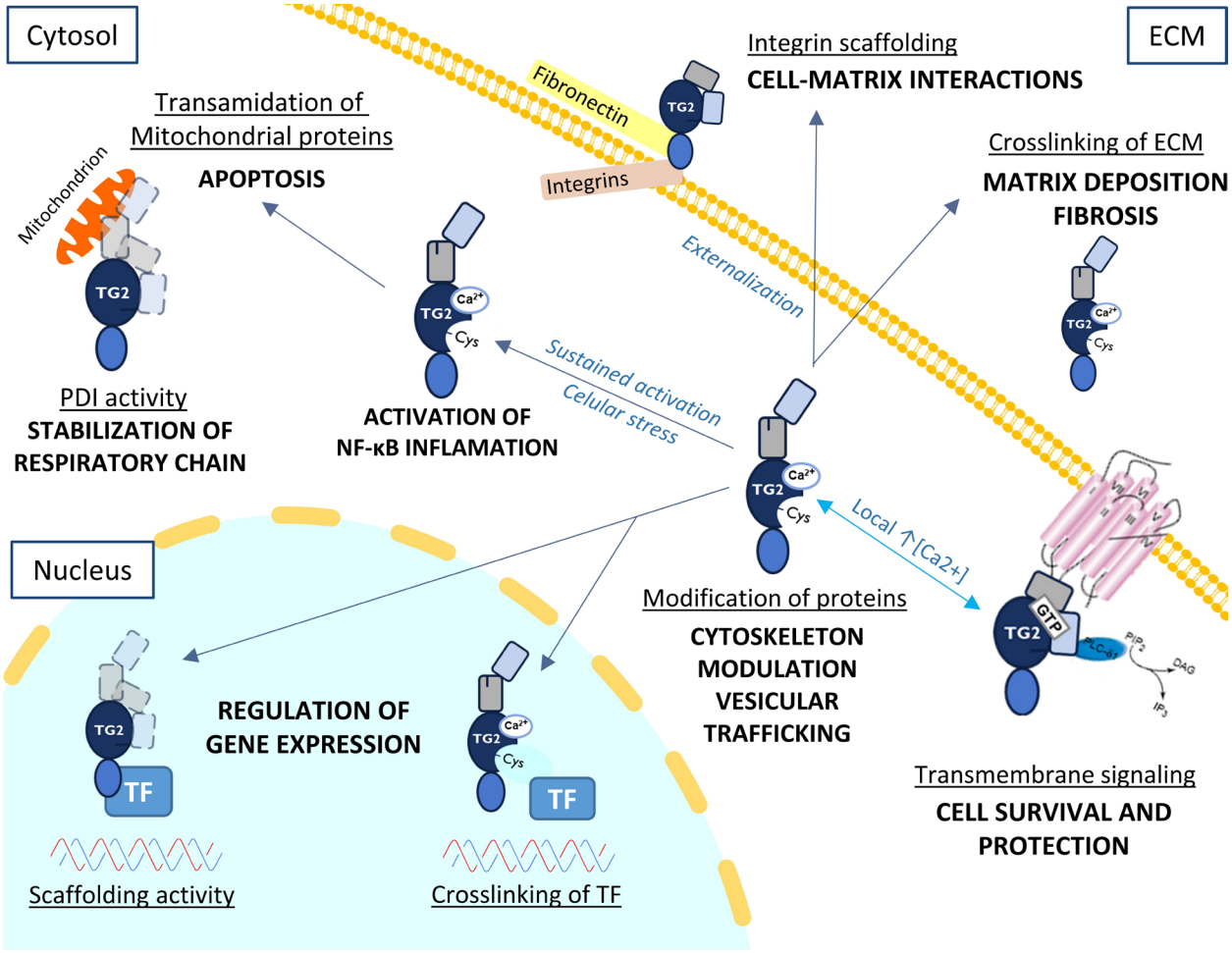


**Figure 3.** Schematic representation of different cellular functions of TG2 depending on its activity, conformation and location. TF = Transcriptional factor.

TG2 gene expression is increased during tissue remodeling, endoplasmic reticulum stress, inflammation, viral infection, cancer and apoptosis, and it is mediated by interleukins 1 and 6, TNF-α, epidermal growth factor, retinoic acid, HIF-1, NF-κB and TGFβ1 (18). With these two last factors, a positive-feedback loop exists as TG2 plays an essential role in their activation. The transcriptional regulation of TG2 suggests its importance as a marker of cellular stress.

### 3.4 TG2 in the vascular system health and disease

Although TG2 is the most widely expressed member of the transglutaminase family of enzymes in the vascular wall, including endothelial and VSMCs, some other transglutaminases have been found in the vasculature of rodents, such as TG1 and TG4 in rat aortae and vena cava (138). In rat small mesenteric arteries, PCR studies showed a weak band for TG1 mRNA besides a marked expression of TG2, however TG1 protein expression was not detected by immunoblotting (15). Another important transglutaminase in the cardiovascular system is Factor XIIIa, which is primarily present in bone marrow-derived cells such as platelets, monocytes, and macrophages (139).

#### 3.4.1 S-nitrosylation of TG2 in age-related vascular stiffness

As previously mentioned, NO regulates both the activity and the cell location of TG2 in the vascular system via S-nitrosylation of the protein (10). In cultured human aortic endothelial cells (HAECs), the release of NO by S-nitrosoglutathione reduced the amount of TG2 in the surface of the cell membrane. At the same time, treatment with the NO synthase (NOS) inhibitor L-NG-nitroarginine methyl ester (L-NAME) increased it. Aortic rings from aging rats and humans have higher levels of transamidase activity compared to aortae from younger individuals, this difference being abolished by the *ex vivo* treatment with L-NAME. This was correlated with decreased TG2 S-nitrosylation, a higher amount of ECM crosslinks and increased stiffness in arteries from older individuals, while the expression of TG2 remained unchanged (9).

Additionally, *in vivo* treatment with L-NAME increased transamidase activity in aortae from wild type, but not from TG2 knockout mice (9). The role of NO in regulating TG2 location was also confirmed in fibroblasts in addition to endothelial cells (10), and the role TG2 in increased vascular stiffness due to decreased NO was also confirmed using eNOS knockout mice (116). These results suggest that decreased NO bioavailability due to aging increases TG2 externalization. Increased externalization and reduced S-nitrosylation of TG2 lead to elevated transamidase activity in the vasculature, resulting in increased ECM crosslinking and central vascular stiffness. Moreover, recent studies suggest that a similar process could be involved in ventricular stiffness associated with aging (140).

#### 3.4.2 Role of TG2 in endothelial dysfunction in diabetes

The role of TG2 in glucose metabolism is a controversial topic. TG2 knockout mice have been reported to have glucose intolerance and impairment of insulin secretion (141), although later

studies from other groups have not been able to replicate these observations in TG2 knockout mice from a different background (142), pointing at the background as the reason for the altered glucose metabolism in the previous studies instead of the ablation of TG2. On the other hand, three different missense mutations in the TG2 gene have been identified in three families with early-onset diabetes mellitus, while being absent in 600 normoglycemic controls (141). Even though these mutations were not fully penetrant and did not appear to be the only cause of diabetes in these families, when the mutant proteins were overexpressed in a rat insulinoma cell line, this resulted in decreased insulin secretion *in vitro* compared to cells overexpressing wild type TG2 (143). The mutations were identified to alter both the transamidase and the GTP binding activities of TG2, suggesting that both activities could participate in different steps of insulin secretion, although more research is needed to identify the mechanisms involved and their actual relevance in the onset of diabetes (143).

The transamidase activity of TG2 has been shown to mediate endothelial cell death in response to increased extracellular concentrations of glucose in human umbilical vein endothelial cells (HUVECs) (12). Later studies also showed that TG2 transamidase activity was involved in VEGF-induced vascular leakage, and that silencing of the TG2 gene or TG2 inhibition by cystamine was able to prevent it in the retina of streptozotocin-induced diabetic mice (13). Moreover, the same group suggested that a 'vicious cycle' between ROS and TG2 was responsible for the sustained endothelial cells damage present even after blood glucose normalization with insulin in aortae from streptozotocin-induced diabetic mice. Aortic endothelial cells from wild type diabetic mice, but not the ones from TG2 knockout or cystamine-treated diabetic mice, had increased transamidase activity, oxidative stress, expression of inflammatory adhesion molecules, and apoptosis even after blood glucose normalization with insulin (14). These results suggest that the transamidase activity of TG2 plays a harmful role in endothelial dysfunction in diabetes.

A very recent study found that TG2, most likely through its transamidase activity, increased the transcription of glucose transporters GLUT-1 and GLUT-3 in fibroblasts during infection with intracellular bacteria *Chlamydia trachomatis*, increasing glucose import. Moreover, the study found a correlation between TG2 transamidase activity and O-GlcNAcylation of proteins, suggesting that TG2 might be an important player in glucose-derived metabolic pathways in cells (144). Considering the potential contribution of increased and sustained O-GlcNAcylation of proteins to vascular dysfunction in diabetes (60), this could be another possible mechanism to explain the role of TG2 in diabetic-related endothelial dysfunction.

### 3.4.3 TG2 in hypertension and regulation of vascular tone

Sustained vasoconstriction and reduced blood flow lead to inward eutrophic remodeling in resistance arteries, resulting in the reduced arterial lumen (145). Although this mechanism is adaptive and directed to maintain sufficient organ irrigation, it can result in end-organ damage in the end (146). Through its transamidase activity, TG2 has been shown to regulate inward remodeling in resistance arteries (6). In TG2 knockout mice, inward remodeling of small

mesenteric arteries in response to reduced blood flow was delayed compared with wild type mice, although the transamidase activity of Factor XIIIa from macrophages was able to compensate with time (7). In phenylephrine (Phe)-treated rats, *in vivo* treatment with cystamine reduced small artery inward remodeling without affecting blood pressure, as well as reduced small artery outward remodeling in Phe and amlodipine-treated rats (147). It should be noted that cystamine is an unspecific inhibitor with several effects other than transglutaminase inhibition (148), and these results should be interpreted with caution.

The contribution of TG2 during arterial remodeling in hypertension seems to be different in large/conductance arteries, where the expression and transamidase activity of TG2 have been shown to decrease in proliferating aortic VSMCs (149) and aortic VSMCs of hypertensive rat models (150), which would correspond with a proliferative VSMCs phenotype. Moreover, aortic VSMCs from TG2 knockout mice had increased proliferation rates compared with VSMCs from wild type mice (151). These studies suggest that the expression of TG2 is linked with a contractile VSMC phenotype. However, through specific signaling pathways during stress or growth, extracellular TG2 can promote VSMC proliferation and dedifferentiation through its transamidase activity. For example, aortic VSMCs from TG2 knockout mice had reduced proliferation in response to the activation of the platelet-derived growth factor receptor /Akt1 pathway, compared with VSMCs from wild type mice (152).

Moreover, TG2 knockout mice also presented attenuated vessel occlusion in a carotid artery ligation model of neointima formation (152). Another example of a potential mechanism through which TG2 could promote VSMC dedifferentiation is the established link between TG2 and serotonin signaling. In aortic VSMCs, TG2 catalyzes serotonylation of Ras homolog family member A (RhoA), which increases its activation and degradation, leading to increased Akt1 activity and most likely playing a role in the inhibition of vascular contraction after long-term stimulation with serotonin (131). Increased serotonylation of RhoA in pulmonary arteries from hypoxic rats suggest that this mechanism might be relevant in arterial remodeling during pulmonary hypertension (131). In short, the role of TG2 in vascular remodeling is complex and seems to depend on the specific pathophysiological context and level of the vasculature.

Aside from its role in arterial remodeling, TG2 can contribute to hypertension participating in other mechanisms. Isopeptide modification of AT1 receptors by TG2 has been shown to stabilize the receptor preventing its ubiquitination-dependent degradation in a mouse model of preeclampsia (113). This mechanism was also observed in an experimental mouse model of inflammation-induced hypertension (153), where TG2 was shown to be upregulated by interleukin 6 and HIF-1. In this model, transamidase activity was required for the production of agonistic autoantibodies against AT1 receptors, highlighting the potential role of TG2 in inflammation-induced hypertension (154).

TG2 has been suggested to participate in the regulation of vascular tone through different mechanisms. TG2 transamidase activity has been suggested to participate in the modification of

α-actin in the vascular smooth muscle, catalyzing the incorporation of serotonin (132) and noradrenaline (NA) (155). The relevance of these processes in VSMC contraction is unclear and has only been inferred through the inhibitory effects of high concentrations of cystamine on serotonin and NA-induced contraction in myograph-mounted arteries. Cystamine is an unspecific transglutaminase inhibitor and such high concentrations are likely to have several pharmacological effects. Therefore these results should be interpreted with caution. Nevertheless, vasorelaxant effects of cystamine in small mesenteric arteries have been shown to be at least partially dependent on TG2 inhibition and linked to the opening of voltage-gated potassium channels in the smooth muscle (15). Inside-out patch-clamp recordings revealed that the GTP binding activity of TG2 is involved in the opening of $K_{Ca}1.1$ channels in the vascular smooth muscle of rabbit mesenteric arteries (128), which could be related with a potential role of the closed conformation of TG2 in vasorelaxation. This potential role is supported by the observation of increased vasoconstriction to Phe of aortic rings from TG2 knockout mice when compared to aortic rings from wild type mice. These differences were abolished when the endothelium was removed, suggesting the involvement of endothelial pathways that would fit with downstream activation of $K_{Ca}1.1$ channels in the smooth muscle. However, surprisingly no difference was found in endothelial function between aortae from TG2 knockout and wild type mice (151). These results point out to a role of TG2 in the regulation of vascular tone, although more research is needed to uncover the relevant mechanisms and relevance of the different conformational states of TG2.

### 3.4.4 Role of TG2 in atherosclerosis

The role of TG2 in inflammation and ECM deposition has led to hypothesize about its role in atherosclerotic plaque formation and stability. However its contribution to the phenomenon is still a controversial topic. In human atherosclerotic coronary arteries TG2 is overexpressed in the neointimal tissue and vascular wall, and co-localizes with COX-2 and NF-κB (156). Theoretically TG2 could participate in the initial formation of the atherosclerotic plaque through its proinflammatory activities in the vascular wall. However, using a mice model of atherosclerosis with TG2 knockout macrophages resulted in larger atherosclerotic lesions in the aortic valve, due to reduced phagocytic capacity of macrophages lacking TG2 and subsequent accumulation of necrotic cells (157). These findings suggest a protective role of TG2 in macrophages.

Concerning the role of TG2 in atherosclerotic plaque composition, reduced collagen content and increased inflammation were observed in the atherosclerotic lesions of an apolipoprotein E (apoE) and TG2 double knockout model, indicating decreased plaque stability (158). Contrarily, in a similar double knockout model from a different research group, no alterations in the composition of the plaques compared with mice expressing TG2 were found (159). In a mouse model of oscillatory flow in which a tapered perivascular cast was placed around the carotid artery, the arteries from TG2 knockout mice presented significantly fewer monocytes adhered to the endothelium compared to the arteries from wild type mice. However, atherosclerotic lesions were absent in both types of mice. This supports the idea that TG2 might be important in the initial phases of plaque formation. However, when the tapered perivascular cast model was applied to

apoE knockout mice, treatment with a transglutaminase inhibitor increased the size of the lesion in addition to reducing the macrophage number and fat content, but only in the lesions distal to the cast, which were exposed to oscillatory shear stress (160). It should be noted that the inhibitor used in these experiments, L682777, is a potent non-selective transglutaminase inhibitor which also inhibit factor XIIIa (161). Factor XIIIa has been shown to play an important role in the onset of atherosclerosis (162). Therefore it cannot be ruled out whether the observed effects of L68277 might be due to the inhibition of factor XIIIa as well. Vascular calcification is a frequent phenomenon in atherosclerotic lesions and a complication of long-term administration of vitamin K antagonist, warfarin. Genetic ablation of TG2 has been shown to reduce calcium content in warfarin-treated mice (163), supporting the importance of TG2 in this process.

### 3.4.5 TG2 in angiogenesis

TG2 has been reported to present both pro- and antiangiogenic effects. Autoantibodies targeting TG2 in celiac disease are known to interrupt different steps of angiogenesis. However, a recent study shows that activation of Ras homolog family member B (RhoB) is associated with these effects (164), suggesting that the antiangiogenic effect might be due to overactivation of TG2 transamidase activity by those autoantibodies instead of due to its inhibition. Celiac autoantibodies have been shown to increase TG2 and RhoA activation previously, leading to vascular permeability (165) and supporting this hypothesis. Also supporting the role of excessive TG2 transamidase activity in antiangiogenesis, the addition of exogenous TG2 increased fibrosis by ECM crosslinking, which led to reduced angiogenesis and tumor growth in experiments by different groups (107,166). TG2 has been shown to inhibit angiogenesis through other mechanisms such as activation of TGFβ1 in cultured endothelial cells (167). Contrarily, in the context of wound healing, TG2 had tissue stabilizing and proangiogenic effects in the skin (168). Moreover, in hypoxic conditions, which stimulates angiogenesis, TG2 colocalized with the antiangiogenic agent endostatin in the ECM surrounding HUVECs, suggesting a potential proangiogenic role of TG2 during hypoxia by interfering with endostatin signaling (106). However, the interaction between TG2 and endostatin has been linked with antiangiogenic effects and vascular rarefaction in murine age-related kidney fibrosis (107), suggesting that the effects of this interaction in angiogenesis are complex and context-specific. The interaction of TG2 with endostatin is dependent on calcium and therefore occurs with the open conformation of the enzyme (106). TG2 inhibition or knockdown inhibited angiogenesis, reducing matrix-bound VEGF A in HUVECs, supporting a positive role of TG2 in VEGF-mediated angiogenesis which was dependent on its transamidase activity (112). On the other hand, TG2 has also been suggested to participate at different levels of VEGF-signaling exerting negative regulation of angiogenesis; for example, extracellular TG2 seems to interact with VEGF receptor 2 and promotes its trafficking to the nucleus upon its activation, limiting its effects. Therefore, inhibition by cystamine enhanced VEGF-induced migration of cultured cells (169). More recently, TG2 was shown to bind to heparan sulfate proteoglycans, interfering with their binding to $VEGF_{165}$ and inhibiting early stages of angiogenesis. This resulted in transiently enhanced retina vessel formation and increased vascularization of $VEGF_{165}$-

containing matrigel implants in TG2 knockout mice (170). As previously mentioned, the interaction of TG2 with heparan sulfate seems to be favored by the closed conformation of the enzyme (105). In VSMCs, the role of TG2 in motility is equally variable. In murine aortic VSMCs, genetic ablation of TG2 diminished cell migration (151), while in other experiments overexpression of TG2 has been reported to inhibit human aortic VSMC migration by participating in $\alpha_{1B}$-adrenoceptor signaling as a G protein (171), although a negative influence in motility due to increased transamidase activity cannot be completely ruled out.

Thus, the role of TG2 in angiogenesis is complex and seems dependent on the signaling pathway, subcellular location, and stage of the process.

### 3.5 Role of TG2 in the dysfunctional kidney

Fibrotic remodeling is the main pathophysiologic process associated with progression to end-stage renal disease in CKD (172). As previously mentioned, TG2 increases ECM rigidity by fibril crosslinking (109,110) but also participates in ECM deposition by TGFβ1 activation (115). Both the transamidase and the scaffolding activities of TG2 are important in this process (173,174) and have demonstrated to be relevant in renal scarring and fibrosis (175,176). In a 5/6-nephrectomy experimental rat model for CKD, treatment with two active-site directed inhibitors of TG2 (NTU281 and NTU283) reduced the development of glomerulosclerosis and tubulointerstitial fibrosis, preventing a decline in kidney function. The TG2 inhibitor NTU281 had low cell membrane permeability, while NTU283 was membrane permeable. Treatment with either of the inhibitors reduced accumulation of collagen. Still, it did not mitigate TGFβ1 activation in diseased kidneys, suggesting that the beneficial effects were due to the inhibition of direct crosslinking by the extracellular TG2 transamidase activity, rather than by reducing its impact in TGFβ1 signaling (16). The less permeable inhibitor NTU281, was also used in a diabetic nephropathy model of uninephrectomized streptozotocin-induced diabetic rats, where it effectively reduced renal tubulointerstitial scarring, collagen deposition and number of myofibroblasts, reversing the increased serum creatinine and albuminuria in diabetic animals (17). The reduction in the number of myofibroblasts suggests that TG2 might play a role in myofibroblast transformation, which could be related with TGFβ1 signaling. TG2 has also been suggested to be important in myofibroblast transformation during liver fibrosis (177). However, it should be noted that both NTU281 and NTU283 are unspecific transglutaminase inhibitors, affecting Factor XIIIa, TG1 and TG3 equally. Although only Factor XIIIa has been found to be linked with early stages of fibrosis, it cannot be ruled out that the inhibition of other transglutaminases besides TG2 play a role in the effects of NTU281 and NTU283.

Microvascular rarefaction and endothelial dysfunction are important hallmarks in the development of nephrosclerosis, particularly during aging (172). Overexpression and overactivation of TG2 has been shown in the kidneys of aging mice, in parallel with increased crosslinking of ECM and fibrosis and exogenous addition of TG2 reduced angiogenesis. Delivery of endostatin combined with folic acid-induced nephropathy, upregulated TG2. Additionally, subcapsular injection of TG2

and/or endostatin induced kidney fibrosis in young mice, and also increased the proportion of senescent cells. Moreover, the interaction of endostatin with TG2 stabilizing its open conformation was confirmed (107). These results suggest that both endostatin and TG2, besides their role in fibrosis, might be geronic proteins acting synergistically, and hence play a role in the onset of age-derived kidney fibrosis and vascular rarefaction. The interaction between the open conformation of TG2 and endostatin has been previously shown (106), and this study suggests that this interaction might stabilize the open conformation of TG2 and lead to overactivation of the enzyme.

In summary, TG2 plays a role in kidney fibrosis and its overactivation most likely contributes to vascular rarefaction of the fibrotic kidney. Achievement of vasoprotection and inhibition of TG2 could be a promising strategy to prevent the development of CKD.

### 3.6 Pharmacological modulation of TG2

Due to the involvement of TG2 in different pathologies such as celiac disease, neurodegenerative diseases and, as discussed above, fibrotic diseases, a considerable effort has been made in the medicinal chemistry field to develop TG2 inhibitors (178). The recently discovered role of the closed conformation of TG2 in cell survival and cancer has increased the interest particularly in inhibitors able to modulate its conformation (19,179).

#### 3.6.1 Competitive amines, classic unspecific inhibitors

The first TG2 inhibitors used were amines, such as derivatives of cadaverine or putrescine. They are transglutaminase substrates that act as competitive inhibitors preventing the formation of naturally occurring crosslinks (180). Some of these inhibitors are used for probing transglutaminase activity, like 5-(biotinamido)pentylamine (BPA), which can be detected with high specificity by streptavidin (181). Cystamine has been one of the most widely used inhibitors from this family, and besides its inhibitory mechanism as competitive amine, it presents an irreversible mechanism of inhibition that has been recently described. Cystamine has been shown to promote the irreversible formation of a disulfide bond between Cys370 and Cys371 TG2 residues that abolish its transamidase activity (182). When administered *in vivo,* cystamine is rapidly reduced in plasma and cytosol to cysteamine, which seems only to inhibit TG2 by the reversible competitive mechanism (183). Therefore, it has been hypothesized that the inhibition of intracellular TG2 transamidase activity might be due to cysteamine and not to cystamine.

All competitive amines are general inhibitors for transglutaminases, with low specificity for the different isozymes, and high doses are needed to observe an inhibitory effect. The effect of these inhibitors in the conformation of TG2 as well as in its other effects besides the transamidase activity, if any, is unknown. In addition, cystamine has been shown to present several other off-target effects like caspase-3 inhibition (148). For these reasons, competitive amines are being abandoned as inhibitors in the investigation of TG2, and this has forced the development of more specific modulators.

### 3.6.2 Irreversible inhibitors that lock the open conformation of TG2

Several families of compounds targeted at the active site of TG2 have been developed in the last years. Bromodihydroisoxazole (DHI) derivatives, such as ERW1041E, have been used *in vivo* in different animal disease models, such as a mice model for inflammation-related hypertension (153), cardiac fibrosis (184) and pulmonary hypertension (185), with apparently low toxicity and successfully inhibiting transglutaminase activity and its consequences. These inhibitors have been proposed as probes of the open conformation of TG2. However, it is unclear if they can induce the open conformation themselves, reducing their usefulness to study conformation in a physiologically relevant way (186). The main limitations of this family of compounds are their moderate potency and low selectivity for TG2 when compared to other isozymes like TG1, TG3, and factor XIIIa (187). Sulfonium and imidazolium inhibitors like the previously mentioned NTU 281-283 and L682777, respectively, have also been used *in vivo* in animal models of kidney disease (16,17) and atherosclerosis (160), with apparently low toxicity, but presenting selectivity issues with other transglutaminases, particularly with factor XIIIa.

Michael acceptor inhibitors are α, β-unsaturated carbonyl compounds that participate in an addition reaction with thiolated nucleophiles, efficiently inhibiting many enzymes whose active site contains cysteine. Acrylamide inhibitors like NC9, VA4 and VA5 are part of this group and have demonstrated to be potent irreversible TG2 inhibitors. These inhibitors bind to the active site of TG2 and have been shown to lock the enzyme in its open conformation, preventing the conformational change to the GTP-bound form, both in the isolated enzyme (21) and in cells expressing a labeled TG2 for Förster resonance energy transfer (FRET) studies (19), showing also to be membrane permeable, reaching cytosolic TG2. Due to their ability to also inhibit the GTPase activity of TG2, these compounds have been shown to reduce cancer stem cell survival (19). The fluorescence of some of these compounds have allowed for their use as probes for TG2, although they seem to also inhibit factor XIIIa (188).

Another widely used group of active-site targeted inhibitors are the peptidomimetic compounds from the 'DON' (6-diazo-5-oxo-L-norleucine) family, which replaced the Michael acceptor warhead by a 'DON' group, resulting in an increased potency and selectivity for TG2 compared to other transglutaminases. Boc-DON and Z-DON developed by the company Zedira (Darmstadt, Germany) are the most widely used compounds from this family, being non-membrane-permeable and membrane-permeable, respectively (189). Although these compounds are selective for TG2, they also inhibit TG1, TG3 and TG6 at working concentrations (189). Moreover, a crystal structure for Z-DON bound TG2 has been obtained, demonstrating that the compound is also able to lock the enzyme in its open conformation (22). Another inhibitor from this family, ZED1277, developed by Zedira and in Phase IIb clinical trials for celiac disease, is the only small molecule inhibitor of TG2 that has reached the clinical phase.

### 3.6.3 Reversible inhibitors that stabilize the closed conformation of TG2

The first used molecules from this class were nonhydrolyzable GTP analogues, such as GTPγS and GMP-PCP, due to their presumed ability to bind to the GTP-binding pocket of TG2. These analogues have been used as research tools *in vitro* to investigate TG2 GTPase activity (128), but their potential interaction with other GTPases make them not suitable for research *in vivo*.

More recently, acylhydrazide inhibitors were developed and were shown to be reversible allosteric inhibitors of TG2 (23), with slow-binding kinetics and variable mechanism of inhibition depending on the TG2 substrate (24), by binding to a GTP-related pocket. The parent compound of this family, LDN 27219, was shown to be non-competitive when the substrates were large proteins such as N-methylcasein and RN-Boc-Lys-NH-CH2-CH2-NH-dansyl. At the same time, it displayed a competitive mechanism with simpler tetrapeptides (24), suggesting that LDN 27219 was able to bind to different conformational states of TG2. Moreover, the first assays showed that LDN 27219 was able to reduce TG2 transamidase activity inhibition by GTP. Therefore it was initially hypothesized that it could compete with GTP binding. Still, later experiments directly measuring GTP binding revealed that other compounds from the acylhydrazide family did not interfere with TG2 GTP-binding activity (189). These results suggest that LDN 27219 does not bind directly to the GTP pocket of TG2, but to a related site that is able to stabilize the closed conformation of the enzyme, mimicking the inhibitory effect of GTP but without directly competing with its binding. This idea is supported by *in silico* simulations suggesting that LDN 27219 binds to a site near to the GTP-binding pocket and stabilizes the closed conformation. LDN 27219 docking seems to interfere with the regulatory loop between the catalytic core and the first β-barrel (aminoacids 454-478), which, as previously mentioned, is essential for conformational change (25). Although this conformational effect has not been observed experimentally, the selectivity profile of acylhydrazide inhibitors also supports this idea (189), as these compounds are highly selective for TG2 and TG3, the only transglutaminases together with TG5 that are regulated by GTP binding. The selectivity for TG5 of these compounds has not been tested so far.

Cinnamoyl inhibitors are a group of reversible TG2 inhibitors that have been shown to inhibit transamidase activity in a competitive manner to the donor substrate, CP4d being the most potent of this family (190). Photo labeling studies revealed that these inhibitors bind to the acyl-donor substrate-binding pocket of the active site (191). Still, despite this, FRET assays in living cells suggested that CP4d favors the closed conformation of the enzyme (19,123). The effect of these compounds in the GTPase activity of TG2, if any, is not known.

### 3.6.4 Other mechanisms of TG2 inhibition with unknown conformational effects

Acylideneoxoindol inhibitors are potent, non-competitive, and reversible TG2 inhibitors, which in recent studies have been found to bind to a low-affinity calcium-binding site on the catalytic core of TG2 (192). Surprisingly, these compounds were transamidase activity inhibitors only at saturating concentrations of calcium, while they activated TG2 transamidase activity at lower, but

physiologically relevant, calcium concentrations (192). This dual agonistic/antagonistic action highlights the complex regulation of TG2 and offers an interesting tool for its study.

Quinoxaline and thieno[3,4-b]-pyrazine inhibitors were discovered using cancer cell proliferation inhibition assays. One of these molecules, GK921, has been shown to bind to the $NH_3$-terminus of TG2 without interacting with the active site, but somehow inactivating the enzyme and inhibiting its interaction with p53, which results in apoptosis in renal cell carcinoma (193). The mechanism of inhibition of these compounds is not known. However, it has led to the generation of interesting hypothesis like the existence of functional TG2 dimers that might play a physiological role, and whose formation seems to be inhibited by these compounds (193).

To target the essential role of TG2 GTPase activity in epithelial-to-mesenchymal transition, which facilitates cancer migration in adults as well as participating in the onset of pulmonary fibrosis (194), the design of inhibitors that bind to the GTP binding pocket, based on their *in silico* docking score, has been patented. Despite being an exciting approach to TG2 inhibition, the compounds have been neither synthesized nor tested *in vitro* yet (20).

Another potential strategy to selectively inhibit TG2 is the use of antibodies or peptides. The advantage of this approach is that inhibitors can be targeted at particular interactions of TG2 with other molecules, affecting its scaffolding activity. For example, peptides and antibodies against the heparan-sulfate binding site to reduce cell adhesion and migration (105), and peptides to interfere with polymerization of IκB by TG2 and avoid the activation of the NF-κB pathway, have been patented (20). Antibodies targeting the catalytic site of TG2 to reduce transamidase activity and ECM deposition have also been developed, Zampilimab (UCB7858) by UCB Pharma being the most successful example, which is being tested in phase I/II clinical trials for chronic allograft injury after kidney transplant. The effect of peptides and antibodies in TG2 conformation is variable depending on the epitopes that they recognize. Recent studies have shown that autoantibodies from celiac disease patients were able to stabilize different conformations of TG2 (195), activating or inhibiting its transamidase activity accordingly (196). The main limitation of antibody use for TG2 inhibition is that the effect is limited to the extracellular enzyme.

**Table 1**: Example of small-molecule TG2 inhibitors

| Name | Molecule | Specificity | Potency for TG2 | Inhibition mechanism | Effect on conformation | Membrane permeable |
|---|---|---|---|---|---|---|
| Competitive amines | | | | | | |
| Cystamine | 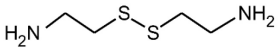 | No specific | $IC_{50}$= 73 µM Data from (186) | Several mechanisms: Competetive reversible. Irreversible formation of disulphide bond in catalytic triad | Unknown | Yes |
| Irreversible inhibitors | | | | | | |
| Z-DON | 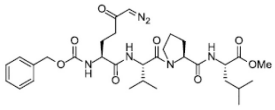 | TG2 > TG6 > TG3 | $IC_{50}$= 0.02 µM Data from (186) | Active site directed | Lock TG2 in the open conformation | Yes |
| Boc-DON | 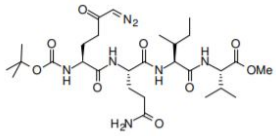 | TG2 >TG6 > TG1 | $IC_{50}$= 0.3 µM Data from (186) | | | No |
| VA5 | 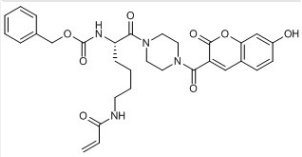 | TG2 > TG1 > FXIIIa | $IC_{50}$ unkown Ki= 11.2 µM Data from (175) | | | Yes |
| Reversible inhibitors | | | | | | |
| GTPγS | 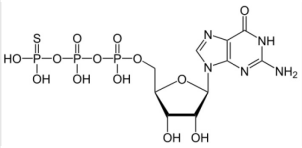 | Probably TG2, TG3, TG5. Interaction with GTPases | $IC_{50}$= 5-48 µM Data from (186) | GTP site directed | Stabilize TG2 closed conformation | Yes |
| LDN 27219 | 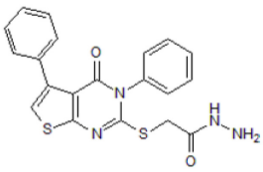 | TG2 = TG3, maybe TG5 | $IC_{50}$= 0.25 - 0.6 µM Data from (23, 24) | Binds to GTP-related site, interacts with regulatory loop. No competitive with GTP | | Yes |
| CP4d | 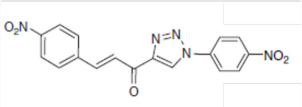 | Unknown | $IC_{50}$= 2.1 µM Data from (187) | Active site directed | | Yes |

## 4. HYPOTHESIS AND AIMS

The hypothesis of the present thesis is that activation of potassium channels and improved endothelium-dependent vasorelaxation by TG2 conformational modulation will prevent vascular dysfunction in aging and diabetes.

The following specific aims were addressed:

1- To assess whether conformational modulation of TG2 by inhibitors stabilizing the closed or the open conformation will affect potassium channel gating in the vascular wall, improving endothelium-dependent vasorelaxation and lowering blood pressure at different ages.

2- To investigate whether *in vivo* treatment with TG2 inhibitors will prevent vascular dysfunction in diabetic mice.

3- To characterize the potassium channels involved in the EDH-induced vasorelaxation in the intrarenal arteries of rats, with the perspective of future application of TG2 modulators.

# 5. MATERIALS AND METHODS

## 5.1 Animal welfare and ethical statements

All animal protocols and care used in this study were approved by the Danish Animal Experiments Inspectorate (permissions 2014-15-2934-0159 and 2019-15-0201-0009) or by the Institutional Animal Care and Use Committee at Complutense University (Madrid, Spain), and were conducted in accordance to the Danish Animal Law which conforms to the European Union Guidelines for the Care and the Use of Laboratory Animals (European Union Directive 2010/63/EU). The animals were housed in the animal facility of the university and in cages (Universal Euro II or III type Long) with standard wood bedding and space for two rats or 4-6 mice. They were maintained on standard chow and water '*ad libitum*', at a temperature of 22-23°C and with a 12 h cycle of light and dark.

The study using human arterial tissue was approved by the Regional Ethics Committee, Central Denmark (permission 1-10-72-120-17) and conducted following the principles of the Helsinki Declaration II for medical research. All participants gave informed consent before participation.

## 5.2 Animal models, study design and tissue preparation

For the experiments in connection with the first aim, Male Wistar Hannover rats at 6-7, 12-14, and 35-40 weeks of age were used. The rats used for the *ex vivo* experiments were randomly selected and euthanized by stunning, decapitation and exsanguination. The intestines were immediately extracted and placed in 4ºC physiological saline solution (PSS), see 'Drug preparation and solutions' for composition. Secondary to tertiary branches of the mesenteric artery were isolated. For *in vivo* blood pressure recordings, animals at 12-14 or 35-40 weeks of age were anesthetized with 35 mg/kg of S-ketamine and 50 mg/kg of pentobarbital sodium administered intraperitoneally (IP) after 8 h fasting and euthanized by pentobarbital overdose at the end of the experiment.

Male Wistar Kyoto rats at 16–18 weeks of age were used for the experiments in connection with the third aim. These rats were decapitated with a guillotine and the kidneys were extracted and placed in 4ºC PSS. First- to third-order branches of the main renal artery, intrarenal arteries, which included the segmental and interlobar arteries, were dissected.

Obese and diabetic db/db mice with a mutation in the leptin receptor and their lean normoglycemic heterozygous db/+ were used as a diabetes model in the experiments related to the second aim. For the *ex vivo* studies on the acute effects of LDN 27219 in isolated arteries, 16-17-week-old diabetic db/db male mice (C57BLKS/J-Lepr$^{db}$/Lepr$^{db}$) and 16-17, 24-25 and 39-40-week-old normoglycemic db/+ (C57BLKS/J-Lepr$^{db}$/+) were used. Prior to euthanasia by cervical dislocation, body weight was registered and blood glucose levels were measured with a Contour Blood Glucose Monitoring System (Bayer, Denmark, Copenhagen S) using tail artery blood samples. The mesenteric bed was then immediately extracted and placed in PSS, and mesenteric arteries were dissected as previously described. For the long-term treatment study, 7-8-week-old

db/db male mice (C57BL/6J-Lepr$^{db}$/ Lepr$^{db}$) were randomly allocated into three groups: 1) treatment with IP injections of LDN 27219 (8 mg/kg/12h) and vehicle drinking water [LDN 27219 treatment group] (*n=12*), or 2) treatment with IP injections of vehicle (each 12 h) and candesartan cilexetil (3 mg/kg/24h) in the drinking water [candesartan treatment group] (*n=12*), or 3) treatment with IP injections of vehicle (each 12 h) and vehicle drinking water [vehicle treatment group] (*n=12*). Age- and sex-matched db/+ mice (C57BL/6J-Lepr$^{db}$/+) were included as healthy controls, receiving the same treatment as the vehicle treatment group. Using a non-compartmental model, pharmacokinetic studies of a single 2 mg/kg IP dose of LDN 27219 in living C57BL/6 mice (*n=3*) showed the half-life of the compound to be 4.94 ± 1.37 (SD) h, being the bioavailability 64.5%. For drug preparation and vehicle composition, see 'Drug preparation and solutions'. Body weight and blood sugar were measured weekly, and food and water consumptions for each cage were registered each 3-4 days, coinciding with change of cages and renewing of water and chow. In half of the animals, blood pressure was also measured weekly using tail-cuff plethysmography (CODA System, Kent Scientific). After three weeks of treatment, mice were euthanized by cervical dislocation and the descending thoracic aortae and small mesenteric arteries were isolated as described above for *ex vivo* examination of endothelial function. The primary endpoint of the long-term study was the treatment of endothelial dysfunction in the peripheral circulation, being secondary endpoints: endothelial dysfunction in large arteries, blood pressure, and the arterial sensitivity to NO and vasoconstrictors.

Human subcutaneous arteries were dissected from fat biopsies of the gluteal region from both male and female patients (30-70 years of age) with or without essential hypertension. A list of patient characteristics can be seen in Table 2.

Table 2: Data from human donors of fat biopsies

| Patient group | Sex | Age (years) | No. of antihypertensive drugs |
|---|---|---|---|
| Hypertension | Female | 43 | 4 |
| Hypertension | Female | 67 | 3 |
| Hypertension | Female | 47 | 2 |
| Healthy Control | Male | 62 | none |
| Healthy Control | Male | 43 | none |
| Healthy Control | Male | 39 | none |
| Healthy Control | Male | 33 | none |
| Healthy Control | Female | 35 | none |

### 5.3 Isometric tension recordings in isolated arteries *ex vivo*

Small mesenteric arteries from rats (internal diameters 200-300 μm) and mice (internal diameter 150-250 μm), rat interlobar arteries (internal diameters 200-300 μm), mice aortic rings (internal diameter >800 μm) and human subcutaneous arteries (internal diameters of 300-400 μm) were cut in segments of approximately 2 mm and mounted in microvascular myographs (Danish Myotechnology, Aarhus, Denmark) using two 25, 40 or 100 μm steel wires, depending on the vessel diameter. PSS solution in the myograph bath was maintained at 37ºC and continuously gassed with 5% CO2,-75% N2-20% O2 to maintain pH (7.4). Small arteries were then normalized to 0.9 times the estimated internal diameter at 100 mmHg of transmural pressure since it has been determined as optimal for force development in most small arteries (197). Aortic rings were stretched to a final force of 5.5 mN (passive tension of 1.38 mN/mm) in 1 mN increments and allowed to equilibrate for at least 30 min. The vessel viability was tested at the beginning of each experiment by measuring the vasoconstrictor responses to a solution with high potassium concentration (KPSS), equivalent to PSS except that NaCl was exchanged for KCl on an equimolar basis. The endothelium was removed in a subset of small arteries by rubbing the lumen with a human scalp hair. The presence or absence of endothelium was checked by addition of ACh ($10^{-5}$ mol/L) after pre-constriction with NA ($10^{-7}$-$5x10^{-6}$ mol/L), arteries with less than 75% of relaxation were discarded except for arteries whose endothelium had been removed and for those from aged or diabetic animals, in which some degree of endothelial dysfunction was expected.

Mesenteric arteries from rats were pre-contracted with the thromboxane analogue, U46619 ($4.10^{-7}$ mol/L) and concentration-response curves (CRCs) for TG2 specific inhibitors, LDN 27219 ($10^{-8}$-$10^{-5}$ mol/L) and Z-DON ($10^{-10}$-$3x10^{-5}$ mol/L) were constructed. To study the role of the endothelial pathways in LDN 27219 relaxation, CRCs in rat mesenteric arteries were constructed for it in presence of a NOS inhibitor, Nω-Nitro-L-arginine (L-NOARG) ($10^{-4}$ mol/L), and in arteries without endothelium. Mesenteric arteries from mice and human subcutaneous arteries were pre-contracted with U46619 ($3x10^{-7}$ - $3x10^{-8}$ mol/L), and CRCs for LDN 27219 ($10^{-8}$-$10^{-4}$ mol/L) were constructed. To discard an effect by the solvent (Dimethyl sulfoxide = DMSO), control CRCs in which only the vehicle was added were performed in every experiment.

Endothelial function of the arteries was assessed by pre-contracting the arteries to approximately 90% of their contraction to KPSS with Phe (usually $3x10^{-6}$ – $10^{-5}$ mol/L for mesenteric arteries and $10^{-7}$ mol/L for aortae) and constructing CRCs for ACh ($10^{-8}$ - $3x10^{-5}$ mol/L). Endothelium-independent vasorelaxation was investigated by constructing CRCs for the NO donor sodium nitroprusside (SNP) ($10^{-8}$ - $3x10^{-5}$ mol/L in mesenteric arteries and $10^{-9}$-$3x10^{-5}$ for aortae) in Phe-contracted arteries. To study the acute effect of LDN 27219 on endothelial function and on endothelium-independent vasorelaxation, ACh and SNP CRCs were constructed after 25 min incubation with either vehicle or LDN 27219 ($10^{-6}$ - $3x10^{-6}$ mol/L). To study the effect of other TG2 inhibitors that lock the enzyme in its open conformation (21,22), CRCs for ACh and SNP were constructed in rat mesenteric arteries after 1h incubation with either Z-DON ($4x10^{-5}$ mol/L), Boc-DON ($10^{-5}$ mol/L), VA5 ($10^{-5}$ mol/L) or vehicle. Differences in incubation time account for

the different membrane permeability of the compounds.

To investigate which endothelial pathways are involved in LDN 27219 potentiation of ACh-induced vasorelaxation, CRCs for ACh in absence and presence of LDN 27219 were repeated in arteries from rats after incubation with blockers of $K_{Ca}2$ and $K_{Ca}3.1$ channels, UCL 1684 ($10^{-6}$ mol/L) and TRAM-34 ($10^{-6}$ mol/L) respectively, L-NOARG ($10^{-4}$ mol/L), $K_{Ca}1.1$ channel blocker iberiotoxin (IbTx) ($10^{-7}$ mol/L) and guanylate cyclase inhibitor ODQ ($3x10^{-6}$ mol/L).

To assess the EDH component in interlobar arteries, CRCs for ACh were performed in the presence of L-NOARG ($10^{-4}$ mol/L) and COX inhibitor indomethacin ($10^{-6}$ mol/L). Then the role of calcium-activated potassium channels in the EDH-mediated relaxation was assessed in the absence and presence of the IbTx ($10^{-7}$ mol/L), TRAM-34 ($10^{-6}$ mol/L), and UCL 1684 ($10^{-6}$ mol/L). To confirm the functional expression of $K_{Ca}1.1$ channels on the endothelium of interlobar arteries, CRCs for $K_{Ca}1.1$ channel opener NS110216 ($10^{-8}$ - $10^{-4}$ mol/L) (198) were constructed on Phe-contracted ($10^{-6}$ mol/L) arteries with and without endothelium, in the absence and presence of IbTx ($10^{-7}$ mol/L). Functional expression of $K_{Ca}2.3$ channels was studied performing CRCs for the $K_{Ca}3.1$ and $K_{Ca}2$ channel opener SKA-31 ($10^{-8}$ - $10^{-4}$ mol/L) (199) in the presence of TRAM-34 ($10^{-6}$ mol/L) alone or in combination with UCL 1684 ($10^{-6}$ mol/L).

Vessel reactivity to vasoconstrictors was also examined in the long-term treatment study with db/db mice constructing CRCs for NA ($10^{-8}$-$10^{-5}$ mol/L in mesenteric arteries and $10^{-9}$-$10^{-7}$ mol/L in aortae).

### 5.4 Electrophysiological recordings *ex vivo*

#### 5.4.1 Resting membrane potential (Em) measurements in myograph-mounted arteries

Small mesenteric arteries from Wistar Hannover rats were mounted and normalized in a myograph as previously described (200). An Ag/AgCl electrode in the myograph bath was used as reference electrode and KCl-filled glass microelectrodes (40-100 MΩ of resistance) were used to obtain intracellular recordings of resting membrane potential. Input resistance was assessed by observing the change in potential caused by applying current pulses of 1 nA; the electrode resistance was compensated using the amplifier (Intro-710, WPI) before penetrating inside the smooth muscle cell. PSS solution in the myograph chamber was maintained at 37ºC and under light bubbling with 95% $O_2$ - 5% $CO_2$ through the protocol.

The effect of 25 min incubation with LDN 27219 ($10^{-6}$ mol/L) in Em and in ACh- ($10^{-8}$-$10^{-5}$ mol/L) induced hyperpolarization was studied in absence and presence of IbTx ($10^{-7}$ mol/L). To minimize the effect of endothelial potassium channels the protocol was repeated in the presence of TRAM-34 ($10^{-6}$ mol/L) and UCL 1684 ($10^{-6}$ mol/L).

5.4.2 Whole cell voltage clamp studies

For isolation of VSMCs, rat mesenteric arteries were dissected, opened longitudinally and stored in 4 ºC dissociation solution (for composition, see 'Drug preparation and solutions'). Arteries were then equilibrated during 10 min in a dissociation solution with bovine serum albumin (BSA) (1 mg/mL) at 37ºC and then exposed to the same solution supplemented with papain (0.5 mg/mL; Worthington Biochemical Corp., Lakewood, NJ, USA) and dithiothreitol (DTT) (1 mg/mL) at 37ºC for 8 min. Arteries were then washed in 4 ºC dissociation solution and moved to dissociation solution containing BSA (1 mg/mL) and collagenase (0.7 mg/mL type F and 0.4 mg/mL type H; Worthington Biochemical Corp.) at 37°C for 3 min. After washing in 4 ºC dissociation solution, isolated VSMCs were obtained by gentle trituration of the digested arteries with a fire-polished glass pipette into the VSMC extracellular solution (for composition, see 'Drug preparation and solutions').

To isolate rat intrarenal artery endothelial cells (RIAECs), intrarenal arteries were cut open longitudinally and incubated in trypsin/EDTA (0.25%/0.02%) in phosphate buffer saline (PBS) without $Ca^{2+}/Mg^{2+}$ (Biochrom KG, Berlin, Germany) for 30 min at 37º C. Subsequently, arteries were washed in 4 ºC dissociation solution and moved to EC extracellular solution (for composition, see 'Drug preparation and solutions'), and RIAECs were scraped and aspirated from the luminal side using a pipette tip.

Isolated cells were seeded in micro-dishes (ibid GmbH, Martinsried, Germany) and maintained at 4º C until used for electrophysiological recordings within 6 h after the isolation procedure. During the recordings cells were continuously perfused (0.5 ml/min) at room temperature (21–25ºC) with their respective extracellular solutions.

Patch pipettes were made of borosilicate glass capillaries (World Precision Instruments, FL, USA) fabricated using a dual-stage puller PP-830 (Narishige, Tokyo, Japan), the tips were fire polished using a microforge MF-830 (Narishige, Tokyo, Japan) and presented resistances of 4-7 MΩ. For the composition of patch pipette solutions, see 'Drug preparation and solutions.' To study the effect of intracellular GTP in LDN 27219 activity over potassium currents, VSMCs patch pipette solution containing $5x10^{-3}$ mol/L $Na_2GTP$ was used in some experiments.

Membrane currents were recorded under the whole-cell configuration of the patch-clamp technique using an Axon Multiclamp 700A amplifier (Axon Instruments, Molecular Devices, CA, USA). Current recordings were digitized on line at 10 kHz and low pass filtered at 2 kHz using a Digidata 1440 A (Axon Instruments). To acquire and store data, pClamp 10 software was used. Em was recorded in some cells under gap-free conditions (I=0 pA) before starting voltage-clamp recordings. Current-voltage relations were determined using voltage ramps (-100 to 160 mV, 600 msec for VSMCs and -100 to 120 mV, 500 msec for RIAECs) and a holding potential (Vh) of -65 mV for VSMCs and -50 mV for RIAECs under the voltage-clamp configuration.

Drugs used in patch-clamp studies were dissolved in the extracellular solution at the desired concentration and applied to the recording micro-dish via a gravity-fed U-tube microperfusion system connected to a vacuum pump that allowed us to exchange the extracellular media.

In VSMCs amplitudes of potassium currents were measured in control conditions and 12 min after the addition of LDN 27219 ($3x10^{-5}$ mol/L) to the extracellular solution. To address which subtype of potassium channels were involved in LDN 27219 effect, the protocol was repeated in the presence of IbTx ($10^{-7}$ mol/L), and of the voltage-gated potassium channel 7 (Kv7) blocker XE991 ($10^{-5}$ mol/L) was added. To study how conformational modulation of TG2 affected LDN 27219 activity over potassium channels, the initial protocol was repeated after one h incubation with VA5 ($5x10^{-5}$ mol/L) or with $Na_2GTP$ ($5x10^{-3}$ mol/L) present in the intracellular solution.

In RIAECs, potassium currents were recorded under control conditions, after the addition of ACh ($10^{-6}$ mol/L) and to study the calcium-activated potassium channels involved in response to ACh, IbTx ($10^{-7}$ mol/L), TRAM-34 ($10^{-6}$ mol/L) and UCL 1684 ($10^{-6}$ mol/L) were cumulatively added to the extracellular solution.

### 5.5 Immunohistochemistry

Samples from freshly isolated RIAECs were seeded on positively charged surface microscope slides and fixed in 4% paraformaldehyde in 0.1 mol/L sodium phosphate buffer (PB), cryoprotected in 30% sucrose in PB and stored at -20°C. Isolated RIAECs were preincubated in 2% BSA in PB containing 0.1% Triton-X-100 for one h. Then, cells were incubated with either a rabbit anti $K_{Ca}2.3$ channel antibody (Alomone Labs, Jerusalem, Israel) diluted at 1:100, a rabbit anti-$K_{Ca}3.1$ channel antibody diluted at 1:100 or a goat anti-$K_{Ca}1.1$ channel alpha subunit antibody (Alomone Labs, Jerusalem, Israel) diluted at 1:100 for 48 h.

Endothelial cells were visualized for positive immunostaining for mouse anti VWF (Thermo Fisher Scientific, USA, 1:50 dilution). They were then washed and reacted with the second antibodies for 2h at room temperature. Secondary antibodies used were Alexa Fluor 594 (red) goat anti-rabbit (Invitrogen, Life Technologies S.A., Madrid, Spain, 1:200 dilution) and Alexa Fluor 488 (green) goat-antimouse (Invitrogen, 1:200 dilution). The slides were covered with a specific mounting medium with 4′,6-diamidino-2-phenylindole (DAPI) (Molecular Probes, Eugene, USA), which stains all cell nuclei.

Tissue samples from the kidney containing renal artery were fixed in 4 % paraformaldehyde in 0.1 mol/L PB, pH 7.4, for 2 to 4 h at 4º C, and subsequently placed in 30 % sucrose in 0.1 mol/L PB for cryoprotection. The tissue was embedded and frozen in OCT compound (Tissue-Tek®. Sakura Finetek, Europe B.V.), and stored at -80°C. Transversal sections 5 μm thick were obtained by means of a cryostat and preincubated in 10% normal goat serum in PB containing 5% BSA and 0.3% Triton-X-100 for 2-3 h. Then, sections were incubated with rabbit anti-$K_{Ca}3.1$, rabbit anti-$K_{Ca}2.3$, rabbit anti-$K_{Ca}1.1$ and rabbit anti-sloβ1 (Alomone labs, Jerusalem, Israel) at a final concentration of 1:100 and a mouse anti-eNOS (Abcam, Cambridge, UK) at 1:400 during 48 h,

washed and reacted with the second antibody for 3 h at room temperature, Alexa Fluor 594 goat-anti-rabbit and Alexa Fluor 488 goat-anti-mouse (1:200 dilution) (Abcam). The slides were covered with a specific mounting medium containing DAPI. No immunoreactivity could be detected in sections incubated in the absence of the primary antisera.

### 5.6 Blood Pressure measurements

#### 5.6.1 Direct mean arterial pressure (MAP) measurements in anesthetized animals

Wistar Hannover rats (12-14 and 35-40 weeks old) were anesthetized with s-ketamine (35 mg/kg) and pentobarbital (50 mg/kg) administered IP, and placed in a heated blanket to maintain body temperature at 37ºC, which was continuously monitored. Adequate depth of anesthesia was checked periodically by the absence of the toe pinch withdrawal effect, and 1/3 of the initial dose of anesthetics was administered IP when needed (usually each 1.5 h). For electrocardiographic recordings, ECG hypodermic needles were placed in the Einthoven's bipolar lead II configuration, which were recorded by an animal bio-amplifier (AD Instruments). A solid-state catheter (model no. SPR-1000 Millar Inc, Houston, USA) was introduced into the carotid artery to measure MAP. Electrocardiographic and MAP data were continuously recorded on a computerized data acquisition system (PowerLab, ADInstruments) and ECG signals were low-pass filtered by using the standard filter file for ECG recordings. The ADInstruments software automatically obtained different electrocardiographical values.

The rats were infused through a catheter placed into the jugular vein for 3 min with either three doses of LDN 27219 (0.1; 1 and 2 mg/kg) or the corresponding doses of the vehicle (polyethylene glycol 400 = PEG-400), using a syringe infusion pump system (Harvard Apparatus Model 55-2219) and leaving a rest period of 10 min between doses. To study the effect of TG2 inhibitors that lock the open conformation of the enzyme, the animals in the vehicle group were infused with a single dose of VA5 (1 mg/kg) for 3 min at the end of the protocol.

#### 5.6.2 Indirect MAP measurements in conscious animals with non-invasive methods

During the long-term treatment study, the blood pressure of diabetic db/db and healthy db/+ mice was recorded once a week using tail-cuff plethysmography with volume pressure recording (CODA System, Kent Scientific). To reduce the effects of the stress induced by this technique, as well as the variations due to the circadian rhythm, animals were trained during one week before the beginning of the study, animals were placed in the holders at least 10 min before the measurements, and the measurements were always carried out at similar times of the day. The temperature of the animals was continuously monitored and maintained at 37 ºC during the measurements. Measurements were repeated 20 times per animal, and results were averaged, excluding outliers (> 2 Standard Deviations (SD)).

## 5.7 Transglutaminase activity measurements

### 5.7.1 Transglutaminase activity *in vitro*

Liver samples from Wistar Hannover rats, snap-frozen with liquid nitrogen until the assay was performed, were thawed and homogenized in RIPA lysis buffer (for composition, see 'Drug preparation and solutions') with Halt Protease and Phosphatase Inhibitor Cocktail (ThermoFisher Scientifics, Massachusetts, USA). Livers were left 30 min on ice before sonicating for 45 seconds and then centrifuged at 13000 rpm for 10 min at 4 ºC. The supernatant was collected, and the protein concentration was measured by a modified Lowry method. Samples were prepared to achieve a concentration of 8 µg/µL using the diluent buffer of the Specific Tissue Transglutaminase Colorimetric Microassay Kit TG2-CovtTest (Zedira, Darmstadt, Germany). This commercially available test is based on the incorporation of a biotinylated preferred TG2 substrate (Biotin-pepT26) as amine-acceptor into a spermine coated strip as amine-donor. After dilution, 25 µL the of sample were incubated with 25 µl of different concentrations of the inhibitors LDN 27219 ($10^{-7}$ – $10^{-4}$ mol/L) or VA5 ($10^{-7}$ – $10^{-5}$ mol/L), or the vehicle for 20 min on ice. Then, the microtiter strips coated with spermine were washed, and 50 µL of study sample or 50 µL of the standard were added along with 10 µL of diluent buffer and 50 µL of ice-cold assay-mixture (Biotin-pepT26 / $CaCl_2$, 20% DTT). The plate was then incubated for 30 min at 37 ºC, and after pertinent washes with wash buffer and 0.1 mol/L NaOH incubated again with horseradish peroxidase (HRP) streptavidin (1:2000 dilution in wash buffer) for 15 min at 37 ºC. Later, HRP substrate was added for 5 min at room temperature, and subsequently, the reaction was stopped with a blocking reagent. The final optical density was read at 450 nm and data was quantitatively evaluated with the standard curve. Duplicates from each sample or standard were performed, and the average value was calculated in all the study samples.

### 5.7.2 Transglutaminase activity *ex vivo*

To measure transamidase activity *ex vivo*, a dot blot assay based on the incorporation of the transglutaminase substrate BPA to structural proteins was used. Small mesenteric arteries from rats of the different age groups were dissected and immediately incubated in PSS containing BPA ($10^{-4}$ mol/L) and an increased concentration of $Ca^{2+}$ ($2.5x10^{-3}$ mol/L) at 37ºC for four h. During incubation, PSS was continuously bubbled with 5% $CO_2$,-75% $N_2$-20% $O_2$ to maintain pH (7.4). Then, unreacted BPA was washed by rinsing the arteries with PBS before tissue homogenization and protein extraction in RIPA lysis buffer with Halt Protease and Phosphatase Inhibitor Cocktail (ThermoFisher Scientifics, Massachusetts, USA). The amount of extracted protein was quantified by a modified Lowry method, and 10 µg of total proteins were loaded onto a nitrocellulose membrane using the BioRad Dot Blot apparatus. The membrane was blocked in 5% BSA for 2 h and then incubated with HRP-conjugated streptavidin (Amersham Bioscience; dilution 1:10000 in 0.5% BSA) for two h to detect BPA incorporation. The membrane was then washed in TBS-T, removed from the dot blot apparatus, and developed using an ECL-Plus kit (General Electric (GE) Health care, Copenhagen, Denmark). The images were captured by a luminescence camera using

a PXi 4 Touch image analysis system (Syngene). After development, membranes were rinsed in water and stained with amido black (0.1% (w/v) in 10% acetic acid) for total protein staining. Blots were quantified using GeneTools 4 software (Syngene) and normalized to the total amount of protein.

Additionally, small mesenteric arteries from rats at 12-14 weeks of age were used for the inhibition assay *ex vivo.* Arteries were incubated in PSS containing BPA and $Ca^{2+}$ as previously described but in the presence of either vehicle, LDN 27219 ($10^{-6}$ mol/L), Z-DON ($4x10^{-5}$ mol/L) or DTT ($10^{-3}$ mol/L), which has been demonstrated to increase TG2 transamidase activity. Two replicates for each treatment and animal were added in one blot, and the average activity in control conditions was set to 100%.

## 5.8 Molecular biology

### 5.8.1 Native polyacrylamide gel electrophoresis (PAGE)

To study the conformational shift of the enzyme, purified and functional human TG2 ($2.5x10^{-6}$ mol/L) protein produced in insect cells (Zedira. Darmstadt, Germany) was incubated for 30 min at room temperature in preincubation buffer (for composition, see 'Drug preparation and solutions') with or without $Na_2GTP$ ($10^{-3}$ mol/L) or LDN 27219 ($10^{-3}$ mol/L ) before adding Native Sample Buffer for Protein Gels (Bio-Rad) or in preincubation buffer with Z-DON ($2x10^{-4}$ mol/L) 30 min prior addition of $CaCl_2$ ($5x10^{-3}$ mol/L) for 20 min. Native sample buffer was added (dilution 1:2), and 1.5 µg of protein was loaded onto a 4–20% Criterion™ TGX Stain-Free™ gel (Bio-Rad) using Tris-glycine (Bio-Rad) as the running buffer. Electrophoresis was applied at 125 V and 4 ºC for 75 min. The bands were visualized using stain-free technology by exposing the gels to UV light and capturing the image using a PXi 4 Touch image analysis system (Syngene). Band intensity analysis was carried out using GeneTools 4 software (Syngene).

### 5.8.2 Sodium dodecyl sulfate-PAGE (SDS-PAGE)

Small mesenteric arteries from rats of different ages were snap-frozen with liquid nitrogen and kept at -80°C until homogenization. The tissue was homogenized and centrifuged in a lysis buffer (for composition, see 'Drug preparation and solutions') with Halt Protease and Phosphatase Inhibitor Cocktail (ThermoFisher Scientifics, Massachusetts, USA). The amount of protein extracted was quantified by a modified Lowry method, and samples were diluted in Laemmli Sample Buffer (Bio-rad) containing DTT to a final concentration of 1 g/L of total protein. After boiling (99°C for 5 min), the samples were left to refrigerate, and 10 µg of protein were loaded onto 4–20% Criterion™ TGX Stain-Free™ gels (Bio-Rad), using XT MOPS (Bio-Rad) as the running buffer.

125 V were applied for one h before being transfer to a polyvinylidene fluoride (PVDF) membrane by applying 100 V for one h at 4°C using Tris-glycine (Bio-Rad) (20% ethanol) as the transfer buffer. After the transfer, total protein was visualized using stain-free technology by exposing the membranes to UV light, and the images were captured using a PXi 4 Touch image analysis system

(Syngene). The membranes were washed twice for 15 min in PBS-T and TBS-T (for composition, see 'Drug preparation and solutions') for one h and then blocked in 0.3% I-block™ (Applied Biosystems) for 2–4 h before being incubated overnight at 4°C with the primary antibody. Anti-TG2 antibody (ab421, Abcam) at a dilution of 1:200, anti-$K_{Ca}$1.1 alpha antibody (APC-107, Alomone labs) at a dilution of 1:100, and anti-$K_{Ca}$1.1 beta 1 antibody (ab3587, Abcam) at a dilution of 1:250 were used as primary antibodies in TBS-T with 0.3 % I-block™ (Applied Biosystems). The membrane was then washed in TBS-T and incubated for 2 h in the secondary antibody, Goat anti-Rabbit IgG (G-21234, Invitrogen). The membrane was developed using an ECL-Plus kit (General Electric (GE) Health care, Copenhagen, Denmark) and the images were captured by a luminescence camera using a PXi 4 Touch image analysis system (Syngene). Blots were quantified using GeneTools 4 software (Syngene)

### 5.9 Drug preparation and solutions

Unless indicated otherwise, all substances used in this study were dissolved in distilled water. For *ex vivo* experiments, U46619 was dissolved in ethanol and Boc-DON, LDN 27219, ODQ, TRAM-34, UCL 1684, XE991, and Z-DON were dissolved in DMSO and stored at -20ºC. Further dilution of the above-mentioned compounds were made in distilled water. The DMSO concentration in the bath were kept below 0.01% and did not affect vessel contractility. For *in vivo* experiments, LDN 27219 and VA5 were dissolved in PEG-400.

For the long-term *in vivo* treatment, stocks of 20 mg/mL of LDN 27219 dissolved in PEG-400 (100%) were stored at -20ºC until administration. LDN 27219 stock solutions were diluted in saline solution containing sulfobutylether-β-cyclodextrin (SBE-b-CD) to improve solubility (9 mg/mL NaCl; 15 % (w/v) SBE-b-CD) immediately before injection, resulting in a clear solution with a final concentration of 2.00 mg/mL of LDN 27219 in 10% PEG-400 / 90% (15% (w/v) SBE-b-CD in saline solution). For the treatment on the drinking water, stocks solutions of 1 mg/ml of Candesartan cilexetil was dissolved in a vehicle of PEG-400 (10% v/v), ethanol (5% v/v), Kolliphor® EL (2% v/v), and tap water (83% v/v) and the pH was adjusted to 9.0 with 0.5 mol/L Na2CO3, before dilution to the final concentration in tap water. Final concentrations needed to achieve the desired doses of candesartan cilexetil per day in the drinking water were determined by measuring water consumption every 3-4 days.

#### 5.9.1 List of used solutions and compositions

- Physiological saline solution (PSS), composition (mmol/L): 119 NaCl, 4.7 KCl, 1.18 $KH_2PO_4$, 1.17 $MgSO_4$, 1.5 $CaCl_2$, 24.9 $NaHCO_3$, 0.026 EDTA and 5.5 glucose, pH= 7.4

- High potassium PSS (KPSS), composition (mmol/L): 123.7 KCl, 1.18 $KH_2PO_4$, 1.17 $MgSO_4$, 1.5 $CaCl_2$, 24.9 $NaHCO_3$, 0.026 EDTA and 5.5 glucose, pH= 7.4

- Dissociation solution, composition (mmol/L): 119 NaCl, 4.7 KCl, 1.18 $KH_2PO_4$, 1.17 $MgSO_4$, 24.9 $NaHCO_3$, 0.027 EDTA, and 11 glucose, pH= 7.4

- VSMCs Extracellular Patch-Clamp solution, composition (mmol/L): 130 NaCl, 5 KCl, 1.2 $MgCl_2$, 1.5 $CaCl_2$, 10 glucose and 10 HEPES, adjusted to pH 7.3 with NaOH

- VSMCs patch pipette (intracellular) solution, composition (mmol/L): 130 KCl, 1.2 $MgCl_2$, 0.1 EGTA and 10 HEPES, adjusted to pH 7.2 with KOH

- Endothelial Cells Extracellular Patch-Clamp solution, composition (mmol/L): 140 NaCl, 5 KCl, 1 MgSO4, 1 CaCl2, 10 glucose and 10 HEPES, adjusted to pH 7.4 with NaOH

- Endothelial Cells patch pipette (intracellular) solution, composition (mmol/L): 140 KCl, 1 $MgCl_2$, 2 EGTA, 1.71 $CaCl_2$ and 5 HEPES, adjusted to pH 7.2 with KOH

- RIPA lysis buffer, composition (mmol/L): 0.5 tris/HCL, 10 EDTA, 1.5 NaCl, 2.5 % deoxycholic acid, 10 % NP-40, pH= 7.4

- Native PAGE preincubation buffer, composition (mmol/L): 75 imidazole, 0.5 EDTA, 5 DTT, pH= 7.2, 10% DMSO

- SDS-PAGE Lysis buffer, composition (mmol/L): 20 tris/HCL, 5 EGTA, 150 NaCl, 20 glycorophosphate, 10 NaF, 1 % triton X-1000, 0.1 % (v/v) Tween® 20, pH= 7.5

- PBS-T, composition (mmol/L): 150 NaCl, 50 $NaH_2PO_4$, 0.05 % (v/v) Tween® 20

- TBS-T, composition (mmol/L): 10 tris base,100 NaCl, 1 EDTA, 0.1 % (w/v) Tween® 20

**5.10 Randomization, blinding and statistical analysis**

All randomization in this study was performed using a random number generator. Group sizes for the *in vivo* studies were calculated with an expected effect size based on the *in vitro* results, desired power of 95% and an alfa of 0.05. For the long term study, the researcher injecting the animals, changing the drinking water bottles, performing the myograph experiments and analyzing the data was blinded to the treatment the animals were receiving. The vials containing stock solutions of either vehicle or treatment were coded by a colleague and dissolved to their working concentrations immediately before application, being indistinguishable from each other.

Data are expressed as means ± SEM, being "n" the number of animals studied in each group. The normality of the data was verified examining their quantile-quantile (Q-Q) plots against the normal distribution. Native-PAGE results were analyzed by paired two-tailed Student´s t-test. CRCs and I-V relationships were analyzed by two-way ANOVA, in order to assess the potency of the agonists, their pD2 values (-logEC50) were calculated by a variable slope model of non-linear regression (GraphPad Prism 7.02) and, if the two-way ANOVA analysis was significant, compared by an F test. One-way ANOVA was used for multiple testing followed by Dunnett's multiple comparison post hoc analysis against a control group when there was only one independent variable of interest. Values of $P < 0.05$ were considered significant.

## 6. SUMMARY OF RESULTS

A more detailed description of the results can be found in the manuscripts.

### 6.1 Role of TG2 conformation in age-dependent changes of endothelial function

Changes in TG2 conformation were examined using native-PAGE. Confirming the results of previous *in silico* studies (25), *in vitro* incubation of purified and functional human TG2 with the reversible inhibitor LDN 27219 increased the relative abundance of the closed conformation compared to vehicle, while incubation with $Na_2GTP$ forced it into its closed conformation, and the irreversible inhibitor Z-DON in the presence of calcium forced it open (Figure 4A). Measurements of BPA incorporation *ex vivo* revealed that the presence of LDN 27219 was able to inhibit 40.92 ± 4.53 % (n=3) of the transamidase activity in isolated rat mesenteric arteries, similarly to Z-DON (58.93 ± 7.84 %, *n=4*). On the other hand, DTT increased transglutaminase activity of the sample 40.84 ± 7.82 % (*n=4*) (Figure 4B). Moreover, LDN 27219 induced concentration-dependent vasorelaxation of rat small mesenteric and human subcutaneous arteries mounted in isometric myograph, while Z-DON did not affect vessel tension (see Manuscript I).

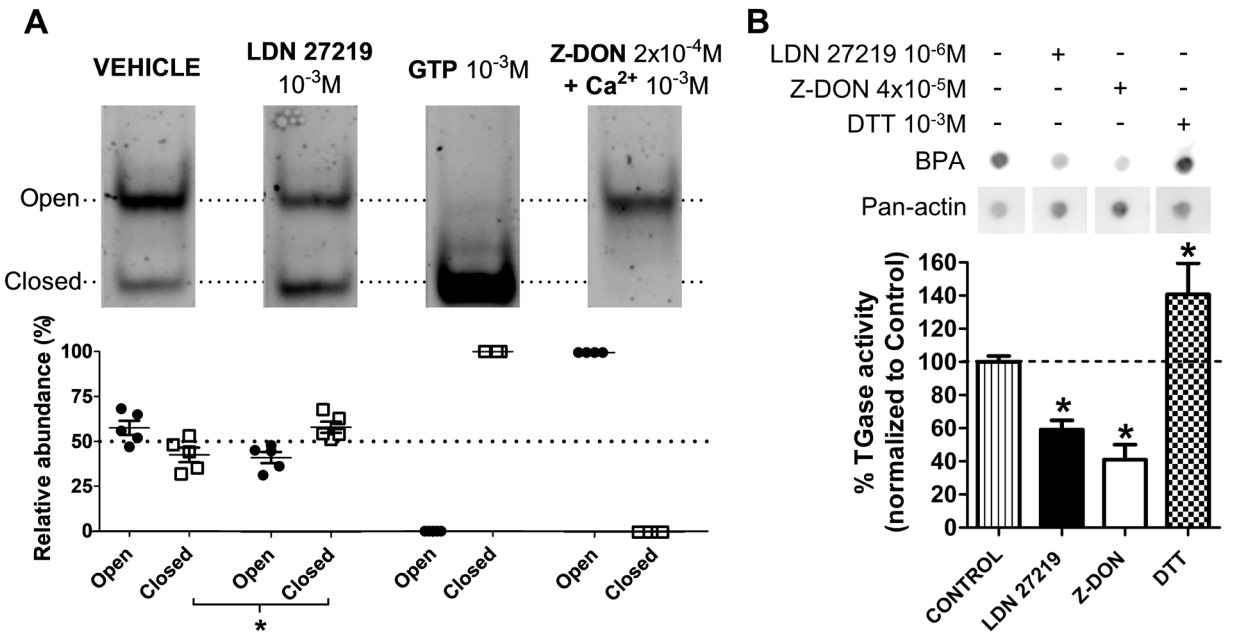


**Figure 4. Effects of different TG2 inhibitors in the conformation *in vitro* and activity *ex vivo* of the enzyme. A.** Study of recombinant human TG2 conformation using Native-PAGE. Top panel: Representative blots of the two visible bands, corresponding to the open and closed conformations, after electrophoresis of human TG2 in the presence of different effectors. Bottom: Average relative abundance of the bands presented as % of total intensity. Data are means ± SEM. *, $P < 0.05$ using paired two-tailed Student´s t-test, $n=5$ replicates in 4 gels **B.** Transglutaminase activity inhibition assay measured as the incorporation of BPA *ex vivo*. Top: Representative dot blot of BPA incorporation in small mesenteric arteries from a 12-14-week-old rat under different incubation conditions and Pan Actin expression as loading control. Bottom: Average transglutaminase (TGase) activity of the experiments shown in the top panel expressed as % of average activity in control conditions. Data are means ± SEM. *, $P < 0.05$ using one-way ANOVA with Dunnett post-test compared to control, $n=3$-$4$. (Modified from Manuscript I).

The effect of conformational modulation of TG2 in endothelial function was investigated using wire myography. Incubation during 20 min with LDN 27219 increased the vasorelaxation induced by ACh CRCs in human subcutaneous arteries ($pD_{2\ Vehicle}$= 7.58 ± 0.06 vs. $pD_{2\ LDN}$= 8.09 ± 0.06. *, $P < 0.05$ using F-test) (Figure 5A) and rat mesenteric artery (not shown in this summary, see Manuscript I). In contrast, incubation with VA5 and Z-DON that are membrane-permeable inhibitors locking TG2 in its open conformation reduced ACh-induced vasorelaxation ($pD_{2\ Vehicle}$= 7.53 ± 0.04; $pD_{2VA5}$= 7.32 ± 0.03*; $pD_{2Z\text{-}DON}$= 7.32 ± 0.05*. *, $P < 0.05$ using F-test compared to vehicle), while the non-permeable inhibitor Boc-DON failed to change it ($pD_{2\ Vehicle}$= 7.50 ± 0.05) (Figure 5B). Additionally, the presence of VA5 or Z-DON prevented the potentiation of endothelium-dependent vasorelaxation ($pD_{2\ VA5}$= 7.32 ± 0.03 vs. $pD_{2\ VA5+LDN}$= 7.25 ± 0.06; $pD_{2\ Z\text{-}DON}$= 7.32 ± 0.05 vs. $pD_{2\ Z\text{-}DON+LDN}$= 7.46 ± 0.03) (Figure 5C, D).

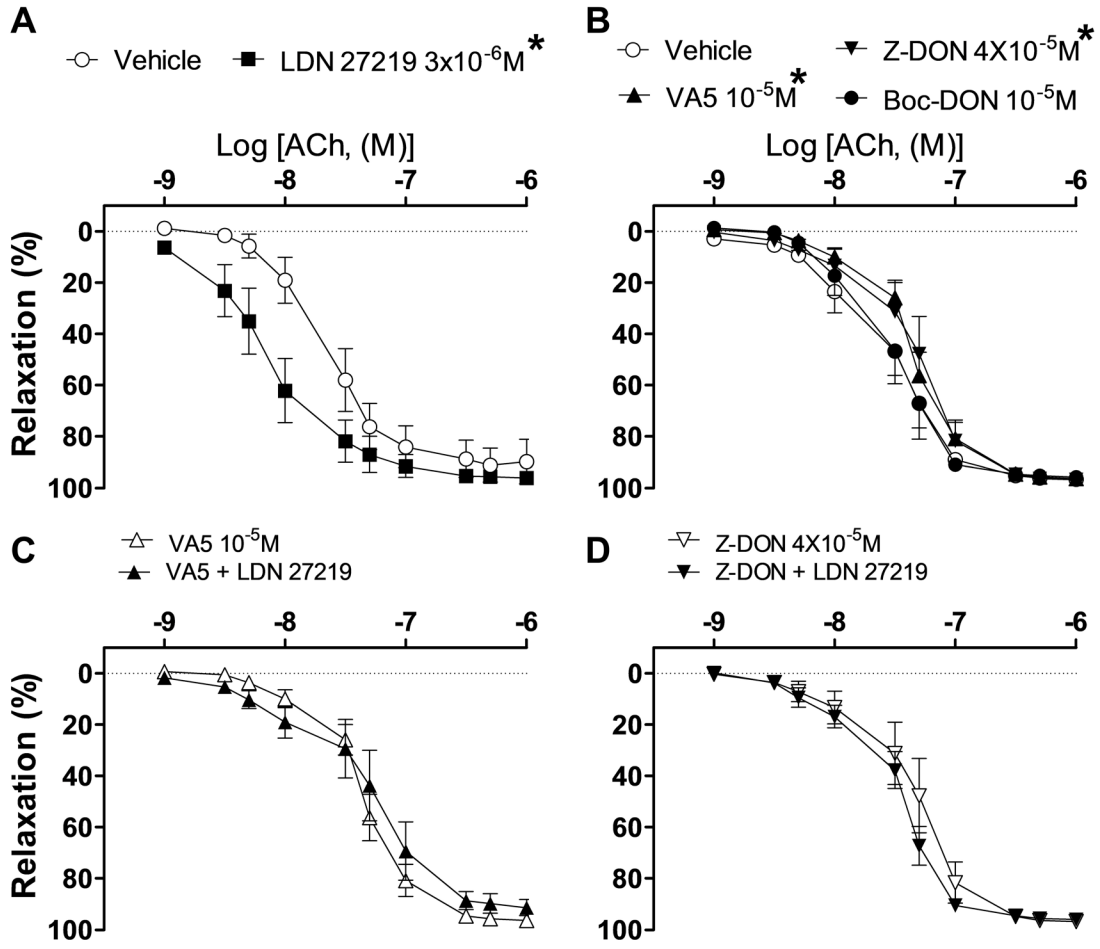


**Figure 5. Effect of conformational modulation of TG2 on endothelium-dependent vasorelaxation *ex vivo*. A.** Average responses to ACh CRCs in Phe-contracted human subcutaneous arteries incubated with either vehicle (DMSO) or reversible TG2 inhibitor LDN 27219, which promotes the closed conformation of the enzyme, *n=7*. **B.** Average responses to ACh CRCs in Phe-contracted rat mesenteric arteries incubated with either vehicle (DMSO) or irreversible and membrane permeable TG2 inhibitors VA5, Z-DON or the non-permeable inhibitor Boc-DON, which promote the open conformation of the enzyme, *n=5-10*. **C.** Average responses to ACh CRCs in Phe-contracted rat mesenteric arteries incubated with either vehicle (DMSO) or LDN 27219 both in presence of VA5, *n=5-6*. **D.** Average responses to ACh CRCs in Phe-contracted human subcutaneous arteries incubated with either vehicle (DMSO) or LDN 27219 both in presence of Z-DON, *n=5*. Data are means ± SEM of % relaxation relative to maximum contraction. *, $P < 0.05$ using two-way ANOVA compared to their respective controls. (Modified from Manuscript I).

To investigate mechanisms involved in the potentiation of ACh-derived vasorelaxation by LDN 27219, different endothelial-pathways were inhibited in rat mesenteric arteries. The presence of $K_{Ca}3.1$ and $K_{Ca}2$ blockers, TRAM-34 ($10^{-6}$ mol/L) and UCL 1684 ($10^{-6}$ mol/L) respectively, failed to prevent the potentiation by LDN 27219 ($10^{-6}$ mol/L) ($pD_{2\ TRAM+UCL+Vehicle} = 6.39 \pm 0.07$ vs. $pD_{2\ TRAM+UCL+LDN} = 6.90 \pm 0.06$ *, $P < 0.05$ using F-test) (Figure 6A). Contrarily, the inhibition of NOS or $K_{Ca}1.1$ channels by L-NOARG ($10^{-4}$ mol/L) or IbTx ($10^{-7}$ mol/L), respectively, abolished the

effect of LDN 27219 ($pD_{2\ L\text{-}NOARG+Vehicle}$= 6.71 ± 0.05 vs. $pD_{2\ L\text{-}NOARG+LDN}$= 6.70 ± 0.05; $pD_{2\ IbTx+Vehicle}$= 6.73 ± 0.05 vs. $pD_{2\ IbTx+LDN}$= 6.70 ± 0.08) (Figure 6B, C). In arteries whose endothelium was removed, incubation with LDN 27219 also potentiated the vasorelaxation in response to SNP ($pD_{2\ Vehicle}$= 6.63 ± 0.07 vs. $pD_{2\ LDN}$= 7.36 ± 0.09 *, *P < 0.05* using F-test) (Figure 6D).

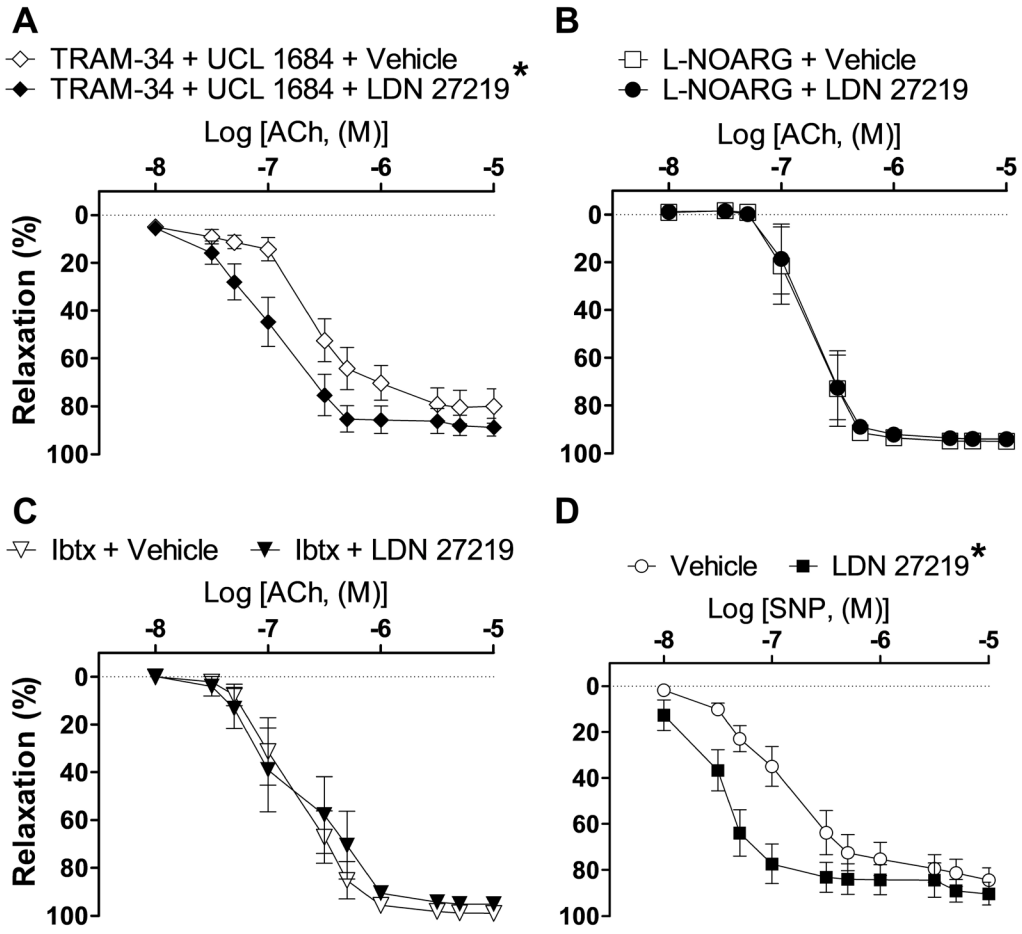


**Figure 6. The mechanism underlying the potentiation of endothelium-dependent vasorelaxation by LDN 27219 *ex vivo*. A.** Average responses to ACh CRCs in Phe-contracted rat mesenteric arteries incubated with either vehicle (DMSO) or reversible TG2 inhibitor LDN 27219, both in the presence of TRAM-34 ($10^{-6}$ mol/L) and UCL 1684 ($10^{-6}$ mol/L), *n=5*. **B.** Average responses to ACh CRCs in Phe-contracted rat mesenteric arteries incubated with either vehicle (DMSO) or reversible TG2 inhibitor LDN 27219, both in the presence of L-NOARG ($10^{-4}$ mol/L), *n=5*. **C.** Average responses to ACh CRCs in Phe-contracted rat mesenteric arteries incubated with either vehicle (DMSO) or reversible TG2 inhibitor LDN 27219, both in the presence of IbTx ($10^{-7}$ mol/L), *n=6*. **D.** Average responses to SNP CRCs in Phe-contracted rat mesenteric arteries without endothelium, incubated with either vehicle (DMSO) or reversible TG2 inhibitor LDN 27219, *n=6*. Data are means ± SEM of % relaxation relative to maximum contraction. *, *P < 0.05* using two-way ANOVA compared to their respective controls. (Modified from Manuscript I).

In isolated VSMCs from rat mesenteric arteries, patch-clamp studies revealed that cells incubated with LDN 27219 ($3x10^{-5}$ mol/L) presented higher potassium current amplitudes than under control

conditions, similarly to cells measured with high concentrations of intracellular $Na_2GTP$ ($5x10^{-3}$ mol/L) (Figure 7). Furthermore, in the presence of high intracellular $Na_2GTP$, addition of LDN 27219 to the extracellular medium failed to increase further potassium currents (not shown in this summary, see Manuscript I). Contrarily, incubation either with VA5 ($5x10^{-5}$ mol/L) or IbTx ($10^{-7}$ mol/L) reduced potassium currents in isolated VSMCs (Figure 7) and prevented LDN 27219 increases in potassium current (not shown in this summary, see Manuscript I).

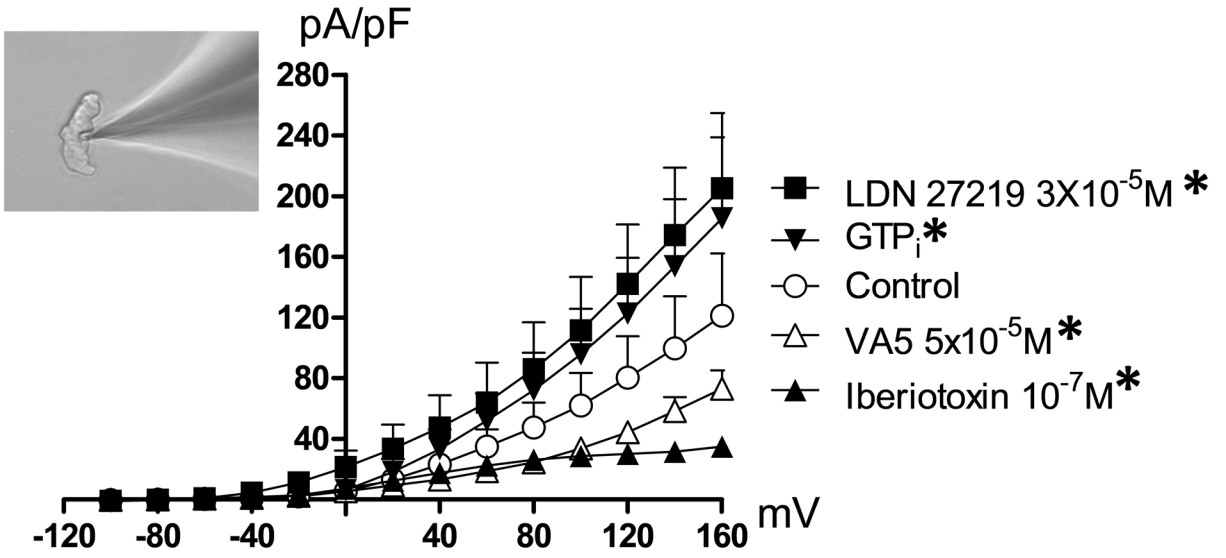


**Figure 7. Effect of TG2 conformational modulation in potassium currents of freshly isolated VSMCs *ex vivo*.** Top left: Picture of freshly isolated VSMCs from rat mesenteric artery and patch pipette during voltage-clamp recordings. Right: Averaged potassium current densities (pA/pF) of VSMCs in different conditions, *n=4-7*. Data are means ± SEM. *, *P < 0.05* using two-way ANOVA compared to control conditions. (Modified from Manuscript I).

The effects of LDN 27219 on endothelial function were studied in mesenteric arteries from rats of different ages. Incubation with LDN 27219 induced a more robust potentiation of endothelium-dependent vasorelaxation in arteries from 35-40-week-old rats when compared to arteries from younger animals. The level of potentiation was calculated as the difference in the area under the curve (AUC) of ACh vasorelaxation between vehicle-incubated and LDN 27219-incubated arteries from the same rat (Figure 8A). This correlated with higher transamidase activity, measured as levels of incorporated BPA, in arteries from older animals (Figure 8B, C). Despite this, they did not present higher expression of TG2 (not shown in this summary, see Manuscript I). Additionally, *in vivo* infusion of LDN 27219 in anesthetized rats showed a dose-dependent blood lowering effect of LDN 27219 that was stronger in 35-40-week-old compared to 12-14-week-old rats. In contrast, infusion of vehicle (PEG-400) induced a dose-dependent increase in blood pressure and injection of VA5 failed to change it (Figure 8D).

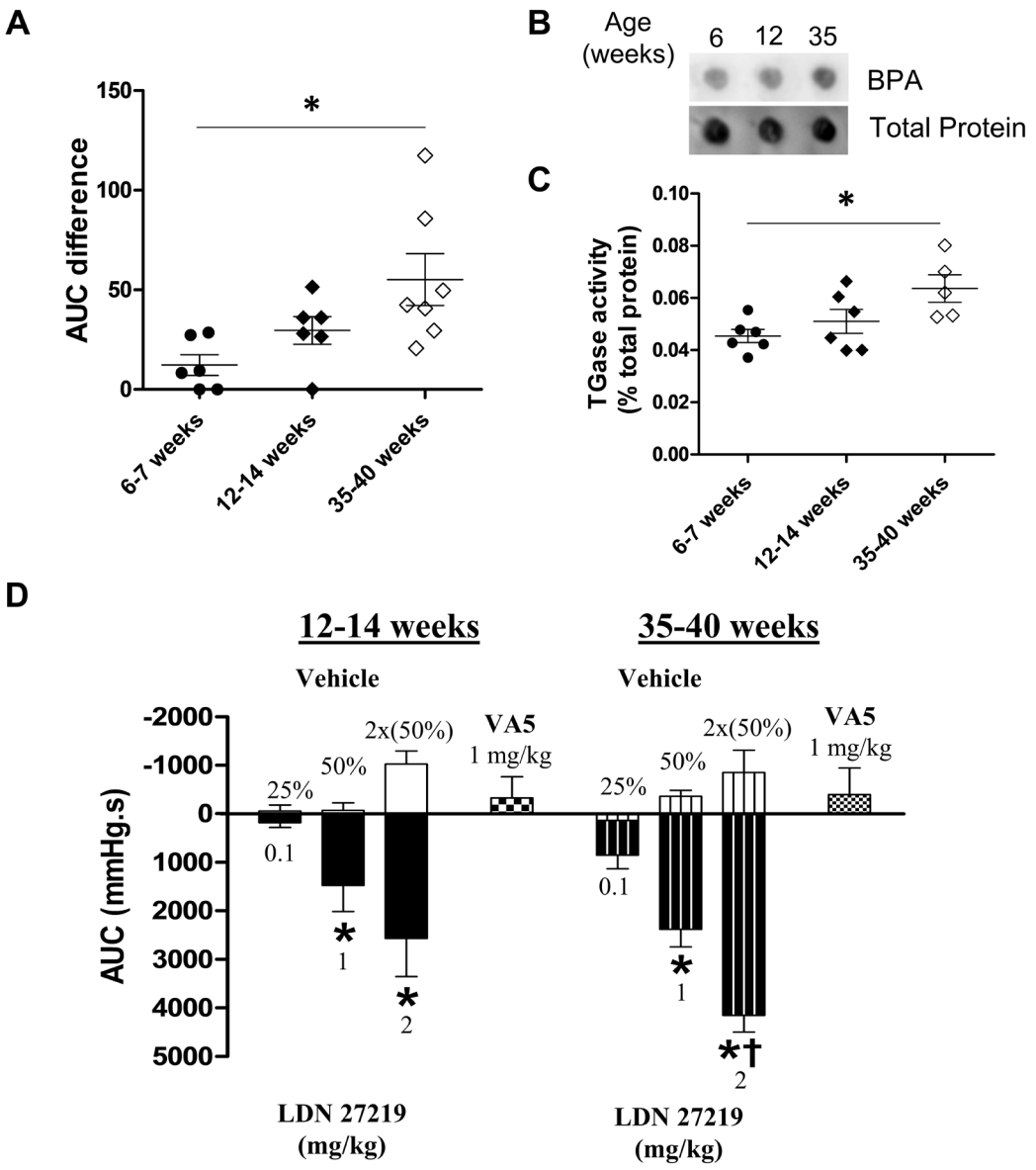


**Figure 8. Age-dependent blood pressure-lowering effects of TG2 modulation to its closed conformation *ex vivo* and *in vivo*. A.** Averaged differences in AUC of ACh-induced relaxations between arteries incubated with vehicle and arteries incubated with LDN 27219 ($10^{-6}$ mol/L) analyzed individually per rat. **B.** Representative dot blot of transamidase (TGase) activity measured as BPA incorporation in rat mesenteric arteries from the different age groups (upper panel) and amido-black staining of total protein corresponding to the blots in the upper panel (lower panel). **C.** Average transamidase activity, as % of total protein in small mesenteric arteries of each age group. Data are means ± SEM. *, $P < 0.05$ using one-way ANOVA with Bonferroni post-test. **D.** AUCs for the changes in blood pressure during 3 min infusion of either increasing doses of LDN 27219, increasing doses of the vehicle (PEG-400) or a single dose of VA5 for the different age groups. $n=5$-$8$. Data are means ± SEM of AUC (mmHg•s). Positive AUCs indicate blood pressure lowering, and negative AUCs indicate increases in blood pressure. *, $P < 0.05$ using two-way ANOVA with Bonferroni post-test compared to Vehicle. † $P < 0.05$ using two-way ANOVA with Bonferroni post-test compared to 12-14-week-old. (Modified from Manuscript I).

## 6.2 Effect of LDN 27219 on small-artery endothelial dysfunction in diabetes

The effect of acute TG2 conformational modulation on endothelial function was also studied in mesenteric arteries from male normoglycemic db/+ mice of different ages and diabetic db/db mice (for weights and blood glucose levels, see Manuscript II). From the 39-40-week-old db/+ mice group, 3 out of the 5 animals used for the study presented severe unilateral hydronephrosis. Vehicle-incubated arteries from db/+ animals presented a reduction in sensitivity to ACh with aging ($pD_{2\ 16\ weeks}$= 7.60 ± 0.08; $pD_{2\ 24\ weeks}$= 6.91 ± 0.08*; $pD_{2\ 39\ weeks}$= 6.49 ± 0.15*†. *, $P < 0.05$ using F-test compared to 16-17-week-old mice. † $P < 0.05$ using F-test compared to 24-25-week-old mice) and arteries from 39-40-week-old db/+ mice presented less maximal vasorelaxation to ACh ($Emax_{\ 16\ weeks}$= 83.67 ± 3.06; $Emax_{\ 24\ weeks}$= 87.25 ± 3.01; $pD_{2\ 39\ weeks}$= 24.62 ± 4.77*† in % of relaxation. *, $P < 0.05$ using F-test compared to 16-17-week-old mice. † $P < 0.05$ using F-test compared to 24-25-week-old mice). Arteries from 16-17-week-old diabetic db/db mice incubated with the vehicle also presented a reduced maximal relaxation to ACh compared to their db/+ counterparts ($Emax_{db/db}$= 25.71 ± 9.45. *, $P < 0.05$ using F-test compared to 16-17-week-old db/+ mice). Incubation during 20 min with LDN 27219 ($3x10^{-6}$ mol/L) failed to change the response to ACh in 16-week-old db/+ mice ($pD_{2\ LDN\ 27219}$= 7.73 ± 0.09) while it potentiated it in arteries from db/+ mice at 24-25 ($pD_{2\ LDN\ 27219}$= 7.31 ± 0.03. *, $P < 0.05$ using F-test compared to vehicle) and 39-40 weeks of age ($Emax_{\ LDN\ 27219}$= 59.28 ± 9.80 in % of relaxation. *, $P < 0.05$ using F-test compared to vehicle), as well as in arteries from 16-17-week-old db/db mice ($Emax_{\ LDN\ 27219}$= 59.23 ± 11.94 in % of relaxation. *, $P < 0.05$ using F-test compared to vehicle) (Figure 9A-D). The differences in AUC of ACh vasorelaxation between vehicle-incubated and LDN 27219-incubated arteries increased with the age of the animals. In contrast, the potentiation in arteries from 16-17-week-old db/db animals was not significantly different than in age-paired db/+ despite a strong tendency (Figure 9E). The potentiation of SNP vasorelaxation by LDN 27219 increased with age in db/+ mice and in diabetic db/db animals compare with age-paired db/+ (Figure 9F). These results confirm the age-dependency of the LDN 27219 effect observed previously in rats and suggest that LDN 27219 may also improve endothelial function in diabetes.

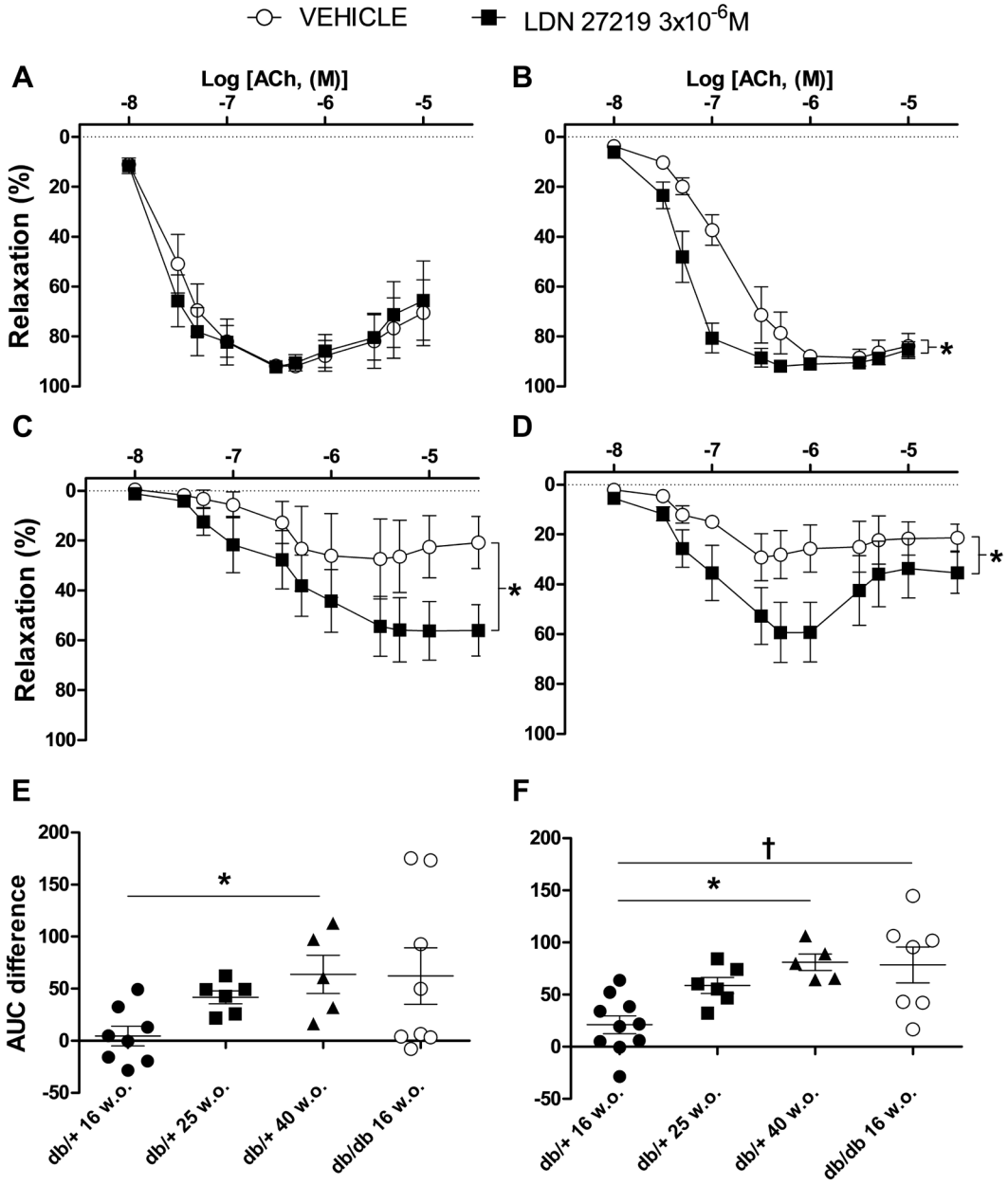


**Figure 9. Effect of LDN 27219 on age- and diabetes-related endothelial dysfunction in mice.** Average responses to ACh CRCs in Phe-contracted mesenteric arteries from db/+ mice at 16-17 (*n=8*) (**A**), 24-25 (*n=6*) (**B**) or 39-40 (*n=5*) (**C**) weeks of age or from 16-17-week-old diabetic db/db mice (n=8) (**D**) incubated with either vehicle (DMSO) or reversible TG2 inhibitor LDN 27219. Data are means ± SEM of % relaxation relative to maximum contraction. *, $P < 0.05$ using two-way ANOVA. **E.** Averaged differences in AUC of ACh-induced relaxations between vehicle-incubated and LDN 27219 ($3x10^{-6}$ mol/L)-incubated arteries analyzed individually per mice. **F.** Averaged differences in AUC of SNP-induced relaxations between vehicle-incubated and LDN 27219 ($3x10^{-6}$ mol/L)-incubated arteries analyzed individually per mice. *, $P < 0.05$ using one-way ANOVA with Bonferroni post-test. †, $P < 0.05$ using unpaired t-test. (Modified from Manuscript II).

Based on these observations, we explored the effect of long-term treatment with LDN 27219 on the onset of endothelial dysfunction in diabetic mice. At the moment of euthanasia before tissue collection, diabetic db/db mice at 10-11 weeks of age presented increased body weight and blood glucose levels compared to their age-paired db/+ counterparts. None of the treatments affected these parameters (for the development of body weight and blood sugar of the mice in the different treatment groups, see Manuscript II). By the end of the treatment, vehicle-treated diabetic db/db animals did not present elevated blood pressure compared to vehicle-treated normoglycemic db/+, and only db/db animals treated with AT1 receptor antagonist candesartan (3 mg/kg/24h) presented lower MAP, whereas treatment with LDN 27219 (8 mg/kg/24h) did not altered blood pressure ($MAP_{db/+\ Vehicle}$= 94.36 ± 7.25; $MAP_{db/db\ Vehicle}$= 90.03 ± 3.33; $MAP_{db/db\ Candesartan}$= 73.55 ± 6.07*; $MAP_{db/db\ LDN\ 27219}$= 95.75 ± 3.39 in mmHg. *, $P < 0.05$ using t-test compared to db/db vehicle) (Figure 10).

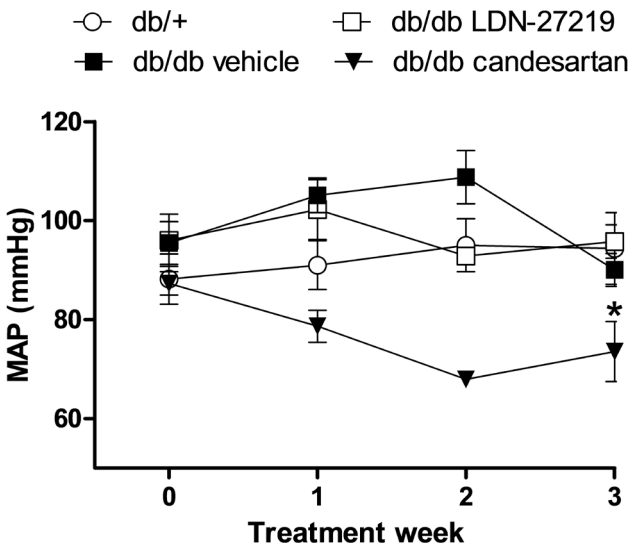


**Figure 10. Development of MAP in the mice in the different treatment groups during long-term treatment study.** Data are means ± SEM of MAP (mmHg), *n= 5-6*. *, $P < 0.05$ using t-test compared to vehicle in the third week of treatment. (Modified from Manuscript II).

Despite the absence of difference in MAP, aortic rings from vehicle-treated db/db animals presented increased maximal vasoconstriction to NA when compared to vehicle treated db/+ mice. In db/db mice, treatment with candesartan reduced the maximal vasoconstriction to NA, while treatment with LDN 27219 failed to significantly change it ($Emax_{db/+\ vehicle}$= 142.10 ± 11.56; $Emax_{db/db\ vehicle}$= 157.50 ± 5.15†; $Emax_{db/db\ candesartan}$= 124.40 ± 11.97*; $Emax_{db/db\ LDN\ 27219}$= 140.70 ± 10.73 in % of KPSS contraction. *, $P < 0.05$ using F-test compared to db/db vehicle. †, $P < 0.05$ using F-test compared to db/+ vehicle) (Figure 8A). Aortic rings from vehicle-treated db/db mice presented similar relaxation to ACh CRCs than rings from their db/+ counterparts, in db/db animals only treatment with candesartan slightly increased relaxation to ACh, although its change in potency ($pD_2$) did not reach significance ($pD_{2\ db/+\ vehicle}$ = 7.57 ± 0.08; $pD_{2\ db/db\ vehicle}$ = 7.34 ± 0.07;

$pD_{2\ db/db\ candesartan}$= 7.61 ± 0.21; $pD_{2\ db/db\ LDN\ 27219}$ = 7.37 ± 0.22) (Figure 11B). Endothelium-independent vasorelaxation, measured by response to SNP CRCs did not change among any of the groups ($pD_{2\ db/+\ vehicle}$ = 7.96 ± 0.06; $pD_{2\ db/db\ vehicle}$ = 7.92 ± 0.13; $pD_{2\ db/db\ candesartan}$= 8.07 ± 0.10; $pD_{2\ db/db\ LDN\ 27219}$ = 7.88 ± 0.17) (Figure 11C).

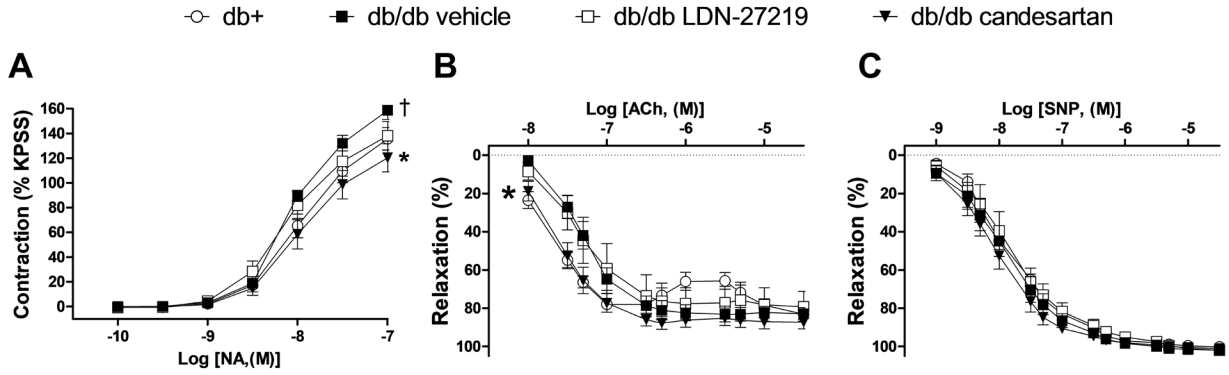


**Figure 11. Effect of long-term treatment with LDN 27219 in aortae from diabetic animals. A.** Average contractions to NA CRCs in aortic rings from mice of the different treatment groups. Data are means ± SEM of % of KPSS contraction, *n=6-12*. **B.** Average vasorelaxations to ACh CRCs in Phe-contracted aortic rings from mice of the different treatment groups, *n=5-12*. **C.** Average vasorelaxations to SNP CRCs in Phe-contracted aortic rings from mice of the different treatment groups, *n=8-12*. Data are means ± SEM of % relaxation relative to maximum contraction. †, $P < 0.05$ using two-way ANOVA compared to db/+. *, $P < 0.05$ using two-way ANOVA compared to db/db vehicle. (Modified from Manuscript II).

In contrast to aortae, small mesenteric arteries from vehicle-treated db/db mice presented slightly reduced contractile response to NA than mesenteric arteries from their db/+ counterparts. In db/db mice, treatment with candesartan slightly increased response to NA compared to vehicle, while treatment with LDN 27219 failed to change it. Despite these small differences, neither changes in $pD_2$ nor maximal constriction to NA were significant ($Emax_{\ db/+\ vehicle}$= 133.90 ± 3.79; $Emax_{\ db/db\ vehicle}$= 127.40 ± 7.41; $Emax_{\ db/db\ candesartan}$= 141.20 ± 5.29; $Emax_{\ db/db\ LDN\ 27219}$= 127.8 ± 7.143 in % of KPSS contraction) (Figure 12A). Arteries from vehicle-treated db/db mice showed reduced relaxation in response to ACh CRCs when compared with db/+ mice. Mesenteric arteries from db/db animals treated with candesartan showed a small improvement in vasorelaxation to ACh compared to arteries from vehicle-treated db/db, while arteries from mice treated with LDN 27219 maintained their response to ACh better than candesartan-treated animals ($Emax_{\ db/+\ vehicle}$= 82.03 ± 4.65; $Emax_{\ db/db\ vehicle}$= 23.08 ± 4.51†; $Emax_{\ db/db\ candesartan}$= 37.85 ± 5.19*; $Emax_{\ db/db\ LDN\ 27219}$= 58.49 ± 4.28*# in % of relaxation relative to maximum contraction. *, $P < 0.05$ using F-test compared to db/db vehicle. †, $P < 0.05$ using F-test compared to db/+ vehicle. #, $P < 0.05$ using F-test compared to db/db candesartan) (Figure 12B). On the other hand, the vasorelaxant response to SNP was not different in any of the treatment groups. ($pD_{2\ db/+\ vehicle}$ = 7.53 ± 0.07; $pD_{2\ db/db\ vehicle}$ = 8.12 ± 0.60; $pD_{2\ db/db\ candesartan}$= 7.30± 0.10; $pD_{2\ db/db\ LDN\ 27219}$ = 8.50 ± 2.22) (Figure 12C).

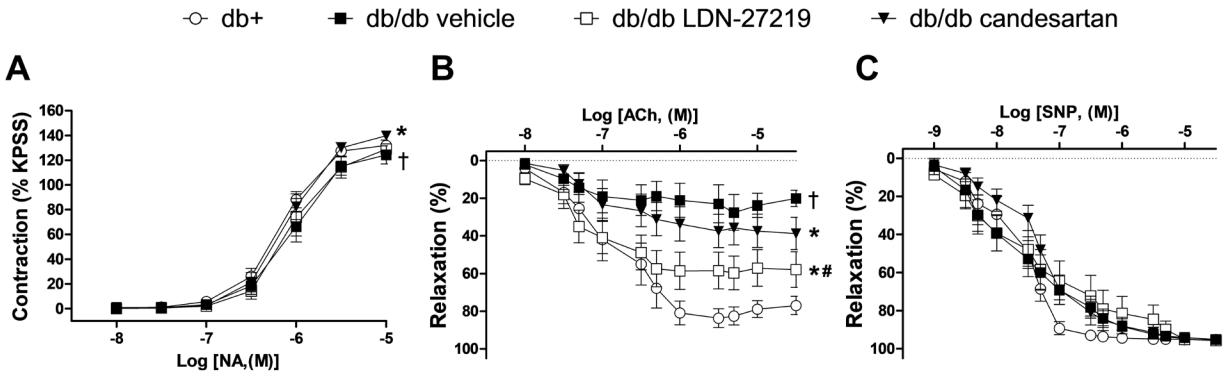


**Figure 12. Effect of long-term treatment with LDN 27219 in small mesenteric arteries from diabetic animals. A.** Average contractions to NA CRCs in mesenteric arteries from mice of the different treatment groups. Data are means ± SEM of % of KPSS contraction. **B.** Average vasorelaxations to ACh CRCs in Phe-contracted mesenteric arteries from mice of the different treatment groups. **C.** Average vasorelaxations to SNP CRCs in Phe-contracted mesenteric arteries from mice of the different treatment groups. Data are means ± SEM of % relaxation relative to maximum contraction, *n=10-11*. $^{\dagger}$, $P < 0.05$ using two-way ANOVA compared to db/+. *, $P < 0.05$ using two-way ANOVA compared to db/db vehicle. $^{\#}$, $P < 0.05$ using two-way ANOVA compared to db/db candesartan. (Modified from Manuscript II).

## 6.3 Characterization of calcium-activated potassium channels involved in the EDH response in rat intrarenal arteries

Isolated RIAECs exhibited a characteristic cobblestone morphology, while the cells in clusters presented a more irregular shape, with visible projections connecting neighbor RIAECs (Figure 13A, B). Concerning their passive electrophysiological properties, non-cultured isolated native RIAECs showed capacitances of 11.40 ± 0.295 pF (*n=10*) and resting membrane potentials of -67.95 ± 3.53 mV (*n=5*) under gap-free recording conditions in the whole-cell configuration. Under voltage-clamp conditions, application of a voltage-ramp (-100 to +120 mV. 600 msec., Vh= -50 mV) on isolated RIAECs activated voltage-dependent outward potassium currents that showed outward rectification at the more positive membrane potentials (Figure 13C, D).

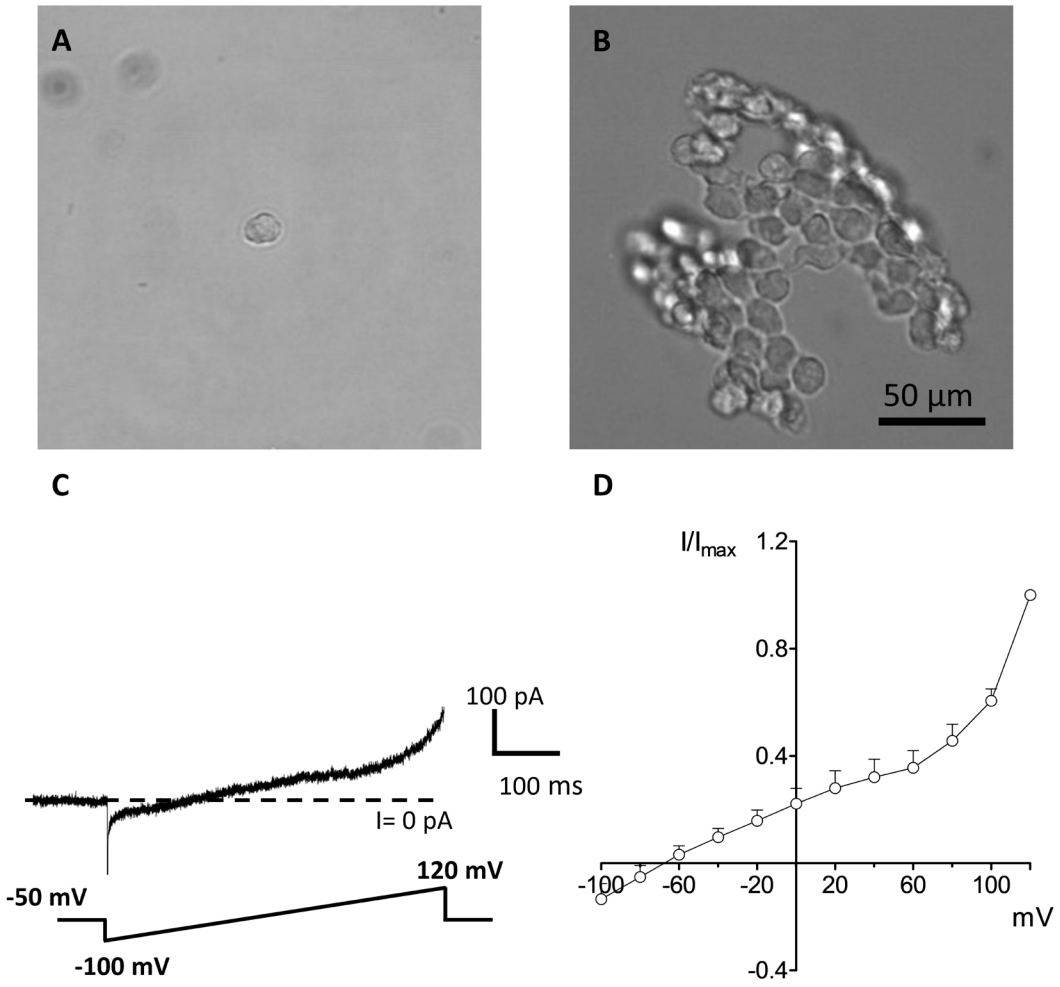


**Figure 13. Morphology of non-cultured, freshly isolated RIAECs and their potassium currents.** Microphotographs of isolated RIAEC (**A**) and clusters (**B**) obtained after enzymatic digestion. Bar: 50 µm. **C.** Representative potassium current in isolated native RIAEC evoked by voltage-ramps under control conditions. **D.** Average I-V relationships for potassium currents from the experiments shown in C. Data are means ± SEM of current amplitude normalized to the maximal amplitude of the current (I/Imax). *n=12*. (Modified from Manuscript III).

When ACh ($10^{-5}$ mol/L) was added to the extracellular solution, a sustained outwardly directed current with an amplitude of 61.29 ± 12.88 pA could be observed at the baseline (Vh=-50 mV) (Figure 14A, B). Subsequent application of a voltage ramp (-100 to +120 mV. 600 msec) increased the amplitude and changed in the shape of the outward currents when compared to those induced by the voltage ramp under control conditions. This change of shape included inward rectification of the currents at the more negative potentials (Figure 14A, B). To identify the calcium-activated potassium channels involved in response to ACh in RIAECs, we repeated the ramps after the cumulatively addition of different blockers for these channels. In the presence of IbTx ($10^{-7}$ mol/L), a blocker of $K_{Ca}1.1$ channels, significant inhibition of the ACh-induced currents at the more positive membrane potentials could be observed without a change neither in the resting outward current nor in the inward current at the more negative potentials. Addition of TRAM-34 ($10^{-6}$ mol/L), a blocker of $K_{Ca}3.1$ channels, blocked the voltage-independent component of the outward currents, as well as the resting outward current and the inward current at more negative potentials. Finally, the blocker of $K_{Ca}2$ channels UCL 1684 ($10^{-6}$ mol/L) significantly inhibited the remaining outward current (Figure 14C, D).

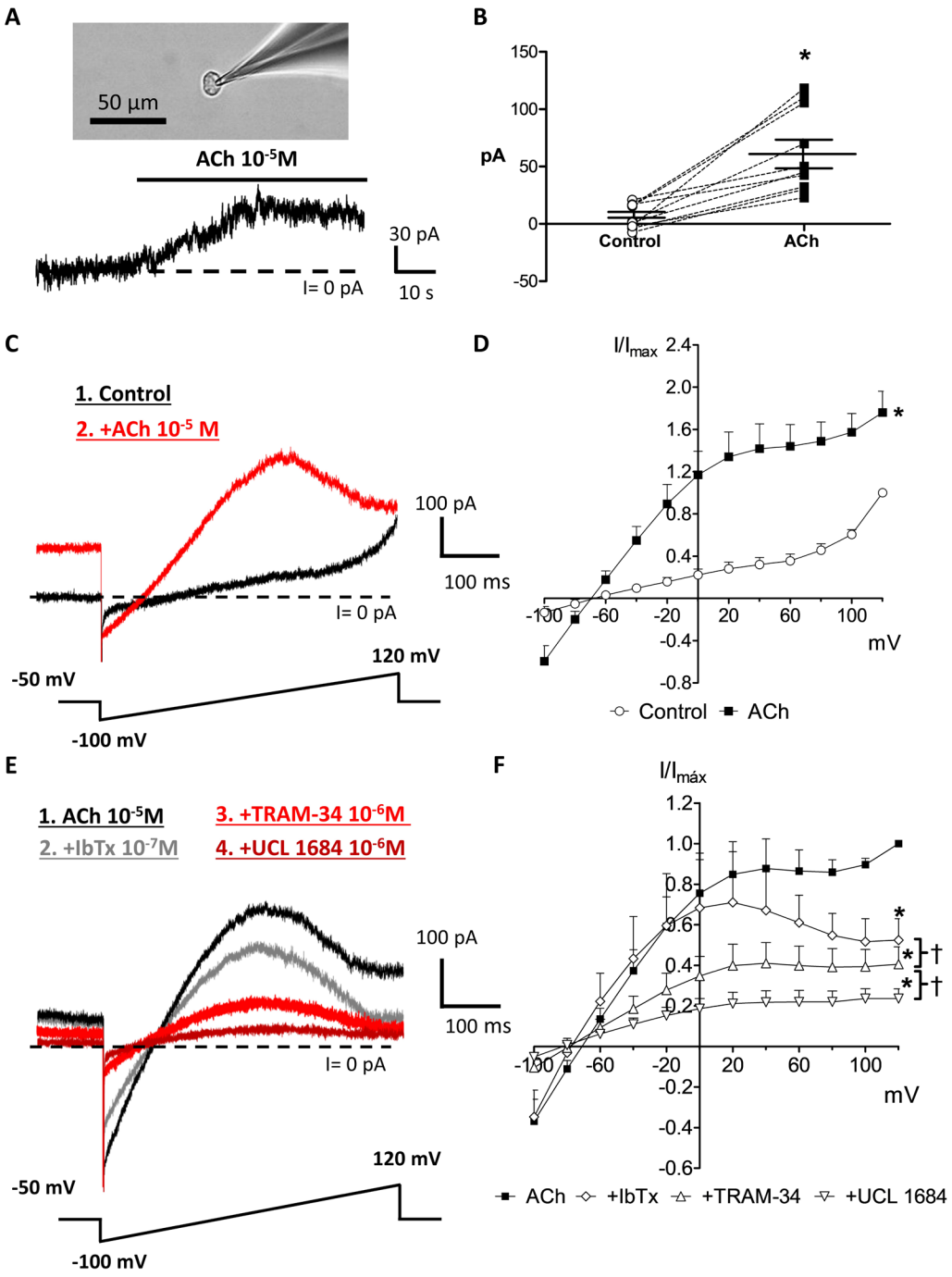


**Figure 14. Contribution of different calcium-activated potassium channels to the ACh-induced currents in RIAECs. A.** Microphotograph of isolated RIAEC under whole-cell configuration (top) and its baseline outward current at a holding potential of -50 mV before and during the addition of ACh to the extracellular solution (bottom). **B.** Average baseline outward currents of RIAECs at holding potential before and after the addition of ACh from the experiments shown in A. Data are means ± SEM. *, $P < 0.05$ using paired two-tailed Student´s t-test compared to control. **C.** Representative outward potassium currents evoked by voltage-ramps from -100 to +120 mV, 600 msec. Vh= -50 mV, in isolated RIAEC under control

conditions and after the addition of ACh to the extracellular solution. **D.** Averaged I-V relationships for potassium currents from the experiments shown in C. Data are means ± SEM of current amplitude normalized to the maximal amplitude of the current under control conditions ($I/I_{max}$). *, $P < 0.05$ using two-way ANOVA compared to control, *n=12*. **E.** Representative potassium currents in the presence of ACh before and after the cumulative addition of IbTx, TRAM-34 and UCL 1684, blockers of $K_{Ca}1.1$, $K_{Ca}3.1$ and $K_{Ca}2$, respectively. **F.** Averaged I-V relationships for $K^+$ currents from the experiments shown in E. Data are means ± SEM of current amplitude normalized to the maximal amplitude of the current after addition of ACh ($I/I_{max}$). *, $P < 0.05$ using two-way ANOVA compared to ACh. †, $P < 0.05$ using two-way ANOVA, *n=6-12*. (Modified from Manuscript III).

The expression of $K_{Ca}1.1$, $K_{Ca}3.1$ and $K_{Ca}2.3$ in RIAECs was confirmed by immunohistochemistry of isolated cells (Figure 15) as well as in tissue slices of the kidney containing intrarenal arteries (data not shown in summary, see Manuscript III). Additionally, staining of VWF was carried out to confirm the endothelial identity of the cells and staining of the cell nuclei was performed using DAPI.

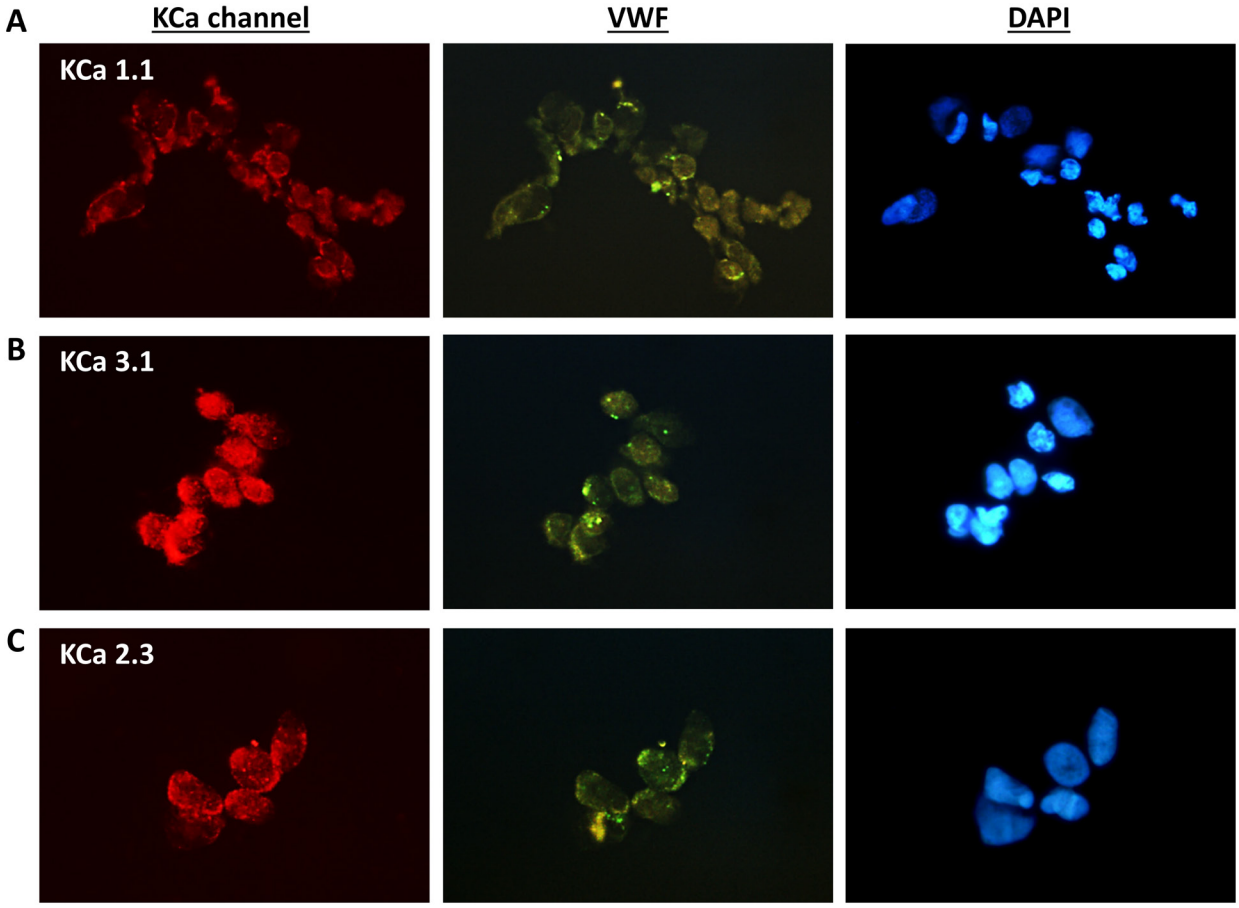


**Figure 15. Expression of calcium-activated potassium channels in freshly isolated RIAECs by immunofluorescence.** Representative pictures of clusters of RIAECs expressing $K_{Ca}1.1$ (**A**), $K_{Ca}3.1$ (**B**) and $K_{Ca}2.3$ (**C**) (left column), VWF (central column) and nuclear staining with DAPI (right column). (Modified from Manuscript III).

To examine the role of the different calcium-activated potassium channels in the EDH-type relaxation, isolated interlobar arteries were subjected to isometric tension measurements in the presence of L-NOARG ($10^{-6}$ mol/L) and indomethacin ($10^{-6}$ mol/L). Blockade of $K_{Ca}1.1$ by IbTx ($10^{-7}$ mol/L) reduced the maximal EDH-type relaxation induced by ACh CRCs ($Emax_{Vehicle}$= 57.45 ± 3.46 vs. $Emax_{IbTx}$= 33.40 ± 3.37 % of relaxation. *,*P < 0.05* using F-test) (Figure 16A,B). To investigate the functional role of $K_{Ca}1.1$ channels in the endothelium of interlobar arteries, CRCs of the specific positive modulator of $K_{Ca}1.1$ channels NS11021 were performed in arteries with and without endothelium under NOS and COX inhibition. NS11021 presented less potent vasorelaxant effects in arteries without endothelium ($PD_{2\ w\ endo}$= 5.40 ± 0.04 vs. $PD_{2\ w/o\ endo}$= 5.02 ± 0.03. *, *P < 0.05* using F-test) (Figure 16C,D) while this difference in potency was abolished in the presence of IbTx ($10^{-7}$ mol/L) ($PD_{2\ w\ endo\ +\ IbTx}$= 4.83 ± 0.03 vs. $PD_{2\ w/o\ endo\ +\ IbTx}$= 4.80 ± 0.03) (Figure 16E,F).

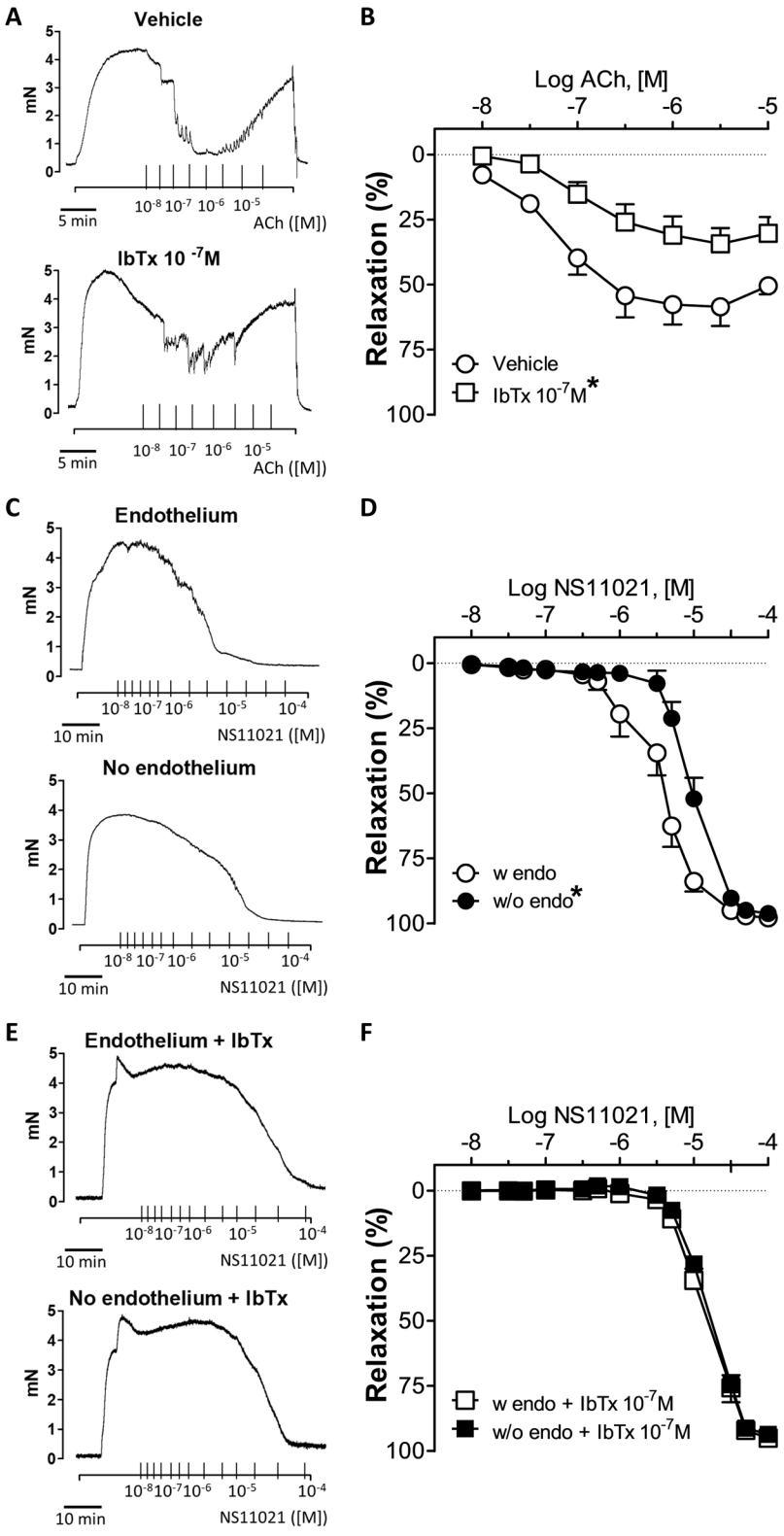


**Figure 16. Role of endothelial $K_{Ca}1.1$ channels in ACh and NS11021-induced EDH relaxation of rat interlobar arteries. A.** Representative traces showing vasorelaxation to ACh in Phe-contracted rat

interlobar arteries in the presence of either vehicle or IbTx, in conditions of NOS and COX inhibition by L-NOARG ($10^{-6}$mol/L) and indomethacin ($10^{-6}$mol/L), respectively. **B.** Averaged ACh CRCs from the experiments shown in A, *n=6*. **C.** Representative traces showing vasorelaxation induced by the $K_{Ca}1.1$ channel opener NS11021 in Phe-contracted rat interlobar arteries with or without endothelium in conditions of NOS and COX inhibition. **D.** Averaged CRCs from the experiments shown in C, *n = 8-9*. **E.** Representative traces showing NS11021-induced vasorelaxation in rat interlobar arteries contracted with Phe, with or without endothelium in conditions of $K_{Ca}1.1$ channel blockade with IbTx and inhibition of NOS and COX. **F.** Averaged CRCs, from the experiments shown in E, *n=6*. Data are means ± SEM of % of relaxation relative to maximum Phe contraction. *, *P<0.05* using two-way ANOVA compared to their respective controls. (Modified from Manuscript III).

Blockade of $K_{Ca}3.1$ channels by TRAM-34 ($10^{-6}$ mol/L) reduced the maximal vasorelaxation of interlobar arteries to ACh CRCs in conditions of NOS and COX inhibition (Emax $_{Vehicle}$= 58.96 ± 4.09 vs. Emax $_{TRAM-34}$= 33.70 ± 3.16 % of relaxation. *, $P < 0.05$ using F-test) (Figure 17A, B). Further, combined blockade of $K_{Ca}1.1$ and $K_{Ca}3.1$ by TRAM-34 ($10^{-6}$ mol/L) and IbTx ($10^{-7}$ mol/L) almost completely abolished relaxation to ACh in these arteries (Emax $_{Vehicle}$= 57.80 ± 4.03 vs. Emax $_{TRAM-34 + IbTx}$= 3.04 ± 10.42 % of relaxation. *, $P < 0.05$ using F-test) (Figure 17A, C).

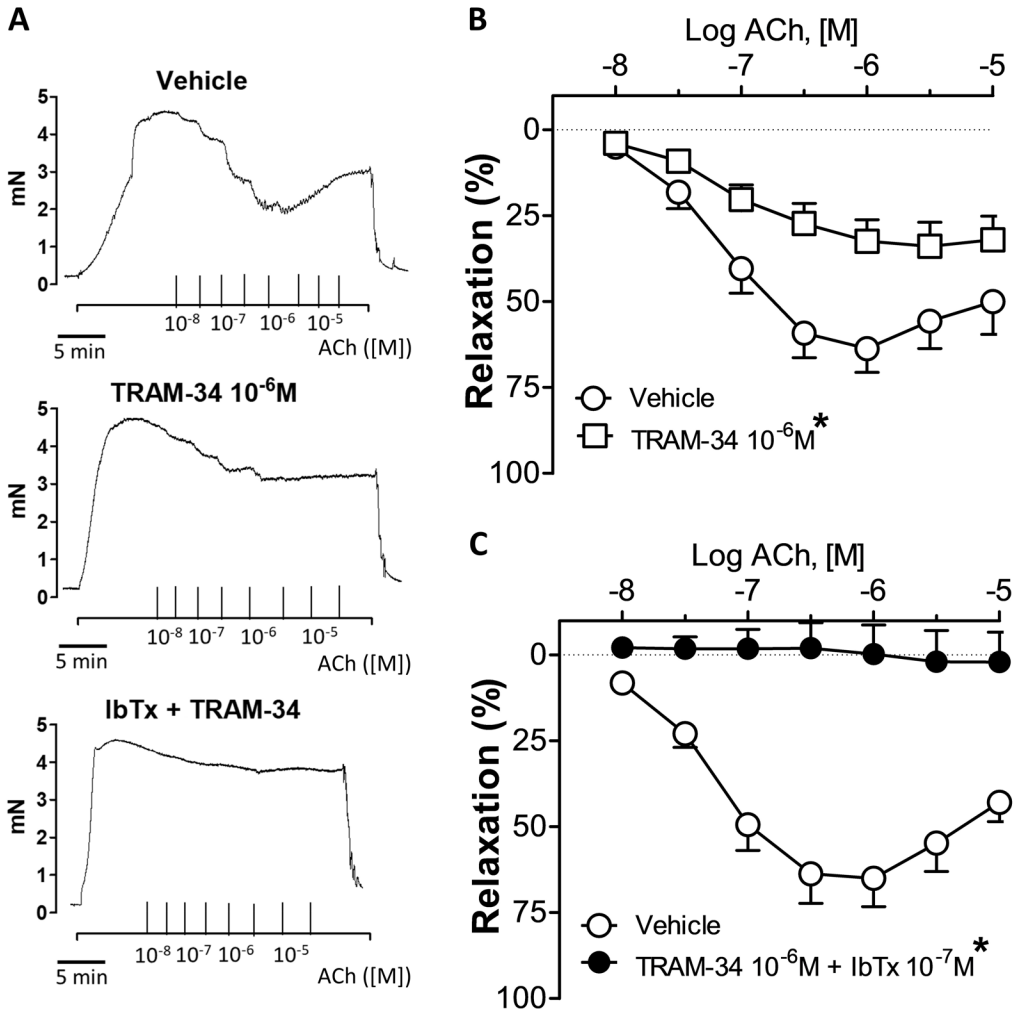


**Figure 17. Role of $K_{Ca}3.1$ channels in ACh-induced EDH relaxation of interlobar arteries. . A.** Representative traces of ACh-induced vasorelaxation in Phe-contracted rat interlobar arteries in the presence of either vehicle, TRAM-34 alone or a combination of TRAM-34 plus IbTx, in conditions of NOS and COX inhibition. **B.** Averaged CRCs in rat interlobar arteries, from the experiments shown in A in the presence of either vehicle or TRAM-34 alone*, n=6*. **C.** Averaged CRCs from the experiments shown in A in presence of either vehicle or a combination of TRAM-34 plus IbTx, *n=6*. Data are means ± SEM of % of relaxation relative to maximum Phe contraction. *, *P<0.05* using two-way ANOVA compared to vehicle.

Incubation with UCL 1684 ($10^{-6}$ mol/L), blocker of $K_{Ca}2$ channels, failed to change the EDH-induced vasorelaxation in rat interlobar arteries (Emax $_{Vehicle}$= 65.33 ± 4.31 vs. Emax $_{UCL\ 1684}$= 74.39 ± 4.58 % of relaxation) (Figure 18A, B). To confirm the presence of $K_{Ca}2.3$ channels in intrarenal arteries, CRCs of SKA-31, an opener of both $K_{Ca}3.1$ and $K_{Ca}2$ channels, were constructed in the presence of TRAM-34 ($10^{-6}$ mol/L) alone or in combination with UCL 1684 ($10^{-6}$ mol/L). $K_{Ca}2$ blockade by UCL 1684 reduced the vasorelaxant potency of SKA-31 in the presence of TRAM-34 ($PD_{2\ TRAM-34}$= 4.93 ± 0.06 vs. $PD_{2\ TRAM-34\ +\ UCL\ 1684}$= 4.59 ± 0.05. *, *P < 0.05* using F-test) (Figure 18C, D).

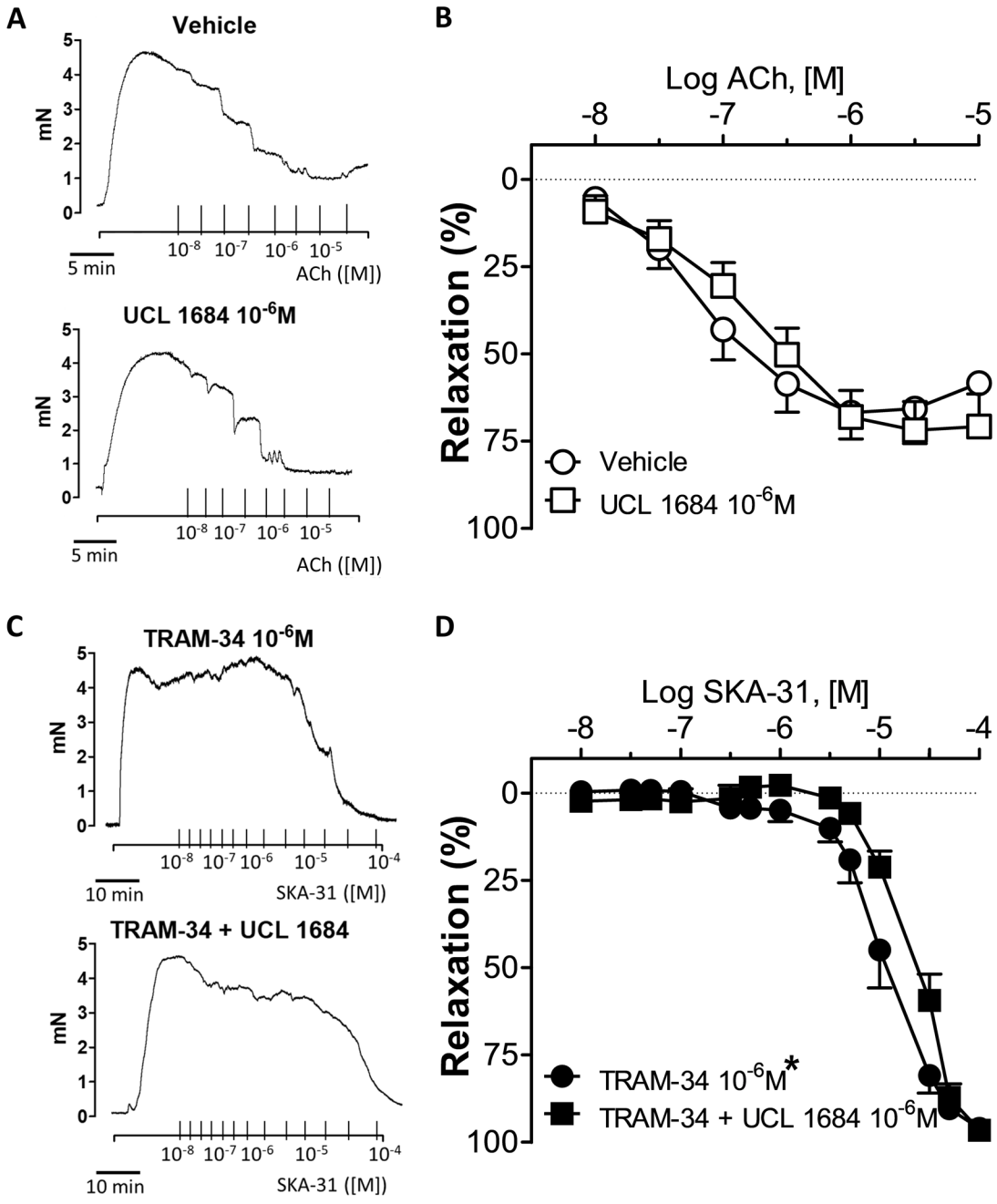


**Figure 18. Role of endothelial $K_{Ca}2.3$ channels in the EDH-type vasorelaxation of rat interlobar arteries. A.** Representative ACh-induced vasorelaxation in Phe-contracted rat interlobar arteries in the presence of either vehicle or UCL 1684 in conditions of NOS and COX inhibition. **B.** Averaged CRCs from the experiments shown in A, *n=6*. **C.** Representative traces of vasorelaxation induced by the $K_{Ca}3.1$ and $K_{Ca}2$ channel opener SKA-31 in Phe-contracted rat interlobar arteries in the presence of either TRAM-34 alone or a combination of TRAM-34 plus UCL 1684, in conditions of NOS and COX inhibition. **D.** Averaged CRCs from the experiments shown in C, *n=5*. Data are means ± SEM of % relaxation relative to maximum Phe contraction. *, *P<0.05* using a two-way ANOVA test compared to their respective controls.

# 7. DISCUSSION

## 7.1 Limitations

### 7.1.1 Limitations of TG2 conformational shift and activity studies

Native-PAGE studies in purified TG2 have demonstrated to be a useful approach to observe the conformational shift of the enzyme in response to different effectors (100,195), although the technique has important limitations. The incubation conditions and the presence of GTP and calcium are highly controlled in these experiments, being very different from the cellular context in which several effectors are present at the same time in different concentrations. This might explain why higher concentrations of LDN 27219, which is an allosteric inhibitor thought to be able to bind to different conformations of TG2 (24), are needed to observe an effect in conformation in the absence of other effectors- while lower concentrations of LDN 27219 show TG2-dependent effects in the arterial wall. To overcome these limitations, a mCerulean-TG2-eYFP FRET biosensor has been developed, so that when transfected into cultured cells and measured with fluorescence lifetime imaging microscopy (FLIM) allows for the measurement of the TG2 construct conformation in living cells (19,123). Although this method allows quantification of the conformational change of TG2 in a cellular context, it is costly, and the extent to which the mCerulean-TG2-eYFP construct presents different behavior than the native TG2 enzyme is currently unclear.

Transglutaminase activity assays, both *ex vivo* and *in vitro*, are normally based on measuring the transglutaminase-dependent incorporation of biotinylated substrates to other proteins using streptavidin conjugated with a reporter molecule to detect the biotin group. One of the main limitations of this technique is that the measured reaction is common to all transglutaminases, although a certain level of specificity to measure TG2 activity can be obtained using different substrates. The selection of substrates for *in vitro* testing, however, can affect the inhibitory kinetics and potency of some allosteric inhibitors, as it has been shown for LDN 27219 (24). The main advantage of the *in vitro* test used in our experiments is that it uses a substrate (pepT26) that has demonstrated a strong preference for TG2 compared to TG1, TG3, and Factor XIIIa (201). Samples for *in vitro* transamidase activity assays have to be protein extracts, in which TG2 is not present in its cellular context, which is essential for the regulation of its activity as previously discussed (see Figure 3).

Moreover, DTT is added in these assays to achieve maximal activation of transamidase activity in the sample at controlled calcium concentrations (202); this makes *in vitro* assays useful for inhibitor testing but does not inform of the transamidase activity of the sample in more physiological conditions. For these reasons, we used the BPA incorporation assay in arteries *ex vivo* to measure transglutaminase activity inhibition in a more physiological context, as well as to compare TG2 activation in samples from animals of different ages. This method is an accepted technique that has been widely used in different tissues and animal models (10,185). Although the

incorporation reaction in this assay takes place in a more physiological environment, with TG2 in a cellular and tissue contexts, it cannot be discarded that the stress caused to the arterial wall during tissue dissection might activate transglutaminase activity. Another limitation of this approach is the previously mentioned lack of specificity of BPA as a transglutaminase substrate (203). Therefore we cannot wholly discard that the activity of other transglutaminases may contribute to the signal we observe, even though we have only found the protein expression of TG2 in mesenteric arteries from Wistar Hannover rats (15). Additionally, some substrates, like biotinylated spermine, are poor probes for *in situ* measurements of TG2 transamidase activity in cells compared to BPA (204). These findings indicate that selection of substrates can also be a limitation when studying TG2 activity *ex vivo*, leading to over- or underrepresentation of its transamidase activity.

### 7.1.2 Animal model limitations

Although the use of small animals in cardiovascular research presents important limitations, particularly concerning cardiac function (205), murine models are well accepted for vascular research when studying regulation of vascular tone. Moreover, we validate our results with LDN 27219 in small arteries of mice and rats using subcutaneous arteries from human donors. Sex differences are important and a topic of growing interest in cardiovascular studies. One of the limitations of the present study is that we only used male rats and mice. Although half of the donors of human subcutaneous arteries were female, the study did not have enough power to analyze the influence of sex in the response to LDN 27219.

We study mice and rats of different ages to examine changes in endothelium-dependent and endothelium-independent vasorelaxation with aging. Although we did not use a model of accelerated aging, we were able to observe reduced relaxations in response to ACh and SNP in Wistar Hannover rats of 35-40 weeks of age, and in db/+ mice at 24-25 and 39-40 weeks of age compared to younger animals. These reductions in endothelium-dependent and independent vasorelaxation are consistent with the more aggravated changes observed by others as aging progress (1,28,49,55). It has to be noted that 3 out of 5 db/+ mice at 39-40 weeks of age used in our experiments presented severe unilateral hydronephrosis, despite not showing apparent symptoms of kidney disease. Although acquired hydronephrosis is not rare in laboratory mice during aging and usually the remaining kidney can compensate (206), we cannot exclude that, besides aging, other factors related to altered kidney function could play a role in the decrease of endothelium-dependent vasorelaxation in these mice.

As a model for endothelial dysfunction in diabetes, we used the db/db model, which presents a mutation in the leptin receptor, making the homozygous mice obese and hyperglycemic. This model presents important cardiovascular differences when compared to diabetic human patients, for example, it presents unaltered or even reduced systemic blood pressure, as well as reduced heart rate and systolic contractility, not making it a good model for the macrovascular complications of diabetes (207). There are conflicting reports concerning the structural remodeling

taking place in the peripheral circulation of db/db mice, with some studies showing outward remodeling, increased blood flow, and unchanged collagen content (208); and others showing inward remodeling, increased stiffness and fibrotic markers (209). However, numerous studies have described endothelial dysfunction in conductance and resistance arteries from db/db mice as young as 6-8 weeks of age and progressing with aging (210–214). They are, therefore considered a valid model for endothelial dysfunction and microvascular complications in diabetes.

### 7.1.3 Limitation of *ex vivo* vascular studies compared to *in vivo* results

The translation of *ex vivo* vascular results to *in vivo* is ambiguous, several factors are lost in the process of isolation of arteries or cells for their study and play an essential role in the control of vascular tone, the influence of the central nervous system being one of the most important ones. It should also be noted that changes in vascular tone were studied in isometric conditions. Although isometric myographs are accepted methods to study small vessels, and have shown generally good translatability, the results they offer can present substantial differences compared to the physiological state of arteries. Another approach is to mount arteries in isobaric pressure myographs (215). For these reasons, we measured the effect of TG2 inhibitors in the blood pressure *in vivo* on anesthetized animals, where we were able to validate the blood pressure lowering effects and age-dependency of the promotion of the closed TG2 conformation by LDN 27219 (see Figure 8). We cannot discard, however, that the intravenous anesthesia could be affecting the observed results.

To avoid the changes in ion channel expression that can take place during cell culture, which may influence the interpretation and translation of patch-clamp results (216,217), we used non-cultured, freshly isolated VSMCs and RIAECs for our studies. In the experiments related to Manuscript III, we obtained RIAECs of 10-15 μm in diameter with a characteristic cobblestone appearance, which is consistent with the morphology reported by other groups studying non-cultured, freshly isolated endothelial cells from other vascular beds, such as in rat small pulmonary arteries (218) and aortae (219). We also report a value of Em of -67.96 ± 3.53 mV (n=5) for isolated RIAECs, which is more hyperpolarized than what has been published by other groups in endothelial cells of different vascular beds, which Em varied from -15 to -52.4 mV (218,220–223). This difference in Em may be explained by the free calcium concentration ($10^{-6}$ mol/L) present in our intracellular solution to activate calcium-activated potassium channels, which most likely causes RIAECs hyperpolarization.

### 7.1.4 Pharmacological limitations

One of the most discussed limitations when using TG2 inhibitors to study the function of the enzyme is their selectivity. From the TG2 inhibitors that force the protein in its open conformation used in our study, Z-DON and Boc-DON show good selectivity for TG2, although they also inhibited TG1, TG3, and TG6 at working concentrations (189). At the same time, VA5 has not been directly tested. However, compounds of the VA5 family seem to possess high selectivity for

TG2, although they can inhibit Factor XIIIA (179,188). LDN 27219 has not been tested itself either, but some of its derivatives show similarly high selectivity for TG2 and TG3 (189). This is not surprising since LDN 27219 seems to bind at a GTP related site of the enzyme, and TG2 and TG3 have GTP binding activities. TG5 is another transglutaminase which has been shown to be modulated by GTP (104). Therefore, inhibition of TG5 by LDN 27219 cannot be discarded. As previously mentioned, in small mesenteric arteries from Wistar Hannover rats, only expression of TG1 and TG2 was found using PCR, although only TG2 protein was detected using western blotting (15). Moreover, the vascular effects of LDN 27219 both in isolated arteries and VSMCs were prevented by incubation with VA5 or Z-DON (See Figures 5 and 7), so it seems unlikely that the effects of LDN 27219 in our *ex vivo* experiments are due to off-target effects. Equally unlikely seems to be that the blood pressure lowering effects of LDN 27219 *in vivo* are due to its action on other transglutaminases, since TG3 and TG5 seems mainly present in the epidermis (224) as well as in the ear and testes of the rat (15). However, other off-target effects cannot be completely ruled out neither in these experiments nor in long-term multiple-dose studies.

As previously mentioned in the methods section, a single-dose pharmacokinetic study in C57BL/6 mice showed the half-life of LDN 27219 to be approximate 5 h. The posology for the three-week treatment study on db/db mice was based on these data, although the pharmacokinetic study was carried out in lean mice. As drug distribution and metabolism are known to change during obesity (225), particularly for lipophilic substances such as LDN 27219, it is highly likely that its half-life is substantially different in db/db mice. For several lipophilic drugs, it has been described how adipocytes can accumulate the substance and become slowly emptying reservoirs (226), this would increase the volume of distribution of the drug, leading to longer half-life but lower maximal plasma concentrations. However, this did not seem to affect the effect of LDN 27219 effect on endothelial function.

Despite the animals in the long-term study did not present any behavioral change, neither reduced weight nor any macroscopic alterations, and initial tests have shown low cytotoxicity for LDN 27219 derivatives (189), very little is known about the chronic toxicity of LDN 27219. Therefore, toxic effects of the three-week treatment cannot be discarded.

### 7.2 Main findings

The abundant expression of TG2 in the vasculature has led to different hypotheses concerning its role in vascular biology. Despite the first events where TG2 was shown to play a role are related to long-term remodeling processes such as increment of ECM stiffness, arterial inward remodeling and angiogenesis, its role in the short-term regulation of vascular tone has long been suspected. However, the exact mechanisms and the relevance of TG2 different conformational states have not been characterized to date.

Our findings link for the first time the closed conformation of TG2 with vasorelaxant and endothelium-dependent vasorelaxation potentiating effects, and suggest that increasing amounts

of TG2 in its open conformation during aging and diabetes could play a role in the decreased VSMC sensitivity to NO by reduced $K_{Ca}1.1$ channel gating.

Moreover, we characterize the calcium-activated potassium channels that are involved in the endothelium-dependent vasorelaxation of small intrarenal arteries from rats, showing expression of $K_{Ca}1.1$ channels in the endothelium and their controversial role in the EDH response.

### 7.2.1 Vascular effects of the pharmacological modulation of TG2 to its closed conformation in rats throughout the aging

The main findings of this study are that the closed conformation of TG2 has a vasorelaxant effect. Our results indicate that LDN 27219 by binding to TG2 promotes the closed conformation, leading to vasorelaxation both *ex vivo* in resistance arteries and to lowering of MAP *in vivo*. Incubation with LDN 27219 also induced potentiation of endothelium-dependent vasorelaxation by increasing VSMC sensitivity to NO through the opening of $K_{Ca}1.1$ channels. Contrarily, inhibitors that lock the open conformation of TG2 have neither direct effect on vascular wall tension nor blood pressure lowering effects *in vivo*, and they slightly reduce endothelium-dependent vasorelaxation and $K_{Ca}1.1$ channel opening. Moreover, we find an increased potentiation of endothelium-dependent vasorelaxation and decrease in blood pressure by LDN 27219 in older compared to younger rats and mice. These results suggest that an increased amount of TG2 in the open conformation may play a role in age-related endothelial dysfunction and that the modulation of TG2 towards closed conformation may be a suitable strategy to restore age-dependent changes in endothelial function.

As previously mentioned, LDN 27219 is a potent, slow-binding, reversible inhibitor that has been reported to dock at a GTP binding-related site of TG2 (24), and has been suggested to stabilize the closed conformation by *in silico* docking simulation (25). Native-PAGE studies have been previously used to study the conformational shift of TG2 (100,195), therefore our results provide direct evidence that LDN 27219 promotes the closed conformation of TG2. Moreover, the present results show an apparent endothelium-dependent vasorelaxation with LDN 27219 that involves the NO pathway (see Manuscript I). The vasorelaxation by LDN 27219 in human subcutaneous arteries suggests for the first time, to the best of our knowledge, that TG2 plays a vital role in the regulation of vascular tone in human arteries. Surprisingly, the more potent TG2 inhibitor Z-DON failed to change the tension of U46619-contracted small mesenteric arteries. This is despite it inhibits transglutaminase activity in arteries *ex vivo*. However, Z-DON has been shown to bind irreversibly to the active site of TG2 and seems to lock the enzyme in its open conformation, as suggested by its complex with TG2 in crystallization studies (22) and our conformation shift studies. These results indicate that the effect of TG2 in vascular tone is independent of its transamidase function and seem to be more related to its conformational state.

Previous patch-clamp studies have reported that, in the presence of GTP, TG2 was able to directly open $K_{Ca}1.1$ channels in VSMCs (128). Moreover, in a recent study, it has been shown that

endothelium-intact aortic rings from TG2 knockout mice are more sensitive to Phe-induced contraction than aortic rings from wild type mice, this difference being abolished in arteries without endothelium. The effect was also reversed by the addition of external TG2 independently of its transglutaminase activity (151). These findings support a potential role of TG2 in vasorelaxation and are in agreement with our current results in both human and rat arteries. We observed a potentiation of ACh-induced vasorelaxation after incubation with LDN 27219, which stabilizes the close conformation of TG2. In contrast, the cell-permeable irreversible inhibitors VA5 and Z-DON, which lock TG2 in the open conformation of TG2, had the opposite effect, reducing ACh-induced and SNP-induced vasorelaxations. Meanwhile, the non-permeable cell inhibitor Boc-DON failed to change ACh-induced vasorelaxation significantly. These results suggested a link between the closed conformation of intracellular TG2 and increased endothelium-dependent vasorelaxation, which is independent of the transamidase activity of the enzyme.

$K_{Ca}3.1$ and $K_{Ca}2.3$ channels are mainly expressed in the endothelium of rat small mesenteric arteries (227), and we observed that the effect of LDN 27219 on ACh-induced vasorelaxation was independent of these channels. In contrast, the inhibition of NOS by L-NOARG abolished the effect of LDN 27219 on ACh relaxation. In agreement with previously mentioned studies (128), we observed that the blockade of $K_{Ca}1.1$ channels by IbTx prevented the effect of LDN 27219 on endothelium-dependent relaxation. Taken together, these observations and the results on endothelium-denuded arteries showing that LDN 27219 incubation also increased SNP-induced vasorelaxation indicate that the effect of LDN 27219 is mainly at the vascular smooth muscle level and through $K_{Ca}1.1$ channel activation. Moreover, we found involvement of $K_{Ca}1.1$ channels and showed that the closed conformation of TG2 was responsible of channel opening using patch clamp recordings in isolated VSMCs. We showed that cells incubated with LDN 27219 presented similarly high potassium conductances to VSMCs measured with GTP in the intracellular solution. Additionally, LDN 27219 was not able to further increase potassium conductances in cells measured with intracellular GTP, suggesting a common mechanism of action. In contrast, arteries incubated with IbTx and VA5, presented smaller potassium conductances (see Figure 7) that were not sensitive to LDN 27219. These findings provide evidence that LDN 27219 through modulation of TG2 to the open conformation leads to opening of $K_{Ca}1.1$ channels in the vascular VSMCs, while inhibitors blocking TG2 in the open conformation has the opposite effect.

Although, in myograph-mounted arteries, blockade of $K_{Ca}1.1$ channels by IbTx abolished the effect of LDN 27219 on ACh-induced vasorelaxation, in our patch-clamp recordings, we observed a minor involvement of Kv7 channels in the LDN 27219-induced currents in VSMCs. This is consistent with previous results from our group that link the vasorelaxant effect of cystamine with Kv7 channel opening (15) and therefore, we cannot exclude their involvement in the vascular effects of LDN 27219.

Previous studies have shown that with aging, TG2 S-nitrosylation decreases leading to increased externalization of TG2 and over-activation of its transamidase activity, resulting in increased vascular stiffness in arteries from both rats and humans without changing TG2 protein expression

(9,10,151). This may be explained by a decrease in NO bioavailability with aging, as we also suggest since arteries from 35-40-week-old rats showed a decreased ACh- and SNP-induced vasorelaxation compared to younger rats. Accordingly, we found increased transamidase activity, without increases in TG2 expression; together with an increased potentiation of ACh-induced vasorelaxation by LDN 27219 in arteries from old animals (see Figure 8). These results suggest that an increased amount of TG2 in the open conformation due to decreased NO-bioavailability may play a role in early age-dependent changes in endothelial function, and that this can be alleviated by the modulation of TG2 to its closed conformation

Several more specific and active-site directed TG2 inhibitors, that supposedly lock the enzyme in its open conformation, have shown no effect on MAP nor heart rate when administered *in vivo* in mice (184,185,228). This is consistent with our results concerning VA5 infusion, which failed to change MAP in anesthetized rats. Contrarily, intravenous infusion of LDN 27219 dose-dependently decreased MAP in rats from all age groups, and in agreement with the potentiating effect *ex vivo*, this effect was bigger in the 35-40 weeks old rats than in the 12-14 weeks old rats. These findings support that the conformation of TG2 rather than the transamidase activity plays a role in the regulation of blood pressure and suggest a role for TG2 in early age-dependent changes of vascular function.

In conclusion, our study suggests that LDN 27219 is able to promote the closed conformation of TG2, and by this mechanism to open $K_{Ca}1.1$ channels in VSMCs leading to potentiation of endothelium-dependent vasorelaxation and lowering blood pressure as well. Moreover, these effects seem to increase with aging, suggesting that modulation of TG2 conformation could be a potential strategy to treat age-related changes in endothelial function.

### 7.2.2 *In vivo* treatment with a TG2 modulator for prevention of small artery endothelial dysfunction in diabetic mice

In the db/db model of diabetic and obese mice, we investigated the effect of acute treatment with LDN 27219 in diabetes-induced endothelial dysfunction. Additionally, we evaluated the effects of long-term LDN 27219 treatment to prevent endothelial dysfunction in db/db mice, compared with long-term treatment with an AT1 receptor antagonist (candesartan). Consistently with our previous results in rats, we observed age-dependent potentiation of ACh- and SNP-induced small artery vasorelaxation by LDN 27219 in normoglycemic db/+ mice of different ages. Additionally, we found a similar increase in LDN 27219-potentiation of endothelium-dependent and endothelium-independent vasorelaxation in arteries from diabetic db/db animals compared to their age-paired normoglycemic counterparts. Finally, we found that three-week treatment with IP injections of LDN 27219 was able to prevent endothelial dysfunction in db/db animals more effectively than treatment with candesartan, being this effect specific for small arteries.

As previously mentioned, reduced NO bioavailability during aging has been linked with increased TG2 externalization and activity in the vasculature (9,10,151), and we showed that in rats, this was

correlated with increased potentiation of ACh and SNP vasorelaxation by acute incubation with LDN 27219 in small arteries. Obesity and diabetes have been also linked with decreased NO synthesis, and therefore endothelial dysfunction in both humans and rodents (2). In this study, we found reduced sensitivity to ACh and SNP with aging and the same age-dependent effect of LDN 27219 in the potentiation of these responses in db/+ mice, as we previously described in rats. Additionally, we found decreased ACh- and SNP-induced vasorelaxation in arteries from diabetic mice, consistently with what has been observed by others (211,214), and an increased potentiation of those vasorelaxations by acute incubation with LDN 27219 compared to arteries from their normoglycemic counterparts. This suggests that similarly to aging, reduced NO bioavailability in diabetes and obesity could also lead to increases in the open conformation of TG2 in the vasculature. The increase in the open conformation could play a role in decreasing $K_{Ca}1.1$ channel activation and reducing relaxation to NO, being these alleviated by acute treatment with LDN 27219, which promotes the closed conformation of TG2.

Most interestingly, we observed a considerable variation of the data in the potentiation of ACh by LDN 27219 in arteries from diabetic animals (see Figure 9E), showing that in half of the arteries, LDN 27219 caused nearly no potentiation. In contrast, in the others, it presented a significant effect, resulting in a bimodal distribution of the data. Considering the poor basal endothelium-dependent vasorelaxation of these arteries, this could suggest that for LDN 27219 to exert a potentiating effect, a minimum level of NO production is needed. This idea seems to be supported by the change towards normality in the data distribution when the direct NO donor SNP was used (see Figure 9F).

The role of TG2 in glucose intolerance and insulin secretion is controversial, and conflicting results have been presented (141–143). During our three-week treatment study with LDN 27219 and candesartan in 7-8-week old mice, we observed increased weight and blood glucose in db/db compared to db/+ mice as previously reported, and none of the treatments caused a significant change in these parameters. Even though we did not explore glucose tolerance specifically, our results seem to indicate that TG2 inhibition was not sufficient to alter glucose metabolism at a systemic level.

Diabetic db/db mice have been previously reported to present similar or even reduced MAP when compared to their heterozygous littermates (207,208). Accordingly, we found no difference in MAP measured in the conscious animals between vehicle-treated db/db mice and vehicle-treated db/+ mice, and only treatment with candesartan reduced MAP significantly in db/db mice. We showed previously that LDN 27219 lowered MAP in anesthetized rats, which suggests that conscious and normotensive db/db mice might be able to compensate for the blood pressure-lowering effect of LDN 27219 during long-term administration. Another possible explanation for this might be the difference in pharmacokinetics between lean and obese animals, which could translate to reduced plasma concentrations of LDN 27219 in db/db animals as discussed in the Pharmacological limitations section.

Several studies in conductance and resistance arteries from diabetic mice and patients have shown that AT1 receptor inhibitors, which are used in the clinic to treat cardiovascular complications in diabetes, reduce sensitivity to vasoconstrictors and improve endothelium-dependent vasorelaxation (229,230). Consistently with these results, we found that long-term treatment with candesartan was able to reduce vasoconstriction to NA in aortae from db/db mice, which presented increased aortic sensitivity to this vasoconstrictor compared with their db/+ littermates. Candesartan also increased ACh-induced vasorelaxation in aortae from db/db mice and prevented endothelial dysfunction in resistance arteries of these animals. Surprisingly, we found no statistically significant endothelial dysfunction in aortae from db/db animals despite a marked tendency in this direction. These result differ from the previous literature finding endothelial dysfunction in aortae from db/db mice of approximately this age (210), and could be explained by the reduced glycemia of the mice used in our experiments.

Previous studies have also demonstrated the role of TG2 transamidase activity in endothelial cell apoptosis (12,14) and increased endothelial leakage in diabetes (13), and have shown that pharmacological inhibition or genetic silencing of TG2 were able to prevent these processes. However, the effects of TG2 inhibition in the preservation of endothelium-dependent vasorelaxation have not been previously explored. We observed that treatment with LDN 27219 prevented endothelial dysfunction in small mesenteric arteries more effectively than candesartan, although it had no significant effect in aortae. Surprisingly, the vasorelaxation to SNP was unaltered by long-term treatment with LDN 27219 and unaffected in db/db animals. These results suggest that preservation of the endothelium-dependent vasorelaxation by long-term treatment with LDN 27219 acts by a different mechanism than the opening of $K_{Ca}1.1$ channels described in rats during acute incubation of isolated arteries. This mechanism might be related with the previously mentioned decrease in endothelial cell death induced by TG2 inhibitors (12–14).

In conclusion, our long-term results suggest a specific effect in the prevention of endothelial dysfunction by LDN 27219 in resistance arteries. This could be explained by the reduced harm in the endothelium of large arteries from these animals, but might also be evidence of the less important role of TG2 in the remodeling of large arteries, which has been shown in other pathophysiological states such as hypertension (150).

### 7.2.3 Calcium-activated potassium channels in the intrarenal EDH response in rats

With the perspective of using TG2 modulators in kidney diseases that could benefit from additional vasoprotection, we examined RIAECs and interlobar arteries to characterize the potassium channels involved in preglomerular endothelium-dependent vasorelaxation. The main findings of this study are that $K_{Ca}1.1$, $K_{Ca}3.1$, and $K_{Ca}2.3$ channels are expressed in the endothelium of intrarenal arteries. However only $K_{Ca}1.1$ and $K_{Ca}3.1$ channels played a role in EDH-type relaxation on renal interlobar arteries ex vivo under isometric conditions.

While the presence of $K_{Ca}3.1$ and $K_{Ca}2.3$ channels in endothelial cells of intrarenal arteries has been extensively reported by others (231–235), the expression of $K_{Ca}1.1$ currents has been found only in the endothelium of larger porcine renal arteries by inside-out patch-clamp experiments (42). In smaller intrarenal arteries, immunofluorescence experiments detected $K_{Ca}1.1$ channel protein in endothelial cells from mouse preglomerular arterioles (43), but its functional role remains unclear. In isolated RIAECs, we observed ACh-activated potassium currents that were blocked by the consecutive addition of blockers of $K_{Ca}1.1$, $K_{Ca}3.1$ and $K_{Ca}2$ channels (Figure 14). Iberiotoxin-sensitive currents were mainly present at the more depolarized potentials and were voltage-dependent, while TRAM-34- and UCL 1684-sensitive currents were voltage-independent. In addition, TRAM-34-sensitive currents presented an inward rectification at more negative voltages that has been previously described as characteristic of $K_{Ca}3.1$ channels (236,237). Our results suggest that $K_{Ca}1.1$, $K_{Ca}3.1$ and $K_{Ca}2.3$ channels are functionally expressed in the endothelium of RIAECs and participate in ACh-induced hyperpolarization of endothelial cells. The expression of the proteins of these channels in the endothelium was confirmed by immunohistochemistry both in isolated RIAECs and in renal tissue slices containing intrarenal arteries.

Several animal models and preparations *ex vivo* as well as *in vivo* has been used to investigate the role of the EDH in intrarenal vasodilation. However, the role of the different calcium-activated potassium channels, particularly of $K_{Ca}1.1$ channels, remains controversial. Hence, IbTx decreased the relaxation induced by EDH in rat small renal arteries under isometric conditions and NOS inhibition, although the location of these channels was not addressed in the study (238). However, $10^{-3}$ mol/L tetraethylammonium (TEA) failed to change the EDH-type response in arteries from rat hydronephrotic kidneys under isobaric conditions, casting a doubt about the role of $K_{Ca}1.1$ channels at least in a pathological state (82). Moreover, several studies have shown the inhibitory effect of charybdotoxin (ChTx), which inhibits both $K_{Ca}1.1$ and $K_{Ca}3.1$ channels- on EDH-induced vasorelaxation of isolated preglomerular arteries from different species including humans (231,235,239–242), which could also indicate a role for $K_{Ca}1.1$ channels. *In vivo* experiments addressing the role of $K_{Ca}1.1$ in the renal circulation have also shown contradicting results. While the infusion of IbTx in rats neither reduced the renal blood flow under resting conditions nor changed the renal response to vasoconstrictors, a reduction of renal blood flow was observed after infusion of $10^{-3}$ mol/L of TEA under similar experimental conditions in the same study (243) as well as in others (43). As TEA at that concentration is considered to be relatively specific for $K_{Ca}1.1$ channels, these results seem to contradict the lack of effect of IbTx. However, this discrepancy might be explained by the short pre-treatment time (4-5 min) with IbTx in Magnusson et al. (243), which could be insufficient to achieve maximum blockade of $K_{Ca}1.1$ channels considering the slow-binding kinetics of the peptide (244,245) that usually requires much longer incubation times even in *ex vivo* experiments. On the other hand, TEA has fast-binding kinetics (244,246) that could achieve $K_{Ca}1.1$ channel blockade in the same incubation period. However, the involvement of other potassium channels in the TEA-induced reduction of renal blood flow cannot be ruled out.

Most importantly, experiments in these studies cannot discriminate between $K_{Ca}1.1$ channels expressed in the endothelium or in VSMCs, informing only of the overall contribution of these channels in renal circulation. In our study, we observe that $K_{Ca}1.1$ channels blockade with IbTx was able to reduce the EDH-induced vasorelaxation on rat interlobar arteries mounted in isometric myographs, under conditions of NOS and COX inhibition. Moreover, we showed that the vasorelaxation induced by the selective $K_{Ca}1.1$ channel opener NS11021 was larger in arteries with intact endothelium compared to those without endothelium, and that this difference was abolished after incubation with IbTx (see Figure 16). These result demonstrated the functional expression of $K_{Ca}1.1$ channels in the endothelium of interlobar arteries, which was also confirmed by immunohistochemistry. However, $H_2O_2$ has been shown to induce vasorelaxation in human coronary arterioles indirectly activating $K_{Ca}1.1$ channels in VSMCs (247), and in previous work we shown that $H_2O_2$ acts as an hyperpolarizing factor mediating intrarenal artery relaxation to ACh under NOS and COX inhibition (248). Therefore, we cannot exclude that the opening of $K_{Ca}1.1$ channels by $H_2O_2$ in VSMC may contribute to the EDH-induced vasorelaxation of intrarenal arteries.

The role of $K_{Ca}3.1$ and $K_{Ca}2.3$ channels in the renovascular EDH response has been studied mainly in combined blockade with other channels. The unspecific calcium-activated potassium channel blocker ChTx either alone (82,239–241) or in combination with the $K_{Ca}2$ blocker apamin (231,235,242) has been shown to reduce EDH-induced vasorelaxation in intrarenal arteries. These result support the importance of calcium-activated potassium channels in the intrarenal EDH response, but do not allow discrimination between channel subtypes. The more specific blocker of $K_{Ca}3.1$ channels, TRAM-34 has been used recently in combination with apamin, reducing the vasorelaxation induced by EDH in myograph-mounted rat and mice renal interlobar arteries under isometric conditions (232,249). Still, the individual contribution of the $K_{Ca}3.1$ and $K_{Ca}2$ channels was not assessed in these studies. In small renal arteries from rats and pigs under isometric conditions, ChTx plus apamin induced an additional reduction of the EDH-mediated vasorelaxation compared to ChTx alone (240,250), although inhibition with apamin alone failed to change the EDH response (250), suggesting a minor role for $K_{Ca}2.3$ channels only detectable when $K_{Ca}1.1$ and $K_{Ca}3.1$ were blocked. This is consistent with *in vivo* experiments where infusion of apamin alone did not change renal blood flow by itself under resting conditions, requiring a combined inhibition of several potassium channels to observe an effect (43). This is consistent with our results, where inhibition of $K_{Ca}2$ channels with UCL 1684 alone did not change EDH vasorelaxation despite these channels being functionally expressed in the endothelium as demonstrated by the patch-clamp studies and by relaxation to SKA-31.

Another potential reason why we did not observe an effect of $K_{Ca}2$ channel inhibition is related to its specific functions and subcellular location. $K_{Ca}2.3$ channels are expressed in endothelial cells near homocellular gap junctions and in the caveolae (251), which could indicate that the primary role for these channels is in the vasodilation associated with mechanosensation or other processes related to the caveolae, including NO release, that cannot be observed under our isometric

experimental conditions and NOS inhibition (252–254). Although the opening of both $K_{Ca}3.1$ and $K_{Ca}2.3$ channel has been linked to NO release (200,255), experiments using $K_{Ca}2.3$ and $K_{Ca}3.1$ channel knock-out mice showed that genetic deletion of $K_{Ca}2.3$ reduced shear stress-induced dilator responses and ACh-induced vasodilation with intact NO synthesis in small arteries under isobaric conditions, but failed to change it under NOS and COX inhibition. Contrarily, genetic deletion of $K_{Ca}3.1$ significantly reduced EDH-type response under NOS and COX inhibition (256), supporting a differential role of these channels.

Results *in vivo* addressing the role of $K_{Ca}3.1$ and $K_{Ca}2.3$ in renal EDH-type relaxation seem to support our results suggesting a major role of both $K_{Ca}1.1$ and $K_{Ca}3.1$ channels, since inhibition with ChTx plus apamin significantly inhibited the ACh-induced increase of renal blood flow under NOS and COX inhibition in streptozotocin-induced diabetic Wistar rats (257), while infusion of the more specific $K_{Ca}3.1$ blocker TRAM-34 plus apamin failed to significantly change it in Sprague-Dawley rats in a similar setting, although there was a tendency in that direction (232).

In summary, we show in this study that $K_{Ca}1.1$, $K_{Ca}3.1$ and $K_{Ca}2.3$ channels are functionally expressed in the freshly isolated RIAECs and mediate endothelial cell hyperpolarization. However, only $K_{Ca}1.1$ and $K_{Ca}3.1$ seem to play a significant role in the EDH-induced vasorelaxation of these arteries in isometric conditions, suggesting that $K_{Ca}2.3$ channels might be important for other processes that cannot be observed in our experimental conditions, such as NO release or shear stress-induced vasodilation. The results of this study elucidated the role of $K_{Ca}1.1$ channels in the endothelium of the preglomerular circulation, and suggest that positive modulation of these channels might be an effective strategy to improve renovascular endothelium-dependent vasorelaxation.

## 8. CONCLUSIONS

The present Ph.D. project was based on the hypothesis that TG2 modulation can improve endothelium-dependent vasorelaxation through the opening of potassium channels and, therefore, be an effective strategy for the prevention of endothelial dysfunction in aging and diabetes; conditions with increased vascular levels of TG2 in the open conformation. Furthermore, we aimed to characterize the potassium channels involved in the EDH response in the intrarenal circulation.

The main findings of our project were:

1- The reversible TG2 inhibitor LDN 27219 stabilizes the closed conformation of TG2 and inhibits its transamidase activity in resistance arteries.

2- Promotion of the closed conformation of TG2 by LDN 27219 in arteries *ex vivo* results in a direct vasorelaxant effect and potentiates endothelium-dependent vasorelaxation by increasing the sensitivity of VSMCs to NO, through the opening of $K_{Ca}1.1$ channels.

3- The potentiation of endothelium-dependent vasorelaxation by LDN 27219 increases with aging. This correlates with increased transamidase activity levels in the vasculature of aging subjects, which could indicate higher amounts of TG2 in the open conformation.

4- *In vivo*, infusion of LDN 27219 dose-dependently lowers MAP, increasing this effect with the age of the animal.

5- TG2 inhibitors that lock the enzyme in its opening conformation, reduce endothelium-dependent vasorelaxation and opening of potassium channels, and failed to change MAP *in vivo*.

6- The potentiation of endothelium-dependent vasorelaxation by LDN 27219 also increases in arteries from diabetic mice compared with those from normoglycemic control mice.

7- Long-term treatment with LDN 27219 administered IP prevents small artery endothelial dysfunction in pre-diabetic animals more effectively than oral candesartan, without affecting blood pressure or SNP-induced vasorelaxation.

8- In the preglomerular renal circulation $K_{Ca}1.1$, $K_{Ca}3.1$ and $K_{Ca}2.3$ channels are functionally expressed in the endothelium of rat intrarenal arteries and they are activated upon muscarinic stimulation with ACh.

9- $K_{Ca}1.1$ and $K_{Ca}3.1$ play a major role in EDH-derived vasorelaxation of intrarenal arteries, whereas blockade of $K_{Ca}2$ channels failed to change ACh-induced vasorelaxation.

In summary, we find that modulation of TG2 to its closed conformation is a promising new strategy to counteract changes in endothelial function of small vessels resulting from aging and diabetes, in which increased amounts of TG2 in the open conformation could play a role in the reduced vascular sensitivity to NO by decreasing $K_{Ca}1.1$ opening. Additionally, $K_{Ca}1.1$ channels are a potential new target to improve endothelium-dependent vasorelaxation in the preglomerular circulation.

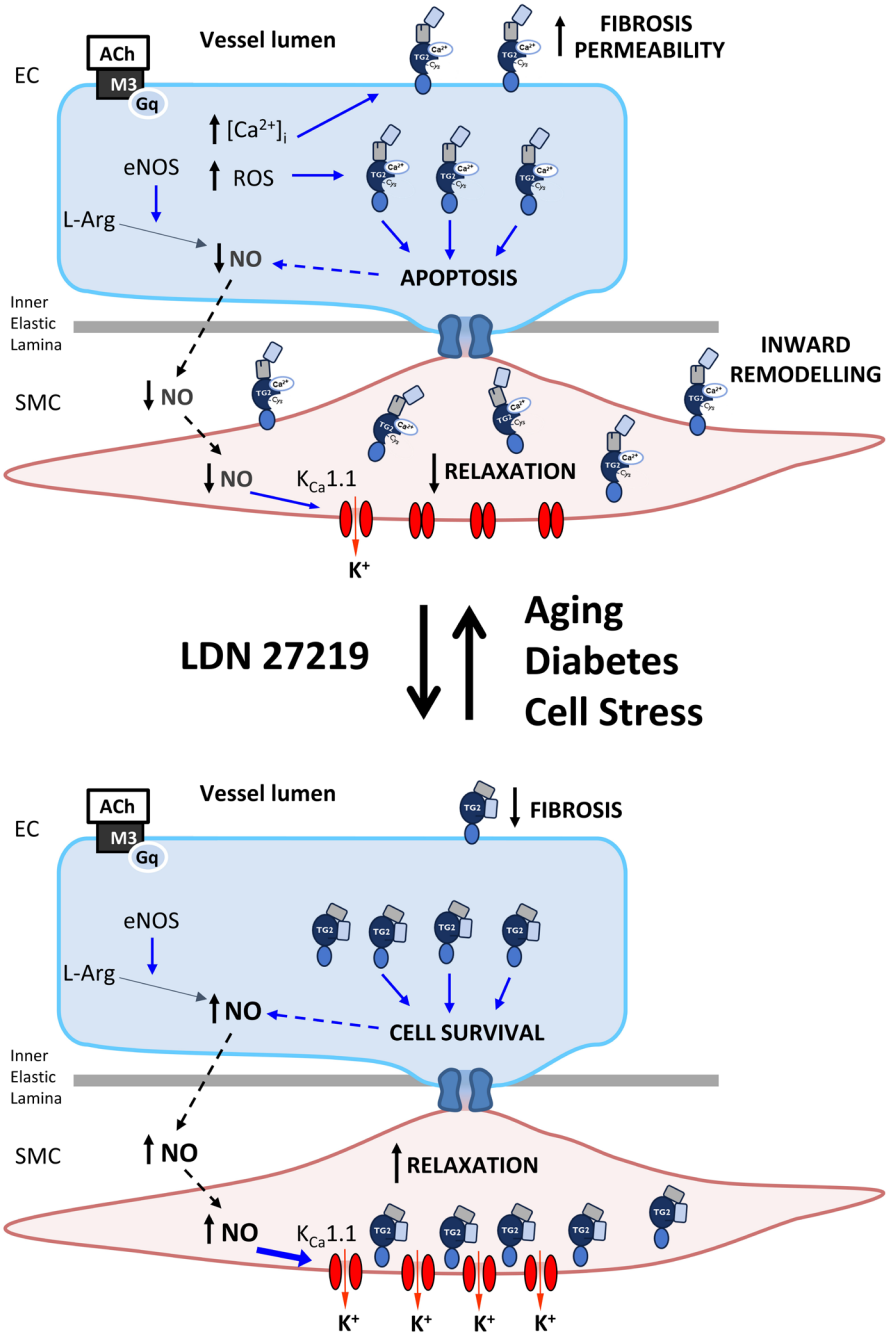


**Figure 19. Proposed model for the role of TG2 conformation in vascular dysfunction during aging and diabetes.**

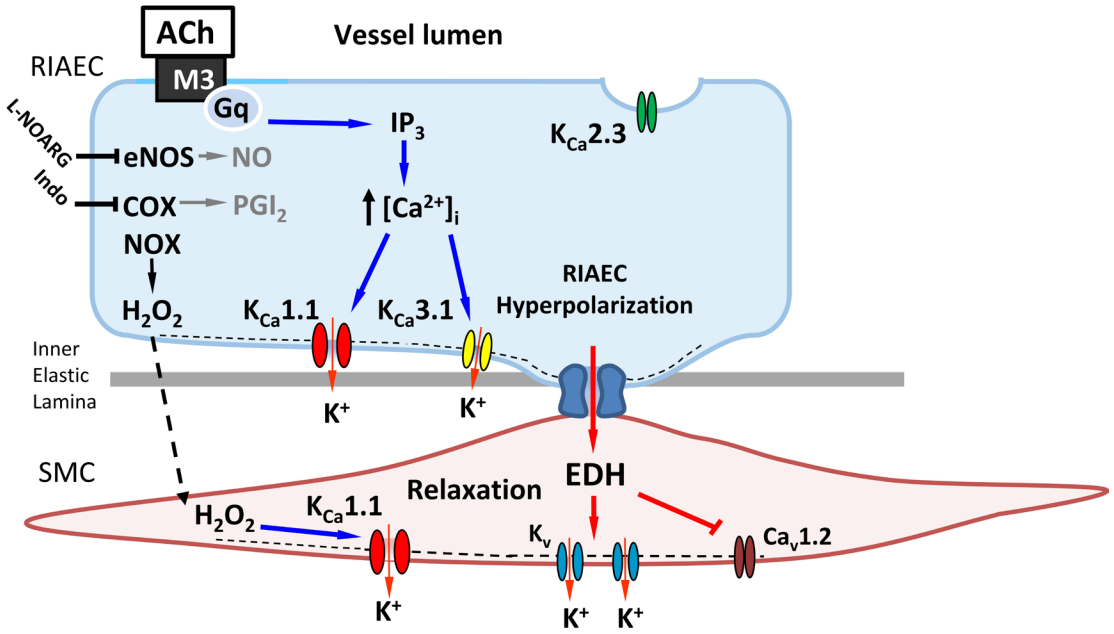


**Figure 20. Scheme describing the suggested involvement of $K_{Ca}1.1$ and $K_{Ca}3.1$ in the EDH (e.g. $H_2O_2$ and myoendothelial gap junctions)-induced vasorelaxation of intrarenal arteries.**

## 9. PERSPECTIVES

We have shown that pharmacological modulation of TG2 to its closed conformation inhibits transamidase activity and offers additional vasoprotection compared to other mechanisms of TG2 inhibition. Moreover, we outline the possibility of using TG2 inhibitors that stabilize the closed conformation in fibrotic kidney diseases. Other TG2 inhibitors lacking a vasoprotective effects have demonstrated efficacy in fibrotic kidney diseases. An additional benefit of inhibitors stabilizing the closed conformation are expected due to their effect improving endothelium-dependent vasorelaxation through $K_{Ca}1.1$ channel modulation. This could be particularly interesting considering the strong dependence of the preglomerular endothelial function on $K_{Ca}1.1$ channels. Considering this potential synergy between the antifibrotic effect of transglutaminase activity inhibition and the vasoprotection resulting from the closed conformation, it would be interesting to explore the long-term application of TG2 inhibitors stabilizing the closed conformation for fibrotic diseases, e.g. CKD and pulmonary hypertension.

Although the conformation of TG2 has been shown to be of great importance in several pathophysiological processes, and its modulation has demonstrated to be a promising therapeutic strategy, very little is known about the value of TG2 as a biomarker especially in cardiovascular diseases. The use of irreversible TG2 inhibitors as positron emission tomography (PET) tracers has been recently proposed as a potential tool to study TG2 conformation *in vivo*, particularly in cancer (258,259). However, these irreversible inhibitors are known to force the enzyme into the open conformation and, therefore, cannot inform of the natural conformational state of the enzyme *in vivo*, although they might be useful for the detection of extracellular TG2. Our work suggest that a negative feedback loop might exist between NO and the open conformation of TG2. Thus, it has been previously shown that reduced NO bioavailability in the vascular system leads to increased externalization and activation of TG2 in its open conformation (9,10,151). On the other hand, we show that increased amounts of TG2 in its open conformation might lead to lower $K_{Ca}1.1$ channel opening in the VSMC with the consequent loss of NO-dependent vasorelaxation, even before endothelial dysfunction becomes apparent. This idea implies that the amount of TG2 in the open conformation in the resistance vasculature will increase with aging and diabetes and could be correlated with increased risk of microvascular complications. To address this hypothesis, it would be interesting to combine the use of PET tracers to study externalization of TG2 *in vivo* with the examination of vasoreactivity in resistance arteries *ex vivo* in diabetic mice/patients. For the moment, we plan to carry out extensive studies in resistance arteries from human patients in order explore the relationship between the diabetic state, aging, elevated transamidase activity, vascular function and sensitivity to TG2 inhibitors.

With this thesis, we elucidated the role of the different conformation of TG2 in the regulation of vascular tone. However, a lot of work is yet to be done to understand the complex role of TG2 in the cardiovascular system. Its elusive and varied externalization mechanisms (120) and its emerging role in inflammation and autophagy (18) seem a promising development for the field of TG2 research, which hopefully will continue to be fruitful and exciting in the upcoming years.

Particularly relevant for our findings in this thesis is the very recent association between the transamidase activity of TG2 and O-GlcNAcylation of proteins, which suggests an important role of TG2 in glucose metabolism at the cellular level (144). This fits well with recent reports on the importance of TG2 activation in the sustained damage on the endothelium of diabetic animals even after successful glycemic normalization (14), and makes the effect of TG2 modulators on post-translational modification of proteins in diabetes an interesting direction for future research.

Finally, at the moment of publication of this thesis, two TG2-targeted therapies are in clinical trials, suggesting that years of basic research on this enzyme might soon translate into a benefit for the patients. Considering the translational potential of the present work, which has led to a patent application, we plan to continue the development of acylhydrazide inhibitors to promote the closed conformation of TG2, studying their potential toxicity, target selectivity and developing scalable screening assays focused on the enzyme conformation.

## 10. BIBLIOGRAPHY


1. Higashi Y, Kihara Y, Noma K. Endothelial dysfunction and hypertension in aging. *Hypertens Res*. 2012;**35**:1039–1047

2. Shi Y, Vanhoutte PM. Macro- and microvascular endothelial dysfunction in diabetes. J Diabetes. 2017;**9**:434–449

3. Eckert RL, Kaartinen MT, Nurminskaya M, Belkin AM, Colak G, Johnson GVW et al. Transglutaminase regulation of cell function. *Physiol Rev*. 2014;**94**:383–417

4. Nurminskaya M V., Belkin AM. Cellular Functions of Tissue Transglutaminase. *Int Rev Cell Mol Biol*. 2012;**294**:1–97

5. Sane DC, Kontos JL, Greenberg CS. Roles of transglutaminases in cardiac and vascular diseases. *Front Biosci*. 2007;**12**:2530–2545

6. Bakker ENTP, Buus CL, Spaan JAE, Perree J, Ganga A, Rolf TM et al. Small Artery Remodeling Depends on Tissue-Type Transglutaminase. *Circ Res*. 2004;**96**:119–126

7. Bakker ENTP, Pistea A, Spaan JAE, Rolf T, De Vries CJ, Van Rooijen N et al. Flow-dependent remodeling of small arteries in mice deficient for tissue-type transglutaminase: Possible compensation by macrophage-derived factor XIII. *Circ Res*. 2006;**99**:86–92

8. van den Akker J, VanBavel E, van Geel R, Matlung HL, Guvenc Tuna B, Janssen GMC et al. The redox state of transglutaminase 2 controls arterial remodeling. *PLoS One*. 2011;**6**:e23067

9. Santhanam L, Tuday EC, Webb AK, Dowzicky P, Kim JH, Oh YJ et al. Decreased S-nitrosylation of tissue transglutaminase contributes to age-related increases in vascular stiffness. *Circ Res*. 2010;**107**:117–125

10. Jandu SK, Webb AK, Pak A, Sevinc B, Nyhan D, Belkin AM et al. Nitric oxide regulates tissue transglutaminase localization and function in the vasculature. *Amino Acids*. 2013;**44**:261–269

11. Steppan J, Bergman Y, Viegas K, Armstrong D, Tan S, Wang H et al. Tissue Transglutaminase Modulates Vascular Stiffness and Function Through Crosslinking-Dependent and Crosslinking-Independent Functions. *J Am Heart Assoc*. 2017;**6**:e004161

12. Bhatt MP, Lim Y-C, Hwang J, Na S, Kim Y-M, Ha K-S. C-Peptide Prevents Hyperglycemia-Induced Endothelial Apoptosis Through Inhibition of Reactive Oxygen Species-Mediated Transglutaminase 2 Activation. *Diabetes*. 2013;**62**:243–253

13. Lee Y-J, Jung S-H, Kim S-HS-Y, Kim M-S, Lee S, Hwang J et al. Essential Role of Transglutaminase 2 in Vascular Endothelial Growth Factor–Induced Vascular Leakage in the Retina of Diabetic Mice. *Diabetes*. 2016;**65**:2414–2428

14. Lee J-YY, Lee Y-JJ, Jeon H-YY, Han E-TT, Park WS, Hong S-HH et al. The vicious cycle between transglutaminase 2 and reactive oxygen species in hyperglycemic memory–induced endothelial dysfunction. *FASEB J*. 2019;**33**:12655–12667

15. Engholm M, Pinilla E, Mogensen S, Matchkov V, Hedegaard ER, Chen H et al. Involvement of transglutaminase 2 and voltage-gated potassium channels in cystamine vasodilatation in rat mesenteric small arteries. *Br J Pharmacol*. 2016;**173**:839–855

16. Johnson TS, Fisher M, Haylor JL, Hau Z, Skill NJ, Jones R et al. Transglutaminase inhibition reduces fibrosis and preserves function in experimental chronic kidney disease. *J Am Soc Nephrol*. 2007;**18**:3078–3088

17. Huang L, Haylor JL, Hau Z, Jones RA, Vickers ME, Wagner B et al. Transglutaminase inhibition ameliorates experimental diabetic nephropathy. *Kidney Int*. 2009;**76**:383–394

18. Tatsukawa H, Furutani Y, Hitomi K, Kojima S. Transglutaminase 2 has opposing roles in the regulation of cellular functions as well as cell growth and death. *Cell Death Dis*. 2016;**7**:1–12

19. Kerr C, Szmacinski H, Fisher ML, Nance B, Lakowicz JR, Akbar A et al. Transamidase site-targeted agents alter the conformation of the transglutaminase cancer stem cell survival protein to reduce GTP binding activity and cancer stem cell survival. *Oncogene*. 2017;**36**:2981–2990

20. Keillor JW, Apperley KYP. Transglutaminase inhibitors: a patent review. *Expert Opin Ther Pat*. 2016;**26**:49–63

21. Mironov GG, Clouthier CM, Akbar A, Keillor JW, Berezovski M V. Simultaneous analysis of enzyme structure and activity by kinetic capillary electrophoresis-MS. *Nat Chem Biol*. 2016;**12**:918–922

22. Lindemann I, Heine A, Klebe G. Transglutaminase 2 in complex with a novel inhibitor. *PDB ID 3S3J*.;:10.2210/pdb3S3J/pdb

23. Duval E, Case A, Stein RL, Cuny GD. Structure-activity relationship study of novel tissue transglutaminase inhibitors. *Bioorganic Med Chem Lett*. 2005;**15**:1885–1889

24. Case A, Stein RL. Kinetic analysis of the interaction of tissue transglutaminase with a nonpeptidic slow-binding inhibitor. *Biochemistry*. 2007;**46**:1106–1115

25. Fisher O. *Subcloning, Enzymatic Characterization, and in silico Docking of Transglutaminase 2*. 2009http://hdl.handle.net/10192/23253

26. Michel CC, Curry FE. Microvascular permeability. *Physiol Rev*. 1999;**79**:703–761

27. Michiels C. Endothelial cell functions. *J Cell Physiol*. 2003;**196**:430–443

28. Vanhoutte PM, Shimokawa H, Feletou M, Tang EHC. Endothelial dysfunction and

vascular disease – a 30th anniversary update. *Acta Physiol*. 2017;**219**:22–96

29. Mistry DK, Garland CJ. Nitric oxide (NO)-induced activation of large conductance Ca2+-dependent K+ channels (BK(Ca)) in smooth muscle cells isolated from the rat mesenteric artery. *Br J Pharmacol*. 1998;**124**:1131–1140

30. Archer SL, Huang JMC, Hampl V, Nelson DP, Shultz PJ, Weir EK. Nitric oxide and cGMP cause vasorelaxation by activation of a charybdotoxin-sensitive K channel by cGMP-dependent protein kinase. *Proc Natl Acad Sci U S A*. 1994;**91**:7583–7587

31. Shimokawa H, Yasutake H, Fujii K, Owada MK, Nakaike R, Fukumoto Y et al. The importance of the hyperpolarizing mechanism increases as the vessel size decreases in endothelium-dependent relaxations in rat mesenteric circulation. *J Cardiovasc Pharmacol*. 1996;**28**:703–711

32. Tomioka H, Hattori Y, Fukao M, Sato A, Liu MY, Sakuma I et al. Relaxation in different-sized rat blood vessels mediated by endothelium- derived hyperpolarizing factor: Importance of processes mediating precontractions. *J Vasc Res*. 1999;**36**:311–320

33. Ellinsworth DC, Sandow SL, Shukla N, Liu Y, Jeremy JY, Gutterman DD. Endothelium-Derived Hyperpolarization and Coronary Vasodilation: Diverse and Integrated Roles of Epoxyeicosatrienoic Acids, Hydrogen Peroxide, and Gap Junctions. *Microcirculation*. 2016;**23**:15–32

34. Garland CJ, Dora KA. EDH: endothelium-dependent hyperpolarization and microvascular signalling. *Acta Physiol*. 2017;**219**:152–161

35. Chauhan SD, Nilsson H, Ahluwalia A, Hobbs AJ. Release of C-type natriuretic peptide accounts for the biological activity of endothelium-derived hyperpolarizing factor. *Proc Natl Acad Sci U S A*. 2003;**100**:1426–1431

36. Kun A, Kiraly I, Pataricza J, Marton Z, Krassoi I, Varro A et al. C-Type natriuretic peptide hyperpolarizes and relaxes human penile resistance arteries. *J Sex Med*. 2008;**5**:1114–1125

37. Edwards G, Dora KA, Gardener MJ, Garland CJ, Weston AH. K+ is an endothelium-derived hyperpolarizing factor in rat arteries. *Nature*. 1998;**396**:269–272

38. Köhler R, Oliván-Viguera A, Wulff H. Endothelial Small- and Intermediate-Conductance K Channels and Endothelium-Dependent Hyperpolarization as Drug Targets in Cardiovascular Disease. *Adv Pharmacol*. 2016;**77**:65–104

39. Jiang Z, Wallner M, Meera P, Toro L. Human and rodent MaxiK channel β-subunit genes: Cloning and characterization. *Genomics*. 1999;**55**:57–67

40. Jackson WF, Blair KL. Characterization and function of Ca2+ -activated K+ channels in arteriolar muscle cells. *Am J Physiol - Heart Circ Physiol*. 1998;**274**:27–34

41. Hill MA, Yang Y, Ella SR, Davis MJ, Braun AP. Large conductance, Ca2+-activated K+ channels (BKCa) and arteriolar myogenic signaling. *FEBS Lett*. 2010;**584**:2033–2042

42. Brakemeier S, Eichler I, Knorr A, Fassheber T, Köhler R, Hoyer J. Modulation of Ca 2+-activated K+ channel in renal artery endothelium in situ by nitric oxide and reactive oxygen species. *Kidney Int*. 2003;**64**:199–207

43. Sorensen CM, Giese I, Braunstein TH, Holstein-Rathlou NH, Salomonsson M. Closure of multiple types of K + channels is necessary to induce changes in renal vascular resistance in vivo in rats. *Pflugers Arch Eur J Physiol*. 2011;**462**:655–667

44. Vanhoutte PM, Luscher TF, Graser T. Endothelium-dependent contractions. In: *Blood Vessels*. 1991: 74–83.

45. Flammer AJ, Anderson T, Celermajer DS, Creager MA, Deanfield J, Ganz P et al. The assessment of endothelial function: From research into clinical practice. *Circulation*. 2012;**126**:753–767

46. Deanfield JE, Halcox JP, Rabelink TJ. Endothelial function and dysfunction: Testing and clinical relevance. *Circulation*. 2007;**115**:1285–1295

47. Suwaidi J Al, Hamasaki S, Higano ST, Nishimura RA, Holmes DR, Lerman A. Long-term follow-up of patients with mild coronary artery disease and endothelial dysfunction. *Circulation*. 2000;**101**:948–954

48. Schächinger V, Britten MB, Zeiher AM. Prognostic impact of coronary vasodilator dysfunction on adverse long- term outcome of coronary heart disease. *Circulation*. 2000;**101**:1899–1906

49. Kong BWC, Man RYK, Gao Y, Vanhoutte PM, Leung SWS. Reduced activity of SKCa and Na-K ATPase underlies the accelerated impairment of EDH-type relaxations in mesenteric arteries of aging spontaneously hypertensive rats. *Pharmacol Res Perspect*. 2015;**3**:1–11

50. Santhanam L, Lim HK, Lim HK, Miriel V, Brown T, Patel M et al. Inducible NO synthase-dependent S-nitrosylation and activation of arginase1 contribute to age-related endothelial dysfunction. *Circ Res*. 2007;**101**:692–702

51. Ng HH, Jelinic M, Parry LJ, Leo CH. Increased superoxide production and altered nitric oxide-mediated relaxation in the aorta of young but not old male relaxin-deficient mice. *Am J Physiol - Heart Circ Physiol*. 2015;**309**:H285–H296

52. Csiszar A, Ungvari Z, Edwards JG, Kaminski P, Wolin MS, Koller A et al. Aging-induced phenotypic changes and oxidative stress impair coronary arteriolar function. *Circ Res*. 2002;**90**:1159–1166

53. Lesniewski LA, Durrant JR, Connell ML, Folian BJ, Donate AJ, Seals DR. Salicylate treatment improves age-associated vascular endothelial dysfunction: Potential role of

nuclear factor κb and forkhead box o phosphorylation. *Journals Gerontol - Ser A Biol Sci Med Sci*. 2011;**66 A**:409–418

54. Higashi Y, Sasaki S, Nakagawa K, Kimura M, Noma K, Hara K et al. Tetrahydrobiopterin improves aging-related impairment of endothelium-dependent vasodilation through increase in nitric oxide production. *Atherosclerosis*. 2006;**186**:390–395

55. Klö S, Bouloumié A, Mülsch A. Aging and Chronic Hypertension Decrease Expression of Rat Aortic Soluble Guanylyl Cyclase. *Hypertension*. 2000;**35**:43

56. Jansson PA. Endothelial dysfunction in insulin resistance and type 2 diabetes. *J Intern Med*. 2007;**262**:173–183

57. Madonna R, Massaro M, De Caterina R. Insulin potentiates cytokine-induced VCAM-1 expression in human endothelial cells. *Biochim Biophys Acta - Mol Basis Dis*. 2008;**1782**:511–516

58. Simsek S, Van Den Oever IAM, Raterman HG, Nurmohamed MT. Endothelial dysfunction, inflammation, and apoptosis in diabetes mellitus. *Mediators Inflamm*. 2010;**2010** doi:10.1155/2010/792393

59. M.a. J, Hart GW. Protein O-GlcNAcylation in diabetes and diabetic complications. *Expert Rev Proteomics*. 2013;**10**:365–380

60. Wright JLN, Collins HE, Wende AR, Chatham JC. O-GlcNAcylation and cardiovascular disease. *Biochem Soc Trans*. 2017;**45**:545–553

61. Ramos-Alves FE, De Queiroz DB, Santos-Rocha J, Duarte GP, Xavier FE. Effect of age and COX-2-derived prostanoids on the progression of adult vascular dysfunction in the offspring of diabetic rats. *Br J Pharmacol*. 2012;**166**:2198–2208

62. Rafnsson A, Böhm F, Settergren M, Gonon A, Brismar K, Pernow J. The endothelin receptor antagonist bosentan improves peripheral endothelial function in patients with type 2 diabetes mellitus and microalbuminuria: A randomised trial. *Diabetologia*. 2012;**55**:600–607

63. Schneider JG, Tilly N, Hierl T, Sommer U, Hamann A, Dugi K et al. Elevated plasma endothelin-1 levels in diabetes mellitus. *Am J Hypertens*. 2002;**15**:967–972

64. Rask-Madsen C, King GL. Vascular complications of diabetes: Mechanisms of injury and protective factors. *Cell Metab*. 2013;**17**:20–33

65. Oparil S, Acelajado MC, Bakris GL, Berlowitz DR, Cífková R, Dominiczak AF et al. Hypertension. *Nat Rev Dis Prim*. 2018;**4**:18014

66. Brandes RP. Endothelial dysfunction and hypertension. *Hypertension*. 2014;**64**:924–928

67. Michel FS, Man RYK, Vanhoutte PM. Increased spontaneous tone in renal arteries of

spontaneously hypertensive rats. *Am J Physiol - Heart Circ Physiol*. 2007;**293**:1673–1681

68. Virdis A, Bacca A, Colucci R, Duranti E, Fornai M, Materazzi G et al. Endothelial dysfunction in small arteries of essential hypertensive patients: Role of cyclooxygenase-2 in oxidative stress generation. *Hypertension*. 2013;**62**:337–344

69. Moorhouse RC, Webb DJ, Kluth DC, Dhaun N. Endothelin antagonism and its role in the treatment of hypertension. *Curr Hypertens Rep*. 2013;**15**:489–496

70. Palei AC, Spradley FT, Warrington JP, George EM, Granger JP. Pathophysiology of hypertension in pre-eclampsia: A lesson in integrative physiology. *Acta Physiol*. 2013;**208**:224–233

71. Tonelli M, Wiebe N, Culleton B, House A, Rabbat C, Fok M et al. Chronic kidney disease and mortality risk: A systematic review. *J Am Soc Nephrol*. 2006;**17**:2034–2047

72. Khandelwal P, Murugan V, Hari S, Lakshmy R, Sinha A, Hari P et al. Dyslipidemia, carotid intima-media thickness and endothelial dysfunction in children with chronic kidney disease. *Pediatr Nephrol*. 2016;**31**:1313–1320

73. Verbeke FH, Pannier B, Guérin AP, Boutouyrie P, Laurent S, London GM. Flow-Mediated vasodilation in end-stage renal disease. *Clin J Am Soc Nephrol*. 2011;**6**:2009–2015

74. Recio-Mayoral A, Banerjee D, Streather C, Kaski JC. Endothelial dysfunction, inflammation and atherosclerosis in chronic kidney disease - a cross-sectional study of predialysis, dialysis and kidney-transplantation patients. *Atherosclerosis*. 2011;**216**:446–451

75. Jourde-Chiche N, Dou L, Cerini C, Dignat-George F, Brunet P. Vascular Incompetence in Dialysis Patients-Protein-Bound Uremic Toxins and Endothelial Dysfunction. *Semin Dial*. 2011;**24**:327–337

76. Duranton F, Cohen G, De Smet R, Rodriguez M, Jankowski J, Vanholder R et al. Normal and pathologic concentrations of uremic toxins. *J Am Soc Nephrol*. 2012;**23**:1258–1270

77. Isermann B, Vinnikov IA, Madhusudhan T, Herzog S, Kashif M, Blautzik J et al. Activated protein C protects against diabetic nephropathy by inhibiting endothelial and podocyte apoptosis. *Nat Med*. 2007;**13**:1349–1358

78. Hohenstein B, Hausknecht B, Boehmer K, Riess R, Brekken RA, Hugo CPM. Local VEGF activity but not VEGF expression is tightly regulated during diabetic nephropathy in man. *Kidney Int*. 2006;**69**:1654–1661

79. Jaimes EA, Hua P, Tian RX, Raij L. Human glomerular endothelium: Interplay among glucose, free fatty acids, angiotensin II, and oxidative stress. *Am J Physiol - Ren Physiol*. 2010;**298**:125–132

80. Sutariya B, Jhonsa D, Saraf MN. TGF-β: The connecting link between nephropathy and fibrosis. *Immunopharmacol Immunotoxicol*. 2016;**38**:39–49

81. Jourde-Chiche N, Fakhouri F, Dou L, Bellien J, Burtey S, Frimat M et al. Endothelium structure and function in kidney health and disease. *Nat Rev Nephrol*. 2019;**15**:87–108

82. Wang X, Loutzenhiser R. Determinants of renal microvascular response to ACh: afferent and efferent arteriolar actions of EDHF. *Am J Physiol Renal Physiol*. 2002;**282**:F124-32

83. Salomonsson M, Brasen JC, Sorensen CM. Role of renal vascular potassium channels in physiology and pathophysiology. *Acta Physiol*. 2017;**221**:14–31

84. Holman RR, Paul SK, Bethel MA, Neil HAW, Matthews DR. Long-term follow-up after tight control of blood pressure in type 2 diabetes. *N Engl J Med*. 2008;**359**:1565–1576

85. King P, Peacock I, Donnelly R. UKPDS: clinical and therpeutic implications for DM2. *Br J Clin Pharmacol*. 1999;:1–6

86. Lund SS, Rossing P, Vaag AA. Follow-up of intensive glucose control in type 2 diabetes. *N Engl J Med*. 2009;**360**:416–418

87. Paneni F, Volpe M, Lüscher TF, Cosentino F. SIRT1, p66Shc, and set7/9 in vascular hyperglycemic memory: Bringing all the strands together. *Diabetes*. 2013;**62**:1800–1807

88. Pirola L, Balcerczyk A, Okabe J, El-Osta A. Epigenetic phenomena linked to diabetic complications. *Nat Rev Endocrinol*. 2010;**6**:665–675

89. Shigiyama F, Kumashiro N, Miyagi M, Ikehara K, Kanda E, Uchino H et al. Effectiveness of dapagliflozin on vascular endothelial function and glycemic control in patients with early-stage type 2 diabetes mellitus: DEFENCE study. *Cardiovasc Diabetol*. 2017;**16**:1–12

90. Ravassa S, Zudaire A, Díez J. GLP-1 and cardioprotection: From bench to bedside. *Cardiovasc Res*. 2012;**94**:316–323

91. Zhang L, Gong DX, Li SH, Zhou XL. Meta-analysis of the effects of statin therapy on endothelial function in patients with diabetes mellitus. *Atherosclerosis*. 2012;**223**:78–85

92. Virdis A, Ghiadoni L, Taddei S. Effects of antihypertensive treatment on endothelial function. *Curr Hypertens Rep*. 2011;**13**:276–281

93. Schmidt AM. Diabetes Mellitus and Cardiovascular Disease. *Arterioscler Thromb Vasc Biol*. 2019;**39**:558–568

94. Goszcz K, Deakin SJ, Duthie GG, Stewart D, Leslie SJ, Megson IL. Antioxidants in Cardiovascular Therapy: Panacea or False Hope? *Front Cardiovasc Med*. 2015;**2**:1–22

95. Stankevičius E, Lopez-Valverde V, Rivera L, Hughes AD, Mulvany MJ, Simonsen U.

Combination of Ca 2+-activated K + channel blockers inhibits acetylcholine-evoked nitric oxide release in rat superior mesenteric artery. *Br J Pharmacol*. 2006;**149**:560–572

96. Köhler R, Kaistha BP, Wulff H. Vascular KCa-channels as therapeutic targets in hypertension and restenosis disease. *Expert Opin Ther Targets*. 2010;**14**:143–155

97. Griffin M, Casadio R, Bergamini CM. Transglutaminases: Nature's biological glues. *Biochem J*. 2002;**368**:377–396

98. Gundemir S, Colak G, Tucholski J, Johnson GVW. Biochimica et Biophysica Acta Transglutaminase 2 : A molecular Swiss army knife. *BBA - Mol Cell Res*. 2012;**1823**:406–419

99. Lai T-S, Liu Y, Li W, Greenberg CS. Identification of two GTP-independent alternatively spliced forms of tissue transglutaminase in human leukocytes, vascular smooth muscle, and endothelial cells. *FASEB J*. 2007;**21**:4131–4143

100. Pinkas DM, Strop P, Brunger AT, Khosla C. Transglutaminase 2 undergoes a large conformational change upon activation. *PLoS Biol*. 2007;**5**:2788–2796

101. Lai TS, Slaughter TF, Peoples KA, Hettasch JM, Greenberg CS. Regulation of human tissue transglutaminase function by magnesium- nucleotide complexes. Identification of distinct binding sites for Mg-GTP and Mg-ATP. *J Biol Chem*. 1998;**273**:1776–1781

102. Nakaoka H, Perez DM, Baek KJ, Das T, Husain A, Misono K et al. Gh: A GTP-Binding protein with transglutaminase activity and receptor signaling function. *Science (80- )*. 1994;**264**:1593–1596

103. Hitomi K, Ikura K, Maki M. GTP, an linhibitor of transglutaminases, is hydrolyzed by tissue-type transglutaminase (TGase 2) but not by epidermal-type transglutaminase (TGase 3). *Biosci Biotechnol Biochem*. 2000;**64**:657–659

104. Candi E, Paradisi A, Terrinoni A, Pietroni V, Oddi S, Cadot B et al. Transglutaminase 5 is regulated by guanine-adenine nucleotides. *Biochem J*. 2004;**381**:313–319

105. Wang Z, Collighan RJ, Pytel K, Rathbone DL, Li X, Griffin M. Characterization of heparin-binding site of tissue transglutaminase: Its importance in cell surface targeting, matrix deposition, and cell signaling. *J Biol Chem*. 2012;**287**:13063–13083

106. Faye C, Inforzato A, Bignon M, Hartmann DJ, Muller L, Ballut L et al. Transglutaminase-2: A new endostatin partner in the extracellular matrix of endothelial cells. *Biochem J*. 2010;**427**:467–475

107. Lin CHS, Chen J, Zhang Z, Johnson GVW, Cooper AJL, Feola J et al. Endostatin and transglutaminase 2 are involved in fibrosis of the aging kidney. *Kidney Int*. 2016;**89**:1281–1292

108. Hasegawa G, Suwa M, Ichikawa Y, Ohtsuka T, Kumagai S, Kikuchi M et al. A novel

function of tissue-type transglutaminase: Protein disulphide isomerase. *Biochem J*. 2003;**373**:793–803

109. Nelea V, Nakano Y, Kaartinen MT. Size distribution and molecular associations of plasma fibronectin and fibronectin crosslinked by transglutaminase 2. *Protein J*. 2008;**27**:223–233

110. Spurlin TA, Bhadriraju K, Chung KH, Tona A, Plant AL. The treatment of collagen fibrils by tissue transglutaminase to promote vascular smooth muscle cell contractile signaling. *Biomaterials*. 2009;**30**:5486–5496

111. Wang Z, Griffin M. TG2, a novel extracellular protein with multiple functions. *Amino Acids*. 2012;**42**:939–949

112. Wang Z, Perez M, Caja S, Melino G, Johnson TS, Lindfors K et al. A novel extracellular role for tissue transglutaminase in matrix-bound VEGF-mediated angiogenesis. *Cell Death Dis*. 2013;**4** doi:10.1038/cddis.2013.318;

113. Liu C, Wang W, Parchim N, Irani R a., Blackwell SC, Sibai B et al. Tissue transglutaminase contributes to the pathogenesis of preeclampsia and stabilizes placental angiotensin receptor type 1 by ubiquitination-preventing isopeptide modification. *Hypertension*. 2014;**63**:353–361

114. Lai TS, Hausladen A, Slaughter TF, Eu JP, Stamler JS, Greenberg CS. Calcium regulates S-nitrosylation, denitrosylation, and activity of tissue transglutaminase. *Biochemistry*. 2001;**40**:4904–4910

115. Telci D, Collighan RJ, Basaga H, Griffin M. Increased TG2 expression can result in induction of transforming growth factor β1, causing increased synthesis and deposition of matrix proteins, which can be regulated by nitric oxide. *J Biol Chem*. 2009;**284**:29547–29558

116. Jung SM, Jandu S, Steppan J, Belkin A, An SS, Pak A et al. Increased tissue transglutaminase activity contributes to central vascular stiffness in eNOS knockout mice. *Am J Physiol Heart Circ Physiol*. 2013;**305**:H803-10

117. Upchurch HF, Conway E, Patterson MK, Birckbichler PJ, Maxwell MD. Cellular transglutaminase has affinity for extracellular matrix. *Vitr Cell Dev Biol*. 1987;**23**:795–800

118. Siegel M, Strnad P, Watts RE, Choi K, Jabri B, Omary MB et al. Extracellular transglutaminase 2 is catalytically inactive, but is transiently activated upon tissue injury. *PLoS One*. 2008;**3** doi:10.1371/journal.pone.0001861

119. Antonyak MA, Li B, Boroughs LK, Johnson JL, Druso JE, Bryant KL et al. Cancer cell-derived microvesicles induce transformation by transferring tissue transglutaminase and fibronectin to recipient cells. *Proc Natl Acad Sci U S A*. 2011;**108**:4852–4857

120. Furini G, Schroeder N, Huang L, Boocock D, Scarpellini A, Coveney C et al. Proteomic profiling reveals the transglutaminase-2 externalization pathway in kidneys after unilateral ureteric obstruction. *J Am Soc Nephrol*. 2018;**29**:880–905

121. Zemskov EA, Mikhailenko I, Hsia RC, Zaritskaya L, Belkin AM. Unconventional secretion of tissue transglutaminase involves phospholipid-dependent delivery into recycling endosomes. *PLoS One*. 2011;**6** doi:10.1371/journal.pone.0019414

122. Adamczyk M, Griffiths R, Dewitt S, Knäuper V, Aeschlimann D. P2X7 receptor activation regulates rapid unconventional export of transglutaminase-2. *J Cell Sci*. 2015;**128**:4615–4628

123. Caron NS, Munsie LN, Keillor JW, Truant R. Using FLIM-FRET to Measure Conformational Changes of Transglutaminase Type 2 in Live Cells. *PLoS One*. 2012;**7**:e44159

124. Mhaouty-Kodja S. Ghα/tissue transglutaminase 2: An emerging G protein in signal transduction. *Biol Cell*. 2004;**96**:363–367

125. Lin YF, Tseng MJ, Hsu HL, Wu YW, Lee YH, Tsai YH. A novel follicle-stimulating hormone-induced Gαh/phospholipase C-δ1 signaling pathway mediating rat Sertoli cell Ca2+-influx. *Mol Endocrinol*. 2006;**20**:2514–2527

126. Lee KH, Lee N, Lim S, Jung H, Ko YG, Park HY et al. Calreticulin inhibits the MEK1,2-ERK1,2 pathway in α1-adrenergic receptor/Gh-stimulated hypertrophy of neonatal rat cardiomyocytes. *J Steroid Biochem Mol Biol*. 2003;**84**:101–107

127. Gentile V, Porta R, Chiosi E, Spina A, Valente F, Pezone R et al. tTGase/Gαh protein expression inhibits adenylate cyclase activity in Balb-C 3T3 fibroblasts membranes. *Biochim Biophys Acta - Mol Cell Res*. 1997;**1357**:115–122

128. Lee MY, Chung S, Bang HW, Baek KJ, Uhm D. Modulation of large conductance Ca2+-activated K+ channel by Galphah (transglutaminase II) in the vascular smooth muscle cell. *Pflugers Arch*. 1997;**433**:671–673

129. Lee J, Kim YS, Choi DH, Moon SB, Tai RH, Joh TH et al. Transglutaminase 2 induces nuclear factor-κB activation via a novel pathway in BV-2 microglia. *J Biol Chem*. 2004;**279**:53725–53735

130. Maiuri L, Luciani A, Giardino I, Raia V, Villella VR, D'Apolito M et al. Tissue Transglutaminase Activation Modulates Inflammation in Cystic Fibrosis via PPARγ Down-Regulation. *J Immunol*. 2008;**180**:7697–7705

131. Guilluy C, Rolli-Derkinderen M, Tharaux PL, Melino G, Pacaud P, Loirand G. Transglutaminase-dependent RhoA activation and depletion by serotonin in vascular smooth muscle cells. *J Biol Chem*. 2007;**282**:2918–2928

132. Watts SW, Priestley JRC, Thompson JM. Serotonylation of vascular proteins important to

contraction. *PLoS One*. 2009;**4**:e5682

133. Guilluy C, Eddahibi S, Agard C, Guignabert C, Izikki M, Tu L et al. RhoA and Rho kinase activation in human pulmonary hypertension: Role of 5-HT signaling. *Am J Respir Crit Care Med*. 2009;**179**:1151–1158

134. Kumar S, Mehta K. Tissue Transglutaminase Constitutively Activates HIF-1α Promoter and Nuclear Factor-κB via a Non-Canonical Pathway. *PLoS One*. 2012;**7** doi:10.1371/journal.pone.0049321

135. Mastroberardino PG, Farrace MG, Viti I, Pavone F, Fimia GM, Melino G et al. 'Tissue' transglutaminase contributes to the formation of disulphide bridges in proteins of mitochondrial respiratory complexes. *Biochim Biophys Acta - Bioenerg*. 2006;**1757**:1357–1365

136. Battaglia G, Farrace MG, Mastroberardino PG, Viti I, Fimia GM, Van Beeumen J et al. Transglutaminase 2 ablation leads to defective function of mitochondrial respiratory complex I affecting neuronal vulnerability in experimental models of extrapyramidal disorders. *J Neurochem*. Published Online First: 2007 doi:10.1111/j.1471-4159.2006.04140.x

137. Filiano AJ, Bailey CDC, Tucholski J, Gundemir S, Johnson GVW. Transglutaminase 2 protects against ischemic insult, interacts with HIF1β, and attenuates HIF1 signaling. *FASEB J*. 2008;**22**:2662–2675

138. Johnson KB, Petersen-Jones H, Thompson JM, Hitomi K, Itoh M, Bakker ENTP et al. Vena cava and aortic smooth muscle cells express transglutaminases 1 and 4 in addition to transglutaminase 2. *Am J Physiol - Heart Circ Physiol*. 2012;**302**:1355–1366

139. Muszbek L, Bereczky Z, Bagoly Z, Komáromi I, Katona É. Factor XIII: A coagulation factor with multiple plasmatic and cellular functions. *Physiol Rev*. 2011;**91**:931–972

140. Oh YJ, Pau VC, Steppan J, Sikka G, Bead VR, Nyhan D et al. Role of tissue transglutaminase in age-associated ventricular stiffness. *Amino Acids*. 2016;**49**:695–704

141. Porzio O, Massa O, Cunsolo V, Colombo C, Malaponti M, Bertuzzi F et al. Missense mutations in the TGM2 gene encoding transglutaminase 2 are found in patients with early-onset type 2 diabetes. Mutation in brief no. 982. Online. *Hum Mutat*. 2007;**28**:1150

142. Iismaa SE, Aplin M, Holman S, Yiu TW, Jackson K, Burchfield JG et al. Glucose Homeostasis in Mice Is Transglutaminase 2 Independent. *PLoS One*. 2013;**8** doi:10.1371/journal.pone.0063346

143. Salter NW, Ande SR, Nguyen HK, Grégoire Nyomba BL, Mishra S. Functional characterization of naturally occurring transglutaminase 2 mutants implicated in early-onset type 2 diabetes. *J Mol Endocrinol*. 2012;**48**:203–216

144. Maffei B, Laverrière M, Wu Y, Triboulet S, Perrinet S, Duchateau M et al. Infection-

driven activation of transglutaminase 2 boosts glucose uptake and hexosamine biosynthesis in epithelial cells. *EMBO J*. 2020;**e102166**:1–19

145. Mulvany MJ. Small artery remodelling in hypertension. *Basic Clin Pharmacol Toxicol*. 2012;**110**:49–55

146. Schiffrin EL. Vascular remodeling in hypertension: Mechanisms and treatment. *Hypertension*. 2012;**59**:367–374

147. Eftekhari A, Rahman A, Schæbel LH, Chen H, Rasmussen CV, Aalkjær C et al. Chronic cystamine treatment inhibits small artery remodelling in rats. *J Vasc Res*. 2007;**44**:471–482

148. Lesort M, Lee M, Tucholski J, Johnson GVW. Cystamine inhibits caspase activity: Implications for the treatment of polyglutamine disorders. *J Biol Chem*. 2003;**278**:3825–3830

149. Vincan E, Neylon CB, Jacobsen AN, Woodcock EA. Reduction in Gh protein expression is associated with cytodifferentiation of vascular smooth muscle cells. *Mol Cell Biochem*. 1996;**157**:107–110

150. Petersen-Jones HG, Johnson KB, Hitomi K, Tykocki NR, Thompson JM, Watts SW. Transglutaminase activity is decreased in large arteries from hypertensive rats compared with normotensive controls. *Am J Physiol - Heart Circ Physiol*. 2015;**308**:H592–H602

151. Steppan J, Bergman Y, Viegas K, Armstrong D, Tan S, Wang H et al. Tissue transglutaminase modulates vascular stiffness and function through crosslinking-dependent and crosslinking-independent functions. *J Am Heart Assoc*. 2017;**6**:e004161

152. Nurminskaya M, Beazley KE, Smith EP, Belkin AM. Transglutaminase 2 promotes PDGF-mediated activation of PDGFR/Akt1 and β-catenin signaling in vascular smooth muscle cells and supports neointima formation. *J Vasc Res*. 2014;**51**:418–428

153. Liu C, Luo R, Wang W, Peng Z, Johnson GVW, Kellems RE et al. Tissue transglutaminase-mediated AT1 receptor sensitization underlies pro-inflammatory cytokine LIGHT-induced hypertension. *Am J Hypertens*. 2019;**32**:476–485

154. Luo R, Liu C, Elliott SE, Wang W, Parchim N, Iriyama T et al. Transglutaminase is a critical link between inflammation and hypertension. *J Am Heart Assoc*. 2016;**5**:1–12

155. Johnson KB, Thompson JM, Watts SW. Modification of proteins by norepinephrine is important for vascular contraction. *Front Physiol*. 2010;**1 OCT**:1–8

156. Cho BR, Kim MK, Suh DH, Hahn JH, Lee BG, Choi YC et al. Increased tissue transglutaminase expression in human atherosclerotic coronary arteries. *Coron Artery Dis*. 2008;**19**:459–468

157. Boisvert WA, Rose DM, Boullier A, Quehenberger O, Sydlaske A, Johnson KA et al.

Leukocyte transglutaminase 2 expression limits atherosclerotic lesion size. *Arterioscler Thromb Vasc Biol*. 2006;**26**:563–569

158. Van Herck JL, Schrijvers DM, De Meyer GRY, Martinet W, Van Hove CE, Bult H et al. Transglutaminase 2 deficiency decreases plaque fibrosis and increases plaque inflammation in apolipoprotein-E-deficient mice. *J Vasc Res*. 2010;**47**:231–240

159. Williams H, Pease RJ, Newell LM, Cordell PA, Graham RM, Kearney MT et al. Effect of transglutaminase 2 (TG2) deficiency on atherosclerotic plaque stability in the apolipoprotein E deficient mouse. *Atherosclerosis*. 2010;**210**:94–99

160. Matlung HL, Neele AE, Groen HC, van Gaalen K, Tuna BG, van Weert A et al. Transglutaminase activity regulates atherosclerotic plaque composition at locations exposed to oscillatory shear stress. *Atherosclerosis*. 2012;**224**:355–362

161. Freund KF, Doshi KP, Gaul SL, Stern AM, Claremon DA, Remy DC et al. Transglutaminase Inhibition by 2-[(2-Oxopropyl)thio]imidazolium Derivatives: Mechanism of Factor XIIIa Inactivation. *Biochemistry*. 1994;**33**:10109–10119

162. Abdalla S, Lother H, Langer A, El Faramawy Y, Quitterer U. Factor XIIIA transglutaminase crosslinks AT1 receptor dimers of monocytes at the onset of atherosclerosis. *Cell*. 2004;**119**:343–354

163. Beazley KE, Deasey S, Lima F, Nurminskaya M V. Transglutaminase 2-mediated activation of β-catenin signaling has a critical role in warfarin-induced vascular calcification. *Arterioscler Thromb Vasc Biol*. 2012;**32**:123–130

164. Martucciello S, Lavric M, Boglarka T, Korponay-Szabo I, Nadalutti C, Myrsky E et al. RhoB is associated with the anti-angiogenic effects of celiac patient transglutaminase 2-targeted autoantibodies. *J Mol Med*. 2012;**90**:817–826

165. Myrsky E, Caja S, Simon-Vecsei Z, Korponay-Szabo IR, Nadalutti C, Collighan R et al. Celiac disease IgA modulates vascular permeability in vitro through the activity of transglutaminase 2 and RhoA. *Cell Mol Life Sci*. 2009;**66**:3375–3385

166. Jones RA, Kotsakis P, Johnson TS, Chau DYS, Ali S, Melino G et al. Matrix changes induced by transglutaminase 2 lead to inhibition of angiogenesis and tumor growth. *Cell Death Differ*. 2006;**13**:1442–1453

167. Kojima S, Nara K, Rifkin DB. Requirement for transglutaminase in the activation of latent transforming growth factor-β in bovine endothelial cells. *J Cell Biol*. 1993;**121**:439–448

168. Haroon ZA, Hettasch JM, Lai T, Dewhirst MW, Greenberg CS. Tissue transglutaminase is expressed, active, and directly involved in rat dermal wound healing and angiogenesis. *FASEB J*. 1999;**13**:1787–1795

169. Dardik R, Inbal A. Complex formation between tissue transglutaminase II (tTG) and vascular endothelial growth factor receptor 2 (VEGFR-2): Proposed mechanism for

modulation of endothelial cell response to VEGF. *Exp Cell Res*. 2006;**312**:2973–2982

170. Beckouche N, Bignon M, Lelarge V, Mathivet T, Pichol-Thievend C, Berndt S et al. The interaction of heparan sulfate proteoglycans with endothelial transglutaminase-2 limits VEGF165-induced angiogenesis. *Sci Signal*. 2015;**8**:1–9

171. Kang SK, Yi KS, Kwon NS, Park KH, Kim UH, Baek KJ et al. α1B-adrenoceptor signaling and cell motility: GTPase function of Gh/transglutaminase 2 inhibits cell migration through interaction with cytoplasmic tail of integrin α subunits. *J Biol Chem*. 2004;**279**:36593–36600

172. Webster AC, Nagler E V., Morton RL, Masson P. Chronic Kidney Disease. *Lancet*. 2017;**389**:1238–1252

173. Verderio E, Gaudry C, Gross S, Smith C, Downes S, Griffin M. Regulation of cell surface tissue transglutaminase: Effects on matrix storage of latent transforming growth factor-β binding protein-1. *J Histochem Cytochem*. 1999;**47**:1417–1432

174. Furini G, Verderio EAM. Spotlight on the Transglutaminase 2-Heparan Sulfate Interaction. *Med Sci*. 2019;**7**:5

175. Burhan I, Furini G, Lortat-Jacob H, Atobatele AG, Scarpellini A, Schroeder N et al. Interplay between transglutaminases and heparan sulphate in progressive renal scarring. *Sci Rep*. 2016;**6**:1–18

176. Shweke N, Boulos N, Jouanneau C, Vandermeersch S, Melino G, Dussaule JC et al. Tissue transglutaminase contributes to interstitial renal fibrosis by favoring accumulation of fibrillar collagen through TGF-β activation and cell infiltration. *Am J Pathol*. 2008;**173**:631–642

177. Schnabel C, Sawitza I, Tag CG, Lahme B, Gressner AM, Breitkopf K. Expression of cytosolic and membrane associated tissue transglutaminase in rat hepatic stellate cells and its upregulation during transdifferentiation to myofibroblasts in culture. *Hepatol Res*. 2004;**28**:140–145

178. Szondy Z, Korponay-Szabó I, Király R, Sarang Z, Tsay GJ. Transglutaminase 2 in human diseases. *BioMedicine*. 2017;**7**:1–13

179. Akbar A, McNeil NMR, Albert MR, Ta V, Adhikary G, Bourgeois K et al. Structure-Activity Relationships of Potent, Targeted Covalent Inhibitors That Abolish Both the Transamidation and GTP Binding Activities of Human Tissue Transglutaminase. *J Med Chem*. 2017;**60**:7910–7927

180. Siegel M, Khosla C. Transglutaminase 2 inhibitors and their therapeutic role in disease states. *Pharmacol Ther*. 2007;**115**:232–245

181. Zhuang R, Khosla C. Substrates, inhibitors, and probes of mammalian transglutaminase 2. *Anal Biochem*. 2020;**591**:113560

182. Palanski BA, Khosla C. Cystamine and Disulfiram Inhibit Human Transglutaminase 2 via an Oxidative Mechanism. *Biochemistry*. 2018;**57**:3359–3363

183. Jeitner TM, Pinto JT, Cooper AJL. Cystamine and cysteamine as inhibitors of transglutaminase activity in vivo. *Biosci Rep*. 2018;**38**:4–10

184. Shinde A V., Su Y, Palanski BA, Fujikura K, Garcia MJ, Frangogiannis NG. Pharmacologic inhibition of the enzymatic effects of tissue transglutaminase reduces cardiac fibrosis and attenuates cardiomyocyte hypertrophy following pressure overload. *J Mol Cell Cardiol*. 2018;**117**:36–48

185. Diraimondo TR, Klöck C, Warburton R, Herrera Z, Penumatsa K, Toksoz D et al. Elevated Transglutaminase 2 Activity Is Associated with Hypoxia-Induced Experimental Pulmonary Hypertension in Mice. *ACS Chem Biol*. 2014;**9**:266–275

186. Dafik L, Khosla C. Dihydroisoxazole analogs for labeling and visualization of catalytically active transglutaminase 2. *Chem Biol*. 2011;**18**:58–66

187. Song M, Hwang H, Im CY, Kim SY. Recent progress in the development of transglutaminase 2 (TGase2) Inhibitors: Miniperspective. *J Med Chem*. 2017;**60**:554–567

188. Al-Jallad HF, Myneni VD, Piercy-Kotb SA, Chabot N, Mulani A, Keillor JW et al. Plasma membrane factor XIIIA transglutaminase activity regulates osteoblast matrix secretion and deposition by affecting microtubule dynamics. *PLoS One*. 2011;**6** doi:10.1371/journal.pone.0015893

189. Schaertl S, Prime M, Wityak J, Dominguez C, Munoz-Sanjuan I, Pacifici RE et al. A profiling platform for the characterization of transglutaminase 2 (TG2) inhibitors. *J Biomol Screen*. 2010;**15**:478–487

190. Pardin C, Roy I, Lubell WD, Keillor JW. Reversible and competitive cinnamoyl triazole inhibitors of tissue transglutaminase. *Chem Biol Drug Des*. 2008;**72**:189–196

191. Pardin C, Roy I, Chica RA, Bonneil E, Thibault P, Lubell WD et al. Photolabeling of tissue transglutaminase reveals the binding mode of potent cinnamoyl inhibitors. *Biochemistry*. 2009;**48**:3346–3353

192. Yi MC, Palanski BA, Quintero SA, Plugis NM, Khosla C. An unprecedented dual antagonist and agonist of human Transglutaminase 2. *Bioorganic Med Chem Lett*. 2015;**25**:4922–4926

193. Kim S-Y. New Insights into Development of Transglutaminase 2 Inhibitors as Pharmaceutical Lead Compounds. *Med Sci*. 2018;**6**:87

194. Wang K, Zu C, Zhang Y, Wang X, Huan X, Wang L. Blocking TG2 attenuates bleomycin-induced pulmonary fibrosis in mice through inhibiting EMT. *Respir Physiol Neurobiol*. 2020;**276**:103402

195. Iversen R, Mysling S, Hnida K, Jørgensen TJD, Sollid LM. Activity-regulating structural changes and autoantibody epitopes in transglutaminase 2 assessed by hydrogen/deuterium exchange. *Proc Natl Acad Sci U S A*. 2014;**111**:17146–17151

196. Hnida K, Stamnaes J, Du Pré MF, Mysling S, Jørgensen TJD, Sollid LM et al. Epitope-dependent functional effects of celiac disease autoantibodies on transglutaminase 2. *J Biol Chem*. 2016;**291**:25542–25552

197. Mulvany MJ, Halpern W. Contractile properties of small arterial resistance vessels in spontaneously hypertensive and normotensive rats. *Circ Res*. 1977;**41**:19–26

198. Bentzen BH, Nardi A, Calloe K, Madsen LS, Olesen SP, Grunnet M. The small molecule NS11021 is a potent and specific activator of Ca 2+-activated big-conductance K+ channels. *Mol Pharmacol*. 2007;**72**:1033–1044

199. Sankaranarayanan A, Raman G, Busch C, Schultz T, Zimin PI, Hoyer J et al. Naphtho[1,2-d]thiazol-2-ylamine (SKA-31), a new activator of KCa2 and KCa3.1 potassium channels, potentiates the endothelium-derived hyperpolarizing factor response and lowers blood pressure. *Mol Pharmacol*. 2009;**75**:281–295

200. Stankevicius E, Dalsgaard T, Kroigaard C, Beck L, Boedtkjer E, Misfeldt MW et al. Opening of small and intermediate calcium-activated potassium channels induces relaxation mainly mediated by nitric-oxide release in large arteries and endothelium-derived hyperpolarizing factor in small arteries from rat. *J Pharmacol Exp Ther*. 2011;**339**:842–850

201. Perez Alea M, Kitamura M, Martin G, Thomas V, Hitomi K, El Alaoui S. Development of an isoenzyme-specific colorimetric assay for tissue transglutaminase 2 cross-linking activity. *Anal Biochem*. 2009;**389**:150–156

202. Stamnaes J, Pinkas DM, Fleckenstein B, Khosla C, Sollid LM. Redox regulation of transglutaminase 2 activity. *J Biol Chem*. 2010;**285**:25402–25409

203. Slaughter TF, Achyuthan KE, Lai TS, Greenberg CS. A microtiter plate transglutaminase assay utilizing 5-(biotinamido)pentylamine as substrate. *Anal Biochem*. 1992;**205**:166–171

204. Jeon JH, Kim CW, Shin DM, Kim K Il, Cho SY, Kwon JC et al. Differential incorporation of biotinylated polyamines by transglutaminase 2. *FEBS Lett*. 2003;**534**:180–184

205. Tsang HG, Rashdan NA, Whitelaw CBA, Corcoran BM, Summers KM, MacRae VE. Large animal models of cardiovascular disease. *Cell Biochem Funct*. 2016;**34**:113–132

206. Springer DA, Allen M, Hoffman V, Brinster L, Starost MF, Bryant M et al. Investigation and identification of etiologies involved in the development of acquired hydronephrosis in aged laboratory mice with the use of high-frequency ultrasound imaging. *Pathobiol Aging Age-related Dis*. 2014;**4**:24932

207. Wang B, Chandrasekera PC, Pippin JJ. Leptin- and Leptin Receptor-Deficient Rodent Models : Relevance for Human Type 2 Diabetes. *Curr Diabetes Rev*. 2014;**10**:131–145

208. Souza-Smith FM, Katz PS, Trask AJ, Stewart JA, Lord KC, Varner KJ et al. Mesenteric resistance arteries in type 2 diabetic db/db mice undergo outward remodeling. *PLoS One*. 2011;**6**:4–13

209. Nguyen Dinh Cat A, Callera GE, Friederich-Persson M, Sanchez A, Dulak-Lis MG, Tsiropoulou S et al. Vascular dysfunction in obese diabetic db/db mice involves the interplay between aldosterone/mineralocorticoid receptor and Rho kinase signaling. *Sci Rep*. 2018;**8**:1–11

210. Miike T, Kunishiro K, Kanda M, Azukizawa S, Kurahashi K, Shirahase H. Impairment of endothelium-dependent ACh-induced relaxation in aorta of diabetic db/db mice-possible dysfunction of receptor and/or receptor-G protein coupling. *Naunyn Schmiedebergs Arch Pharmacol*. 2008;**377**:401–410

211. Pannirselvam M, Verma S, Anderson TJ, Triggle CR. Cellular basis of endothelial dysfunction in small mesenteric arteries from spontaneously diabetic (db/db -/-) mice: Role of decreased tetrahydrobiopterin bioavailability. *Br J Pharmacol*. 2002;**136**:255–263

212. Piercy V, Taylor SG. A comparison of spasmogenic and relaxant responses in aortae from C57/BL/KsJ diabetic mice with those from their non-diabetic litter mates. *Pharmacology*. 1998;**56**:267–275

213. Sallam N, Fisher A, Golbidi S, Laher I. Weight and inflammation are the major determinants of vascular dysfunction in the aortae of db/db mice. *Naunyn Schmiedebergs Arch Pharmacol*. 2011;**383**:483–492

214. Silva MAB, Bruder-Nascimento T, Cau SBA, Lopes RAM, Mestriner FLAC, Fais RS et al. Spironolactone treatment attenuates vascular dysfunction in type 2 diabetic mice by decreasing oxidative stress and restoring NO/GC signaling. *Front Physiol*. 2015;**6**:1–11

215. Buus NH, VanBavel E, Mulvany MJ. Differences in sensitivity of rat mesenteric small arteries to agonists when studied as ring preparations or as cannulated preparations. *Br J Pharmacol*. 1994;**112**:579–587

216. Köhler R, Brakemeier S, Kühn M, Degenhardt C, Buhr H, Pries A et al. Expression of ryanodine receptor type 3 and TRP channels in endothelial cells: Comparison of in situ and cultured human endothelial cells. *Cardiovasc Res*. 2001;**51**:160–168

217. Sandow SL, Grayson TH. Limits of isolation and culture: Intact vascular endothelium and BK Ca. *Am J Physiol - Heart Circ Physiol*. 2009;**297**:1–7

218. Hogg DS, McMurray G, Kozlowski RZ. Endothelial cells freshly isolated from small pulmonary arteries of the rat possess multiple distinct K+ current profiles. *Lung*. 2002;**180**:203–214

219. Hughes JM, Riddle MA, Paffett ML, Gonzalez Bosc L V., Walker BR. Novel role of endothelial BK Ca channels in altered vasoreactivity following hypoxia. *Am J Physiol - Heart Circ Physiol*. 2010;**299**:1439–1450

220. Olschewski A, Olschewski H, Bräu ME, Hempelmann G, Vogel W, Safronov B V. Basic electrical properties of in situ endothelial cells of small pulmonary arteries during postnatal development. *Am J Respir Cell Mol Biol*. 2001;**25**:285–290

221. Behringer EJ, Socha MJ, Polo-Parada L, Segal SS. Electrical conduction along endothelial cell tubes from mouse feed arteries: Confounding actions of glycyrrhetinic acid derivatives. *Br J Pharmacol*. 2012;**166**:774–787

222. Behringer EJ, Segal SS. Tuning electrical conduction along endothelial tubes of resistance arteries through Ca 2+-Activated K + channels. *Circ Res*. 2012;**110**:1311–1321

223. Dora KA, Gallagher NT, McNeish A, Garland CJ. Modulation of endothelial cell KCa3.1 channels during endothelium-derived hyperpolarizing factor signaling in mesenteric resistance arteries. *Circ Res*. 2008;**102**:1247–1255

224. Aeschlimann D, Koeller MK, Allen-Hoffmann BL, Mosher DF. Isolation of a cDNA encoding a novel member of the transglutaminase gene family from human keratinocytes. Detection and identification of transglutaminase gene products based on reverse transcription-polymerase chain reaction with degenerate primers. *J Biol Chem*. 1998;**273**:3452–3460

225. Smit C, De Hoogd S, Brüggemann RJM, Knibbe CAJ. Obesity and drug pharmacology: a review of the influence of obesity on pharmacokinetic and pharmacodynamic parameters. *Expert Opin Drug Metab Toxicol*. 2018;**14**:275–285

226. Abernethy DR, Greenblatt DJ. Drug Disposition in Obese Humans: An Update. *Clin Pharmacokinet*. 1986;**11**:199–213

227. Félétou M. Calcium-activated potassium channels and endothelial dysfunction: Therapeutic options? *Br J Pharmacol*. 2009;**156**:545–562

228. Wang Z, Stuckey DJ, Murdoch CE, Camelliti P, Lip GYH, Griffin M. Cardiac fibrosis can be attenuated by blocking the activity of transglutaminase 2 using a selective small-molecule inhibitor. *Cell Death Dis*. 2018;**9**:613

229. Matsumoto S, Shimabukuro M, Fukuda D, Soeki T, Yamakawa K, Masuzaki H et al. Azilsartan, an angiotensin II type 1 receptor blocker, restores endothelial function by reducing vascular inflammation and by increasing the phosphorylation ratio Ser(1177)/Thr(497) of endothelial nitric oxide synthase in diabetic mice. *Cardiovasc Diabetol*. 2014;**13**:30

230. Malik RA, Schofield IJ, Izzard A, Austin C, Bermann G, Heagerty AM. Effects of angiotensin type-1 receptor antagonism on small artery function in patients with type 2 diabetes mellitus. *Hypertension*. 2005;**45**:264–269

231. Büssemaker E, Popp R, Binder J, Busse R, Fleming I. Characterization of the endothelium-derived hyperpolarizing factor (EDHF) response in the human interlobar artery. *Kidney Int*. 2003;**63**:1749–1755

232. Rasmussen KMB, Braunstein TH, Salomonsson M, Brasen JC, Sorensen CM. Contribution of K+ channels to endothelium-derived hypolarization-induced renal vasodilation in rats in vivo and in vitro. *Pflugers Arch Eur J Physiol*. 2016;**468**:1139–1149

233. Simonet S, Isabelle M, Bousquenaud M, Clavreul N, Félétou M, Vayssettes-Courchay C et al. K Ca3.1 channels maintain endothelium-dependent vasodilatation in isolated perfused kidneys of spontaneously hypertensive rats after chronic inhibition of NOS. *Br J Pharmacol*. 2012;**167**:854–867

234. Waeckel L, Bertin F, Clavreul N, Damery T, Köhler R, Paysant J et al. Preserved regulation of renal perfusion pressure by small and intermediate conductance KCa channels in hypertensive mice with or without renal failure. *Pflügers Arch - Eur J Physiol*. 2015;**467**:817–831

235. Wang D, Borrego-Conde LJ, Falck JR, Sharma KK, Wilcox CS, Umans JG. Contributions of nitric oxide, EDHF, and EETS to endothelium-dependent relaxation in renal afferent arterioles. *Kidney Int*. 2003;**63**:2187–2193

236. Oliván-Viguera A, Valero MS, Pinilla E, Amor S, García-Villalón ÁL, Coleman N et al. Vascular Reactivity Profile of Novel KCa3.1-Selective Positive-Gating Modulators in the Coronary Vascular Bed. *Basic Clin Pharmacol Toxicol*. 2016;**119**:184–192

237. Sforna L, Megaro A, Pessia M, Franciolini F, Catacuzzeno L. Structure, Gating and Basic Functions of the Ca2+-activated K Channel of Intermediate Conductance. *Curr Neuropharmacol*. 2018;**16**:608–617

238. Jiang F, Li CG, Rand MJ. Mechanisms of nitric oxide-independent relaxations induced by carbachol and acetylcholine in rat isolated renal arteries. *Br J Pharmacol*. 2000;**130**:1191–1200

239. Brandes RP, Behra A, Lebherz C, Böger RH, Bode-Böger SM, Phivthong-Ngam L et al. N(G)-nitro-L-arginine- and indomethacin-resistant endothelium-dependent relaxation in the rabbit renal artery: Effect of hypercholesterolemia. *Atherosclerosis*. 1997;**135**:49–55

240. Jiang F, Dusting GJ. Endothelium-dependent vasorelaxation independent of nitric oxide and K(+) release in isolated renal arteries of rats. *Br J Pharmacol*. 2001;**132**:1558–1564

241. Karagiannis J, Rand M, Li C-G. Role of gap junctions in endothelium-derived hyperpolarizing factor-mediated vasodilatation in rat renal artery. *Acta Pharmacol Sin*. 2004;**25**:1031–1037

242. Gschwend S, Buikema H, Navis G, Henning RH, De Zeeuw D, Van Dokkum RPE. Endothelial dilatory function predicts individual susceptibility to renal damage in the 5/6

nephrectomized rat. *J Am Soc Nephrol*. 2002;**13**:2909–2915

243. Magnusson L, Sorensen CM, Braunstein TH, Holstein-Rathlou NH, Salomonsson M. Renovascular BKCa channels are not activated in vivo under resting conditions and during agonist stimulation. *Am J Physiol - Regul Integr Comp Physiol*. 2007;**292**:345–353

244. Giangiacomo KM, Garcia ML, McManus OB. Mechanism of Iberiotoxin Block of the Large-Conductance Calcium-Activated Potassium Channel from Bovine Aortic Smooth Muscle. *Biochemistry*. 1992;**31**:6719–6727

245. Koschak A, Koch RO, Liu J, Kaczorowski GJ, Reinhart PH, Garcia ML et al. [125I]iberiotoxin-D19Y/Y36F, the first selective, high specific activity radioligand for high-conductance calcium-activated potassium channels. *Biochemistry*. 1997;**36**:1943–1952

246. Miller C. Competition for block of a Ca2+-activated K+ channel by charybdotoxin and tetraethylammonium. *Neuron*. 1988;**1**:1003–1006

247. Zhang DX, Borbouse L, Gebremedhin D, Mendoza SA, Zinkevich NS, Li R et al. H2O2-induced dilation in human coronary arterioles: Role of protein kinase G dimerization and large-conductance Ca 2+-activated K + channel activation. *Circ Res*. 2012;**110**:471–480

248. Muñoz M, López-Oliva ME, Pinilla E, Martínez MP, Sánchez A, Rodríguez C et al. CYP epoxygenase-derived H2O2 is involved in the endothelium-derived hyperpolarization (EDH) and relaxation of intrarenal arteries. *Free Radic Biol Med*. 2017;**106**:168–183

249. Brasen JC, de Wit C, Sorensen CM. Myoendothelial coupling through Cx40 contributes to EDH-induced vasodilation in murine renal arteries: evidence from experiments and modelling. *Acta Physiol*. 2018;**222**:1–12

250. Büssemaker E, Wallner C, Fisslthaler B, Fleming I. The Na-K-ATPase is a target for an EDHF displaying characteristics similar to potassium ions in the porcine renal interlobar artery. *Br J Pharmacol*. 2002;**137**:647–654

251. Absi M, Burnham MP, Weston AH, Harno E, Rogers M, Edwards G. Effects of methyl β-cyclodextrin on EDHF responses in pig and rat arteries; Association between SK Ca channels and caveolin-rich domains. *Br J Pharmacol*. 2007;**151**:332–340

252. Yu J, Bergaya S, Murata T, Alp IF, Bauer MP, Lin MI et al. Direct evidence for the role of caveolin-1 and caveolae in mechanotransduction and remodeling of blood vessels. *J Clin Invest*. 2006;**116**:1284–1291

253. McNeish AJ, Sandow SL, Neylon CB, Chen MX, Dora KA, Garland CJ. Evidence for involvement of both IKCa and SKCa channels in hyperpolarizing responses of the rat middle cerebral artery. *Stroke*. 2006;**37**:1277–1282

254. Du J, Ma X, Shen B, Huang Y, Birnbaumer L, Yao X. TRPV4, TRPC1, and TRPP2 assemble to form a flow-sensitive heteromeric channel. *FASEB J*. 2014;**28**:4677–4685

255. Dalsgaard T, Kroigaard C, Misfeldt M, Bek T, Simonsen U. Openers of small conductance calcium-activated potassium channels selectively enhance NO-mediated bradykinin vasodilatation in porcine retinal arterioles. *Br J Pharmacol*. 2010;**160**:1496–1508

256. Brähler S, Kaistha A, Schmidt VJ, Wölfle SE, Busch C, Kaistha BP et al. Genetic deficit of SK3 and IK1 channels disrupts the endothelium-deerived hyperpolarizing factor vasodilator pathway and causes hypertension. *Circulation*. 2009;**119**:2323–2332

257. Edgley AJ, Tare M, Evans RG, Skordilis C, Parkington HC. In vivo regulation of endothelium-dependent vasodilation in the rat renal circulation and the effect of streptozotocin-induced diabetes. *Am J Physiol - Regul Integr Comp Physiol*. 2008;**295**:829–839

258. Wildt B Van Der, Wilhelmus MMM, Beaino W, Kooijman EJM, Schuit RC, Bol JGJM et al. In vivo evaluation of two tissue transglutaminase PET tracers in an orthotopic tumour xenograft model. *Eur J Nucl Med Mol Imaging*. 2018;**8**:39

259. Wildt B Van Der, Lammertsma AA, Drukarch B, Windhorst AD. Strategies towards in vivo imaging of active transglutaminase type 2 using positron emission tomography. *Amino Acids*. 2017;**49**:585–595

## 11. APPENDIX 1: MANUSCRIPT I

**The transglutaminase 2 inhibitor LDN 27219 age-dependently lowers blood pressure and improves endothelium-dependent vasodilation in resistance arteries.**

Estéfano Pinilla, Simon Comerma-Steffensen, Judit Prat-Duran, Luis, Vladimir Matchkov, Niels Henrik Buus, and Ulf Simonsen.

Submitted for publication.

**The transglutaminase 2 inhibitor LDN 27219 age-dependently lowers blood pressure and improves endothelium-dependent vasodilation in resistance arteries**

Estéfano Pinilla MPharm. [1,2], Simon Comerma-Steffensen DVM. MSc. PhD[1,3], Judit Prat-Duran MSc.[1], Luis Rivera DVM . PhD[2], Vladimir Matchkov MSc. PhD[1], Niels Henrik Buus MD. PhD[1,4], Ulf Simonsen MD. PhD[1]

[1]Department of Biomedicine, Pulmonary and Cardiovascular Pharmacology, Aarhus University, Denmark; [2]Departament of Physiology, Faculty of Pharmacy, Complutense University of Madrid, Spain; [3]Department of Biomedical Sciences/ Animal Physiology, Veterinary Faculty, Central University of Venezuela, Maracay, Aragua, Venezuela; [4]Department of Renal Medicine, Aarhus University Hospital, Denmark

**Short title:** TG2 modulation age-dependently lowers BP

**Word count: 5933**

**Abstract: 243**

**Figures: 6**

**Address correspondence to:**

Estéfano Pinilla

Department of Biomedicine

Aarhus University

Ole Worms Allé 4, Blg 1160

8000 Aarhus C. Denmark

estefanopinilla@biomed.au.dk

Tel. No. 004550255722

**ABSTRACT**

Tissue transglutaminase 2 (TG2) is an enzyme which in the open conformation state exerts transamidase activity, leading to protein cross-binding and development of fibrosis. In the closed conformation state, TG2 seems important for transmembrane signaling. The unspecific transglutaminase inhibitor cystamine causes vasodilation. However, the role of TG2 conformation in vascular function is unknown. We investigated the vascular effects of several TG2 inhibitors, by measurements of relaxation in isolated rat and human small arteries, patch-clamp studies on vascular smooth muscle cells and blood pressure measurements during intravenous infusion in anesthetized rats. LDN 27219 promoted the closed TG2 conformation and inhibited transamidase activity in small arteries. In contrast to inhibitors promoting the open conformation of TG2 (Z-DON, VA5), LDN 27219 concentration-dependently relaxed rat and human small arteries. LDN 27219 potentiated acetylcholine-induced relaxation by increasing sensitivity to nitric oxide through opening of smooth muscle large-conductance calcium-activated potassium channels; these effects were abolished by membrane permeable TG2 inhibitors promoting the open conformation. In isolated arteries from older rats, transamidase activity was increased and LDN 27219 improved acetylcholine-induced relaxation more than in younger rats. Infusion of LDN 27219 decreased blood pressure more effectively in 35-week than 12-week-old rats. In summary, pharmacological modulation of TG2 to the closed conformation leads to age-dependent blood pressure lowering and potentiation of endothelium-dependent vasorelaxation by opening potassium channels. Our findings suggest that promotion of the closed conformation of TG2 is a potential strategy to treat age-related endothelial dysfunction and to lower blood pressure.

**Keywords:** transglutaminase 2, aging, endothelial dyfunction, nitric oxide, blood pressure

## GRAPHICAL ABSTRACT

**The transglutaminase 2 inhibitor LDN 27219 age-dependently lowers blood pressure and improves endothelium-dependent vasodilation in resistance arteries**

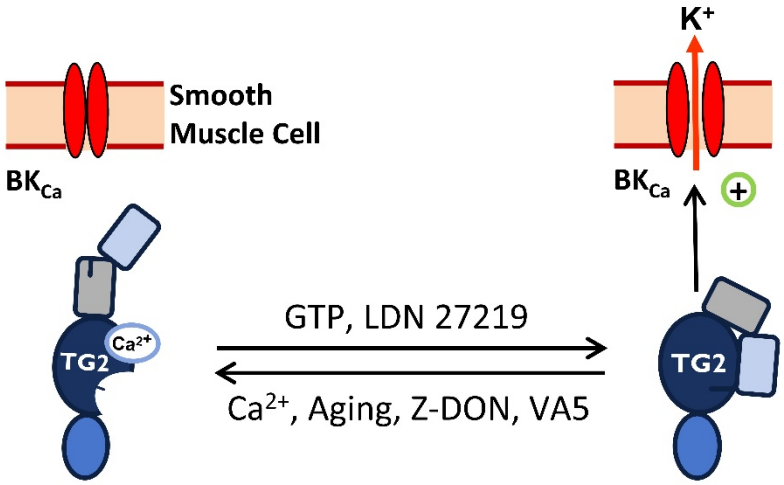


**OPEN conformation of TG2**

- No effect on tone
- Decreased sensitivity to NO
- No effect on blood pressure *in vivo*

**CLOSED conformation of TG2**

- Direct vasorelaxation
- Increased sensitivity to NO
- Blood pressure lowering effect *in vivo*

**Perspectives:** Pharmacological modulation of tissue transglutaminase (TG2) to its closed conformation is a potential new strategy to reverse age-related endothelial dysfunction.

## INTRODUCTION

Transamidase activity and externalization of tissue transglutaminase (TG2) are involved in structural changes in the vasculature such as cardiovascular stiffness in aging,[1–3] vascular remodeling in response to reduced blood flow,[4,5] and endothelial dysfunction in diabetes.[6,7] Moreover, recent studies by our group and others suggest that TG2 plays a role in the regulation of vascular tone.[8,9]

TG2 is a member of the transglutaminase family of enzymes (TG1-7 and Factor XIII) and it is highly expressed in both endothelial and smooth muscle cells throughout the vascular tree.[10] TG2 has several functions depending on its cellular location, conformation and microenvironment (redox state, availability of $Ca^{2+}$ and nucleotides).[11,12] In the $Ca^{2+}$-bound open conformation TG2 has transamidase activity, leading to covalent crosslinking of structural proteins while in the closed conformation TG2 has GTP-binding activity functioning as a G protein ($G_h\alpha$).[13] As these two activities are mutually exclusive and despite TG2 is in dynamic equilibrium, transamidase activity is thought to be mainly present in extracellular TG2 and during local intracellular $Ca^{2+}$ increments. In contrast, intracellular TG2 in the closed/GTP-bound enzymatic state, constitutively exerts transmembrane signaling by linking several G protein coupled receptors with signaling cascades.

There has been an interest to develop new TG2 irreversible inhibitors that modulate the enzyme into its open conformation, such as Z-DON[14] or VA5,[15] inhibiting at the same time the transamidase and GTP binding activities.[16] On the other hand, there are some reversible TG2 inhibitors like LDN 27219, which is a potent, slow-binding, inhibitor that has been reported to dock at a GTP binding-related site of TG2.[17] Additionally, *in silico* docking simulations of LDN 27219 binding to TG2 have suggested that it might stabilize the closed conformation of the enzyme.[18] Although we found vasorelaxant effects of some TG2

inhibitors,[8] it is unclear whether the conformation of the TG2 protein plays a role in the regulation of the vascular tone, particularly in vascular aging.

We hypothesized that pharmacological modulation promoting the closed conformation of TG2 would lead to vasorelaxation by opening of potassium channels, and hence restore the age-related changes in endothelial function and blood pressure (BP). This study for the first time links the closed conformation of TG2 with vasodilatory effects *ex vivo* and *in vivo* and with an increased sensitivity to nitric oxide (NO) in the vascular smooth muscle through the opening of large-conductance calcium-activated potassium channels ($BK_{Ca}$). These effects increase with age and correlate to transamidase activity in small arteries, suggesting that conformational modulation of TG2 is a potential strategy to restore endothelial function during aging.

## METHODS

For a more detailed description of the methods and composition of used solutions, see Data Supplement.

### Animals and tissue preparation:

Male Wistar Hannover rats at 6-7, 12-14 and 35-40 weeks of age were used. For *ex vivo* studies, animals were randomly selected and euthanized by decapitation and exsanguination. The mesenteric bed was immediately removed and mesenteric resistance arteries (internal lumen diameters 200-300 μm) were isolated. Animal protocols and care were approved by the Danish Animal Experiments Inspectorate (permission 2014-15-2934-0159 and 2019-15-0201-00009) and followed Aarhus University institutional guidelines and the NIH guidelines.[19]

Human subcutaneous resistance arteries were obtained from fat biopsies of the gluteal region from both male and female patients (30-70 years of age) with or without essential hypertension (for details, see Table S1), and isolated for *ex vivo* studies. The study using human tissue was approved by the Regional Ethics Committee, Central Denmark (permission: 1-10-72-120-17) and conducted in accordance with the principles of the Helsinki Declaration II for medical research and Aarhus University institutional guidelines. All participants gave informed consent prior to participation.

**Native-PAGE**

To study the effect of different TG2 inhibitors on enzyme conformation, purified and functional human TG2 produced in insect cells was obtained from Zedira (Darmstadt, Germany) and native gel electrophoresis experiments were performed as previously described.[20,21]

**Transamidase activity assay in intact arteries**

A dot blot assay was used to determine 5-biotin(amido)pentylamine (BPA) incorporation in structural proteins as a measure of transamidase activity *ex vivo* as previously described.[1] Freshly isolated mesenteric resistance arteries were incubated in a BPA solution for 4h, washed and homogenized. Incorporated BPA was quantified by chemiluminescence using HRP-streptavidin.

**Isometric tension studies**

Resistance arteries from rats and human donnors were mounted in microvascular myographs for isometric tension recordings (Danish Myotechnology, Aarhus, Denmark).[8] Changes in tension were recorded in response to different TG2 inhibitors and their effect on

endothelium-dependent vasorelaxation was studied. In a subset of arteries, the endothelium was removed by rubbing the lumen with a human scalp hair.

**Whole-cell voltage-clamp studies**

Freshly isolated smooth muscle cells (SMCs) from rat mesenteric artery were used for patch-clamp recordings within 5 h after the isolation procedure as previously described.[8] Current-voltage relations were determined using voltage ramps.

***In vivo* mean arterial pressure (MAP) and heart rate (HR) measurements**

Male Wistar rats at 12-14 and 35-40 weeks of age were anesthetized with s-ketamine and pentobarbital. Changes in MAP and electrocardiographic signal were studied using solid-state catheterization of the carotid artery and ECG needles.[22]

**Statistical analysis**

Data are expressed as means ± SEM, where "*n"* is the number of animals studied in each group or the number of replicates in the case of native-PAGE studies. Normality of the data was verified examining their quantile-quantile (Q-Q) plots against the normal distribution. Native-PAGE results were analyzed by paired two-tailed Student´s t-test. Concentration–response curves were analyzed by two-way ANOVA followed by Bonferroni post-test for multiple comparisons. One-way ANOVA was used for multiple testing, followed by the appropiate multiple comparison post-test, when there was only one independent variable of interest. Values of $P<0.05$ were considered significant. All analyses were performed using GraphPad Prism Software (version 7.02).

## RESULTS

### Conformational state is important for the effect of TG inhibition on vascular tone

We investigated the effect of LDN 27219 on TG2 conformation using native gel electrophoresis. In accordance with previous *in silico* simulations,[18] incubation of isolated human TG2 with LDN 27219 increased the relative abundance of the closed conformation of the enzyme compared to vehicle *in vitro*. Meanwhile, GTP completely forced the enzyme into its closed conformation and Z-DON in the presence of calcium forced TG2 into its open conformation (Figure 1A). We also studied the capacity of these inhibitors to reduce transamidase activity in rat small mesenteric arteries *ex vivo* using the BPA incorporation assay. We observed that incubation with LDN 27219 and Z-DON inhibited transamidase activity in a similar way, while 1,4-dithiothreitol (DTT) increased transamidase activity as previously reported (Figure 1B). [2,5]

In isolated rat mesenteric resistance arteries contracted with the thromboxane analogue U46619, LDN-27219 induced concentration-dependent relaxations, which were significantly reduced in arteries without endothelium and in the presence of the NO synthase (NOS) inhibitor Nω-Nitro-L-arginine (L-NOARG), indicating that LDN 27219 vasorelaxation is NO-dependent. Contrarily, Z-DON failed to change vessel wall tension (Figure 1C). LDN 27219 also induced relaxation in U46619-contracted human subcutaneous resistance arteries (Figure 1D).

### Pharmacologically induced closed conformation of TG2 potentiates endothelium-dependent relaxation by increasing SMC sensitivity to NO

Incubation with LDN 27219 for 20 min increased the response to acetylcholine (ACh) in phenylephrine (Phe)-contracted subcutaneous arteries from human biopsies (Figure 2A-C).

This effect was also observed in arteries from 12-14-week-old rats (Figure 2D). Contrarily, incubation with VA5 and Z-DON that are irreversible and membrane-permeable TG2 inhibitors and lock the enzyme in its open conformation, caused a slight inhibition of ACh-induced relaxation in rat mesenteric arteries, while a non-permeable TG2 inhibitor Boc-DON failed to change relaxation (Figure 2E and Figure S1A). LDN 27219 potentiation of ACh-induced vasorelaxation was abolished by the presence of the irreversible membrane-permeable TG2 inhibitors (Figure 2F and Figure S1B). Additionally, *in vitro* transamidase activity assays showed that VA5 inhibited transamidase activity more potently than LDN 27219 (Figure S1C). These results indicate that LDN 27219-induced vasorelaxation is mainly due to its capacity to induce the closed conformation of TG2 and not directly related with transamidase activity inhibition.

The potentiating effect of LDN 27219 on endothelium-dependent vasorelaxation was still observed in the presence of $IK_{Ca}$ and $SK_{Ca}$ channel blockers TRAM-34 and UCL 1684 (Figure 3A), while it was abolished after incubation with L-NOARG (Figure 3B), suggesting that, at the level of the endothelium, it was independent of endothelial potassium channels and related to the NO pathway.

At the level of SMCs, LDN 27219 potentiation of ACh-induced vasorelaxation was still present, although apparently reduced, in the presence of the guanylate cyclase inhibitor ODQ (Figure S2), while it was abolished after incubation with the $BK_{Ca}$ channel blocker iberiotoxin (Figure 3C). Additionally, we found that incubation with LDN 27219 was able to hyperpolarize and increase the ACh-induced hyperpolarization in the smooth muscle layer of myograph-mounted arteries in the presence of TRAM-34 and UCL 1684, being these effects abolished by the addition of iberiotoxin (Figure S3). These findings suggested that the effect of LDN 27219 takes place mainly at the SMC level by opening $BK_{Ca}$ channels and therefore

increasing its sensitivity to NO. We confirmed this hypothesis by studying the effect of LDN 27219 incubation on arteries without endothelium, where LDN 27219 also potentiated relaxations induced by the NO donor sodium nitroprusside (SNP) (Figure 3D). Contrarily, incubation with VA5 and Z-DON reduced SNP-induced vasorelaxation (Figure S4).

**Modulation towards TG2 closed conformation induces $BK_{Ca}$ channel opening in SMCs.**

To further understand the role of potassium channels and TG2 conformational changes in the effect of LDN 27219, voltage-clamp studies were performed on SMCs freshly isolated from rat small mesenteric arteries. LDN 27219 markedly enhanced outward potassium currents reaching its maximum effect at 12 min (Figure 4A). In agreement with our previous results, this effect was reduced in SMCs that had been incubated with iberiotoxin. Moreover, a small part of the remaining LDN 27219-elicited potassium current under $BK_{Ca}$ channel blockage was sensitive to the Kv7 channel blocker, XE991 (Figure 4B). Thus, in addition to a major role of $BK_{Ca}$ channels, these results suggest a minor role for Kv7 channels in LDN 27219 vasorelaxation.

We also tested how the conformational modulation of TG2 affected LDN 27219-elicited increases in potassium currents of isolated SMCs. Induction of the TG2 open conformation with VA5, reduced the current density of SMCs compared to control conditions (Figure S5) and completely inhibited the enhancement of potassium currents by LDN 27219 (Figure 4C). GTP, GDP and ATP have been shown to dock TG2 and inducing its closed conformation. SMCs exposed to $Na_2GTP$ in the intracellular solution, showed higher current densities than SMCs under control conditions (Figure S5). This was similar to the potassium current recorded from SMCs stimulated with LDN 27219, and addition of LDN 27219 did not cause further enhancement of these currents (Figure 4D). Taken together, these results suggest that LDN 27219 mimics the effect of GTP by promoting the closed conformation of TG2 and

opens $BK_{Ca}$ channels, while the open conformation of TG2 slightly decrease the activation of $BK_{Ca}$ channels.

**Pharmacological induction of TG2 closed conformation leads to *ex vivo* and *in vivo* age-dependent BP-lowering effects.**

Previous studies suggest the involvement of TG2 in age-related cardiovascular complications.[1,3] To study the effect of age on the potentiation of endothelial function by LDN 27219, we used small mesenteric arteries from 6-7 and 35-40-week-old rats. Arteries from 6-7-week-old rats presented similar responses to ACh and SNP compared to the 12-14-week-old rats. Contrarily, the arteries from rats at 35-40 weeks of age, showed slightly reduced endothelial function and less response to SNP (Table S2). Incubation with LDN 27219 for 20 min produced a potentiation of the response to ACh only in arteries from older animals (Figure 5A-B). The response to SNP in arteries without endothelium was potentiated by incubation with LDN 27219 in both age groups (Fig 5C-D). The differences on area under the curve (AUC) of the responses to ACh and to SNP between vehicle-incubated and LDN 27219-incubated arteries were bigger in rats at 35-40 weeks of age compared to younger rats (Figure 5E and Figure S6). Neither the expressions of TG2, $BK_{Ca}$ alpha nor beta subunits were increased in arteries from older rats in comparison with younger rats (Figure S7), but arteries from 35-40-week-old rats presented increased transamidase activity (Figure 5F), suggesting a larger amount of functional TG2 in the open conformation in arteries from older animals.

*In vivo* intravenous administration of LDN 27219 in anesthetized rats at 12-14 and 35-40 weeks of age induced dose-dependent decreases in MAP that was maintained throughout the 3 min of infusion. This was followed by a transient raise over the baseline immediately after the end of drug administration (Figure 6A) without having any effect neither on HR compared to the vehicle (Figure S8) nor on electrocardiographic parameters (Table S3).

Infusion of the corresponding vehicle (polyethylene glycol 400) slightly increased MAP at the highest dose (Figure 6A) although it reduced HR (Figure S8). Rats at 35-40 weeks of age showed a tendency to higher basal MAP compared with 12-14-week-old rats (111.40 ± 5.55 vs. 97.20 ± 4.02 in mmHg, n=11-15. p=0.065 using unpaired t-test) as well as to lower HR (348.7 ± 9.88 vs. 374.7 ± 10.93 in beats per min, n=11-15. p=0.093 using unpaired t-test). There were not differences in the measured ECG parameters between both age groups. Responses to increasing doses of LDN 27219 had significantly larger AUCs in 35-40-week-old rats compared to 12-14-week-old rats (Figure 6C). This indicates greater effects on BP in older rats, being consistent with *ex vivo* measurements. Infusion of a single dose of VA5 failed to change MAP (Figure 6B-C).

## DISCUSSION

There are three major findings of the present investigation. First, we provide direct evidence that LDN 27219 promotes the closed conformation of TG2 using native-PAGE studies. Secondly, our findings suggest that LDN 27219 by promoting the closed conformation leads to vasodilation and improves endothelium-dependent relaxation in rat and human resistance arteries which is in contrast to the effect of the inhibitors that lock TG2 open, VA5[15] and Z-DON,[14] hence suggesting the effect of vascular tone is independent of TG2 transamidase activity. This points to a mechanism where the closed conformation of TG2 in the smooth muscle layer couples to opening of $BK_{Ca}$ channels. Thirdly, we provide evidence that promoting the closed conformation of TG2 leads to improved endothelium-dependent relaxation of resistance arteries and blood pressure lowering in an age-dependent manner.

Recent studies have shown that only endothelium-intact aortic rings from TG2 knockout mice are more sensitive to Phe-induced contraction compared to arotic rings from wild type mice, being this difference absent in arteries without endothelium. The difference in sensitivity to

Phe endothelium-intact aortic rings from TG2 knockout mice was reversed by the addition of external TG2 independently of its transamidase activity.[9] These results might be explained by patch-clamp studies reporting that, in the presence of GTP, TG2 is able directly to open $BK_{Ca}$ channels in vascular SMCs,[23] which would lead to hyperpolarization and vasodilation. Our findings in human and rat arteries provide a mechanistic explanation for these findings. We observed a potentiation of ACh-induced vasorelaxation after incubation with LDN 27219, which stabilizes the close conformation of TG2. In contrast, the cell permeable irreversible inhibitors VA5 and Z-DON, which lock TG2 in the open conformation of TG2,[14,15] had the opposite effect, reducing ACh-induced and SNP-induced vasorelaxations. Meanwhile, the non-permeable cell inhibitor Boc-DON failed to significantly change ACh-induced vasorelaxation. These results suggest a link between the closed conformation of intracellular TG2 and increased endothelium-dependent vasorelaxation, which is independent of the transamidase activity of the enzyme.

There are several lines of evidence supporting that LDN 27219 affects vascular tone by a specific action on TG2 conformation. First, LDN 27219 induces the TG2 closed conformation similarly to GTP in the native-PAGE studies. Second, previous findings have shown that GTP-bound TG2 opens $BK_{Ca}$ channels,[23] and addition of LDN 27219 in the presence of intracellular GTP, failed to further increase potassium conductance in isolated SMCs suggesting a common mechanism of action for LDN 27219 and GTP. Third, we observed that SMCs incubated with VA5, an irreversible TG2 inhibitor that locks the enzyme in its open conformation,[15] presented smaller potassium currents than under control conditions that were insensitive to LDN 27219. Therefore, our findings show that LDN 27219 by promoting the closed conformation of TG2 leads to activation of $BK_{Ca}$ channels and increased sensitivity to endothelium-derived NO.

TG2 plays an important role in several age-related alterations in the cardiovascular system.[1,3] In large arteries, the decrease in NO bioavailability related to aging has been associated with an increased externalization of TG2 and over-activation of its transamidase activity leading to increased vascular stiffness in both rats and humans.[1,9,24] However, no significant changes in TG2 expression in aging arteries were found.[1] This can be explained by S-nitrosation and redox status of TG2 that regulates TG2 activation and trafficking.[1,5,24] In agreement, we found increased transamidase activity without a significant TG2 expression increase in arteries from 35-40-week-old rats, which presented reduced ACh- and SNP-induced vasorelaxations compared to younger rats, suggesting decreased NO-bioavailability and sensitivity. Accordingly, these arteries from older rats showed an increased potentiation of ACh-derived vasorelaxation by LDN 27219. These results suggest that an increased amount of TG2 in the open conformation due to reduced NO-bioavailability may play a role in early age-dependent changes in endothelial function. This could however be alleviated by the modulation of TG2 to its closed conformation.

Contrarily to cystamine, several active-site directed TG2 inhibitors have shown no effect on BP nor HR when administered *in vivo* in mice.[25,26] In the present study, intravenous infusion of LDN 27219 caused a dose-dependent decrease in MAP in anesthetized rats. Analysis of LDN 27219 pharmacokinetics in male C57BL/6 mice showed that the half-life of the compound in blood is approximately 5 h (data not shown). This suggests that the rapid reversal of the effect of LDN 27219 on MAP is due to compensatory sympathetic vasoconstriction rather than degradation or excretion of the compound. In agreement with the potentiating effect *ex vivo*, the AUC of the decrease in MAP caused by LDN 27219 was larger in the 35-40-week-old than in the 12-14-week-old rats, These findings support a role of TG2 in early age-dependent changes of vascular function, and that TG2 conformation plays

an important role for regulation of BP independently of its transamidase activity, since VA5 failed to change BP.

*Limitations*

In addition to TG2, TG1 and TG4 have been found in rat aorta and vena cava.[27] In rat small mesenteric arteries, we only detected a marked expression of TG2 and a weak band for TG1 in RT-PCR studies but no TG1 protein was detected by immunoblotting.[8] Although little is known about the selectivity of LDN 27219 against other transglutaminases, analysis of other hydrazide inhibitors from the same family showed a high selectivity for TG2 and TG3.[28] TG3 is mainly located in the epidermis[29] as well as in the ear and testes of the rat.[8] Considering that observed *ex vivo* effects of LDN 27219 on arteries and isolated SMCs were completely inhibited by other selective TG2 inhibitors, it seems unlikely that the inhibition of other transglutaminases or off-target mechanisms contribute to the BP lowering *in vivo* induced by LDN 27219.

**PERSPECTIVES**

In conclusion, our study suggests that LDN 27219 is able to modify the dynamic equilibrium of TG2 towards the closed conformation, leading to direct relaxation and potentiation of NO-dependent vasorelaxation by positive modulation of the $BK_{Ca}$ channels in SMCs. These effects are present in rats and human resistance arteries and seem to increase with animal aging. Besides the role of TG2 in the development of vascular stiffness,[1,2,9] elevated amounts of TG2 in its open conformation might also participate in age-related endothelial dysfunction. A potential strategy to reverse this is by pharmacological modulation of TG2 to its closed conformation.

## ACKNOWLEDGEMENTS

We thank laboratory technician Heidi Schou Knudsen for performing the immunoblotting for TG2 and $BK_{Ca}$ channel alpha and beta subunits. We thank Ms. Diana Feiteira for her technical assistance.

## SOURCES OF FUNDING

U. Simonsen was supported by grants from the Danish Heart Foundation (16-R107-A6681-22967), the NovoNordisk Foundation (NNF130C0007739; NNF190C0055688), and the Danish Research Council (DFF-6110-00622B). N.H. Buus was supported by Aarhus University Research Foundation (AUFF-F-2018-7-2).

## DISCLOSURES

None.

## REFERENCES

1. Santhanam L, Tuday EC, Webb AK, Dowzicky P, Kim JH, Oh YJ, Sikka G, Kuo M, Halushka MK, MacGregor AM, et al. Decreased S-nitrosylation of tissue transglutaminase contributes to age-related increases in vascular stiffness. *Circ Res*. 2010;107:117-125. doi:10.1161/CIRCRESAHA.109.215228
2. Jung SM, Jandu S, Steppan J, Belkin A, An SS, Pak A, Choi EY, Nyhan D, Butlin M, Viegas K, Avolio A, Berkowitz DE, Santhanam L. Increased tissue transglutaminase activity contributes to central vascular stiffness in eNOS knockout mice. *Am J Physiol Heart Circ Physiol*. 2013;305:H803-10. doi:10.1152/ajpheart.00103.2013
3. Oh YJ, Pau VC, Steppan J, Sikka G, Bead VR, Nyhan D, Levine BD, Berkowitz DE,

Santhanam L. Role of tissue transglutaminase in age-associated ventricular stiffness. *Amino Acids*. 2016;49:695-704. doi:10.1007/s00726-016-2295-z

4. Bakker ENTP, Pistea A, Spaan JAE, Rolf T, De Vries CJ, Van Rooijen N, Candi E, Vanbavel E. Flow-dependent remodeling of small arteries in mice deficient for tissue-type transglutaminase: Possible compensation by macrophage-derived factor XIII. *Circ Res*. 2006;99:86-92. doi:10.1161/01.RES.0000229657.83816.a7

5. van den Akker J, VanBavel E, van Geel R, Matlung HL, Guvenc Tuna B, Janssen GMC, van Veelen PA, Boelens WC, de Mey JGR, Bakker ENTP. The redox state of transglutaminase 2 controls arterial remodeling. *PLoS One*. 2011;6:e23067. doi:10.1371/journal.pone.0023067

6. Lee Y-J, Jung S-H, Kim S-HS-Y, Kim M-S, Lee S, Hwang J, Kim S-HS-Y, Kim Y-M, Ha K-S. Essential Role of Transglutaminase 2 in Vascular Endothelial Growth Factor–Induced Vascular Leakage in the Retina of Diabetic Mice. *Diabetes*. 2016;65:2414-2428. http://diabetes.diabetesjournals.org/content/65/8/2414.abstract.

7. Lee J-Y, Lee Y-J, Jeon H-Y, Han E-T, Park WS, Hong S-H, Kim Y-M, Ha K-S. The vicious cycle between transglutaminase 2 and reactive oxygen species in hyperglycemic memory–induced endothelial dysfunction. *FASEB J*. 2019;33:12655-12667. doi:10.1096/fj.201901358rr

8. Engholm M, Pinilla E, Mogensen S, Matchkov V, Hedegaard ER, Chen H, Mulvany MJ, Simonsen U. Involvement of transglutaminase 2 and voltage-gated potassium channels in cystamine vasodilatation in rat mesenteric small arteries. *Br J Pharmacol*. 2016;173:839-855. doi:10.1111/bph.13393

9. Steppan J, Bergman Y, Viegas K, Armstrong D, Tan S, Wang H, Melucci S, Hori D, Park SY, Barreto SF, et al. Tissue transglutaminase modulates vascular stiffness and

function through crosslinking-dependent and crosslinking-independent functions. *J Am Heart Assoc*. 2017;6:e004161. doi:10.1161/JAHA.116.004161

10. Sane DC, Kontos JL, Greenberg CS. Roles of transglutaminases in cardiac and vascular diseases. *Front Biosci*. 2007;12:2530-2545. doi:2253 [pii]

11. Eckert RL, Kaartinen MT, Nurminskaya M, Belkin AM, Colak G, Johnson GVW, Mehta K. Transglutaminase regulation of cell function. *Physiol Rev*. 2014;94:383-417. doi:10.1152/physrev.00019.2013

12. Han BG, Cho JW, Cho YD, Jeong KC, Kim SY, Lee B Il. Crystal structure of human transglutaminase 2 in complex with adenosine triphosphate. *Int J Biol Macromol*. 2010;47:190-195. doi:10.1016/j.ijbiomac.2010.04.023

13. Nurminskaya M V., Belkin AM. Cellular Functions of Tissue Transglutaminase. *Int Rev Cell Mol Biol*. 2012;294:1-97. doi:10.1016/B978-0-12-394305-7.00001-X

14. Lindemann I, Heine A, Klebe G. Transglutaminase 2 in complex with a novel inhibitor. *PDB ID 3S3J*.:10.2210/pdb3S3J/pdb.

15. Mironov GG, Clouthier CM, Akbar A, Keillor JW, Berezovski M V. Simultaneous analysis of enzyme structure and activity by kinetic capillary electrophoresis-MS. *Nat Chem Biol*. 2016;12:918-922. doi:10.1038/nchembio.2170

16. Keillor JW, Apperley KYP, Akbar A. Inhibitors of tissue transglutaminase. *Trends Pharmacol Sci*. 2015;36:32-40. doi:10.1016/j.tips.2014.10.014

17. Case A, Stein RL. Kinetic analysis of the interaction of tissue transglutaminase with a nonpeptidic slow-binding inhibitor. *Biochemistry*. 2007;46:1106-1115. doi:10.1021/bi061787u

18. Fisher O. Subcloning, Enzymatic Characterization, and in silico Docking of Transglutaminase 2. 2009. http://hdl.handle.net/10192/23253.

19. National Research Council (US) Committee for the Update of the Guide for the Care and Use of Laboratory Animals. *Guide for the Care and Use of Laboratory Animals*. 8th ed. (National Academies Press, ed.). Washington, DC; 2011. doi:10.17226/12910

20. Pinkas DM, Strop P, Brunger AT, Khosla C. Transglutaminase 2 undergoes a large conformational change upon activation. *PLoS Biol*. 2007;5:2788-2796. doi:10.1371/journal.pbio.0050327

21. Iversen R, Mysling S, Hnida K, Jørgensen TJD, Sollid LM. Activity-regulating structural changes and autoantibody epitopes in transglutaminase 2 assessed by hydrogen/deuterium exchange. *Proc Natl Acad Sci U S A*. 2014;111:17146-17151. doi:10.1073/pnas.1407457111/-/DCSupplemental

22. Corydon KK, Matchkov V, Fais R, Abramochkin D, Hedegaard ER, Comerma-Steffensen S, Simonsen U. Effect of ischemic preconditioning and a Kv7 channel blocker on cardiac ischemia-reperfusion injury in rats. *Eur J Pharmacol*. 2020;866. doi:10.1016/j.ejphar.2019.172820

23. Lee MY, Chung S, Bang HW, Baek KJ, Uhm D. Modulation of large conductance Ca2+-activated K+ channel by Galphah (transglutaminase II) in the vascular smooth muscle cell. *Pflugers Arch*. 1997;433:671-673. doi:10.1007/s004240050330

24. Jandu SK, Webb AK, Pak A, Sevinc B, Nyhan D, Belkin AM, Flavahan NA, Berkowitz DE, Santhanam L. Nitric oxide regulates tissue transglutaminase localization and function in the vasculature. *Amino Acids*. 2013;44:261-269. doi:10.1007/s00726-011-1090-0

25. Wang Z, Stuckey DJ, Murdoch CE, Camelliti P, Lip GYH, Griffin M. Cardiac fibrosis can be attenuated by blocking the activity of transglutaminase 2 using a selective small-molecule inhibitor. *Cell Death Dis*. 2018;9:613. doi:10.1038/s41419-018-0573-2

26. Shinde A V., Su Y, Palanski BA, Fujikura K, Garcia MJ, Frangogiannis NG. Pharmacologic inhibition of the enzymatic effects of tissue transglutaminase reduces cardiac fibrosis and attenuates cardiomyocyte hypertrophy following pressure overload. *J Mol Cell Cardiol*. 2018;117:36-48. doi:10.1016/j.yjmcc.2018.02.016

27. Johnson KB, Petersen-Jones H, Thompson JM, Hitomi K, Itoh M, Bakker ENTP, Johnson GVW, Cola G, Watts SW. Vena cava and aortic smooth muscle cells express transglutaminases 1 and 4 in addition to transglutaminase 2. *Am J Physiol - Hear Circ Physiol*. 2012;302:1355-1366. doi:10.1152/ajpheart.00918.2011

28. Schaertl S, Prime M, Wityak J, Dominguez C, Munoz-Sanjuan I, Pacifici RE, Courtney S, Scheel A, Macdonald D. A profiling platform for the characterization of transglutaminase 2 (TG2) inhibitors. *J Biomol Screen*. 2010;15:478-487. doi:10.1177/1087057110366035

29. Aeschlimann D, Koeller MK, Allen-Hoffmann BL, Mosher DF. Isolation of a cDNA encoding a novel member of the transglutaminase gene family from human keratinocytes. Detection and identification of transglutaminase gene products based on reverse transcription-polymerase chain reaction with degenerate primers. *J Biol Chem*. 1998;273:3452-3460. doi:10.1074/jbc.273.6.3452

## NOVELTY AND SIGNIFICANCE

### What is new?

- Promotion of the closed conformation of transglutaminase 2 (TG2) in the vasculature by the reversible inhibitor LDN 27219 is linked with: a direct vasorelaxant effect, an increased nitric oxide sensitivity in the vascular smooth muscle caused by opening of

potassium channels, which potentiates endothelium-derived vasorelaxation, as well as a blood pressure lowering effect during intravenous infusion.

- Contrarily, TG2 inhibitors locking the open conformation fail to change vascular tone, reduce endothelium-dependent vasorelaxation and do not lower blood pressure.
- Arteries from older animals have more TG2 in its open conformation, which translates in stronger vasoprotective effects of pharmacological induction of the TG2 closed conformation with aging.

**What is relevant?**

- The open conformation of TG2 presents transamidase activity, which is profibrotic and linked to age-related vascular alterations.
- TG2 inhibitors promoting the closed conformation might offer extensive vascular protection by inhibition of transamidase activity, improvement of endothelial function and lowering of blood pressure.

**Summary**

In isolated small arteries from rats and humans, promotion of the closed conformation of transglutaminase 2 (TG2) by LDN 27219 resulted in direct vasorelaxation and increased endothelium-dependent vasorelaxation by opening of smooth muscle potassium channels. Infusion of LDN 27219 in anesthesized rats induced concentration-dependent blood pressure lowering. Both the *in vitro* and *in vivo* effects increased with the age of the animal, and correlated with an increased TG2 transamidase activity in the arteries.

**FIGURES**

**Figure 1**

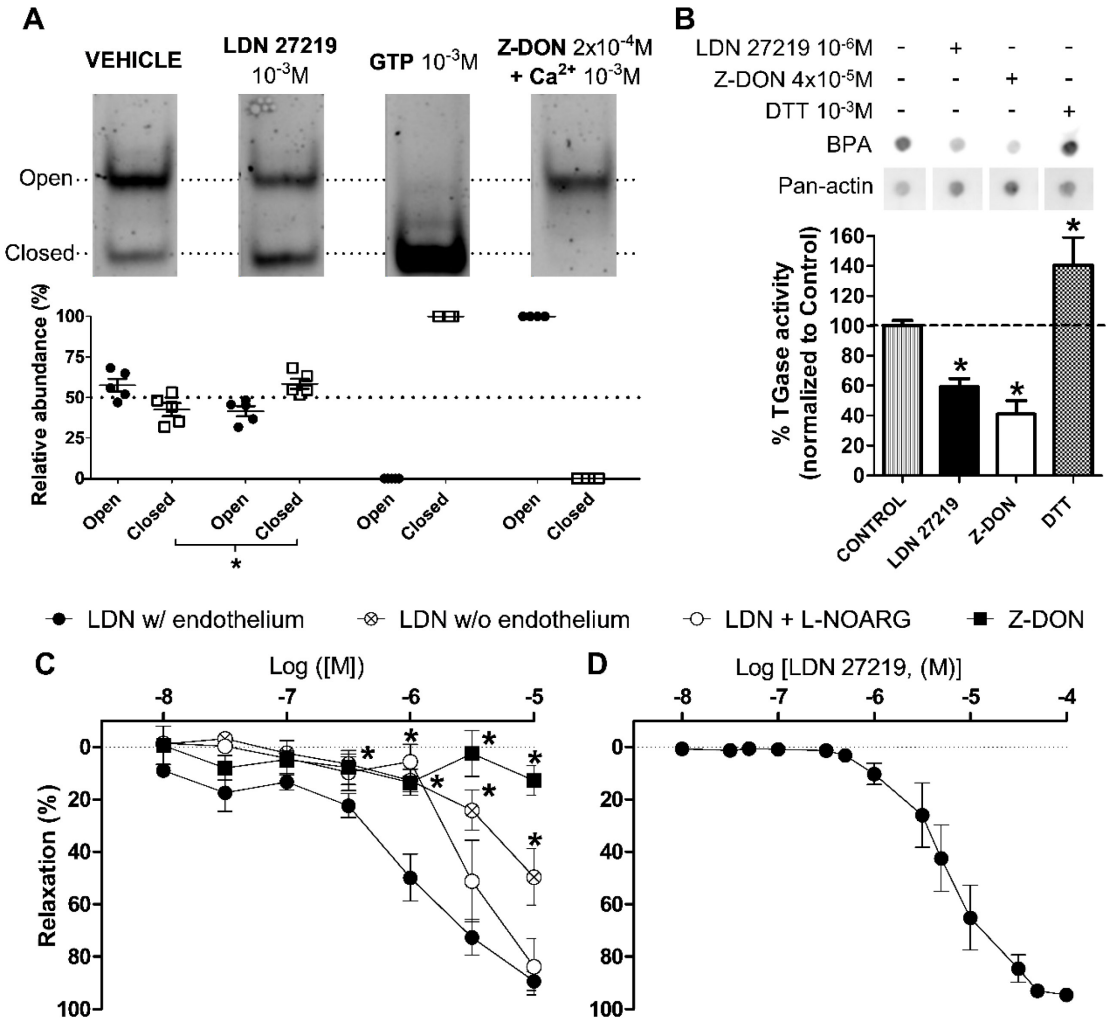


**Figure 1. Effects of pharmacological modulation of tissue transglutaminase (TG2) conformation on vessel tension *ex vivo*. A.** Native-PAGE conformational study of recombinant human TG2. Top panel: representative blots from the same gel after electrophoresis of purified TG2 treated with different effectors. Bottom: average relative abundance (presented as % of total intensity) of the two visible bands, corresponding to the open and to the closed conformation of the enzyme. Data are means ± SEM. *, $P<0.05$ using paired two-tailed Student´s t-test**,** $n=5$ replicates in 4 gels. **B.** Transglutaminase inhibition in mesenteric arteries by LDN 27219 and Z-DON. Top panel: Representative dot blot of 5-

biotin(amido)pentylamine (BPA) incorporation, as a measure of transamidase (TGase) activity in 12-14-week-old rat mesenteric arteries incubated under different conditions and pan-actin expression as loading control. Bottom: Average transamidase activity, as % normalized to control conditions. $n$=3-4. Data are means ± SEM. *, $P$<0.05 using one-way ANOVA with Dunnett post-test compared to control. **C.** Isometric tension studies of U46619-contracted small mesenteric arteries from male rats at 12-14 weeks of age: average concentration-response curves for LDN 27219 in the presence or absence of nitric oxide synthase inhibitor Nω-Nitro-L-arginine (L-NOARG) ($10^{-4}$ mol/L), and Z-DON. $n$=6-9. **D.** Averaged concentration-response curves for LDN 27219 in U46619-contracted subcutaneous arteries from human patients. $n$=8. Data are means ± SEM of % relaxation relative to maximum contraction. *, $P<0.05$ using two-way ANOVA with Bonferroni post-test compared to LDN 27219 in arteries with endothelium.

**Figure 2**

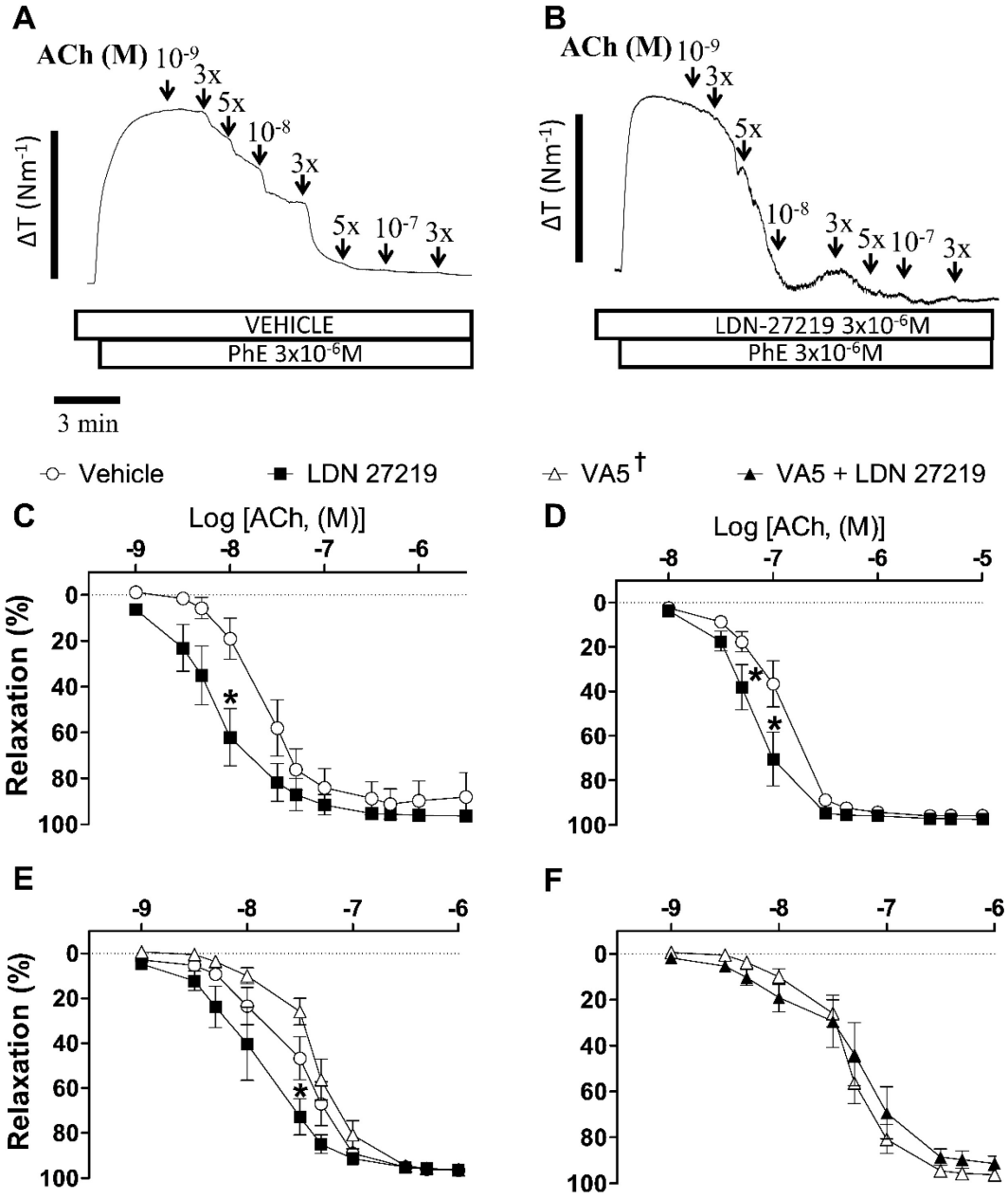


**Figure 2. Effects of pharmacological modulation of tissue transglutaminase (TG2) conformation on endothelium-dependent vasorelaxation *ex vivo*. A-B.** Original traces showing acetylcholine (ACh)-induced vasorelaxation in phenylephrine (Phe)-contracted human subcutaneous arteries after treatment with reversible TG2 inhibitor LDN 27219 ($3x10^{-6}$ mol/L) or vehicle during 20 min. **C.** Averaged concentration-response curves from the experiments shown in A-B, *n*=7. **D.** Averaged ACh concentration-response curves after

incubation with LDN 27219 ($10^{-6}$ mol/L) or vehicle in Phe-contracted small mesenteric arteries from male rats at 12-14 weeks of age, $n$=6. **E.** Averaged ACh concentration-response curves after incubation with cell-permeable irreversible inhibitor VA5 ($10^{-5}$ mol/L), which locks the open conformation of the enzyme, LDN 27219 ($10^{-6}$ mol/L) on the same set of experiments (positive control) or vehicle in Phe-contracted small mesenteric arteries from male rats $n$=4-10. **F.** Averaged ACh concentration-response curves after incubation with LDN 27219 ($10^{-6}$ mol/L) or vehicle, both in presence of VA5 ($10^{-5}$ mol/L) in Phe-contracted small mesenteric arteries from male rats. Data are means ± SEM of % relaxation relative to maximum contraction. *, $P$<0.05 using two-way ANOVA with Bonferroni post-test compared to vehicle. †, $P$<0.05 using two-way ANOVA compared to vehicle.

## Figure 3

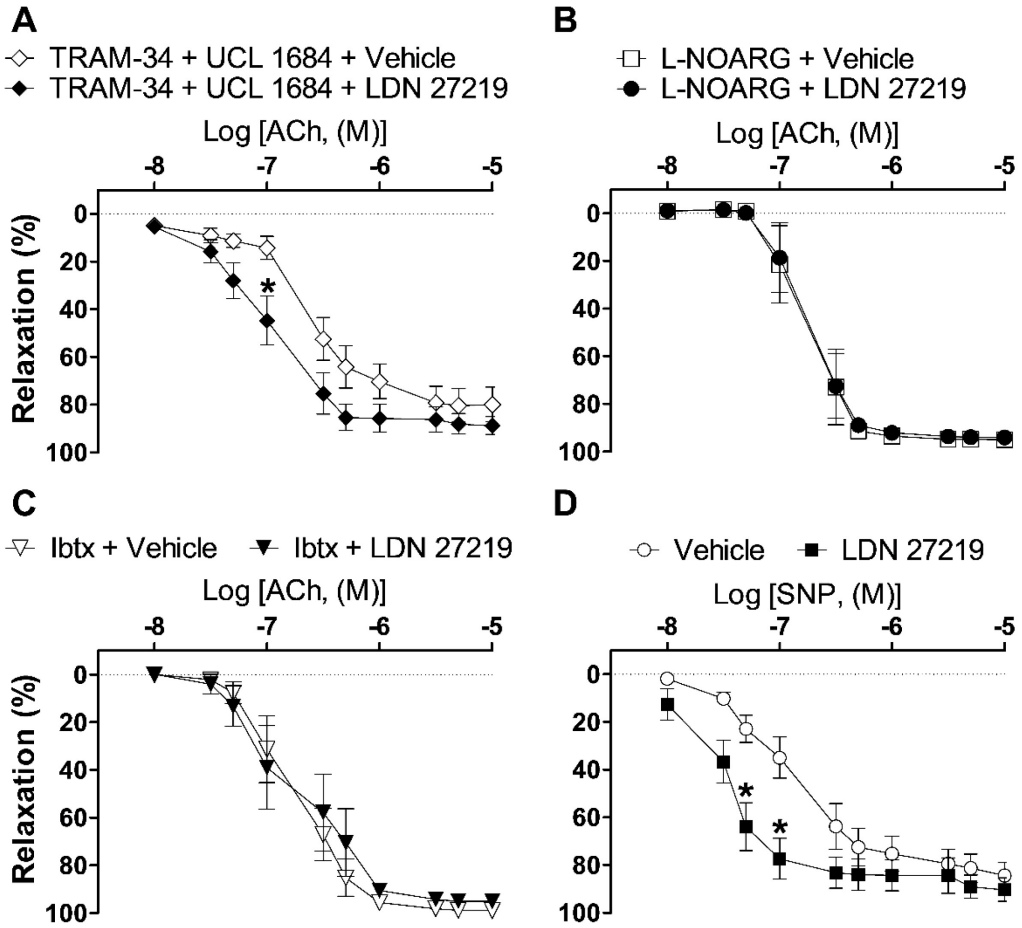


**Figure 3. Mechanisms behind the potentiation of endothelium-derived vasorelaxation by LDN 27219. A-D.** Averaged concentration-response curves for acetylcholine (ACh) in phenylephrine (Phe)-contracted small mesenteric arteries from male rats at 12-14 weeks of age, after 20 min incubation with either vehicle or LDN 27219 ($10^{-6}$ mol/L) in the presence of: **A.** TRAM-34 and UCL 1684, inhibitors of intermediate and small-conductance calcium-activated potassium channels ($IK_{Ca}$ and $SK_{Ca}$), respectively, *n*=5. **B.** Nitric oxide synthase inhibitor Nω-Nitro-L-arginine (L-NOARG), *n*=5. **C.** Large-conductance calcium-activated potassium channel **(**$BK_{Ca}$) blocker iberiotoxin, *n*=6. **D.** Averaged concentration-response curves for nitric oxide donor sodium nitroprusside (SNP) in Phe-contracted rat small mesenteric arteries without endothelium, after incubation with either vehicle or LDN 27219,

$n$=6. Data are means ± SEM of % relaxation relative to maximum contraction. *, $P$<0.05 using two-way ANOVA with Bonferroni post-test compared to vehicle.

## Figure 4

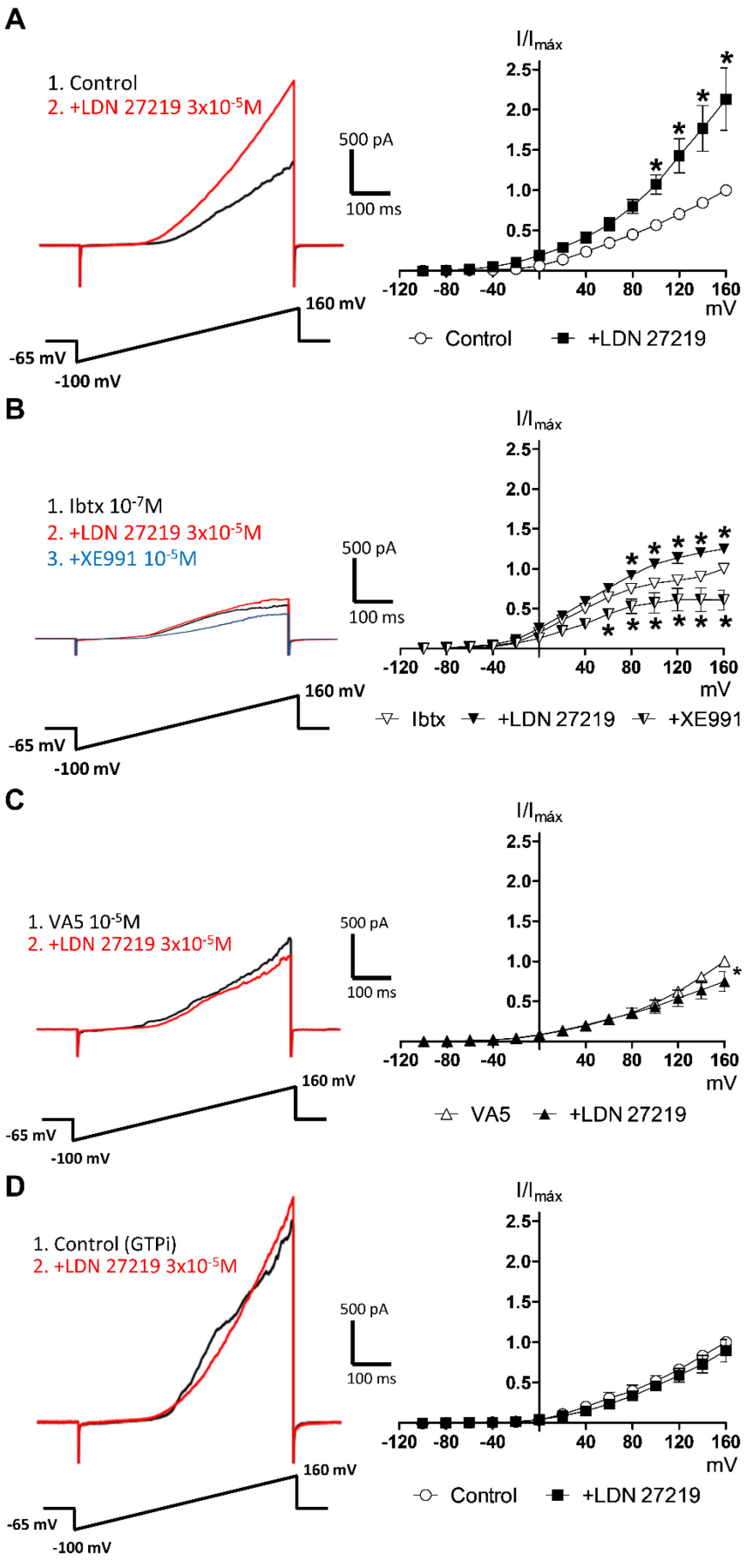
A
1. Control
2. +LDN 27219 3x10-5M
500 pA
100 ms
160 mV
-65 mV
-100 mV
I/Imáx
2.5
2.0
1.5
1.0
0.5
-120 -80 -40 40 80 120 160
mV
Control
+LDN 27219
B
1. Ibtx 10-7M
2. +LDN 27219 3x10-5M
3. +XE991 10-5M
500 pA
100 ms
160 mV
-65 mV
-100 mV
I/Imáx
2.5
2.0
1.5
1.0
0.5
-120 -80 -40 40 80 120 160
mV
Ibtx
+LDN 27219
+XE991
C
1. VA5 10-5M
2. +LDN 27219 3x10-5M
500 pA
100 ms
160 mV
-65 mV
-100 mV
I/Imáx
2.5
2.0
1.5
1.0
0.5
-120 -80 -40 40 80 120 160
mV
VA5
+LDN 27219
D
1. Control (GTPi)
2. +LDN 27219 3x10-5M
500 pA
100 ms
160 mV
-65 mV
-100 mV
I/Imáx
2.5
2.0
1.5
1.0
0.5
-120 -80 -40 40 80 120 160
mV
Control
+LDN 27219

**Figure 4. Effect of LDN 27219 on potassium currents in freshly isolated smooth mucle cells (SMCs).** Left: representative potassium currents in SMCs isolated from 12-14-week-old rat small mesenteric artery evoked by voltage-ramps between -100 and +160 mV. Right: averaged I-V relations for potassium currents from the experiments shown in the left. Effect of 12 min incubation with LDN 27219 in: **A.** Control conditions, *n*=7. **B.** Presence of large-conductance calcium-activated potassium channel **(**$BK_{Ca}$) blocker iberiotoxin before and after the addition of Kv7 channel blocker XE991, *n*=5. **C.** Presence of TG2 irreversible inhibitor VA5, which locks the enzyme in its open conformation, *n*=6. **D.** Presence of GTP in the intracellular pipette solution (GTPi), *n*=5. Data are means ± SEM of current amplitude normalized to maximal amplitude of the current under control condition ($I/I_{max}$). *, $P<0.05$ using two-way ANOVA with Bonferroni post-test compared to control.

## Figure 5

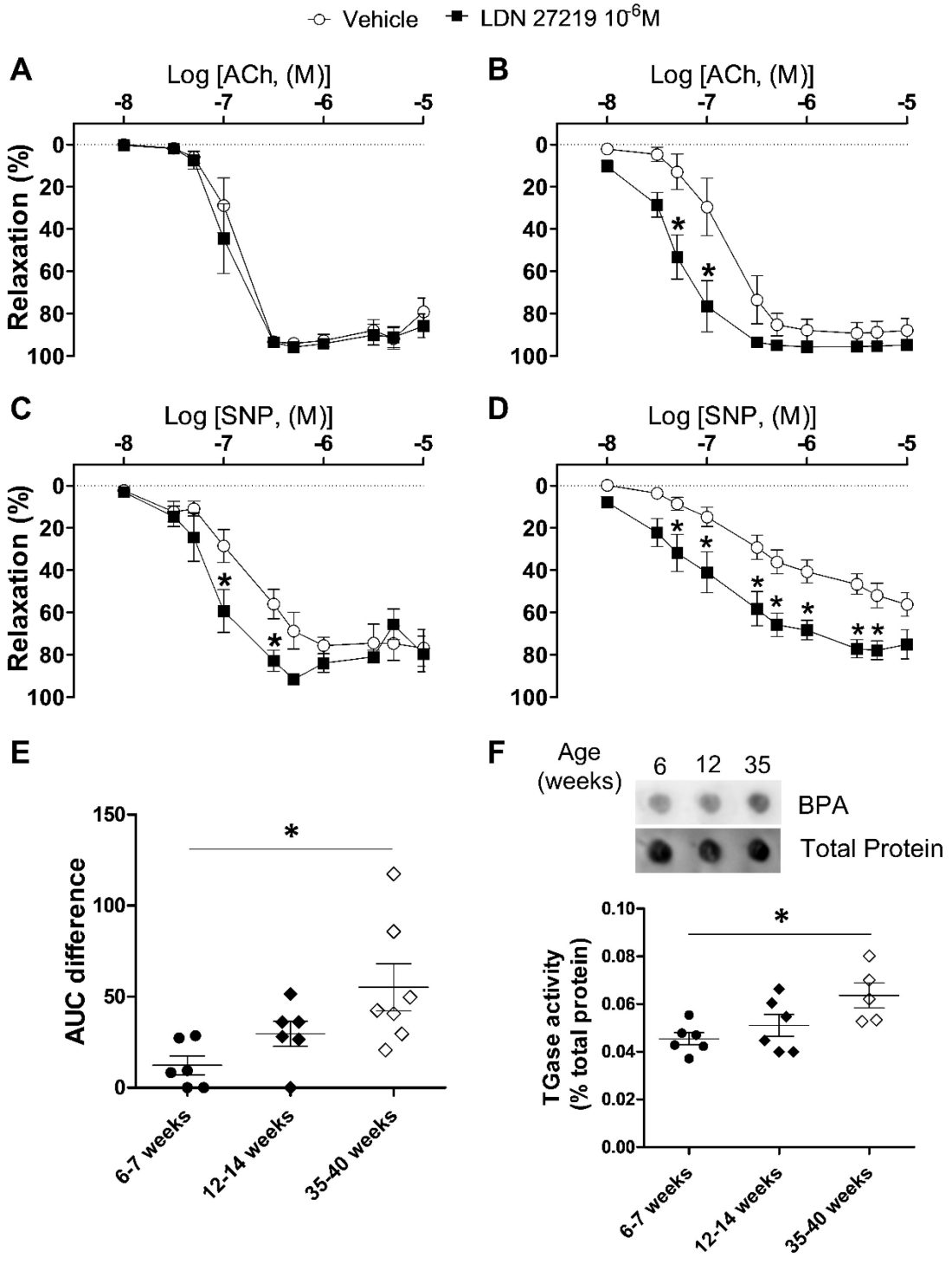


**Figure 5. Age-dependence effect on endothelial function of pharmacological modulation of tissue transglutaminase (TG2) to its closed conformation by LDN 27219.** Averaged concentration-response curves for acetylcholine (ACh) in phenylephrine (Phe)-contracted

myograph-mounted small mesenteric arteries, treated with either LDN 27219 or vehicle for 20 min, from male rats at: **A.** 6-7 weeks of age, $n$=6. **B.** 35-40 weeks of age, $n$=7. Averaged concentration-response curves for nitric oxide donor sodium nitroprusside (SNP) in Phe-contracted small mesenteric arteries without endothelium, treated with either LDN 27219 or vehicle for 20 min, from male rats at: **C.** 6-7 weeks of age, $n$=5. **D.** 35-40 weeks of age, $n$=7. Data are means ± SEM of % relaxation relative to maximum contraction. *, $P < 0.05$ using two-way ANOVA with Bonferroni post-test compared to vehicle. **E.** Averaged differences in area under the curve (AUC) of the response to ACh between vehicle-incubated and LDN 27219-incubated ($10^{-6}$ mol/L) arteries analysed individually per rat. **F.** Top panel: Representative dot blot of 5-biotin(amido)pentylamine (BPA) incorporation, as a measure of transamidase (TGase) activity in rat mesenteric arteries from the different age groups and their corresponding total protein amido-black staining. Bottom: Average TGase activity, as % of total protein in small mesenteric arteries of each age group. Data are means ± SEM. *, $P<0.05$ using one-way ANOVA with Bonferroni post-test.

**Figure 6**

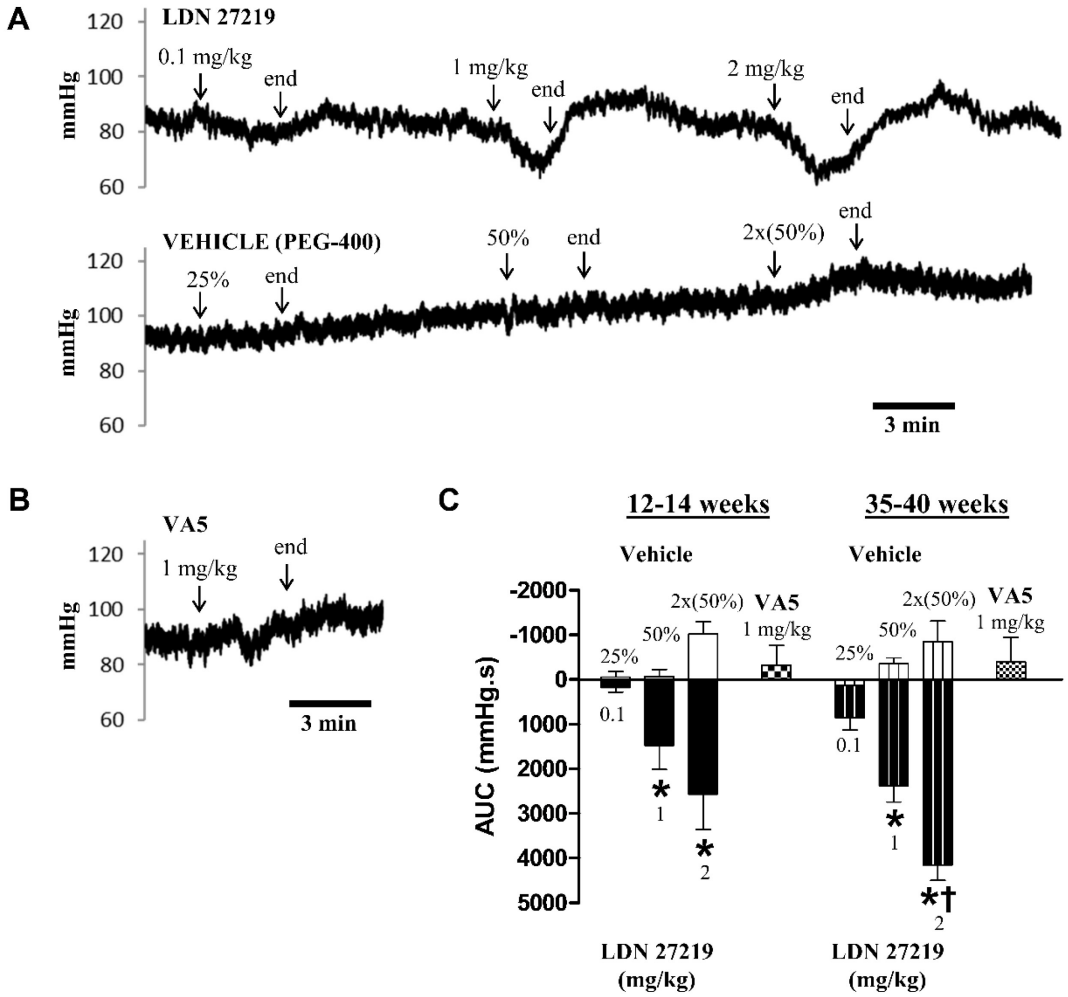


**Figure 6. Age-dependent effect on mean arterial pressure (MAP) of pharmacological modulation of tissue transglutaminase (TG2) conformation by LDN 27219 *in vivo*. A.** Representative MAP measurements of two anesthetized rats at 12 weeks of age infused with three doses of either LDN 27219 (top) or vehicle (PEG-400 = polyethylene glycol 400) (bottom) during 3 min. **B.** Representative MAP measurement of an anesthetized 12-week-old rat during the 3 min infusion of a single dose of VA5. **C**. Averaged area under the curves (AUCs) for the experiments presented in A and B for the different age groups. $n$=5-8. Data are means ± SEM of AUC (mmHg•s). Negative AUCs indicate contraction. *, $P$<0.05 using two-way ANOVA with Bonferroni post-test compared to Vehicle. † $P$<0.05 using two-way ANOVA with Bonferroni post-test compared to 12-14-week-old.

**ONLINE DATA SUPPLEMENT**

# The transglutaminase 2 inhibitor LDN 27219 age-dependently lowers blood pressure and improves endothelium-dependent vasodilation in resistance arteries.

Estéfano Pinilla MPharm. [1,2], Simon Comerma-Steffensen DVM. MSc. PhD[1,3], Judit Prat-Duran MSc.[1], Luis Rivera DVM . PhD[2], Vladimir Matchkov MSc. PhD[1], Niels Henrik Buus MD. PhD[1,4], Ulf Simonsen MD. PhD[1]

[1]Department of Biomedicine, Pulmonary and Cardiovascular Pharmacology, Aarhus University, Denmark; [2]Departament of Physiology, Faculty of Pharmacy, Complutense University of Madrid, Spain; [3]Department of Biomedical Sciences/ Animal Physiology, Veterinary Faculty, Central University of Venezuela, Maracay, Aragua, Venezuela; [4]Department of Renal Medicine, Aarhus University Hospital, Denmark

## DETAILED METHODS

### Animals and tissue preparation:

Male Wistar rats at 6-7, 12-14 and 35-40 weeks of age, weighing 200-250, 300-400 and 600-700 g, respectively, were obtained from Taconic Denmark ApS (Rye, Denmark) and housed in the animal facility of Aarhus University in cages (Universal Euro III type Long) with standard wood bedding and space for two rats. There was a 12 h cycle of light and dark, and rats were maintained on standard chow and water *ad libitum*. Human subcutaneous arteries were obtained from fat biopsies of the gluteal region from both male and female Caucasian patients (30-70 years of age) with or without essential hypertension. A list of patient characteristics can be seen in Table S1. For '*ex vivo*' studies, animals were randomly selected and euthanized by decapitation and exsanguination following the NIH guidelines for the care and use of laboratory animals.[1] The mesenteric bed was immediately extracted and placed in 4ºC physiological saline solution (PSS, pH= 7.4) of the following composition (mmol/L): 119 NaCl, 4.7 KCl, 1.18 $KH_2PO_4$, 1.17 $MgSO_4$, 1.5 $CaCl_2$, 24.9 $NaHCO_3$, 0.026 EDTA and 5.5 glucose. Mesenteric second-order branches (internal diameters of 200-300 μm) were isolated. Human subcutaneous arteries (internal diameters of 300-400 μm) were dissected from the biopsies under the same conditions as mentioned above for the rat mesenteric arteries. For '*in vivo*' experiments animals were fasted 8 h before anesthesia with 35 mg/kg of S-ketamine and 50 mg/kg of pentobarbital sodium administered intraperitoneally. Animal protocols and care were approved by the Danish Animal Experiments Inspectorate (permission 2014-15-2934-0159) and followed the NIH guidelines. The study using human arterial tissue was approved by the Regional Ethics Committee, Central Denmark (permission 1-10-72-120-17) and conducted in accordance with the principles of the Helsinki Declaration II for medical research. All participants gave informed consent prior to participation.

### Native-PAGE

Purified and functional human TG2 protein produced in insect cells was obtained from Zedira (Darmstadt, Germany) and native gel electrophoresis experiments were performed using a method similar to those previously described.[2,3] Briefly, TG2 ($2.5x10^{-6}$ mol/L) was incubated for 30 min at room temperature in buffer (75 mmol/L imidazole, 0.5 mmol/L EDTA, 5 mmol/L DTT [pH 7.2], 10% DMSO) with or without $GTPNa_2$ ($10^{-3}$ mol/L) or LDN 27219 ($10^{-3}$ mol/L ) before adding Native Sample Buffer for Protein Gels (Bio-Rad) or in preincubation buffer with Z-DON ($2x10^{-4}$ mol/L) 30 min prior addition of $CaCl_2$ ($5x10^{-3}$ mol/L) for 20 min. Native sample buffer was added (dilution 1:2), and 1.5 μg of protein was loaded onto a 4–20% Criterion™ TGX Stain-Free™ gel (Bio-Rad) using Tris-glycine (Bio-Rad) as the running buffer. For 75 min, 125 V was applied at 4 ºC. The bands were visualized using stain-free technology by exposing the gels to UV light and capturing the image using a PXi 4 Touch image analysis system (Syngene). Band intensity analysis was carried out using GeneTools 4 software (Syngene) and results were expressed as relative abundance of the two observable bands, corresponding to the open and the closed conformation of TG2, in each lane.

**Isometric tension studies**

Small mesenteric arteries and human subcutaneous arteries (approximately 2 mm length) were mounted in microvascular myographs (Danish Myotechnology, Aarhus, Denmark) using two 40 μm wires and stretched to their optimal diameter for isometric tension recordings, which corresponded to 0.9 times the estimated internal diameter at 100 mmHg of transmural pressure.[4] PSS solution in the myograph bath was heated to 37ºC and continuously bubbled with 5% $CO_2$,-75% $N_2$-20% $O_2$ to maintain pH (7.4). The vessel viability was tested at the beginning of each experiment by measuring the vasoconstrictor responses to a solution with a high $K^+$ concentration (KPSS), equivalent to PSS except that NaCl was exchanged for KCl on an equimolar basis, giving a final concentration of 123.7 mmol/L $K^+$ and the presence of endothelium was confirmed by addition of acetylcholine (ACh) ($10^{-5}$ mol/L) after pre-constriction with noradrenaline ($5 \cdot 10^{-6}$ mol/L), arteries with less than 75% of relaxation were discarded.

Mesenteric arteries from rats were pre-contracted with the thromboxane analogue, U46619 ($4x10^{-7}$ mol/L) and concentration-response curves for TG2 specific inhibitors, LDN 27219 ($10^{-8}$-$10^{-5}$ mol/L) and Z-DON ($10^{-10}$-$3x10^{-5}$ mol/L) were constructed. To study the role of the endothelial pathways in relaxation, concentration-response curves for LDN 27219 were constructed in the presence of an eNOS inhibitor, Nω-Nitro-L-arginine (L-NOARG) ($10^{-4}$ mol/L), and in arteries whose endothelium had been removed mechanically by rubbing the lumen repeatedly with a human scalp hair. Successful endothelial removal was examined by absence of relaxation to ACh ($10^{-5}$ mol/L). Human subcutaneous arteries were contracted with U46619 ($3x10^{-8}$ mol/L) and concentration-response curves for LDN 27219 ($10^{-8}$-$10^{-4}$ mol/L) were constructed.

To investigate the effect of TG2 conformational modulation in endothelial function, arteries from animals of different ages were contracted with Phenylephrine (Phe) ($10^{-5}$ mol/L). Afterwards, ACh concentration-response curves were constructed after 25 min incubation with LDN 27219 ($10^{-6}$ mol/L) together with 1 h incubation of the irreversible TG2 inhibitors: Z-DON ($4x10^{-5}$ mol/L), Boc-DON ($10^{-5}$ mol/L) or VA5 ($10^{-5}$ mol/L) which had shown to lock the enzyme in its open conformation,[24] or with vehicle (DMSO). Differences in incubation time account for the different membrane permeability of the compounds. Human subcutaneous arteries were contracted with Phe ($3x10^{-6}$ mol/L) and ACh concentration-response curves were constructed after 25 min incubation with LDN 27219 ($3x10^{-6}$ mol/L) or with vehicle.

To investigate the endothelial pathways involved in potentiation of endothelium-dependent vasodilation in arteries from rats, concentration-response curves for ACh were constructed in the absence and the presence of LDN 27219 plus blockers of small and intermediate conductance calcium-activated potassium channels ($SK_{Ca}$ and $IK_{Ca}$) UCL 1684 ($10^{-6}$ mol/L) and TRAM-34 ($10^{-6}$ mol/L), respectively, L-NOARG ($10^{-4}$ mol/L), large conductance calcium-activated potassium channel ($BK_{Ca}$) blocker iberiotoxin ($10^{-7}$ mol/L), or the guanylate cyclase inhibitor ODQ ($3 \cdot 10^{-6}$ mol/L).

To assess if effects observed were mainly at the smooth muscle cell level, concentration-response curves for the NO donor sodium nitroprusside (SNP) ($10^{-8}$-$10^{-5}$ mol/L) were also constructed in presence and absence of LDN 27219 in rat arteries whose endothelium had been removed by rubbing the lumen with a human scalp hair.

Relaxations were expressed as percentage relative to the contraction level and differences in Area Under the Curve (AUC) for ACh and SNP responses between vehicle-incubated arteries and LDN 27219-incubated arteries were calculated for each age group using Graphpad Prism 7.2 (GraphPad Software, San Diego, California, USA).

### *'Ex vivo'* transamidase activity assay

To measure transamidase activity *'ex vivo'*, a dot blot assay based on the incorporation of the tranglustaminase substrate 5-(biotinamido)pentylamine (BPA) to structural proteins was used as previously described.[5] Small mesenteric arteries from rats of the different age groups were dissected and immediately incubated in PSS containing BPA ($10^{-4}$ mol/L) and an increased concentration of $Ca^{2+}$ ($2.5x10^{-3}$ mol/L) at 37ºC for 4 h. During incubation, PSS was continuously bubbled with 5% $CO_2$,-75% $N_2$-20% $O_2$ to maintain pH (7.4). Then, unreacted BPA was washed by rinsing the arteries with PBS before tissue homogenization and protein extraction in RIPA lysis buffer (0.5 mmol/L tris/HCL pH 7.4, 10 mmol/L EDTA, 1.5 mmol/L NaCl, 2.5 % deoxycholic acid, 10 % NP-40) with Halt Protease and Phosphatase Inhibitor Cocktail (ThermoFisher Scientifics, Massachusetts, USA). The amount of extracted protein was quantified by a modified Lowry method and 10 μg of total proteins were loaded onto a nitrocellulose membrane using the BioRad Dot Blot apparatus (Bio-Dot® Apparatus). The membrane was blocked in 5% BSA for 2 h and then incubated with HRP-conjugated streptavidin (Amersham Bioscience; dilution 1:10,000 in 0.5% BSA) for 2 h to detect BPA incorporation. The membrane was then washed in TBS-T, removed from the dot blot apparatus and developed using an ECL-Plus kit (General Electric (GE) Health care, Copenhagen, Denmark). The images were captured by a luminescence camera using a PXi 4 Touch image analysis system (Syngene). After development, membranes were rinsed in water and stained with amido black (0.1% (w/v) in 10% acetic acid) for total protein staining. Blots were quantified using GeneTools 4 software (Syngene) and normalized to the total protein. For each sample results are the average intensity expressed as % of total protein of two replicates.

Additionally, small mesenteric arteries from rats at 12-14 weeks of age were used for the inhibition assay '*ex vivo*'. Arteries were incubated in PSS containing BPA and $Ca^{2+}$ as previously described but in presence of either vehicle, LDN 27219 ($10^{-6}$ mol/L), Z-DON ($4 \cdot 10^{-5}$ mol/L) or dithiothreitol (DTT) ($10^{-3}$ mol/L), which has been demonstrated to increase TG2 transamidase activity. Two replicates for each treatment and animal were added in one blot, the average activity under control conditions was set to 100% and the results are expressed as % of transamidase activity normalized to control conditions and presented in Figure 1.

### *'In vitro'* transamidase activity inhibition assay

To measure transamidase activity *'in vitro'* an assay based on the incorporation of a biotinylated preferred TG2 substrate (Biotin-pepT26) as amine-acceptor into a spermine coated strip as amine-donnor was used. Liver samples from young (6-7-week-old) and old rats (35-40-week-old) snap frozen with liquid nitrogen until the assay was performed. The samples were thawed and homogenized in RIPA lysis buffer (0.5 mmol/L tris/HCL pH 7.4, 10 mmol/L EDTA, 1.5 mmol/L NaCl, 2.5 % deoxycholic acid, 10 % NP-40) with Halt Protease and Phosphatase Inhibitor Cocktail (ThermoFisher Scientifics, Massachusetts, USA). Livers were left 30 min on ice before sonicating for 45 seconds and then centrifuged at 13000 rpm for 10 min at 4 ºC. The supernatant was

collected, and the protein concentration was measured by a modified Lowry method. Samples were prepared to achieve a concentration of 8 µg/µL using the diluent buffer of the Specific Tissue Transglutaminase Colometric Microassay Kit TG2-CovtTest (Zedira, Darmstadt, Germany). Then, 25 µL of sample were incubated with 25 µl of different concentrations of the inhibitors LDN 27219 ($10^{-7}$ – $10^{-4}$ mol/L) or VA-5 ($10^{-7}$ – $10^{-5}$ mol/L), or the vehicle for 20 min on ice. The assay was performed following the manufacturer's protocol.

In short, microtiter strips coated with spermine were washed and 50 µL of study sample or 50 µL of standard were added along with 10 µL of diluent buffer and 50 µL of ice-cold assay-mixture (Biotin-pepT26 / $CaCl_2$, 20% DTT). The plate was then incubated for 30 min at 37 ºC, and after pertinent washes with wash buffer and 0.1 mol/L NaOH, incubated again with horseradish peroxidase streptavidin (1:2000 dilution in wash buffer) for 15 min at 37 ºC. Later, HRP substrate was added for 5 min at room temperature and subsequently, the reaction was stopped with a blocking reagent. The final optical density was read at 450 nm and data was quantitatively evaluated with the standard curve. Duplicates from each sample or standard were performed, and the average value was calculated in all the study samples. Results are presented as % of transamidase activity under control conditions.

**Resting membrane potential measurements**

Small mesenteric arteries were mounted and normalized in a myograph as described above. KCl-filled glass microelectrodes (40-100 MΩ of resistance) were used to obtain intracellular recordings of resting membrane potential, placing an Ag/AgCl electrode in the myograph bath as reference electrode. Input resistance was assessed by observing the change in potential caused by applying current pulses of 1 nA; the electrode resistance was compensated using the amplifier (Intro-710, WPI) before penetrating inside the smooth muscle cell. PSS solution in the myograph bath was heated to 37ºC and light bubbling with 95% $O_2$ - 5% $CO_2$ was maintained through the protocol.

The effect of 25 min incubation with LDN 27219 ($10^{-6}$ mol/L) on resting membrane potential and on ACh ($10^{-8}$-$10^{-5}$ mol/L) induced hyperpolarization was studied in the absence and the presence of iberiotoxin ($10^{-7}$ mol/L). To minimize the effect of endothelial potassium channels the protocol was repeated in the presence of TRAM-34 ($10^{-6}$ mol/L) and UCL 1684 ($10^{-6}$ mol/L). Resting membrane potential was expressed in absolute values (mV).

**Experimental procedure for electrophysiological studies**

**Cell isolation**

For isolation of SMCs, rat mesenteric arteries were dissected, opened longitudinally and stored in ice-cold dissociation solution containing (mmol/L): 119 NaCl, 4.7 KCl, 1.18 $KH_2PO_4$, 1.17 $MgSO_4$, 24.9 $NaHCO_3$, 0.027 EDTA, and 11 glucose, pH= 7.4. Arteries were then equilibrated during 10 min in a dissociation solution with BSA (1 mg/mL) at 37ºC and then exposed to the same solution supplemented with papain (0.5 mg/mL; Worthington Biochemical Corp., Lakewood, NJ, USA) and DTT (1 mg/mL) at 37ºC for 8 min. Arteries were then washed in ice-cold dissociation solution and moved to dissociation solution containing BSA (1 mg/mL) and collagenase (0.7 mg/mL type F and 0.4 mg/mL type H; Sigma.) at 37°C for 3 min. After washing

in ice-cold dissociation solution, isolated SMCs were obtained by gentle trituration of the digested arteries with a fire polished glass pipette into the SMC extracellular solution (for composition, see below).

After the digestion protocol, SMCs were seeded in micro-dishes (ibidi GmbH, Martinsried, Germany) and used for patch clamp recordings 15 min after the isolation protocol and within the next 5 hs.

**Whole cell voltage clamp studies**

Extracellular patch-clamp solution for SMCs contained the following (mmol/L): 130 NaCl, 5 KCl, 1.2 $MgCl_2$, 1.5 $CaCl_2$, 10 glucose and 10 HEPES (adjusted to pH 7.3 with NaOH). The patch pipette (intracellular) solution for SMCs contained the following (mmol/L): 130 KCl, 1.2 $MgCl_2$, 0.1 EGTA and 10 HEPES (adjusted to pH 7.2 with KOH). To study the effect of intracellular GTP in LDN 27219 activity over potassium currents, patch pipette solution with 5 mmol/L $Na_2GTP$ was used in some experiments.

Membrane currents were recorded under the whole-cell configuration of the patch-clamp technique using an Axon Multiclamp 700A amplifier (Axon instruments, Molecular Devices, CA, USA). Patch pipettes were made of borosilicate glass capillaries (World Precision Instruments, FL, USA) fabricated using a dual-stage puller PP-830 (Narishige, Tokyo, Japan) and had resistances of 4-7 MΩ. Current recordings were digitized on line at 10 kHz and low pass filtered at 2 kHz using a Digidata 1440 A (Axon Instruments), to acquire and store data pClamp 10 software was used. Current-voltage relations were determined using 600 ms voltage ramps from -100 to 160 mV and a holding potential (Vh) of -65 mV for SMCs.[4]

In SMCs amplitudes of $K^+$-outward currents were measured under control conditions and 12 min after the addition of LDN 27219 ($3x10^{-5}$ mol/L) to the extracellular solution by a perfusion system. To address which potassium channels were involved in LDN 27219 effect, the protocol was repeated in presence of iberiotoxin ($10^{-7}$ mol/L), and Kv7 blocker XE991 ($10^{-5}$ mol/L) was added. To study how conformational modulation of TG2 affected LDN 27219 activity over potassium channels, the initial protocol was repeated after 1 h incubation with VA5 ($5x10^{-5}$ mol/L) or with GTP present in the intracellular solution.

**Immunoblotting for TG2 and $BK_{Ca}$ channels**

Small mesenteric arteries from rats of different ages were snap frozen with liquid nitrogen and kept at -80°C, until homogenization. The tissues were homogenized and centrifuged in a lysis buffer (20 mmol/L tris/HCL, 5 mmol/L EGTA, 150 mmol/L NaCl, 20 mmol/L glycorophosphate, 10 mmol/L NaF, 1 % triton X-1000, 0.1 % tween-20, pH 7.5) with Halt Protease and Phosphatase Inhibitor Cocktail (ThermoFisher Scientifics, Massachusetts, USA). The amount of protein extracted was quantified by a modified Lowry method and samples were diluted in Laemmli Sample Buffer (Bio-rad) containing DTT to a final concentration of 1 g/L of total protein. After boiling (99°C for 5 min), the samples were left to refrigerate and 10 μg of protein was loaded onto 4–20% Criterion™ TGX Stain-Free™ gels (Bio-Rad), using XT MOPS (Bio-Rad) as the running buffer.

The samples were subjected to electrophoresis for 1 h at 125 V, before being transferred to a polyvinylidene fluoride (PVDF) membrane by applying 100 V for 1 h at 4°C using Tris-glycine (Bio-Rad) (20% ethanol) as the transfer buffer. After the transfer, total protein was visualized using stain-free technology by exposing the membranes to UV light and the images were captured using a PXi 4 Touch image analysis system (Syngene). The membranes were washed twice for 15 min in PBS-T (150 mmol/L NaCl, 50 mmol/L $NaH_2PO_4$, 0.05 % (v/v) Tween® 20) and TBS-T (10 mmol/L tris base,100 mmol/L NaCl, 1 mmol/L EDTA, 0.1 % (w/v) Tween® 20) for 1 h and then blocked in 0.3% I-block™ (Applied Biosystems) for 2–4 h before being incubated overnight at 4°C with the primary antibody. Anti-Transglutaminase 2 antibody (ab421, Abcam) at a dilution of 1:200, anti-$BK_{Ca}$ alpha antibody (APC-107, Alomone labs) at a dilution of 1:100, and anti-$BK_{Ca}$ beta 1 antibody (ab3587, Abcam) at a dilution of 1:250 were used as primary antibodies in TBS-T with 0.3 % I-block™ (Applied Biosystems). The membrane was then washed in TBS-T and incubated for 2 h in the secondary antibody, Goat anti-Rabbit IgG (G-21234, Invitrogen). The membrane was developed using an ECL-Plus kit (General Electric (GE) Health care, Copenhagen, Denmark) and the images were captured by a luminescence camera using a PXi 4 Touch image analysis system (Syngene). Blots were quantified using GeneTools 4 software (Syngene) and normalized to the total protein intensity in their lane.

**'*In vivo*' mean arterial pressure (MAP) and heart rate (HR) measurements**

Male Wistar rats at 12-14 and 35-40 weeks of age were used for the 'in vivo' experiments. Group sizes were calculated with an expected effect size f of 1, desired power of 95% and an alfa of 0.05 and age-paired animals were randomly assigned to treatment or vehicle group.

Rats were anesthetized with intraperitoneal injections of s-ketamine (35 mg/kg) and pentobarbital (50 mg/kg) and placed in a heated blanket to maintain body temperature at 37ºC. ECG needles were installed in the Einthoven configuration for electrocardiographic recordings of the standard lead II derivation, which were obtained by an animal bio-amplifier (AD Instruments), and a solid state catheter (model no. SPR-1000 Millar Inc, Houston, USA) was introduced into the carotid artery to measure MAP. MAP and electrocardiographic data was continuously recorded on a computerized data acquisition system (PowerLab, ADInstruments) and ECG signals were low-pass filtered by using the standard filter file for ECG recordings. The ADInstruments software automatically obtained the different electrocardiographical values. Adequate depth of anesthesia was checked periodically by absence of the toe pinch withdrawal effect and 1/3 of the initial dose of anesthetics was administered intraperitoneally when needed (usually each 90 min).

The rats were infused through a catheter in the jugular vein for 3 min with either three doses of LDN 27219 (0,1; 1 and 2 mg/kg) or the corresponding doses of vehicle (PEG-400), using a syringe infusion pump (Hardvard Apparatus Model 55-2219) and leaving a rest period of 10 min between the doses. To study the effect of TG2 inhibitors that lock the open conformation of the enzyme, the animals in the vehicle group were infused with a single dose of VA5 (1 mg/kg) for 3 min at the end of the protocol. MAP and HR values before, during and two min after the infusion were expressed as means ± SEM. AUCs for changes in MAP during the infusion were also calculated for each age group using Graphpad Prism 7.2 (GraphPad Software, San Diego, California, USA).

## Materials

For the conformational shift assay using native polyacrylamide gel electrophoresis (native-PAGE) purified and functional human TG2 protein produced in insect cells was obtained from Zedira (Darmstadt, Germany).

The following drugs were used: ACh, $Na_2GTP$ (guanosine 5′-triphosphate sodium salt), Indomethacin, Nω-Nitro-L-arginine (L-NOARG), ODQ (1H-[1,2,4]Oxadiazolo[4,3-a]quinoxalin-1-one), Phenylephrine, sodium nitroprusside (SNP), U46619 (9α- epoxymethanoprostaglandin F2α) and XE991 (10,10-bis(4-pyridinylmethyl)-9(10H)-anthracenone dihydrochloride) from Sigma (St. Louis, MO, USA). Iberiotoxin, LDN 27219, TRAM-34 and UCL 1684 were obtained from Tocris Bioscience (Bristol, UK). Boc-DON and Z-DON were obtained from Zedira (Darmstadt, Germany). VA5 was from ChemShuttle (Hayward, CA, USA). Unless otherwise stated all substances were dissolved in distilled water. For 'ex vivo' experiments U46619 was dissolved in ethanol and Boc-DON, LDN 27219, ODQ, TRAM-34, UCL 1684, XE991 and Z-DON were dissolved in DMSO and stored at -20ºC. Further dilution of the above mentioned compounds were made in distilled water. The DMSO concentration in the bath were kept below 0.01% and did not affect vessel contractility. For '*in vivo*' experiments, LDN 27219 and VA5 were dissolved in PEG-400.

## SUPPLEMENTAL REFERENCES


1. National Research Council (US) Committee for the Update of the Guide for the Care and Use of Laboratory Animals. *Guide for the Care and Use of Laboratory Animals*. 8th ed. (National Academies Press, ed.). Washington, DC; 2011. doi:10.17226/12910
2. Pinkas DM, Strop P, Brunger AT, Khosla C. Transglutaminase 2 undergoes a large conformational change upon activation. *PLoS Biol*. 2007;5:2788-2796. doi:10.1371/journal.pbio.0050327
3. Iversen R, Mysling S, Hnida K, Jørgensen TJD, Sollid LM. Activity-regulating structural changes and autoantibody epitopes in transglutaminase 2 assessed by hydrogen/deuterium exchange. *Proc Natl Acad Sci U S A*. 2014;111:17146-17151. doi:10.1073/pnas.1407457111/-/DCSupplemental
4. Engholm M, Pinilla E, Mogensen S, Matchkov V, Hedegaard ER, Chen H, Mulvany MJ, Simonsen U. Involvement of transglutaminase 2 and voltage-gated potassium channels in cystamine vasodilatation in rat mesenteric small arteries. *Br J Pharmacol*. 2016;173:839-855. doi:10.1111/bph.13393
5. Santhanam L, Tuday EC, Webb AK, Dowzicky P, Kim JH, Oh YJ, Sikka G, Kuo M, Halushka MK, MacGregor AM, et al. Decreased S-nitrosylation of tissue transglutaminase contributes to age-related increases in vascular stiffness. *Circ Res*. 2010;107:117-125. doi:10.1161/CIRCRESAHA.109.215228

## SUPPLEMENTAL TABLES

### Table S1: Data from human donors of fat biopsies

| Patient group | Sex | Age (years) | No. of antihypertensive drugs |
|---|---|---|---|
| Hypertension | Female | 43 | 4 |
| Hypertension | Female | 67 | 3 |
| Hypertension | Female | 47 | 2 |
| Healthy Control | Male | 62 | none |
| Healthy Control | Male | 43 | none |
| Healthy Control | Male | 39 | none |
| Healthy Control | Male | 33 | none |
| Healthy Control | Female | 35 | none |

**Table S2: Level of contraction induced by different vasoconstrictors and Emax and pD2 values of different vasodilators in the presence of different drug incubations.**

| | Conditions | n | Vasoconstrictor | Contraction level ($Nm^{-1}$) | Vasodilator | $E_{max}$ (Relaxation %) | $pD_2$ |
|---|---|---|---|---|---|---|---|
| Figure 1E | Control | 12 | U46619 ($1\text{-}4x10^{-7}$ mol/L) | 3.06 ± 0.30 | LDN 27219 | 89.35 ± 3.58 | 5.99 ± 0.07 |
| | w/o endothelium | 6 | | 2.53 ± 0.28 | LDN 27219 | 49.59 ± 10.76 * | 4.97 ± 0.12 * |
| | L-NOARG ($10^{-4}$ mol/L) | 7 | | 2.99 ± 0.30 | LDN 27219 | 83.87 ± 10.79 | 5.48 ± 0.07 * |
| | Control | 9 | | 2.14 ± 0.17 | Z-DON | 13.48 ± 4.92 * | ND |
| Figure 1F | Control | 8 | U46619 ($3x10^{-8}$ mol/L) | 4.19 ± 0.44 | LDN 27219 | 94.52 ± 1.73 | 5.14 ± 0.09 |
| Figure 2C | Vehicle | 7 | Phe ($3x10^{-6}$ mol/L) | 4.42 ± 0.47 | ACh | 91.75 ± 6.68 | 7.58 ± 0.06 |
| | LDN 27219 ($3x10^{-6}$ mol/L) | 7 | | 3.97 ± 0.48 | | 96.02 ± 1.58 | 8.09 ± 0.06 * |
| Figure 2D | Vehicle | 6 | Phe ($10^{-5}$ mol/L) | 3.20 ± 0.38 | ACh | 94.97 ± 1.28 | 6.90 ± 0.03 |
| | LDN 27219 ($10^{-6}$ mol/L) | 6 | | 3.74 ± 0.30 | | 97.44 ± 0.93 | 7.18 ± 0.03 * |
| Figure 2E | Vehicle | 10 | Phe ($10^{-5}$ mol/L) | 3.54 ± 0.12 | ACh | 96.61 ± 0.72 | 7.53 ± 0.04 |
| | VA5 ($10^{-6}$ mol/L) | 6 | | 3.37 ± 0.18 | | 96.33 ± 0.60 | 7.32 ± 0.03 * |
| | LDN 27219 ($10^{-6}$ mol/L) | 4 | | 3.35 ± 0.36 | | 96.27 ± 0.68 | 7.86 ± 0.05 * |
| Figure 2F | VA5 ($10^{-6}$ mol/L) + Vehicle | 6 | Phe ($10^{-5}$ mol/L) | 3.37 ± 0.18 | ACh | 96.33 ± 0.60 | 7.32 ± 0.03 |
| | VA5 ($10^{-6}$ mol/L) + LDN 27219 ($10^{-6}$ mol/L) | 5 | | 2.88 ± 0.24 | | 91.37 ± 3.10 | 7.24 ± 0.06 |
| Figure 3A | TRAM-34 ($10^{-6}$ mol/L) + UCL 1684 ($10^{-6}$ mol/L) + Vehicle | 5 | Phe ($10^{-5}$ mol/L) | 2.49 ± 0.56 | ACh | 80.29 ± 6.97 | 6.39 ± 0.07 |
| | TRAM-34 ($10^{-6}$ mol/L) + UCL 1684 ($10^{-6}$ mol/L) + LDN 27219 ($10^{-6}$ mol/L) | 5 | | 2.35 ± 0.59 | | 88.81 ± 3.73 | 6.90 ± 0.06* |
| Figure 3B | L-NOARG ($10^{-4}$ mol/L) + Vehicle | 5 | Phe ($10^{-5}$ mol/L) | 3.37 ± 0.23 | ACh | 94.88 ± 1.25 | 6.71 ± 0.05 |
| | L-NOARG ($10^{-4}$ mol/L) + LDN 27219 ($10^{-6}$ mol/L) | 5 | | 4.47 ± 0.22 * | | 93.97 ± 1.63 | 6.70 ± 0.05 |
| Figure 3C | Ibtx ($10^{-7}$ mol/L) + Vehicle | 6 | Phe ($10^{-5}$ mol/L) | 4.15 ± 0.28 | ACh | 98.94 ±1.38 | 6.71 ± 0.05 |
| | Ibtx ($10^{-7}$ mol/L) + LDN 27219 ($10^{-6}$ mol/L) | 6 | | 4.23 ± 0.29 | | 95.12 ± 0.89 | 6.68 ± 0.08 |
| Figure 3D | Vehicle - w/o endo | 6 | Phe ($10^{-5}$ mol/L) | 3.72 ± 0.47 | SNP | 84.37 ± 5.36 | 6.63 ±0.07 |
| | LDN 27219 ($10^{-6}$ mol/L) - w/o endo | 6 | | 3.23 ± 0.35 | | 90.33 ± 4.96 | 7.36 ± 0.09 * |
| Figure 5A | Vehicle | 6 | Phe ($10^{-5}$ mol/L) | 2.77 ± 0.23 | ACh | 94.01 ± 1.77 | 6.86 ± 0.04 |
| | LDN 27219 ($10^{-6}$ mol/L) | 6 | | 2.78 ± 0.16 | | 95.78 ± 0.5 | 6.96 ± 0.04 |
| Figure 5B | Vehicle | 7 | Phe ($10^{-5}$ mol/L) | 3.36 ± 0.34 | ACh | 88.66 ± 4.81 | 6.76 ± 0.06 † |
| | LDN 27219 ($10^{-6}$ mol/L) | 7 | | 3.77 ± 0.33 | | 94.87 ± 2.04 | 7.30 ± 0.04 * |
| Figure 5C | Vehicle - w/o endo | 5 | Phe ($10^{-5}$ mol/L) | 2.54 ± 0.44 | SNP | 86.28 ± 5.47 | 6.48 ± 0.08 |
| | LDN 27219 ($10^{-6}$ mol/L) - w/o endo | 5 | | 2.53 ± 0.50 | | 90.47 ± 2.60 | 7.01 ± 0.07 * |
| Figure 5D | Vehicle - w/o endo | 7 | Phe ($10^{-5}$ mol/L) | 4.17 ± 0.26 | SNP | 53.43 ± 4.43 † | 5.43 ± 0.09 † |
| | LDN 27219 ($10^{-6}$ mol/L) - w/o endo | 7 | | 4.47 ± 0.37 | | 71.87 ± 5.27 * | 6.60 ± 0.09 * |

Values are means ± SEM and are calculated from the data in figures indicated in the left column. n: number of animals used. *, $P < 0.05$ compared to control/vehicle conditions using paired two-tailed Student´s t-test , except in the pD2 values where an F-test was used. †, $P < 0.05$ compared to vehicle conditions in 12 - 14 weeks old animals using paired two-tailed Student´s t-test , except in the pD2 values where an F-test was used. ND: Not determined because Emax was less than 50%

**Table S3: ECG parameters of rats from the different age groups before, during and two minutes after the intravenous infusion of different doses of LDN 27219.**

| | | | LDN 27219 dose | | | | | | | | |
|---|---|---|---|---|---|---|---|---|---|---|---|
| | | | 0,1 mg/kg | | | 1 mg/kg | | | 2 mg/kg | | |
| Age | n | | Before | During | After | Before | During | After | Before | During | After |
| 12 - 14 weeks old | 6 | P duration (s) | 0.0181 ± 0.003 | 0.0187 ± 0.003 | 0.0185 ± 0.003 | 0.0188 ± 0.003 | 0.0187 ± 0.003 | 0.0201 ± 0.003 | 0.0202 ± 0.004 | 0.0232 ± 0.007 | 0.0218 ± 0.005 |
| | | P amplitude (mV) | 0.1393 ± 0.018 | 0.1361 ± 0.018 | 0.1382 ± 0.018 | 0.1385 ± 0.017 | 0.1276 ± 0.014 | 0.1293 ± 0.013 | 0.1191 ± 0.014 | 0.1033 ± 0.014 | 0.1123 ± 0.015 |
| | | PR interval (s) | 0.0476 ± 0.002 | 0.0489 ± 0.002 | 0.0480 ± 0.002 | 0.0480 ± 0.002 | 0.0485 ± 0.002 | 0.0498 ± 0.002 | 0.0487 ± 0.003 | 0.0499 ± 0.004 | 0.0492 ± 0.003 |
| | | QRS interval (s) | 0.0163 ± 0.001 | 0.0161 ± 0.001 | 0.0160 ± 0.001 | 0.0154 ± 0.002 | 0.0160 ± 0.001 | 0.0164 ± 0.001 | 0.0165 ± 0.002 | 0.0153 ± 0.002 | 0.0176 ± 0.001 |
| | | QTc (s) | 0.1540 ± 0.016 | 0.1555 ± 0.016 | 0.1594 ± 0.015 | 0.1515 ± 0.017 | 0.1558 ± 0.017 | 0.1539 ± 0.014 | 0.1461 ± 0.020 | 0.1409 ± 0.029 | 0.1519 ± 0.019 |
| 35-40 weeks old | 7 | P duration (s) | 0.0163 ± 0.001 | 0.0181 ± 0.002 | 0.0182 ± 0.002 | 0.0182 ± 0.002 | 0.0166 ± 0.002 | 0.0183 ± 0.002 | 0.0190 ± 0.002 | 0.0193 ± 0.002 | 0.0199 ± 0.002 |
| | | P amplitude (mV) | 0.1458 ± 0.007 | 0.1422 ± 0.008 | 0.1417 ± 0.009 | 0.1420 ± 0.008 | 0.1417 ± 0.004 | 0.1334 ± 0.007 | 0.1355 ± 0.010 | 0.1286 ± 0.004 | 0.1165 ± 0.015 |
| | | PR interval (s) | 0.0462 ± 0.002 | 0.0463 ± 0.002 | 0.0464 ± 0.002 | 0.0460 ± 0.002 | 0.0469 ± 0.002 | 0.0472 ± 0.002 | 0.0462 ± 0.001 | 0.0471 ± 0.002 | 0.0478 ± 0.001 |
| | | QRS interval (s) | 0.0155 ± 0.001 | 0.0158 ± 0.001 | 0.0157 ± 0.001 | 0.0155 ± 0.001 | 0.0159 ± 0.001 | 0.0158 ± 0.001 | 0.0166 ± 0.001 | 0.0162 ± 0.001 | 0.0163 ± 0.001 |
| | | QTc (s) | 0.1755 ± 0.005 | 0.1780 ± 0.005 | 0.1782 ± 0.004 | 0.1758 ± 0.006 | 0.1813 ± 0.007 | 0.1753 ± 0.003 | 0.1791 ± 0.004 | 0.1822 ± 0.006 | 0.1703 ± 0.008 |

Values are means ± SEM. n: number of animals used. The rate-corrected QT interval (QTc) was calculated using the standard Bazett's formula ($QTc = QT \cdot \sqrt{RR}^{-1}$)

**SUPPLEMENTAL FIGURES**

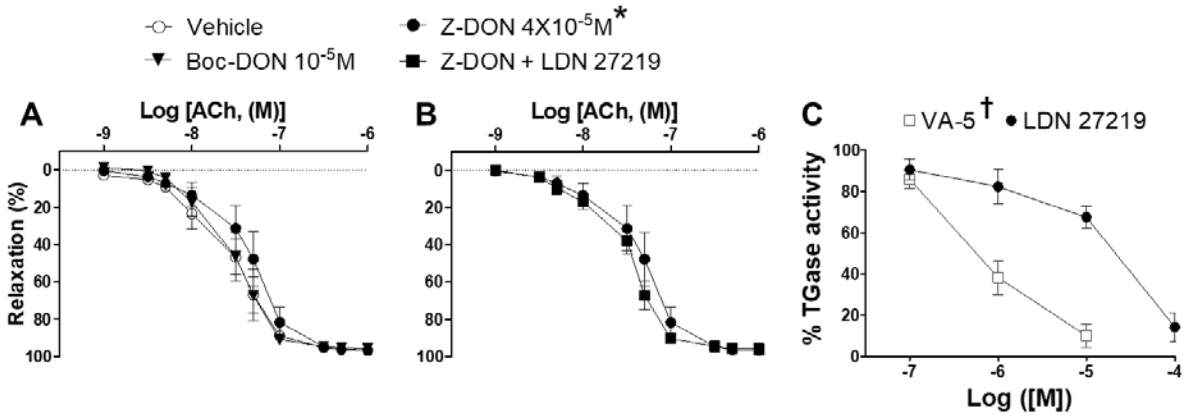


**Figure S1. Effect of incubation with TG2 inhibitors that lock the enzyme open on ACh response. A.** Averaged concentration-response curves for ACh of myograph-mounted small mesenteric arteries from male rats at 12-14 weeks of age, treated with either cell-permeable irreversible TG2 inhibitor Z-DON, cell non-permeable irreversible inhibitor Boc-DON or vehicle. Data are means ± SEM of % relaxation relative to maximum contraction. *, $P > 0.05$ using two-way ANOVA compared to vehicle, n = 5 - 10. **B.** Effect of incubation with LDN 27219 on ACh response in the presence of Z-DON: Averaged concentration-response curves for ACh of myograph-mounted small mesenteric arteries from male rats at 12-14 weeks of age, treated either with LDN 27219 or vehicle, in the presence of Z-DON. Data are means ± SEM of % relaxation relative to maximum contraction, n = 5. **C.** Transamidase activity inhibition assays *'in vitro'*: Averaged concentration-response curves for LDN-27219 or VA5 *'in vitro'*. Data are means ± SEM of % transglutaminase activity relative to control conditions. $pD_{2\ LDN\ 27219}$= 4.41±0.32; $pD_{2\ VA5}$= 6.28±0.24 †, $P< 0.05$ using F test, $n = 4 – 8$.

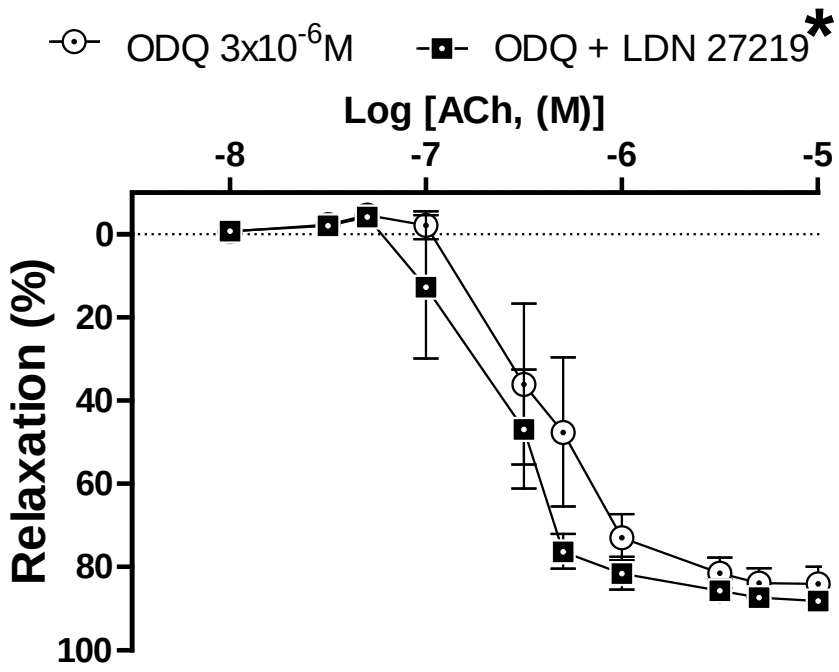


**Figure S2. Effect of incubation with LDN 27219 on ACh response in the presence of ODQ.** Averaged concentration-response curves for ACh of myograph-mounted small mesenteric arteries from male rats at 12-14 weeks of age, treated either with LDN 27219 ($10^{-6}$ mol/L) or vehicle, in the presence of ODQ ($3x10^{-6}$ mol/L). Data are means ± SEM of % relaxation relative to maximum contraction. *P > 0.05 using two-way ANOVA compared to ODQ, n = 5.

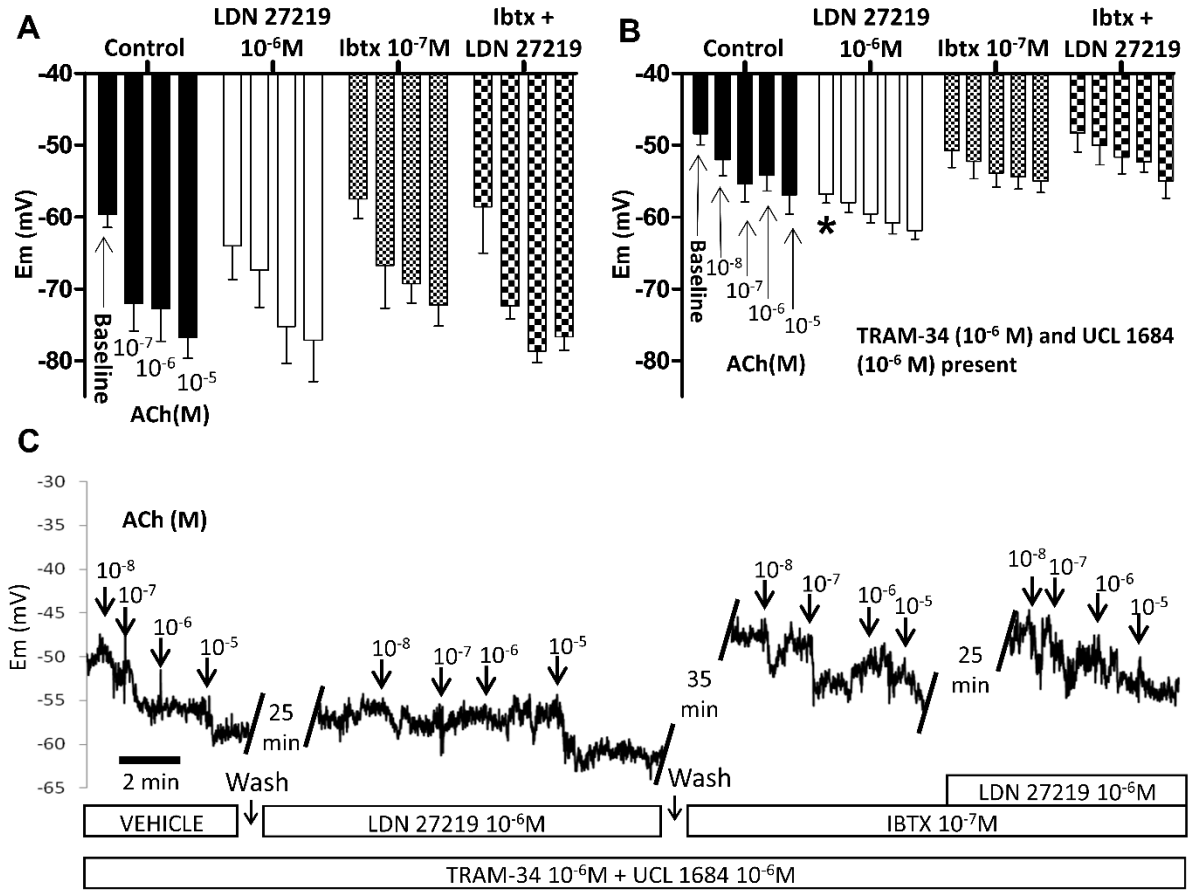


**Figure S3. Effect of LDN 27219 on SMC resting membrane potential in rat small mesenteric arteries.** Resting membrane potential (Em) recordings of SMCs in the vascular wall of myograph-mounted mesenteric arteries from male rats at 12-14 weeks of age. Recordings were performed during addition of increasing doses of ACh in the absence or in the presence of LDN 27219 and/or $BK_{Ca}$ channel blocker iberiotoxin. **A.** Averaged Em values of intact arteries, $n = 5$. **B.** Averaged Em values of arteries in the presence of $IK_{Ca}$ channel blocker TRAM-34 and $SK_{Ca}$ channel UCL 1684, $n = 6$. **C.** Representative trace of Em recordings in the presence of TRAM-34 and UCL 1684. Data are means ± SEM of Em (mV). *, $P < 0.05$ using two-way ANOVA with Bonferroni post-test compared to control.

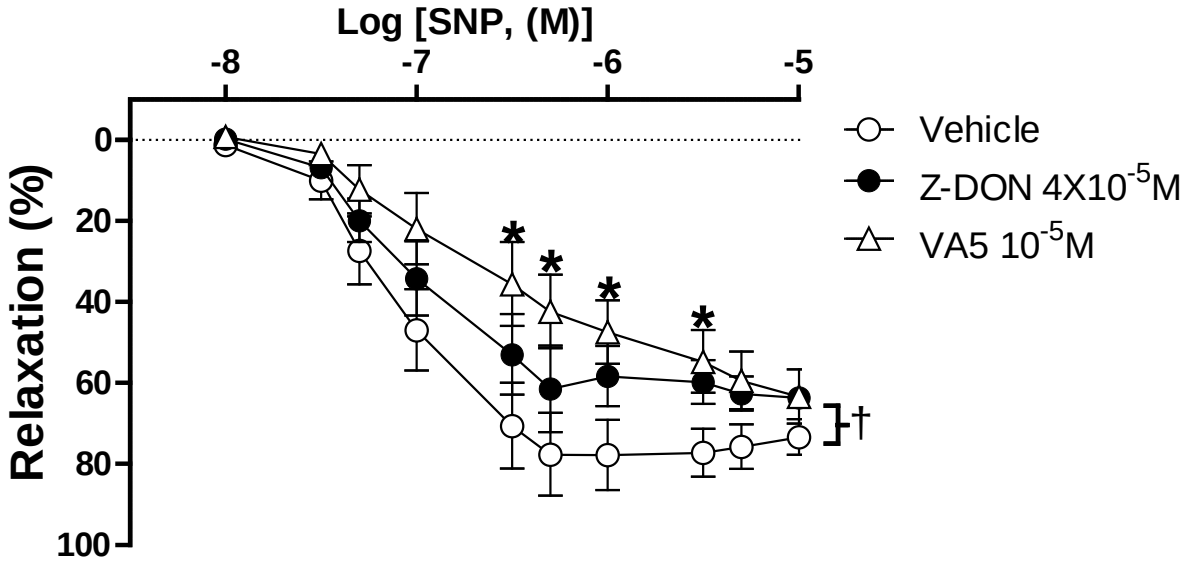


**Figure S4. Effect of incubation with TG2 openers on SNP response in endothelium-denuded arteries.** Averaged concentration-response curves for SNP in myograph-mounted small mesenteric arteries without endothelium from male rats at 12-14 weeks of age, treated either with different cell-permeable irreversible TG2 inhibitors that lock the open conformation of the enzyme or vehicle. Data are means ± SEM of % relaxation relative to maximum contraction. *, $P < 0.05$ using two-way ANOVA with Bonferroni post-test compared to vehicle. †, $P < 0.05$ using two-way ANOVA compared to vehicle, $n = 6$.

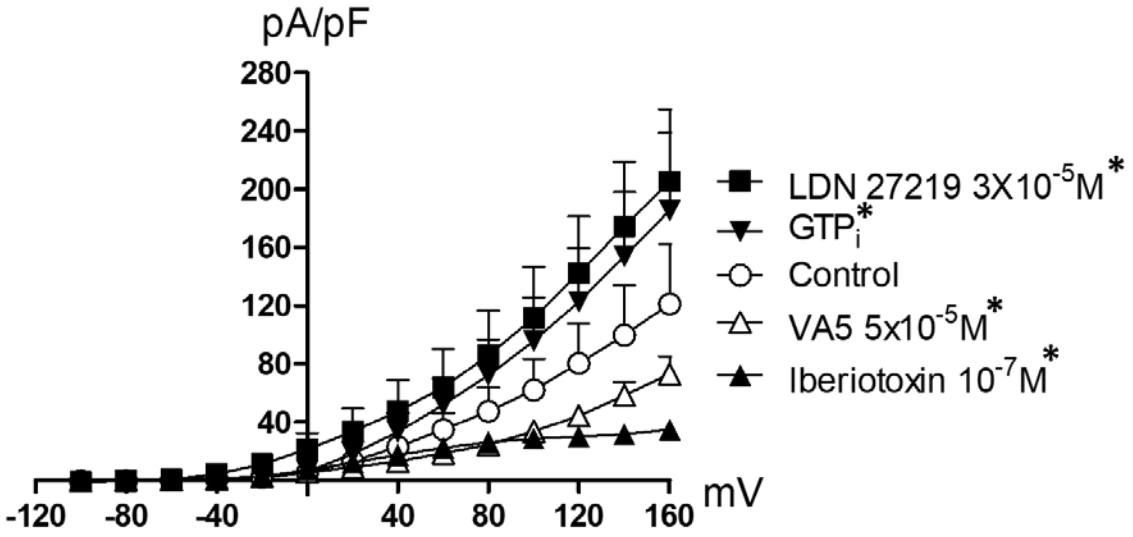


**Figure S5. $K^+$ outward currents expressed as a current density (pA/pF) for SMCs in the presence of different activators/blockers.** Averaged current density (pA/pF) of SMCs exposed to different treatments. Data are means ± SEM of current density (pA/pF). *, $P < 0.05$ using two-way ANOVA compared to control, $n = 4 - 7$.

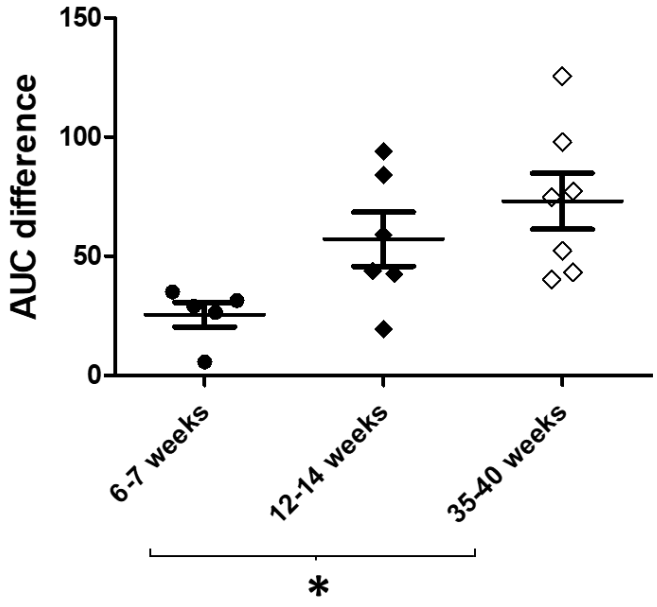


**Figure S6. Area under the curve (AUC) difference between vehicle-incubated and LDN 27219-incubated arteries in response to SNP in the different age groups.** Averaged differences in AUC of the responses to NO donor SNP of arteries incubated with vehicle and arteries incubated with LDN 27219 in each age group. Data are means ± SEM. *, $P < 0.05$ using one-way ANOVA with Bonferroni post-test.

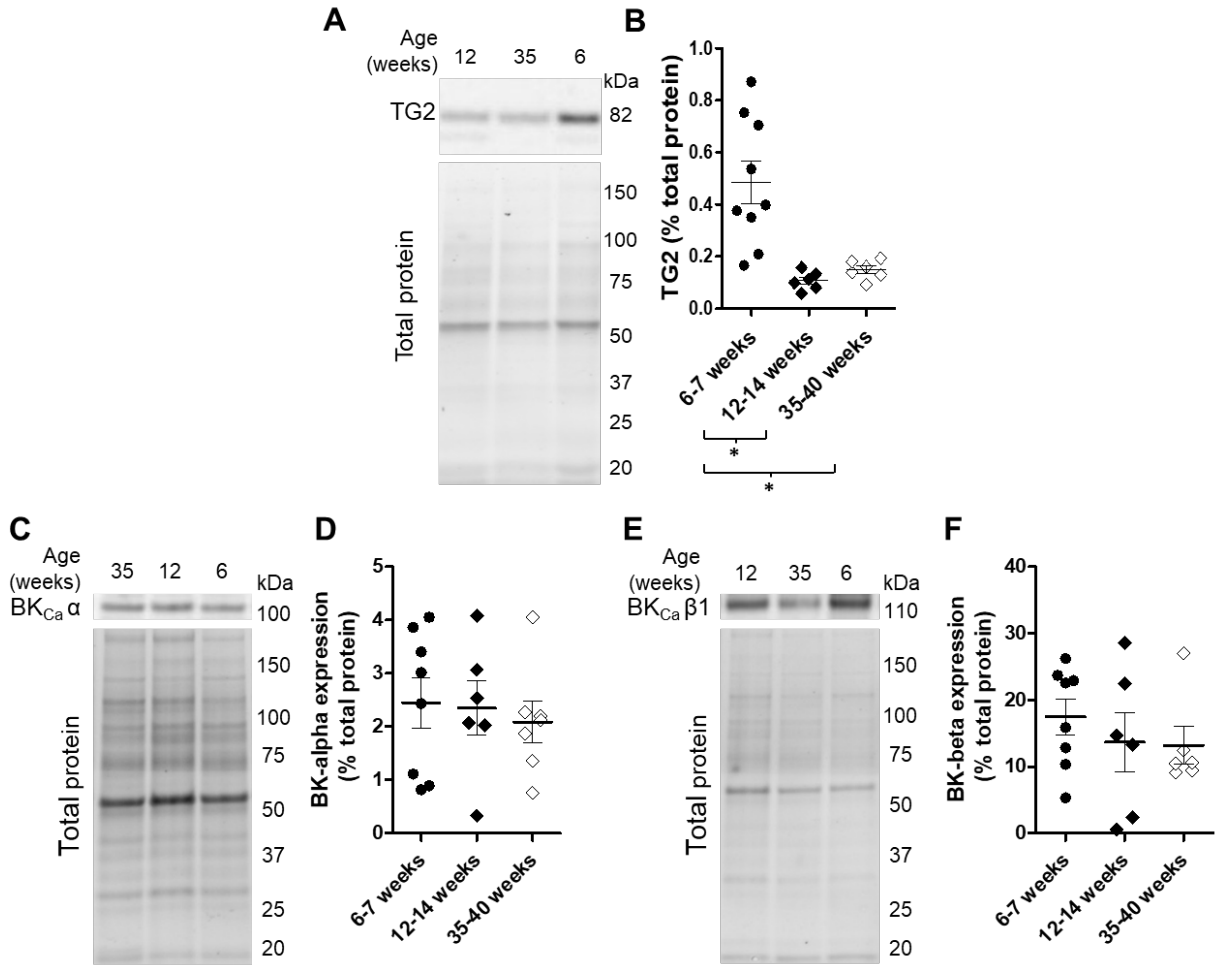


**Figure S7. Protein expression of TG2, $BK_{Ca}$ alpha and beta 1 subunit in different age groups.** **A.** Representative immunoblot of TG2, located at 82 kDa, in rat mesenteric arteries from the different age groups (upper panel). Stain-free total protein of the lanes corresponding to the blots in the upper panel (lower panel). **B.** Average TG2 protein expression, as % of total protein in small mesenteric arteries of each age group. **C.** Representative immunoblot of BK-alpha, located at 100 kDa, in rat mesenteric arteries from the different age groups from the same membrane (upper panel). Stain-free total protein of the lanes corresponding to the blots in the upper panel (lower panel). **D.** Averaged BK-alpha protein expression, as % of total protein in small mesenteric arteries of each age group. **E.** Representative immunoblot of BK-beta 1, located at 110 kDa, in rat mesenteric arteries from the different age groups from the same membrane (upper panel). Stain-free total protein of the lanes corresponding to the blots in the upper panel (lower panel). **F.** Averaged BK-beta 1 protein expression, as % of total protein in small mesenteric arteries of each age group. Data are means ± SEM. *, $P < 0.05$ using one-way ANOVA with Bonferroni post-test.

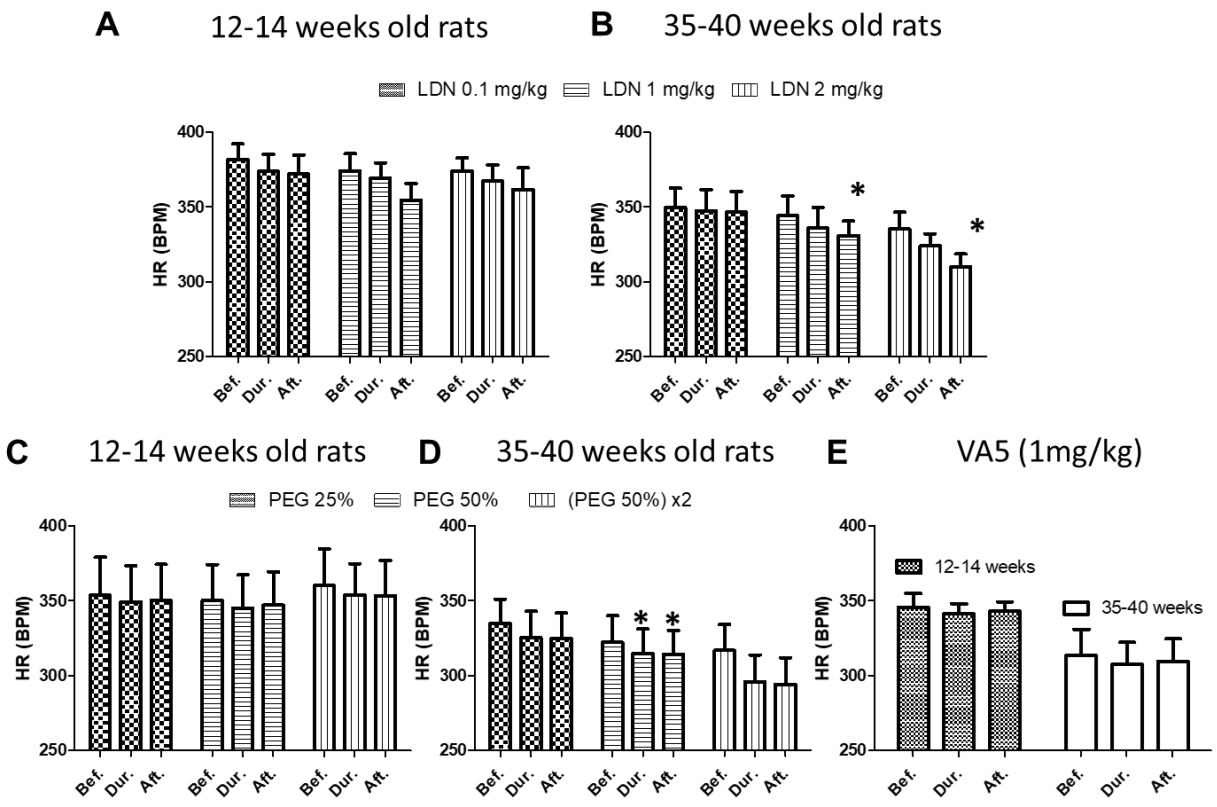


**Figure S8. Effects on heart rate (HR) before, during and after infusion of LDN-27219, PEG-400 and VA5. A.** Averaged HR values measured before (Bef.), during (Dur.) and 2 min after (Aft.) intra-jugular infusion of 3 doses of LDN 27219 to 12-14-week-old rats. $n$ = 6. **B.** Averaged HR values measured before (Bef.), during (Dur.) and 2 min after (Aft.) intra-jugular infusion of 3 doses of LDN 27219 to 35-40-week-old rats, $n$ = 7. **C.** Averaged HR values measured before (Bef.), during (Dur.) and 2 min after (Aft.) intra-jugular infusion of 3 doses of vehicle (PEG-400) to 12-14-week-old rats, $n$ = 5. **D.** Averaged HR values measured before (Bef.), during (Dur.) and 2 min after (Aft.) intra-jugular infusion of 3 doses of vehicle (PEG-400) to 35-40-week-old rats, $n$ = 8. **E.** Averaged HR values measured before (Bef.), during (Dur.) and 2 min after (Aft.) intra-jugular infusion of a single dose of VA5 to 12-14 and 35-40-week-old rats. Data are means ± SEM. *, $P < 0.05$ using paired two-tailed Student´s $t$-test compared to before infusion (Bef.).

## 12. APPENDIX 2: MANUSCRIPT II

**Acute and chronic treatment with the transglutaminase 2 inhibitor LDN 27219 restores endothelium-dependent vasorelaxation in resistance arteries from diabetic db/db mice.**

Estéfano Pinilla and Ulf Simonsen.

In submission for publication.

## 13. APPENDIX 3: MANUSCRIPT III

**Endothelial large- and intermediate-conductance $Ca^{2+}$ -activated $K^+$ channels mediate rat intrarenal artery endothelium derived hyperpolarization response.**

Estéfano Pinilla, Ana Sánchez, María P Martínez, Mercedes Muñoz, Albino García-Sacristán, Ralf Köhler, Dolores Prieto, and Luis Rivera.

Submitted for publication.

## 14. APPENDIX 4: PATENT APPLICATION

**Tissue Transglutaminase Modulators for Medicinal Use.**

Estéfano Pinilla and Ulf Simonsen.

International PCT patent application number WO2020030648A1. 13 Feb. 2020.

(12) INTERNATIONAL APPLICATION PUBLISHED UNDER THE PATENT COOPERATION TREATY (PCT)

(19) World Intellectual Property Organization
International Bureau

(43) International Publication Date
13 February 2020 (13.02.2020)

WIPO | PCT

(10) International Publication Number
WO 2020/030648 A1

(51) International Patent Classification:
*A61K 31/519* (2006.01) *A61P 9/08* (2006.01)
*A61P 9/10* (2006.01) *A61P 9/12* (2006.01)
*A61P 9/14* (2006.01)

(21) International Application Number:
PCT/EP2019/071134

(22) International Filing Date:
06 August 2019 (06.08.2019)

(25) Filing Language: English

(26) Publication Language: English

(30) Priority Data:
18187711.9 07 August 2018 (07.08.2018) EP

(71) Applicant: **AARHUS UNIVERSITET** [DK/DK]; Nordre Ringgade 1, 8000 Aarhus C (DK).

(72) Inventors: **PÉREZ, Estéfano, Pinilla,**; Vikærsvej 21, st., 8240 Risskov (DK). **SIMONSEN, Ulf**; Østermøllevej 13, 8380 Trige (DK).

(74) Agent: **PLOUGMANN VINGTOFT A/S**; Strandvejen 70, 2900 Hellerup (DK).

(81) Designated States *(unless otherwise indicated, for every kind of national protection available)*: AE, AG, AL, AM, AO, AT, AU, AZ, BA, BB, BG, BH, BN, BR, BW, BY, BZ, CA, CH, CL, CN, CO, CR, CU, CZ, DE, DJ, DK, DM, DO, DZ, EC, EE, EG, ES, FI, GB, GD, GE, GH, GM, GT, HN, HR, HU, ID, IL, IN, IR, IS, JO, JP, KE, KG, KH, KN, KP, KR, KW, KZ, LA, LC, LK, LR, LS, LU, LY, MA, MD, ME, MG, MK, MN, MW, MX, MY, MZ, NA, NG, NI, NO, NZ, OM, PA, PE, PG, PH, PL, PT, QA, RO, RS, RU, RW, SA, SC, SD, SE, SG, SK, SL, SM, ST, SV, SY, TH, TJ, TM, TN, TR, TT, TZ, UA, UG, US, UZ, VC, VN, ZA, ZM, ZW.

(84) Designated States *(unless otherwise indicated, for every kind of regional protection available)*: ARIPO (BW, GH, GM, KE, LR, LS, MW, MZ, NA, RW, SD, SL, ST, SZ, TZ, UG, ZM, ZW), Eurasian (AM, AZ, BY, KG, KZ, RU, TJ, TM), European (AL, AT, BE, BG, CH, CY, CZ, DE, DK, EE, ES, FI, FR, GB, GR, HR, HU, IE, IS, IT, LT, LU, LV, MC, MK, MT, NL, NO, PL, PT, RO, RS, SE, SI, SK, SM, TR), OAPI (BF, BJ, CF, CG, CI, CM, GA, GN, GQ, GW, KM, ML, MR, NE, SN, TD, TG).

**Declarations under Rule 4.17:**
— *of inventorship (Rule 4.17(iv))*

**Published:**
— *with international search report (Art. 21(3))*

(54) Title: TISSUE TRANSGLUTAMINASE MODULATORS FOR MEDICINAL USE

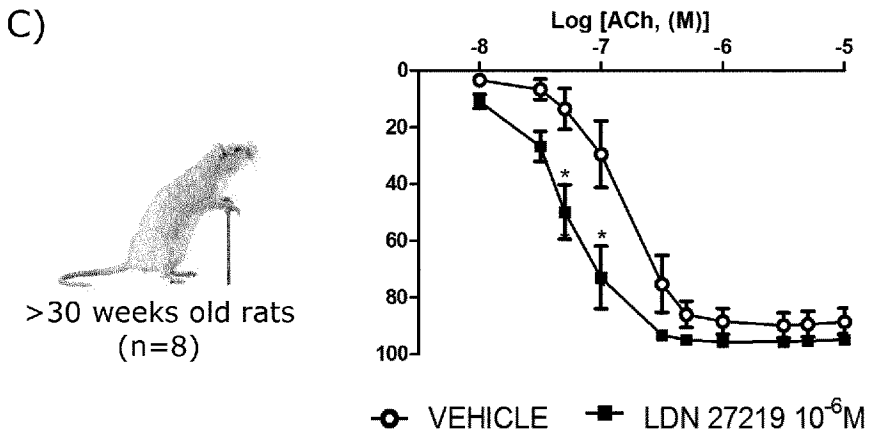


Fig. 1

(57) Abstract: The present invention relates to a compound which is a modulator of tissue transglutaminase (TG2) for use in the treatment of endothelial dysfunction and diseases related thereto or resulting therefrom. In particular the present invention relates to the compound LDN-27219 (Formula II herein) and derivatives thereof for use in the treatment of diseases resulting from endothelial dysfunction, especially in association with aging and diabetic subjects.

WO 2020/030648 A1

# TISSUE TRANSGLUTAMINASE MODULATORS FOR MEDICINAL USE

## Technical field of the invention

The present invention relates to compounds which modulate tissue transglutaminase (TG2) for use in the treatment of endothelial dysfunction and diseases related thereto. In particular the present invention relates to the compound LDN-27219 (formula II herein) and derivatives thereof for use in the treatment of diseases resulting from endothelial dysfunction, especially in association with aging and/or diabetes.

## Background of the invention

The endothelium is a cellular monolayer that coats the luminal surface of the vascular system and plays an essential role in the regulation of vascular tone in response to hemodynamics and chemical signals. The functioning of the endothelial cells is influenced by Tissue Transglutaminase (TG2), which is an enzyme of the transglutaminase family (TG1-7 and Factor XIII). The TG2 enzyme is highly expressed in endothelial and smooth muscle cells. TG2 is located in different intracellular and extracellular compartments and has several functions depending on the location and conformation of the enzyme.

TG2 is found in the body in a closed conformation and in an open confirmation. When TG2 is bound to $Ca^{2+}$, it conforms to an open conformation that shows extracellular transamidase activity and leads to covalent cross-linking of structural proteins. In the closed conformation, it presents intracellular GTP-binding activity that enables it to act as a G protein ($G_h\alpha$).

Elevated levels and/or activity of TG2 is associated with a number of diseases including cancer, neurodegenerative diseases, fibrosis, and celiac diseases, and therefore, different types of TG2 inhibitors have been developed and used to investigate how TG2 inhibition may be used for treatment of these diseases. A plethora of inhibitors have been investigated, including compounds such as cystamine and LDN-27219.

Generally, these studies have however not studied the effects of using compounds which inhibit the open conformation by promoting the closed conformation of TG2, and no compounds have been identified for effective treatment of endothelial dysfunction, particularly in association with secondary conditions including old-age or diabetes, which influence TG2 expression.

Thus, *M. Engholm et al., British J. Pharm. (2016), 173, 839-855* discloses primarily a study of the vasodilatory effects of cystamine in mesenteric small arteries in rats. The study uses LDN-27219 as a comparative TG2 inhibitor and concluded that both compounds have the ability to relax contracted arteries in rats. The study does not disclose the promotion of the closed conformation TG2 or any beneficial effects hereof, nor age- or diabetes related effects of the TG2 inhibitors therein.

*Y.J. Oh et al., Amino Acids, 2017, 49(3), 695-704* discloses the role of TG2 in age-associated ventricular stiffness. Cystamine, a known general TG2 inhibitor, improves the cardiac function in aging rats. The use of TG2 modulators promoting the closed confirmation of TG2, including LDN-27219, is not disclosed.

Thus, *J.W. Keillor et al., Trends in pharmacological sciences, 2015, Vol 36, no 1* discloses a number of inhibitors of TG2 and their effects. TG2 is described as related to particularly celiac disease, fibrosis and cancer. LDN-27219 is disclosed as an allosteric reversible slow binding inhibitor of TG2. The efficacy of LDN-27219 in any particular diseases is not disclosed, and neither is activity relation to endothelial dysfunction. The document discloses the comparative compounds used herein, i.e. Boc-DON and Z-DON (Z013 and Z006 therein respectively).

US 2018/0002700 A1 discloses the use of TG2 inhibitors, such as LDN-27219 for the treatment of diabetic complications caused by vascular leakage (claim 1). There are no data related to LDN-27219. Age and diabetes-related effects of LDN-27219, or any other TG2 inhibitors, are not disclosed or any relation thereof to promotion of the closed conformation of TG2.

WO 2014/057266 discloses the use of specific TG2 inhibitors in the treatment of age-related macular degeneration. LDN-27119 and treatment of age- or diabetes related endothelial dysfunction is not disclosed.

*US 8,614,233* discloses cinnamoyl inhibitors of TG2, and links TG2 with a long list of diseases. LDN-27219 and derivatives are not disclosed.

Hence, an improved control of the effects of TG2 modulator control over the conformation of the enzyme would be advantageous, and in particular a more efficient inhibitor of the open conformation TG2 and promoter of the closed conformation TG2, useful for treatment of endothelial dysfunction, particularly in subjects of old-age or subjects diagnosed with diabetes, would be advantageous.

**Summary of the invention**

The present invention thus uses reversible TG2 modulators, such as LDN-27219, to stabilize the closed conformation of the enzyme TG2. This leads to e.g. relaxation of arteries, improvement of endothelium-derived vasodilation and antihypertensive effects, representing a new pathway for the treatment of diseases related to endothelial dysfunction.

Thus, an object of the present invention relates to the provision of an improved treatment of endothelial dysfunction, particularly in aging and diabetic subjects.

In particular, it is an object of the present invention to provide a treatment of endothelial dysfunction and diseases related thereto, that solves the above mentioned problems of the prior art with TG2 inhibitors that are non-selective and have unknown effect in the conformation of the enzyme or those that are selective, but lock the enzyme in the open conformation. These inhibitors are less effective in the treatment of endothelial dysfunction and more likely to induce undesirable side-effects, particularly in aging and diabetic subjects.

Thus, a first aspect of the present invention relates to a compound which is a modulator of tissue transglutaminase (TG2) for use in the treatment of endothelial dysfunction,

wherein the modulator of tissue transglutaminase (TG2) is a compound of formula (I):

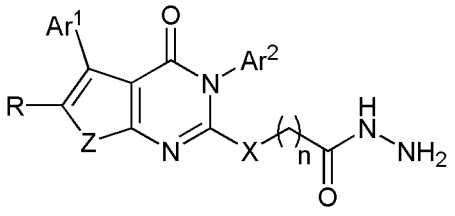

(I)

wherein

- Z is selected from the group consisting of S, $SO_2$, and Se,
- $Ar^1$ and $Ar^2$ are independently selected from the group consisting of optionally substituted phenyl and optionally substituted heteroaryl,
- R is selected from the group consisting of hydrogen, deuterium, halogen, and $C_1$-$C_3$ alkyl,
- X is selected from the group consisting of O, NH, N(Me), and S,

n is an integer selected from the group consisting of 1, 2 and 3.

A second aspect of the invention relates to a method of treating endothelial dysfunction comprising administering to a subject in need thereof a compound which is a modulator of tissue transglutaminase (TG2).

A third aspect of the invention relates to use of a compound which is a modulator of tissue transglutaminase (TG2) for the manufacture of a medicament for use in the treatment endothelial dysfunction.

The present inventors have surprisingly found that modulators of TG2, which inhibit the open conformation of the TG2 enzyme while promoting the closed conformation, such as LDN-27219 and derivatives, are effective in the treatment of endothelial dysfunction and diseases related thereto. Particularly, these compounds are effective in aging and diabetic subjects, where a pronounced effect is seen as compared to control and also compared to TG2 inhibitors that lock the enzyme in its open conformation, or that inhibit the enzyme more generally and/or irreversibly.

**Brief description of the figures**

**Figure 1** shows that treatment with LDN-27219 ($10^{-6}$ mol/L) improves the endothelium-derived relaxation of mesenteric arteries extracted from Male Wistar rats as induced by acetylcholine ($10^{-8}$-$10^{-5}$ mol/L) as compared to the control experiments (vehicle), and that the effect of LDN-27219 is particularly pronounced in older rats. Thus, Figure 1 A) shows relaxation % of the mesenteric arteries in healthy 6-7 week old rats as a function of acetylcholine concentration. Figure 1 B) shows relaxation % of the mesenteric arteries in healthy ≈12 week old rats. Figure 1 C) shows relaxation % of the mesenteric arteries in healthy >30 week old rats.

**Figure 2** shows that LDN-27219 ($3 \cdot 10^{-6}$ mol/L) improves the endothelium-derived relaxation of small mesenteric arteries extracted from male BKS diabetic mice as induced by acetylcholine ($10^{-8}$-$10^{-5}$ mol/L) as compared to the control experiments (vehicle), and that the effect of LDN-27219 is particularly pronounced in older and diabetic mice. Thus, Figure 2 A) shows relaxation % of the mesenteric arteries in 14-16 week old healthy control BKS mice that do not express type 2 diabetes as a function of acetylcholine concentration. Figure 2 B) shows relaxation % of the mesenteric arteries in 24-25 week healthy control BKS mice that do not express type 2 diabetes. Figure 2 C) shows relaxation % of the mesenteric arteries in 16-17 week old mice with diabetes 2.

**Figure 3 A**) Shows that the infusion of three doses of LDN-27219 (0.1, 1.0 and 2.0 mg/kg) each lower the mean blood pressure (mmHg) in the carotid artery (antihypertensive effect), as well as a control experiment infusing the vehicle PEG-400.

**Figure 3 B)** Shows the calculated integral of the blood pressure (AUC) for the three additions of LDN-27219 shown in figure 3 A) and illustrates the increased anti-hypertensive effect in older rats (> 30 weeks old) as compared to younger rats (12-14 weeks old).

**Figure 4)** Shows that LDN-27219 ($10^{-3}$ mol/L) is able to increase the percentage of purified human TG2 in the closed conformation as compared to control conditions (vehicle). Thus, Figure 4 A) shows the two bands corresponding to the

open and closed conformations (above) and their relative abundance in percentage (below) in control conditions. Figure 4 B) shows the two bands corresponding to the open and closed conformations (above) and their relative abundance in percentage (below) in presence of LDN-27219 ($10^{-3}$ mol/L). Figure 4 C) shows the band corresponding to the closed conformation (above) and its relative abundance in percentage (below) in presence of GTP ($10^{-3}$ mol/L), natural ligand of TG2 that is known to force the closed conformation of the enzyme. Figure 4 D) shows the band corresponding to the open conformation (above) and its relative abundance in percentage (below) in presence of Z-DON ($0.2 \cdot 10^{-3}$ mol/L) and $Ca^{2+}$ ($10^{-3}$ mol/L), ligands of TG2 that are known to force the open conformation of the enzyme.

**Figure 5 A)** Shows the average of the current density(pA/pF)-voltage(mV) relationships of isolated vascular smooth muscle cells (VSMCs) exposed to different TG2 modulators. LDN-27219 ($3 \cdot 10^{-5}$ mol/L) increased potassium currents compared to the control conditions in an equivalent way to intracellular GTP, which has been shown to induce TG2 closed conformation, while (S)-Benzyl (6-acrylamido-1-(4-(7-hydroxy-2-oxo-2H-chromene-3-carbonyl)piperazin-1-yl)-1-oxohexan-2-yl)carbamate) (from now on VA-5) ($5 \cdot 10^{-5}$ mol/L), a TG2 irreversible inhibitor that has been shown to lock TG2 into the open conformation decreased potassium currents on these cells.

**Figure 5 B)** Shows the different effects of TG2 inhibitors on the tension of small mesenteric arteries extracted from ≈12 week old Male Wistar rats depending on their effect on the conformation of the enzyme. LDN-27219 ($10^{-8}$-$10^{-5}$ mol/L), that is believed to promote the closed conformation of TG2, induces a direct and dose-dependent relaxation of the arteries, which is sensitive to the removal of the endothelial layer. On the other hand, Z-DON-Val-Pro-Leu-OMe (from now on Z-DON) ($10^{-8}$-$3 \cdot 10^{-4}$ mol/L), an irreversible TG2 inhibitor that has been shown to lock the enzyme in the open conformation in crystallization studies, does not induce relaxation at any tested doses.

**Figure 5 C)** Shows that, in contrast to LDN-27219, membrane permeable inhibitors that force TG2 into the open conformation (Z-DON ($4 \cdot 10^{-5}$ mol/L) and VA-5 ($10^{-5}$ mol/L)) reduce the endothelium-derived relaxation of mesenteric

arteries extracted from ≈12 week Male Wistar rats when induced by acetylcholine ($10^{-8}$-$10^{-5}$ mol/L) and compared to the control experiments (vehicle) and membrane impermeable TG2 inhibitor Boc-DON-Gln-Ile-Val-OMe (from now on Boc-DON) ($10^{-5}$ mol/L).

**Figure 5 D)** Shows that the presence of VA-5 ($10^{-5}$ mol/L) prevents LDN-27219 ($10^{-6}$ mol/L) to produce the improvement in endothelium-derived relaxation of small mesenteric arteries extracted from ≈12 week Male Wistar rats. This experiment was performed under the same conditions as the experiment shown in Figure 1 B, except from the presence of the irreversible TG2 inhibitor VA-5 that lock the enzyme in the open conformation.

**Figure 5 E)** Shows the average mean blood pressure (mmHg) recorded before, during and after the infusion of a single dose of VA-5 (1 mg/kg) and illustrates the lack of anti-hypertensive effect of this compound in both younger rats (12-14 weeks old) and older rats (>30 weeks old).

**Figure 6 A)** Shows that LDN-27219 ($10^{-8}$-$10^{-5}$ mol/L), induces a direct and dose-dependent relaxation of small subcutaneous arteries obtained from human biopsies. These results evidence the translatability to human tissue of the previous results in tissue from rodents (Figure 5B).

**Figure 6 B)** Shows that LDN-27219 ($3 \cdot 10^{-6}$ mol/L) improves the endothelium-derived relaxation of small subcutaneous arteries obtained from human biopsies as induced by acetylcholine ($10^{-8}$-$10^{-5}$ mol/L) as compared to the control experiments (vehicle). These results evidence the translatability to human tissue of the previous results in tissue from rodents (Figure 1).

**Figure 7)** Shows that intraperitoneal injection of LDN-27219 (8 mg/kg/12h) for 3 weeks (long-term '*in vivo*' study) is able to successfully prevent endothelial dysfunction in diabetic BKS mice of 10 weeks of age more effectively than oral candesartan (3 mg/kg/24 h), an anti-hypertensive treatment used in the clinical practice that has previously demonstrated to improve endothelial function in similar disease models of diabetes. As in previous figures, endothelial function is

studied as relaxation of small mesenteric arteries as induced by acetylcholine ($10^{-8}$-$3 \cdot 10^{-5}$ mol/L).

The present invention will now be described in more detail in the following.

**Detailed description of the invention**

Definitions

Prior to discussing the present invention in further details, the following terms and conventions will first be defined:

*Enzyme modulator*

In the present context, an "enzyme modulator" is a compound that changes the activity of an enzyme. The modulator may be an enzyme inhibitor that decreases the activity of the enzyme, or an enzyme inducer that increases the activity of the enzyme. Specifically a "modulator of tissue transglutaminase" (TG2) may for example induce the formation of a closed conformation of TG2, and therefore inhibit the open conformation of TG2. In the present invention, the enzyme modulator may be a small organic molecule, such as a compound of Formula (I), more specifically the compound of Formula (II) [LDN-27219], which changes the conformation of the enzyme and thereby alters the activity of the enzyme.

*Tissue Transglutaminate (TG2)*

In the present context, "Tissue Transglutaminase" (TG2) is an enzyme of the transglutaminase family (comprising TG1-TG7 and Factor XIII). The TG2 enzyme is highly expressed in endothelial and smooth muscle cells and can be found within many different organs of the body, including the brain, the heart, the liver and small intestine. TG2 is located in different intracellular and extracellular compartments and has several functions depending on the location and conformation of the enzyme. The intracellular TG2 is most abundant in the cytosol and in smaller amounts within the nucleus and mitochondria. TG2 is found in the body in a closed conformation and in an open confirmation. When TG2 is bound to $Ca^{2+}$, it conforms to an open conformation that shows extracellular transamidase activity and leads to covalent cross-linking of structural proteins. In the closed

conformation, it presents intracellular GTP-binding activity that enables it to act as a G protein (Ghα) and consequently allow for signal transduction in the cell.

*Endothelial dysfunction*

In the present context, "endothelial dysfunction" is a condition in which the endothelial layer, that coats the luminal surface of the vascular system, fails to function normally. Such a condition is associated with a decreased ability of the endothelial layer to secrete important mediators for control of vasoconstriction and vasodilation. Vasoconstriction is mostly regulated by endothelin-1 and thromboxane A2 mediators, whereas vasodilation is regulated by nitric oxide (NO), prostacyclin or other endothelium-derived hyperpolarization factors. The endothelial cells play an essential role in the regulation of vascular tone in response to hemodynamics and chemical signals. Thus, endothelial dysfunction is e.g. associated with increased blood pressure and cardiovascular diseases in the vascular system. Endothelial dysfunction particularly occurs in association with aging and diabetes. Dysfunction of the endothelial cells may also occur when excessive amounts of low-density lipoprotein (LDL) particles are oxidized within the endothelial layer. Although endothelial dysfunction may be regarded as a cardiovascular risk factor in itself, it is associated to a number of related pathologies/diseases such as for example dementia, Alzheimer's disease, ventricular hypertrophy, vascular calcification, atherosclerosis, ischemic chronic wounds, hypertension, and erectile dysfunction.

*Diabetes*

In the present context, the term "diabetes" refers to the disease diabetes mellitus. It is a type of disease in which the amount of sugar in the blood is far removed from normal levels for a prolonged time period. In most cases the blood will contain an elevated amount of sugar, either because of insufficient production of insulin (diabetes 1) or because the cells do not respond properly to the insulin (diabetes 2). The abnormal levels of sugar in the blood stream cause a decrease in NO production by the endothelial cells and decreased activity of NO. Diabetes 1 is classified as an immune-mediated or idiopathic disease that is characterized by loss of the insulin-producing beta-cells in the pancreatic islets. Diabetes 1 covers roughly 10% of the present 422 million diabetes patients worldwide. Diabetes 2 is characterized by insulin resistance in the cells and is primarily caused by obesity

instigated by lifestyle factors, such as lack of physical activity, poor diet, and stress. Diabetes 2 covers roughly 90% of the present 422 million diabetes patients worldwide.

*Age-associated endothelial dysfunction*

In the present context, the term "age-associated endothelial dysfunction" refers to endothelium dysfunction in which the cells do not secrete the required amount of mediators controlling vascular tone as a consequence of an aging body. It also covers endothelium dysfunctions caused by elevated levels of cholesterol resulting from increasing age. Further, any diseases resulting from endothelial dysfunction may also be age-associated.

*Diabetes-associated endothelial dysfunction*

In the present context, the term "diabetes-associated endothelial dysfunction" refers to endothelial dysfunction caused by diabetes and the resulting impairment of the NO production and activity of nitric oxide. Further, any diseases resulting from endothelial dysfunction may also be diabetes-associated.

*Optionally substituted*

In the present context, the term "optionally substituted" describes any moiety that is obtained if one or more of the hydrogen atoms in any position on the optionally substituted moiety (such as e.g. an aromatic ring) is substituted with another atom or group.

*Heteroaryl*

In the present context, the term "heteroaryl" refers to a compound comprising one or more aromatic rings that consist of carbon atoms and at least one or more heteroatoms, such as O, N or S. Examples of 5, 6, 9 and 10 membered heteroaryls include pyrrole, furane, thiophene, thiazole, isothiazole, oxazole, isooxazole, pyrazole, imidazole, 1,2,3-oxadiazole, 1,2,4-oxadiazole, 1,2,5-oxadiazole, 1,3,4-oxadiazole, 1,2,3-triazole, 1,2,4-triazole, pyridine, pyridazine, pyrimidine, pyrazine, 1,2,4-triazine, 1,3,5-triazine, indole, indolizine, indazole, benzimidazole, 4-azaindole, 5-azaindole, 6-azaindole, 7-azaindole, 7-azaindazole, pyrazolo[1,5-a]pyrimidine, benzofuran, isobenzofuran, benzo[b]thiophene, benzo[c]thiophene, benzo[d]isoxazole, benzo[c]isoxazole, benzo[d]oxazole,

benzo[c]isothiazole, benzo[d]thiazole, benzo[c][1,2,5]thiaciazole, 1H-benzotriazole, quinolone, isoquinoline, quinoxaline, phthalazine, quinazoline, cinnoline, 1,8-naphthyridine, pyrido[3,2-d]pyrimidine, pyrido[4,3-d]pyrimidine, pyrido[3,4-b]pyrazine, pyrido[2,3-b]pyrazine.

*Alkyl*

In the present context, the term "alkyl" means any terminal saturated hydrocarbon chain, including branched or linear chains. Examples include methyl ($-CH_3$), ethyl ($-CH_2CH_3$), propyl ($-CH_2CH_2CH_3$) and isobutyl ($-CH(CH_3)CH_2CH_3$). $C_1$-$C_{10}$ alkyl refers to an alkyl comprising 1-10 carbons.

*Alkenyl*

In the present context, the term "alkenyl" refers to an alkyl as described above, which however is unsaturated and contains at least one or more double bonds within its structure.

*Alkynyl*

In the present context, the term "alkynyl" refers to an alkyl as described above, which however is unsaturated and contains at least one or more triple bonds within its structure.

*Pharmaceutically acceptable*

In the present context, the term "pharmaceutically acceptable" refers to molecular entities and compositions that are physiologically tolerable and do not typically produce an allergic or similar untoward reaction, such as e.g. gastric upset, dizziness and the like, when administered to a human. Preferably, as used herein, the term "pharmaceutically acceptable" means approved by a regulatory agency of the Federal or a state government or listed in the U.S. Pharmacopoeia or other generally recognized pharmacopoeia for use in animals, and more particularly in humans.

*Solution*

In the present context, the term "solution" refers to a homogeneous mixture composed of two or more substances.

*Solid dosage form*

In the present context, the term "solid dosage form" refers to a solid pharmaceutical product consisting of a defined mixture of pharmaceutical active ingredients and inactive components. When apportioned into a specific dose, a solid dosage form may be termed a solid unit dosage form. Solid dosage formulations may be in the form of tablets, capsules, granules, powders, sachets, or chewables.

*An effective amount*

In the present context, the term "effective amount" refers to a dosage sufficient to produce a desired result on a health condition, pathology, and disease of a subject or for a diagnostic purpose. The desired result may comprise a subjective or objective improvement in the recipient of the dosage. "Therapeutically effective amount" refers to that amount of an agent effective to produce the intended beneficial effect on health.

The present invention relates to the treatment of endothelial dysfunction via selective modulation of the tissue transglutaminase (TG2) enzyme using compounds that stabilize the enzyme in the so-called "closed conformation", where GTP binds to the enzyme. As provided above this leads to enhanced endothelial function and a potential new pathway for treating diseases such as for example hypertension, erectile dysfunction and others.

Thus a first aspect of the present invention is a compound which is a modulator of tissue transglutaminase (TG2) for use in the treatment of endothelial dysfunction.

In one embodiment the modulator of tissue transglutaminase (TG2) is for use in the treatment of diseases resulting from endothelial dysfunction.

The present inventors have shown that compounds promoting the closed conformation of TG2 and thus inhibiting or lowering the available amount of the open conformation of TG2 are particularly effective and selective in improving endothelial function. Therefore, the modulator of tissue transglutaminase (TG2) may preferably be a promoter of the closed conformation of tissue transglutaminase, and even more preferably the modulator of tissue

transglutaminase (TG2) may be a promoter of the closed conformation of tissue transglutaminase and an inhibitor of the open conformation of tissue transglutaminase. Preferably, the tissue transglutaminase (TG2) is human tissue transglutaminase (EC 2.3.2.13).

Age and diabetes may lead to increased expression of TG2. In a particularly preferred embodiment the modulator of tissue transglutaminase (TG2) has an effect on endothelial function which is age-dependent. Particularly preferred are compounds which increasingly improve endothelial function with increasing age of a subject, to which the compound is administered. Likewise, compounds which improve endothelial function in particularly in diabetic subjects are preferred.

As described a number of small molecule inhibitors of TG1-7 are known including inhibitors of TG2, but the majority are general inhibitors/modulators of TG2 (i.e. inhibits both the closed and open form). Since promotion of the closed form over the open form is hypothesised to have beneficial effects in endothelial function, compounds achieving such modulation would have potential in the treatment of endothelial dysfunction. The present inventors have found that LDN-27219 and derivatives achieve such promotion of the closed conformation while inhibiting the open conformation. These compounds are superior to non-specific inhibitors and inhibitors that lock the enzyme in the open conformation in terms of treating endothelial dysfunction, particularly in patient sub-groups of old age and sub-groups diagnosed with diabetes. Suitable derivatives of LDN-27219 are described in e.g. US 2006/0183759.

Hence, in a preferred embodiment the modulator of tissue transglutaminase (TG2) is a compound of formula (I):

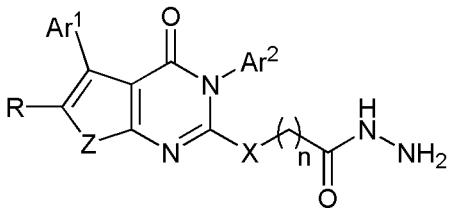


(I)

wherein

- Z is selected from the group consisting of S, $SO_2$, and Se,

- $Ar^1$ and $Ar^2$ are independently selected from the group consisting of optionally substituted phenyl and optionally substituted heteroaryl,
- R is selected from the group consisting of hydrogen, deuterium, halogen, and $C_1$-$C_3$ alkyl,
- X is selected from the group consisting of O, NH, N(Me), and S,
- n is an integer selected from the group consisting of 1, 2 and 3.

In the present context, $SO_2$ is a diradical having the formula  , which bond to other atoms in a molecular structure through covalent bonds to the S in $SO_2$.

In a more preferred embodiment Z is S.

The optional substituents of $Ar^1$ and $Ar^2$ may be selected from the group consisting of $C_1$-$C_{10}$ alkyl, $C_2$-$C_{10}$ alkenyl, $C_2$-$C_{10}$ alkynyl, amino (-$NH_2$), -$CH_2NH(C_1$-$C_{10}$ alkyl), -$CH_2N(C_1$-$C_{10}$ alkyl)$_2$, aminoalkyl (-$NH(C_1$-$C_{10}$ alkyl) or –$N(C_1$-$C_{10}$ alkyl)$_2$, cyano (-CN), -$CONH_2$, -$CONH(C_1$-$C_{10}$ alkyl), -$CON(C_1$-$C_{10}$ alkyl)$_2$, hydroxyl (-OH), $C_1$-$C_{10}$ alkyl hydroxyl (-alkyl-OH), $C_1$-$C_{10}$ alkoxy(-O-alkyl), carboxylic acid (-COOH), $C_1$-$C_{10}$ alkyl esters (-COO-alkyl), $C_1$-$C_{10}$ alkyl acyl (-CO-alkyl), sulfonic acid (-$SO_3H$), $C_1$-$C_{10}$ alkyl sulfonate (-$SO_3$-alkyl), phosphonic acid (-$PO(OH)_2$), $C_1$-$C_{10}$ alkyl phosphonate (-$PO(O\text{-alkyl})_2$), phosphinic acid (-P(O)(H)OH), $SO_2NH_2$, hydroxamic acid (-CONHOH), $C_1$-$C_{10}$ alkyl sulfonylureas (-$NHCONHSO_2$(alkyl)), $C_1$-$C_{10}$ acylsulfonamides (-$SO_2$-NHCO-(alkyl), hydroxyl amine (-NHOH), nitro (-$NO_2$), and halogen.

More preferably the optional substituents of $Ar^1$ and $Ar^2$ are selected from the group consisting of $C_1$-$C_{10}$ alkyl, cyano (-CN), -$CONH_2$, hydroxyl (-OH), $C_1$-$C_{10}$ alkyl hydroxyl (-alkyl-OH), carboxylic acid (-COOH), $C_1$-$C_{10}$ alkyl esters (-COO-alkyl), sulfonic acid (-$SO_3H$), phosphonic acid (-$PO(OH)_2$), nitro (-$NO_2$), and halogen.

Even more preferably the optional substituents of $Ar^1$ and $Ar^2$ are selected from the group consisting of $C_1$-$C_3$ alkyl, hydroxyl (-OH), $C_1$-$C_3$ alkyl hydroxyl (-alkyl-OH), and halogens. Halogens may preferably be selected from the group consisting of fluorine, chlorine, bromine, and iodine, preferably fluorine.

In a preferred embodiment the compound according to Formula (I), is a compound wherein

- $Ar^1$ and $Ar^2$ are optionally substituted phenyl,
- R is hydrogen or halogen
- X is S,
- n is an integer selected from the group consisting of 1, 2 and 3.

In an even more preferred embodiment the compound according to Formula (I), is a compound wherein

- $Ar^1$ and $Ar^2$ are phenyl,
- R is hydrogen
- X is S,
- n is 1.

Thus, in a most preferred embodiment the modulator of tissue transglutaminase (TG2) is a compound of formula (II):

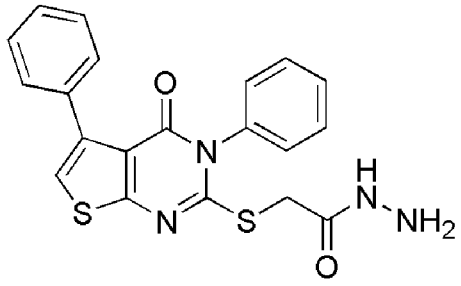


(II).

The compound of formula (II) corresponds to LDN-27219, and hence, in an alternative embodiment the modulator of tissue transglutaminase (TG2) is LDN-27219.

As described above for the present first aspect of the invention, it relates to the treatment of endothelial dysfunction, and diseases resulting therefrom. The present inventors have found that the selective TG2 modulators of the invention are increasingly effective in the treatment of endothelial dysfunction the older the

subjects are. This may be related to the fact that TG2 is increasingly expressed in aging subjects.

Therefore, in a preferred embodiment of the present invention the endothelial dysfunction is associated with increased levels or increased activity of tissue transglutaminase (TG2). More preferably the endothelial dysfunction is age-associated, i.e. associated with changes in endothelial function related to aging.

In terms of age-associated endothelial dysfunction and age-associated diseases resulting from endothelial dysfunction, a patient sub-group may be defined, wherein the compounds of the present invention have pronounced beneficial effects. Thus, in a preferred embodiment the compounds of the invention are administered to human patients between the age of 30-140 years, such as the age of 35-140 years, 40-140 years, 45-140 years, 50-140 years, 55-140 years, 60-140 years, 65-140 years, 70-140 years, such as preferably 30-120 years, 40-100 years, such as most preferably 50-100 years.

Expression of TG2 is also increased in diabetic subjects. The inventors have found that the selective TG2 modulators for the closed conformation in the present invention are especially effective in the treatment of endothelial dysfunction associated with diabetes i.e. associated with changes in endothelial function related to diabetes.

Thus, in a preferred embodiment the endothelial dysfunction is diabetes-associated. Thus, a preferred sub-group of patient may be defined as patients or subjects suffering from diabetes or diagnosed with diabetes, also known as diabetes mellitus. Diabetes may include diabetes-1 or diabetes-2. Thus, in a more preferred embodiment of the present invention the endothelial dysfunction is associated with diabetes-1 or diabetes-2, preferably diabetes-2.

Age and diabetes may often be related, particularly diabetes-2 may develop in aging patient. Hence, in another preferred embodiment of the present invention the endothelial dysfunction is both age-associated and diabetes-associated, particularly it may be both age-associated and diabetes-2 associated.

The subjects or patients treated for the present invention are preferably mammals, such as preferably human subjects or patients.

A number of diseases are known to be a direct or indirect result of endothelial dysfunction, or to be associated with endothelial dysfunction. Such related diseases comprise cardiovascular diseases, diseases related to vasodilative function, but also diseases related to the brain and its function. Also, the well-known antifibrotic effects of TG2 inhibitors, together with the vasoprotective effects observed from the induction of the closed conformation, make LDN-27219 potentially useful in the treatment of fibrotic diseases. Hence, in a preferred embodiment of the present invention the disease resulting from endothelial dysfunction is selected from the group consisting of dementia, Alzheimer's disease, ventricular hypertrophy, vascular calcification, renal fibrosis, cardiac fibrosis, pulmonary fibrosis, atherosclerosis, ischemic chronic wounds, hypertension, pulmonary hypertension, and erectile dysfunction, preferably hypertension and erectile dysfunction.

For treatment of erectile dysfunction, it is possible to define a patient sub-group, in which the compounds of the present invention have a pronounced effect. Thus in the treatment of erectile dysfunction the compounds may preferably be administered to patients of male gender.

In an embodiment of the present invention the compound of the present invention is administered in a composition further comprising a pharmaceutically acceptable carrier or diluent, more preferably in the form of a solution or a solid dosage form, and most preferably as a solid dosage form. In an embodiment of the present invention the solid dosage form is selected from the group consisting of a tablet, a capsule, and a sachet.

The compounds of the present invention and the composition as described above may be administered orally, or parenterally, such as intravenously, intradermally, subcutaneously, or topically. Preferably the compound is administered in a therapeutically effective amount.

One particularly preferred embodiment of the invention is a compound of formula (I):

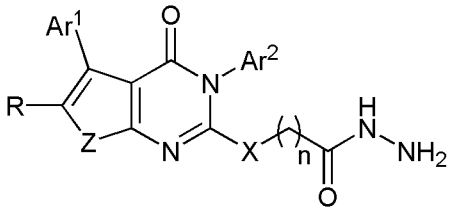

(I)

wherein

- Z is selected from the group consisting of S, $SO_2$, and Se,
- $Ar^1$ and $Ar^2$ are independently selected from the group consisting of optionally substituted phenyl and optionally substituted heteroaryl,
- R is selected from the group consisting of hydrogen, deuterium, halogen, and $C_1$-$C_3$ alkyl,
- X is selected from the group consisting of O, NH, N(Me), and S,
- n is an integer selected from the group consisting of 1, 2 and 3,

for use in the treatment of a disease selected from the group consisting of dementia, Alzheimer's disease, ventricular hypertrophy, vascular calcification, atherosclerosis, ischemic chronic wounds, hypertension, and erectile dysfunction.

Another particularly preferred embodiment of the invention is a compound of formula (I):

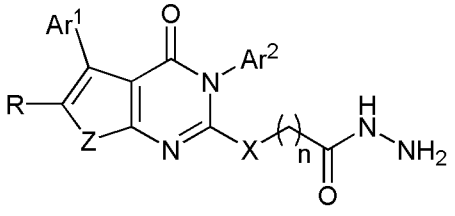

(I)

wherein

- Z is selected from the group consisting of S, $SO_2$, and Se,
- $Ar^1$ and $Ar^2$ are independently selected from the group consisting of optionally substituted phenyl and optionally substituted heteroaryl,
- R is selected from the group consisting of hydrogen, deuterium, halogen, and $C_1$-$C_3$ alkyl,
- X is selected from the group consisting of O, NH, N(Me), and S,
- n is an integer selected from the group consisting of 1, 2 and 3,

for use in the treatment of endothelial dysfunction,
wherein said endothelial dysfunction is age-associated or diabetes-associated.

Yet another particularly preferred embodiment of the invention is a compound of formula (I):

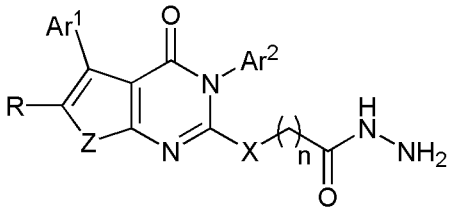

(I)

wherein

- Z is selected from the group consisting of S, $SO_2$, and Se,
- $Ar^1$ and $Ar^2$ are independently selected from the group consisting of optionally substituted phenyl and optionally substituted heteroaryl,
- R is selected from the group consisting of hydrogen, deuterium, halogen, and $C_1$-$C_3$ alkyl,
- X is selected from the group consisting of O, NH, N(Me), and S,
- n is an integer selected from the group consisting of 1, 2 and 3,

for use in the treatment of diseases resulting from endothelial dysfunction, wherein the compound of formula (I) is administered to human patients between the age of 30-140 years.

Yet another particularly preferred embodiment of the invention is a compound of formula (I):

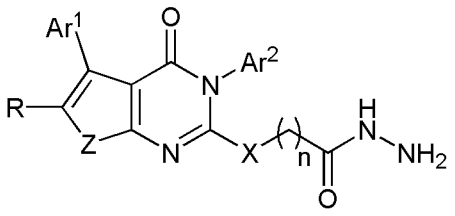

(I)

wherein

- Z is selected from the group consisting of S, $SO_2$, and Se,
- $Ar^1$ and $Ar^2$ are independently selected from the group consisting of optionally substituted phenyl and optionally substituted heteroaryl,

- R is selected from the group consisting of hydrogen, deuterium, halogen, and $C_1$-$C_3$ alkyl,
- X is selected from the group consisting of O, NH, N(Me), and S,
- n is an integer selected from the group consisting of 1, 2 and 3,

for use in the treatment of diseases resulting from endothelial dysfunction, wherein the compound of formula (I) is administered to human patients diagnosed with diabetes.

A second aspect of the present invention is a method of treating endothelial dysfunction comprising administering to a subject in need thereof a compound which is a modulator of tissue transglutaminase (TG2).

A third aspect of the present invention is the use of a compound which is a modulator of tissue transglutaminase (TG2) for the manufacture of a medicament for use in the treatment of endothelial dysfunction.

It should be noted that embodiments and features described in the context of one of the aspects of the present invention also apply to the other aspects of the invention.

All patent and non-patent references cited in the present application, are hereby incorporated by reference in their entirety.

The invention will now be described in further details in the following non-limiting examples.

**Examples**

**Materials and methods**

For the conformational shift assay using native polyacrylamide gel electrophoresis (native-PAGE) purified and functional human TG2 protein produced in insect cells was obtained from Zedira (Darmstadt, Germany).
The following compounds were used: ACh, Candesartan cilexetil, $Na_2GTP$ (guanosine 5′-triphosphate sodium salt), phenylephrine, and U46619 (9α-

epoxymethanoprostaglandin F2α) from Merk (Darmstadt, Germany). LDN-27219 was obtained from Tocris Bioscience (Bristol, UK). Boc-DON and Z-DON were obtained from Zedira (Darmstadt, Germany). Sulfobutyl ether beta-cyclodextrin sodium (SBE-b-CD) was obtained from Glentham Life Sciences (Wiltshire, United Kingdom). VA-5 was from ChemShuttle (Hayward, CA, USA). Synthesis of LDN-27219 is described in US 2006/0183759.

Unless otherwise stated all substances were dissolve in distilled water. For '*ex vivo*' experiments U46619 was dissolved in ethanol and Boc-DON, LDN-27219 VA-5 and Z-DON were dissolved in DMSO and stored at -20ºC. Further dilution of the above mentioned compounds were made in distilled water. The DMSO concentration in the bath were kept below 0,01% and did not affect vessel contractility. For '*in vivo*' experiments LDN-27219 and VA-5 were dissolved in PEG-400.

For long-term '*in vivo*' experiments, stocks of LDN-27219 dissolved in PEG-400 were diluted in saline solution containing SBE-b-CD to improve solubility (9 mg/mL NaCl; 15 % (w/v) SBE-b-CD) immediately after injection, resulting in a final concentration of 2.00 mg/mL of LDN-27219 in 10% PEG-400/90%(15% (w/v) SBE-b-CD in saline solution). For the treatment on the drinking water 1 mg/ml Candesartan cilexetil was dissolved in a vehicle of polyethylene glycol 400 (10% v/v), ethanol (5% v/v), cremophor EL (2% v/v), and tap water (83% v/v) and the pH was adjusted to 9.0 with 0.5 mol/L $Na_2CO_3$ prior to dilution to the final concentration in tap water, as previously described (Seltzer A., et al., Brain Res., 2004, 1028(1), 9-18). Final concentrations needed to achieve the desired dosis of candesartan cilexetil per day were determined by measuring water consumption each 3-4 days.

Animals and tissue preparation

Human subcutaneous arteries were obtained from fat biopsies of the gluteal region from both male and female patients (30-70 years of age) with essential hypertension.

Male Wistar rats of 6-7, 12-14 and 30-35 weeks of age, weighing 200-250, 300-400 and 600-700 g respectively, were obtained from Taconic Denmark ApS (Rye, Denmark) and housed adequately in the animal facility of Aarhus University. Healthy male BKS(D)-Leprdb/JOrlRj heterozygous mice of age 14-16, 24-25 (for '*ex vivo*' studies) and 6-7 weeks (for long-term '*in vivo*' studies) and diabetic homozygous mice of age 16-17 (for '*ex vivo*' studies) and 6-7 (for long-term '*in vivo*' studies) weeks were obtained from Taconic, Ry, Denmark or Janvier Labs (Le Genest-Saint-Isle, France) and housed adequately in the animal facility of Aarhus University.

For '*ex vivo*' studies, animals were randomly selected and euthanized by cervical dislocation and exanguination. The mesenteric arteries were immediately extracted and placed in 4ºC physiological saline solution (PSS, pH= 7.4) of the following composition (mmol/L): 119 NaCl, 4.7 KCl, 1.18 $KH_2PO_4$, 1.17 $MgSO_4$, 1.5 $CaCl_2$, 24.9 $NaHCO_3$, 0.026 EDTA and 5.5 glucose and small mesenteric arteries (internal diameters of 200-300 µm) were isolated. Human subcutaneous arteries (internal diameters of 300-400 µm) were dissected from the biopsies in the same conditions mentioned above for the mesenteric bed from rodents.

For '*in vivo*' experiments Wistar rats of different age were fasted 8 h before anesthesia with 35 mg/kg of S-ketamine and 50 mg/kg of pentobarbital sodium administered intraperitoneally.

For long-term '*in vivo*' studies, diabetic homozygous mice were randomly allocated into three groups: 1) treatment with Intraperitoneal (IP) injections of LDN-27219 (8 mg/kg/12h) and vehicle drinking water [LDN-27219 treatment group], or 2) treatment with IP injections of vehicle (each 12 h) and candesartan cilexetil (3 mg/kg/24h) in the drinking water [candesartan treatment group], or 3) treatment with IP injections of vehicle (each 12 h) and vehicle drinking water [vehicle treatment group]. Age-paired healthy heterozygous animals were included as healthy controls, receiving the same treatment as the vehicle treatment group. After three weeks of treatment, animals were anesthetized with inhalation of isofluorane and euthanized by cervical dislocation. Small mesenteric arteries were obtained as described above.

Animal protocols and care were approved by the Danish Animal Experiments Inspectorate (permission 2014-15-2934-0159) and followed the ARRIVE guidelines (McGrath et al, 2015). The study using human arterial tissue was approved by the Regional Ethics Committee, Central Denmark (permission number: 1-10-72-120-17) and conducted in accordance with the principles of the Helsinki Declaration II for medical research. All participants gave informed consent prior to participation.

**Example 1 – Effects of LDN-27219 in rats of different age (*ex-vivo*)**

Small mesenteric arteries were mounted in microvascular myographs (Danish Myotechnology, Aarhus, Denmark) using two 40 µm wires and stretched to their optimal diameter for isometric tension recordings, which corresponded to 0.9 times the estimated internal diameter at 100 mmHg of transmural pressure. PSS solution in the myograph bath was heated to 37ºC and continuously bubbled with 5% CO2 in air to maintain pH (7.4). The vessel viability was tested at the beginning of each experiment by measuring the vasoconstrictor responses to a solution with a high $K^+$ concentration (KPSS), equivalent to PSS except that NaCl was exchanged for KCl on an equimolar basis, giving a final concentration of 123,7 mmol/L $K^+$ and the presence of endothelium was confirmed by addition of acetylcholine (ACh) ($10^{-5}$) after pre-constriction with noradrenaline ($5 \cdot 10^{-6}$ mol/L), arteries with less than 75% of relaxation were discarded.

Mesenteric arteries from rats of different age were incubated with ($10^{-6}$ mol/L) LDN-27219 or vehicle for 25 minutes and pre-contracted with phenylephrine (Phe) ($10^{-5}$ mol/L). Then cumulative addition of acetylcholine (ACh) caused the relaxation of the mesenteric arteries and the concentration-response curves were constructed.

Rats of 5-7 weeks age, about 12 weeks age, and more than 30 weeks of age were tested respectively. The results of the isometric tension studies are shown in Figure 1, A), B) and C) respectively, each representing a different their age group.

Example 1 demonstrates that LDN-27219 allows a more potent endothelium-dependent relaxation of the mesenteric arteries when compared to the ones

treated with vehicle, and that the effect of LDN-27219 is more pronounced in old rats, than in young rats.

**Example 2 - Effects of LDN-27219 in diabetic mice and healthy control mice of different age (*ex-vivo*)**

In these experiments, healthy control mice of different ages and diabetic adult mice were used and the relaxation measurements were performed as described in Example 1.

Healthy male BKS(D)-Leprdb/JOrlRj heterozygous mice between 14-16 and 24-25 weeks of age, and diabetic homozygous mice between 16-17 weeks of age were tested respectively. The results of the isometric tension studies are shown in Figure 2, A), B) and C) respectively.

Example 2 demonstrates that LDN-27219 allows a more potent endothelium-dependent relaxation of the mesenteric arteries when compared to the vehicle experiments in healthy and diabetic mice, and that the effect of LDN-27219 is more pronounced in older mice, and particularly pronounced in diabetic mice.

**Example 3 - Effects of LDN-27219 rats of different age (*in vivo*)**

Mean arterial pressure (MAP) `*in vivo*´ measurements:

Male Wistar rats with 12-14 and 30-35 weeks of age were anesthetized with s-ketamine (35 mg/kg) and pentobarbital (50 mg/kg) and placed on a heated blanket to maintain body temperature at 37ºC. ECG needles were installed for electrocardiographic measurements and a solid state catheter (Millar Inc, Houston, USA) was introduced into the carotid artery to measure MAP. MAP and electrocardiographic data was continuously recorded on a computerized data acquisition system (PowerLab, ADInstruments). Adequate depth of anesthesia was checked periodically by the absence of the toe pinch withdrawal effect and 1/3 of the initial dose of anesthetics was administered intraperitoneally when needed (usually each 1½ h). Changes in MAP and electrocardiographic signal in response to intrajugular infusion during 3 minutes of different doses of LDN-27219 and the corresponding vehicle (PEG-400) were studied.

The Area Under the Curve (AUC) was calculated using Graphpad Prism 5.1 (GraphPad Software, San Diego, California, USA) for each response to the change in MAP that was collected during the experiments in example 3. The AUC gives information about the maximal response, and about the duration of the effect.

The mean arterial pressure (MAP) over 3 minutes when adding LDN-27219 and control is shown in Figure 3 A), whereas the Area Under the Curve for these MAP measurements are shown for different aged rats in Figure 3 B) as a function of LDN-27219 concentration.

Preliminar *'in vivo'* studies in healthy male BKS(D)-Leprdb/JOrlRj heterozygous mice showed that, additionally to the previously described antyhipertensive effect, mice displayed increased erectile function, measured as peak intracavernosal pressure (PICP) over MAP, upon the administration of LDN-27219.

Example 3 demonstrates that LDN-27219 has an antihypertensive effect *in vivo*, as it lowers the mean blood pressure in the carotid artery. Example 3 further demonstrates the greater effect of LDN-27219 in older animals, which is consistent with the results obtained in Example 1.

**Example 4 – LDN-27219 promotes closed confirmation of TG2 as compared to TG2 inhibitors that lock the enzyme in the open conformation.**

*LDN-27219 is able to increase the percentage of TG2 present in the close conformation 'in vitro' compared to vehicle*.

Native gel electrophoresis experiments were performed using a method similar to those previously described (Pinkas DM, et al., PLoS Biol, 2007, 5(12), 2788–2796.) (Iversen R, et al., Proc Natl. Acad. Sci., 2014, 111(43), 17146-17151). Briefly, TG2 (2.5 uM) was incubated for 30 min at room temperature in preincubation buffer (75 mM imidazole, 0.5 mM EDTA, 5 mM DTT [pH 7.2], 10% DMSO) with or without 1 mM $GTPNa_2$ or 1 mM LDN-27219 before adding Native Sample Buffer for Protein Gels (Bio-Rad) or in preincubation buffer with 0.2 mM Z-

DON 30 min prior addition of 5mM of $CaCl_2$ for 20 min. Native buffer was added (dilution 1:2), and 1.5 ug of protein was loaded onto a 4–20% Criterion™ TGX Stain-Free™ gel (Bio-Rad) using Tris-glycine as the running buffer. For 75 min, 125 V was applied at 4 ºC . The bands were visualized using stain-free technology by exposing the gels to UV light and capturing the image using a PXi 4 Touch image analysis system (Syngene). Band intensity analysis was carried out using GeneTools 4 software (Syngene).

Figure 4 A) and B) show that LDN-27219 is able to increase the relative abundance of the closed conformation, reducing therefore the relative abundance of the open conformation, compared to vehicle. While GTP is able to completely force TG2 to its closed conformation of the enzyme and, contrarily, Z-DON in presence of calcium is able to force its open conformation (Figure 4 C) and D)).

*At the cellular level, LDN-27219 has the same influence in vascular smooth muscle cells (VSMCs) potassium currents as an endogenous promoter of the closed conformation of TG2, while the induction of the open conformation of the enzyme has the opposite effect.*

For isolation of VSMCs, rat mesenteric arteries were dissected as previously described, opened longitudinally and stored in ice-cold dissociation solution containing (mmol/L): 119 NaCl, 4.7 KCl, 1.18 $KH_2PO_4$, 1.17 $MgSO_4$, 24.9 $NaHCO_3$, 0.027 EDTA, and 11 glucose, pH= 7.4. Arteries were then equilibrated during 10 min in a dissociation solution with bovine albumin serum (BSA; 1 mg/mL) at 37ºC and then exposed to the same solution supplemented with papain (0.5 mg/mL; Worthington Biochemical Corp., Lakewood, NJ, USA) and dithiothreitol (DTT; 1 mg/mL) at 37ºC for 8 min. Arteries were then washed in ice-cold dissociation solution and moved to dissociation solution containing BSA (1 mg/mL) and collagenase (0.7 mg/mL type F and 0.4 mg/mL type H; Worthington Biochemical Corp.) at 37°C for 3 min. After washing in ice-cold dissociation solution, isolated SMCs were obtained by gentle trituration of the digested arteries with a fire polished pipette into the SMC extracellular solution (for composition, see below). After the digestion protocol, SMCs were seeded in micro-dishes (ibidi GmbH, Martinsried, Germany) and used for patch clamp recordings 15 min after the isolation protocol and within the next 5 hours.

Extracellular patch-clamp solution for VSMCs contained the following (mmol/L): 130 NaCl, 5 KCl, 1.2 $MgCl_2$, 1.5 $CaCl_2$, 10 glucose and 10 HEPES (adjusted to pH 7.3 with NaOH) .The patch pipette (intracellular) solution for SMCs contained the following (mmol/L): 130 KCl, 1.2 $MgCl_2$, 0.1 EGTA and 10 HEPES (adjusted to pH 7.2 with KOH). To study the effect of intracellular GTP in LDN-27219 activity over potassium currents, patch pipette solution with 5 mmol/L $Na_2GTP$ was used in some experiments.

Membrane currents were recorded under the whole-cell configuration of the patch-clamp technique using an Axon Multiclamp 700A amplifier (Axon instruments, Molecular Devices, CA, USA). Patch pipettes were made of borosilicate glass capillaries (World Precision Instruments, FL, USA) fabricated using a dual-stage puller PP-830 (Narishige, Tokyo, Japan) and had resistances of 4-7 MΩ. Current recordings were digitized on line at 10 kHz and low pass filtered at 2 kHz using a Digidata 1440 A (Axon Instruments), to acquire and store data the pClamp 10 software was used. Current-voltage relations were determined using 600 ms voltage ramps from -100 to 160 mV and a holding potential (Vh) of -65 mV for SMCs.

Amplitudes of $K^+$-outward currents were measured in control conditions and 12 min after the addition of LDN-27219 ($3 \cdot 10^{-5}$ mol/L) to the extracellular solution by a perfusion system. To study how conformational modulation of TG2 affected LDN-27219 activity over potassium channels, the initial protocol was repeated after one hour incubation with VA-5 ($5 \cdot 10^{-5}$ mol/L) and with GTP present in the intracellular solution, as VA-5 has been shown to force TG2 into the open conformation while GTP has been shown to induce the closed conformation.

Figure 5 A) shows that VSMCs treated with LDN-27219 had potassium currents significantly bigger compared to the ones in control conditions, being this currents equivalent to the ones recorded in presence of intracellular GTP. Contrarily, VSMCs treated with VA-5 presented significantly smaller potassium currents compared to those in control conditions. These results suggest that LDN-27219 mimics GTP, inducing the closed conformation of TG2 and leading to the opening of potassium channels, while VA-5 produces the opposite effect.

*Different mechanisms of TG2 inhibition on vascular tone*

The small mesenteric arteries were prepared in the same way is described in example 1.

The small mesenteric arteries were pre-contracted with the thromboxane analogue, U46619 ($4 \cdot 10^{-7}$ mol/L) and concentration-response curves for TG2 specific inhibitors, LDN-27219 ($10^{-8}$-$10^{-5}$ mol/L) and Z-DON ($10^{-8}$-$3 \cdot 10^{-4}$ mol/L) were constructed. To study the role of the endothelial pathways in LDN-27219 relaxation, concentration-response curves were constructed for it in arteries whose endothelium had been removed mechanically by rubbing the lumen repeatedly with a human scalp hair.

LDN-27219 induced relaxation in U46619 pre-contracted arteries as shown in Figure 5B). Furthermore, the results obtained in the same experiment using arteries without an endothelium layer showed a significantly reduced relaxation. Experiments were performed with cystamine in M. Engholm et al., British J. Pharm. (2016), 173, 839-855, showing that general TG2 inhibitors with unkown effects on TG2 conformation lacked effects on endothelial pathways. Also, the irreversible inhibitor Z-DON that has been shown to lock the enzyme in the open conformation, failed to induce any vasodilation. The results presented in Figure 5 B) are consistent with what is shown in Example 1 and indicate that the vasodilatory effects of LDN-27219 are associated with an endothelial pathway and that different mechanisms of TG2 inhibition have completely different effects in the vascular system.

*Pharmacological induction of TG2 closed conformation potentiates endothelial function while promotion of its open conformation reduces endothelium-dependent vasodilation.*

The small mesenteric arteries were prepared in the same way is described in example 1.

To investigate the effect of TG2 conformational modulation in endothelial function, arteries from animals of different age were pre-contracted with phenylephrine (Phe) ($10^{-5}$ mol/L) and ACh concentration-response curves were constructed after a 1 hour incubation with the irreversible TG2 inhibitors Z-DON ($4 \cdot 10^{-5}$ mol/L), Boc-DON ($10^{-5}$ mol/L) and VA-5 ($10^{-5}$ mol/L), which have demonstrated to lock the enzyme in its open conformation.

Incubation with LDN-27219 during 25 min increased the response to ACh in Phe pre-constricted arteries from 12-14 weeks old rats as observed in Example 1 (Figure 1 B). Contrarily, in these experiments, incubation with Z-DON and VA-5, irreversible and membrane permeable TG2 inhibitors that lock the enzyme in its open conformation, caused a slight inhibition of ACh relaxation compared to the vehicle, while non-permeable TG2 inhibitor Boc-DON had no significant effect as shown in Figure 5 C). LDN-27219 potentiation of ACh-induced vasodilation was reduced or completely inhibited by the presence of these TG2 irreversible inhibitors as represented by VA-5 in Figure 5 D) These results indicate that the effects of LDN-27219 are mainly due to its capacity to induce the closed conformation of TG2.

*Inducing TG2 open conformation by pharmacological means has no effects in blood pressure 'in vivo'.*

Rats of different age in these experiments were anesthetized, prepared and catheterized as described in Example 3. Intrajugular infusion during 3 minutes of a single dose (1 mg/kg) of the irreversible TG2 inhibitor VA-5, which have been shown to lock TG2 in the open conformation, did not produce any change in the mean blood pressure of the aorta neither in adult, nor in older animals. These results are shown in Figure 5 E) as average mean arterial pressure (MAP) values (mmHg) measured before (Bef.), during (Dur.) and after (Aft.) the infusion. These results indicate, consistently with the *ex-vivo* results, that inhibitors that lock the enzyme in the open conformation lack the antihypertensive properties of LDN-27219.

This example demonstrates that LDN-27219 is a selective promoter of the closed confirmation of TG2 and that this leads to enhanced endothelial vasodilatory function by opening of potassium channels as compared to specific inhibitors of TG2 that lock the enzyme in the open conformation and which show contrary effects on the vascular system, see Figure 5 E).

**Example 5 – A pharmacokinetic study.**

Using a non-compartmental model, pharmacokinetic studies of a single 2 mg/kg intravenous dose of LDN-27219 in living mice, revealed that the compound remains in the blood for enough time to be adequate for long-term treatments. The estimated values are reported in the following table.

| Compound | Sample size (no of mice) | Volume of distribution (L/kg) | Half-life (h) | Clearance (mL/min·kg) |
|---|---|---|---|---|
| LDN-27219 | 3 | 21.4 | 4.89 | 52.3 |

**Example 6 – Translatability of murine results to human tissue.**

Small human subcutaneous arteries were obtained from fat biopsies from the gluteal region of hypertensive patients and prepared as described in Example 1. Concentration-response curves for LDN-27219 were constructed as described in Example 4 (figure 5B) and relaxation measurements were performed as described in Example 1. The results of the isometric tension studies are shown in Figure 6 A) and B).

This example demonstrates the translatability of the results obtained in murine arteries to human tissue.

**Example 6 – Effect of long-term '*in vivo*' treatment with LDN-27219 in diabetic mice compared to reference treatment.**

In these experiments, age-paired healthy control mice and diabetic mice were used and the relaxation measurements were performed as described in Example 1. Mesenteric arteries from diabetic male BKS(D)-Leprdb/JOrlRj homozygous mice of 10-11 weeks of age were tested after three weeks of treatment with either 8 mg/kg LDN-27219, vehicle or 3 mg/kg candesartan cilexetil. Arteries from healthy male heterozygous mice were also tested after three weeks of treatment with vehicle as a healthy control. The results of the isometric tension studies are shown in Figure 7.

Example 6 demonstrates that long-term '*in vivo*' treatment with LDN-27219 is able to prevent diabetes-related endothelial dysfunction better than the long-term treatment with angiotensin II receptor antagonist candesartan cilexetil.

**Summary of results and conclusion**

Transamidase activity of tissue transglutaminase (TG2), linked to its open conformation, is associated with a series of diseases including cardiovascular disease. Also, TG2 can adopt a closed conformation, presenting GTP binding activity and playing a role in transmembrane signaling. Besides the ability of TG2 inhibitors to inhibit transamidase activity, conformational changes of the enzyme may play a role in their impact on disease. It has been found that general inhibitors (e.g. cystamine) of transglutaminase causes smooth muscle vasodilation. However, it is unclear how these inhibitors affect TG2 conformation and how these different conformations are linked with vascular function.

The present study hypothesized that the closed conformation of TG2 will be associated with vasodilation and antihypertensive effects and may restore age-related changes in endothelial function. It was tested whether LDN-27219 could promote the closed conformation of TG2 and provide improved effects in endothelial function.

Here '*ex vivo*' measurements of vessel tension were performed using isometric myographs in small mesenteric arteries from male Wistar rats, male diabetic healthy control mice and patch-clamp studies in isolated VSMCs. These experiments revealed that induction of the closed conformation of TG2 by LDN-27219 had a direct vasodilatory effect and potentiated the arterial response to acetylcholine through the opening of potassium channels. In contrast, drugs promoting the open conformation of TG2 had no effect in vessel tension and decreased potassium current and acetylcholine response. '*In vivo*' measurements of blood pressure and heart rate revealed that jugular infusion of LDN-27219 induced a drop in blood pressure that was larger in older animals, this was associated with increased expression of TG2 and restoration of endothelial function in isolated arteries from older animals and diabetic animals.

Pharmacological modulation of TG2 to its closed conformation using LDN-27219 presents antihypertensive effects '*in vivo*' and potentiates endothelium-dependent vasodilatation by opening potassium channels, increasing these effects with the age of the animal and in diabetic animals. Our findings suggest that the promotion of TG2 closed conformation using LDN-27219 could be a potential strategy to restore age-associated changes in endothelial function as well as diabetes associated changes.

**References**


- J.W. Keillor et al., Trends in pharmacological sciences, 2015, Vol 36, no 1
- M. Engholm et al., British J. Pharm. (2016), 173, 839-855
- US 8,614,233
- Y.J. Oh et al., Amino Acids, 2017, 49(3), 695-704
- US 2018/0002700 A1
- WO 2014/057266
- US2006/0183759
- McGrath JC, Lilley E (2015). Implementing guidelines on reporting research using animals (ARRIVE etc.): new requirements for publication in BJP. Br J Pharmacol 172: 3189–3193
- Seltzer A., et al., Brain Res., 2004, 1028(1), 9-18).
- Pinkas DM, et al., PLoS Biol, 2007, 5(12), 2788–2796
- Iversen R, et al., Proc. Natl. Acad. Sci., 2014, 111(48), 17146-17151.

**Claims**

1. A compound which is a modulator of tissue transglutaminase (TG2) for use in the treatment of endothelial dysfunction,
wherein the modulator of tissue transglutaminase (TG2) is a compound of formula (I):

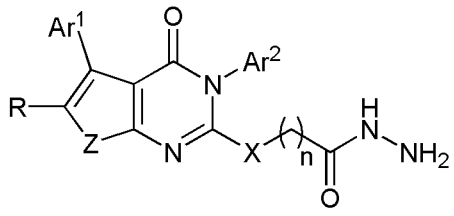

(I)

wherein

- Z is selected from the group consisting of S, $SO_2$, and Se,
- $Ar^1$ and $Ar^2$ are independently selected from the group consisting of optionally substituted phenyl and optionally substituted heteroaryl,
- R is selected from the group consisting of hydrogen, deuterium, halogen, and $C_1$-$C_3$ alkyl,
- X is selected from the group consisting of O, NH, N(Me), and S,

n is an integer selected from the group consisting of 1, 2 and 3.

2. The compound for use according to claim 1, wherein the modulator of tissue transglutaminase (TG2) is for use in the treatment of diseases resulting from endothelial dysfunction.

3. The compound for use according to claim 2, wherein the disease resulting from endothelial dysfunction is selected from the group consisting of dementia, Alzheimer's disease, ventricular hypertrophy, vascular calcification, renal fibrosis, cardiac fibrosis, pulmonary fibrosis, atherosclerosis, ischemic chronic wounds, hypertension, pulmonary hypertension, and erectile dysfunction.

4. The compound for use according to claim 3, wherein the disease resulting from endothelial dysfunction is selected from the group consisting of hypertension and erectile dysfunction.

5. The compound for use according to any of the preceding claims, wherein the modulator of tissue transglutaminase (TG2) is a promoter of the closed conformation of tissue transglutaminase.

6. The compound for use according to any of the preceding claims, wherein Z is S.

7. The compound for use according to any of the preceding claims, wherein the optional substituents of $Ar^1$ and $Ar^2$ are selected from the group consisting of $C_1$-$C_{10}$ alkyl, $C_2$-$C_{10}$ alkenyl, $C_2$-$C_{10}$ alkynyl, amino (-$NH_2$), -$CH_2NH(C_1$-$C_{10}$ alkyl), -$CH_2N(C_1$-$C_{10}$ alkyl)$_2$, aminoalkyl (-NH($C_1$-$C_{10}$ alkyl) or –N($C_1$-$C_{10}$ alkyl)$_2$, cyano (-CN), -$CONH_2$, -CONH($C_1$-$C_{10}$ alkyl), -CON($C_1$-$C_{10}$ alkyl)$_2$, hydroxyl (-OH), $C_1$-$C_{10}$ alkyl hydroxyl (-alkyl-OH), $C_1$-$C_{10}$ alkoxy(-O-alkyl), carboxylic acid (-COOH), $C_1$-$C_{10}$ alkyl esters (-COO-alkyl), $C_1$-$C_{10}$ alkyl acyl (-CO-alkyl), sulfonic acid (-$SO_3H$), $C_1$-$C_{10}$ alkyl sulfonate (-$SO_3$-alkyl), phosphonic acid (-PO(OH)$_2$), $C_1$-$C_{10}$ alkyl phosphonate (-PO(O-alkyl)$_2$), phosphinic acid (-P(O)(H)OH), $SO_2NH_2$, hydroxamic acid (-CONHOH), $C_1$-$C_{10}$ alkyl sulfonylureas (-NHCONHSO$_2$(alkyl)), $C_1$-$C_{10}$ acylsulfonamides (-$SO_2$-NHCO-(alkyl), hydroxyl amine (-NHOH), nitro (-$NO_2$), and halogen.

8. The compound for use according to any of the preceding claims, wherein

- $Ar^1$ and $Ar^2$ are optionally substituted phenyl,
- R is hydrogen or halogen
- X is S,
- n is an integer selected from the group consisting of 1, 2 and 3.

9. The compound for use according to any of the preceding claims, wherein the modulator of tissue transglutaminase (TG2) is a compound of formula (II):

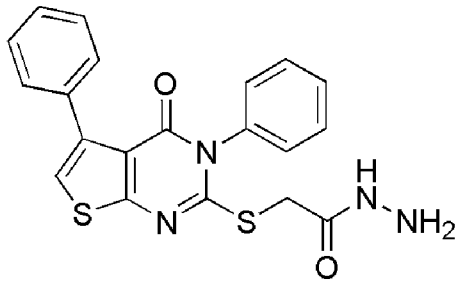


(II).

10. The compound for use according to any of the preceding claims, wherein the modulator of tissue transglutaminase (TG2) is LDN-27219.

11. The compound for use according to any of the preceding claims, wherein the endothelial dysfunction is age-associated.

12. The compound for use according to any of the preceding claims, wherein the compound is administered to human patients between the age of 30-140 years, such as the age of 35-140 years, 40-140 years, 45-140 years, 50-140 years, 55-140 years, 60-140 years, 65-140 years, 70-140 years, such as preferably 30-120 years, 40-100 years, such as most preferably 50-100 years.

13. The compound for use according to any of the preceding claims, wherein the endothelial dysfunction is diabetes-associated.

14. The compound for use according to any of the preceding claims, wherein the endothelial dysfunction is associated with diabetes-1 or diabetes-2, preferably diabetes-2.

15. The compound for use according to any of the preceding claims, wherein the endothelial dysfunction is both age-associated and diabetes-associated.

16. The compound for use according to any of the preceding claims, wherein the compound is administered in a composition further comprising a pharmaceutically acceptable carrier or diluent.

A)

6-7 week old rats
(n=6)

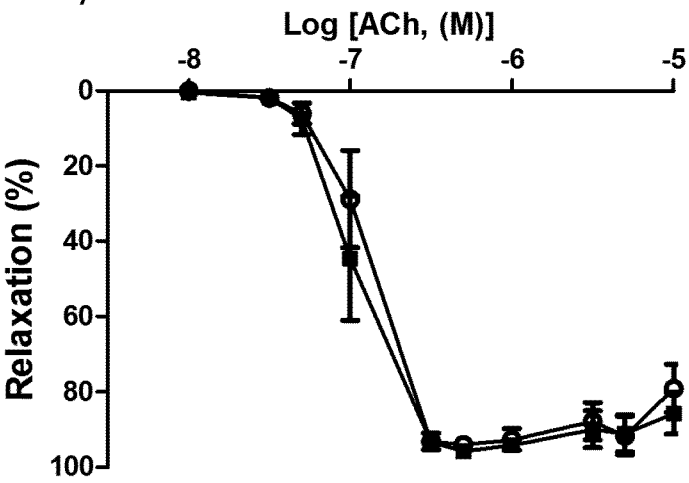


B)

≈12 weeks old rats
(n=6)

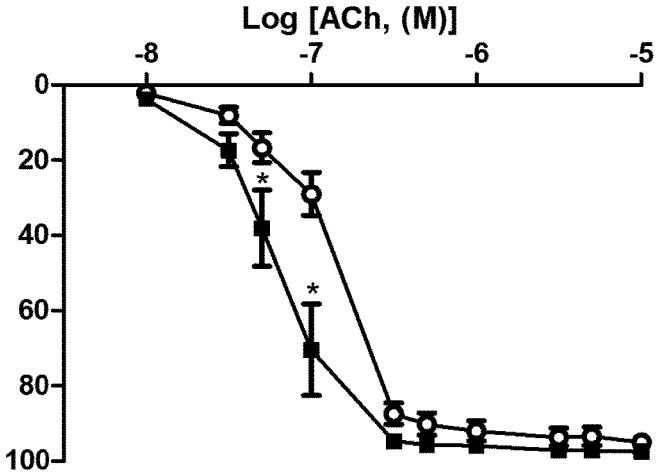


C)

>30 weeks old rats
(n=8)

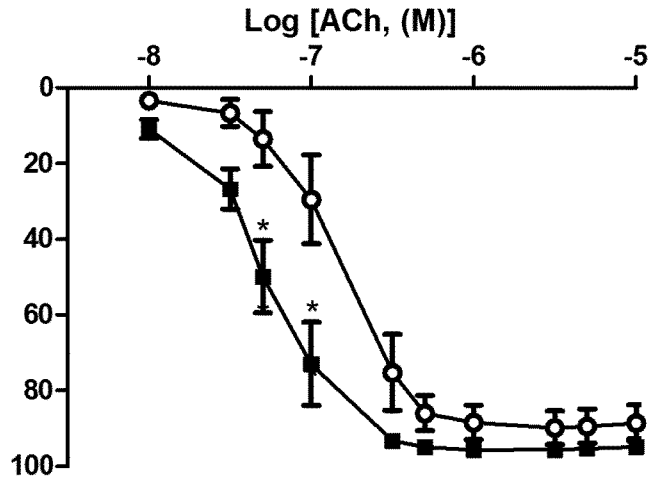


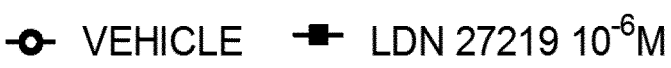


Fig. 1 (A-C)

A)

Healthy control 14-16 weeks old mice (n=8)

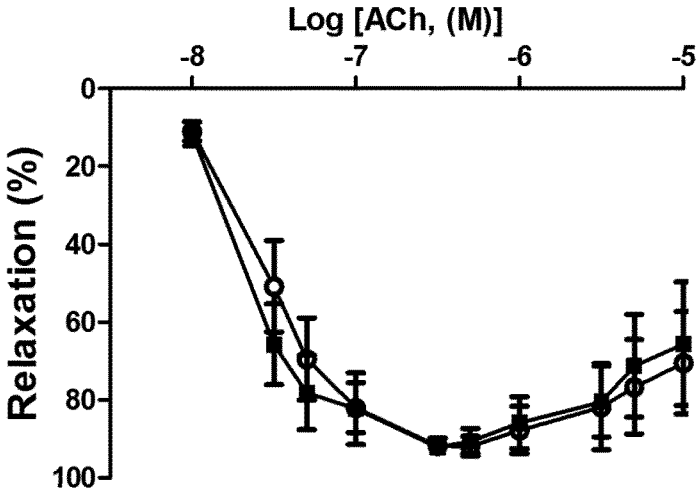


B)

Healthy control 24-25 weeks old mice (n=6)

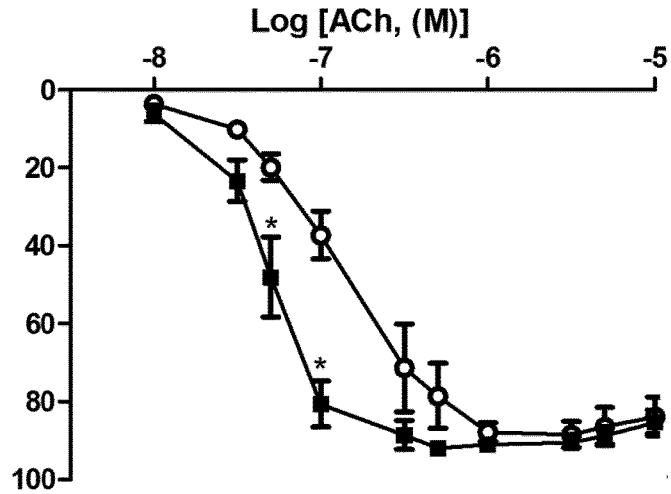


C)

Diabetic mice 16-17 weeks old (n=8)

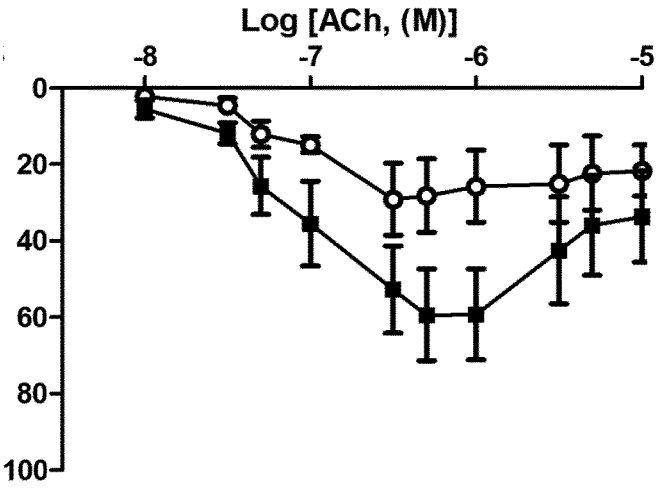


VEHICLE

LDN 27219 $3X10^{-6}M$

Fig. 2 (A-C)

A)

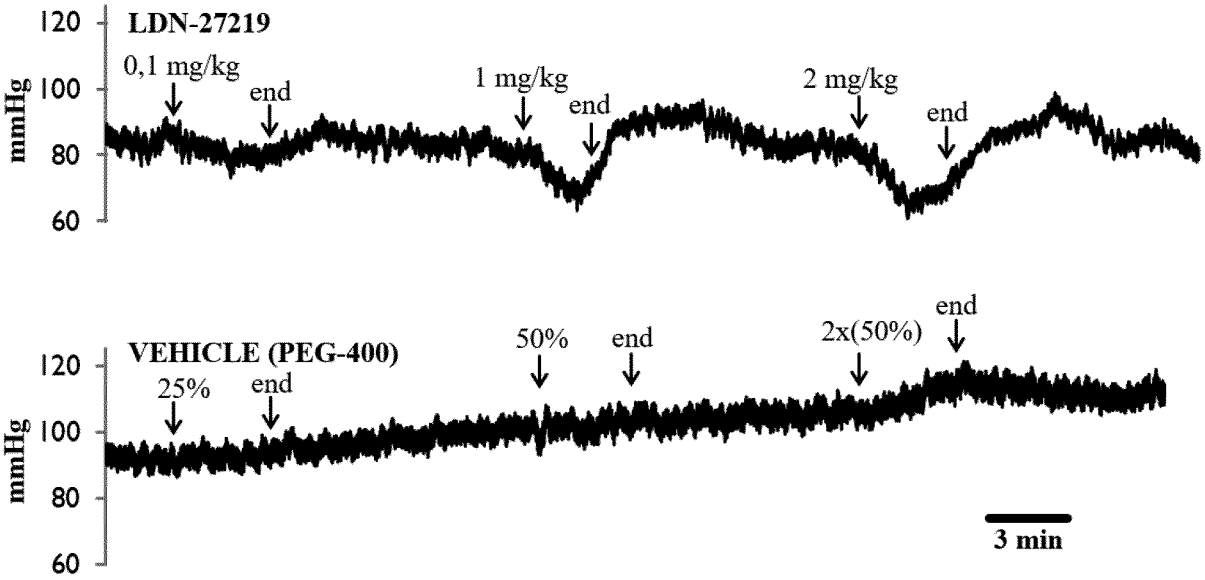
LDN-27219
0,1 mg/kg
end
1 mg/kg
end
2 mg/kg
end
mmHg
120
100
80
60
VEHICLE (PEG-400)
25%
end
50%
end
2x(50%)
end
3 min

B)

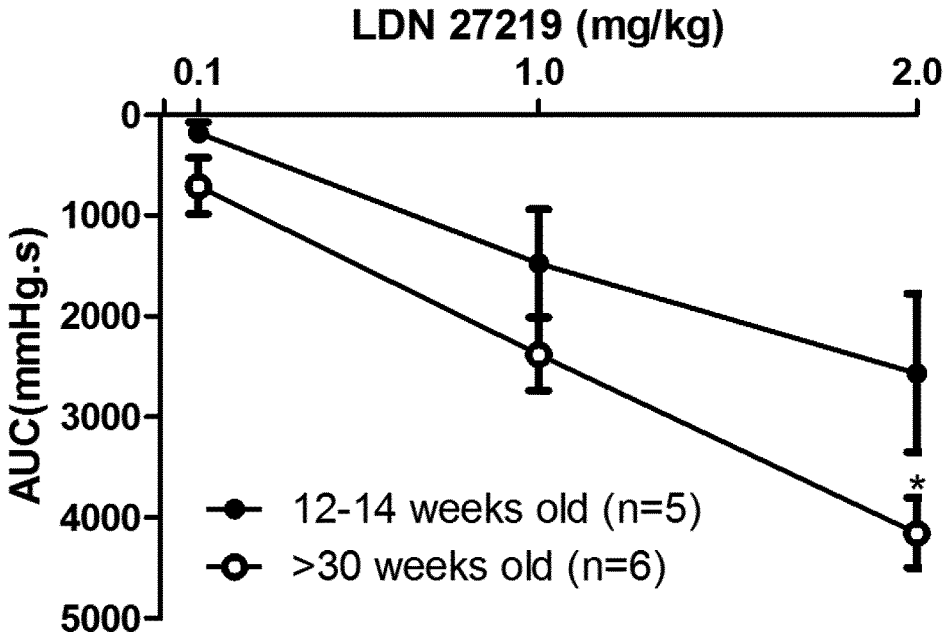
LDN 27219 (mg/kg)
0.1
1.0
2.0
AUC(mmHg.s)
0
1000
2000
3000
4000
5000
*
12-14 weeks old (n=5)
>30 weeks old (n=6)

Fig. 3A-3B

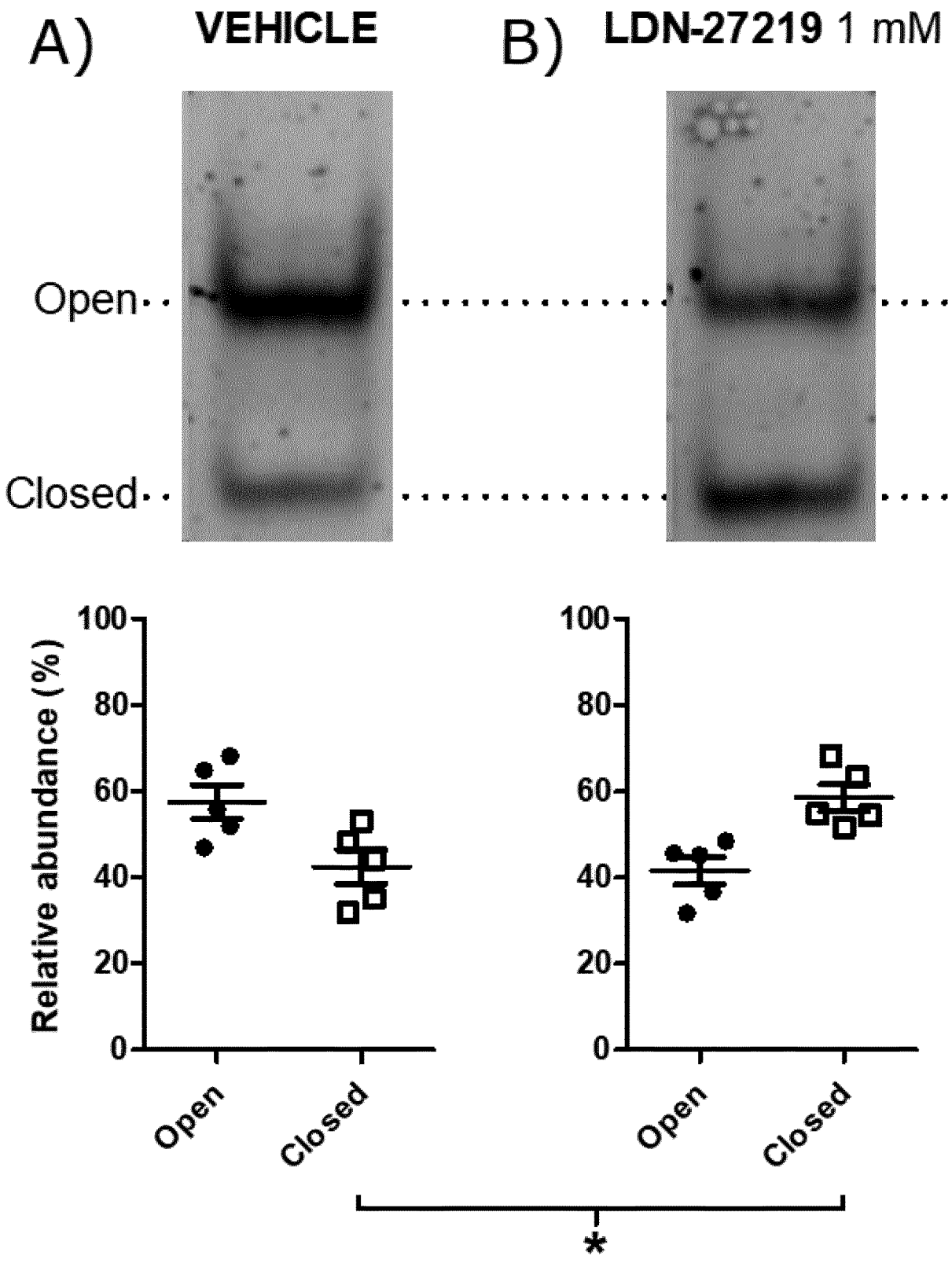
A)
VEHICLE
B)
LDN-27219 1 mM
Open
Closed
Relative abundance (%)
100
80
60
40
20
0
Open
Closed
Open
Closed
*

Fig. 4 (A-B)

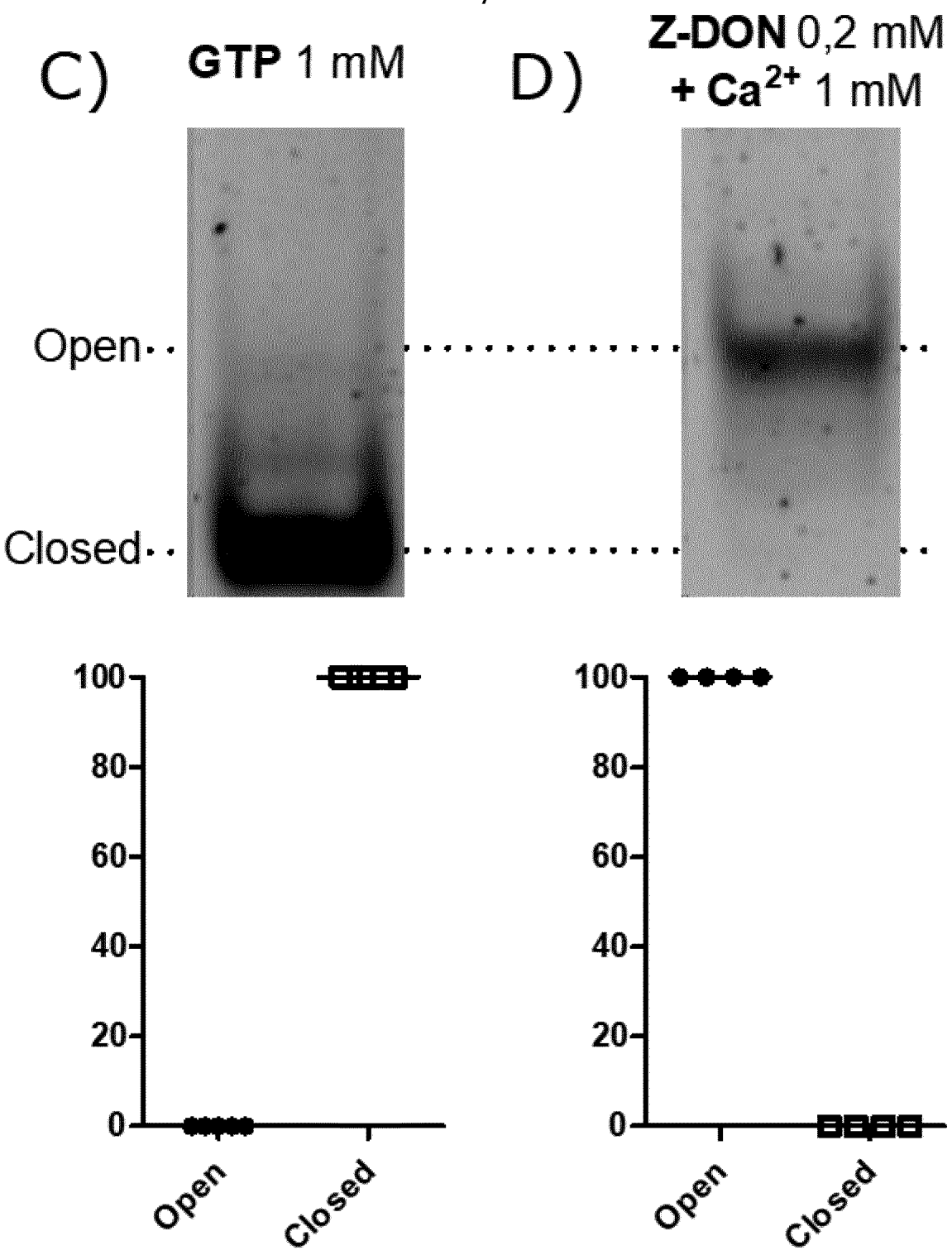
C)
GTP 1 mM
D)
Z-DON 0,2 mM
+ Ca2+ 1 mM
Open
Closed
100
80
60
40
20
0
Open
Closed
100
80
60
40
20
0
Open
Closed

Fig. 4 (C-D)

A)

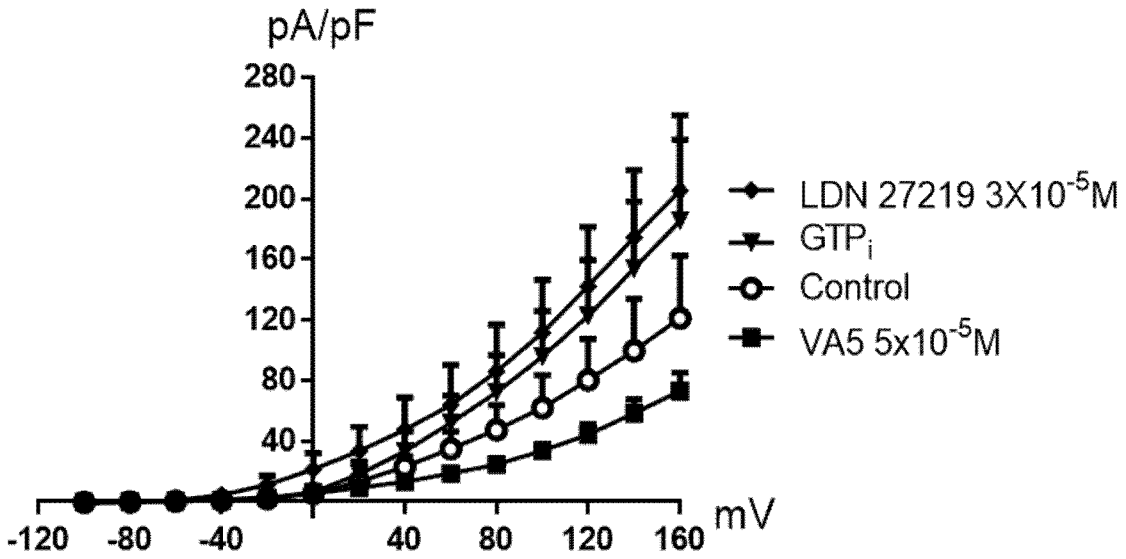
pA/pF
280
240
200
160
120
80
40
-120
-80
-40
40
80
120
160
mV
LDN 27219 3X10-5M
GTPi
Control
VA5 5x10-5M

B)

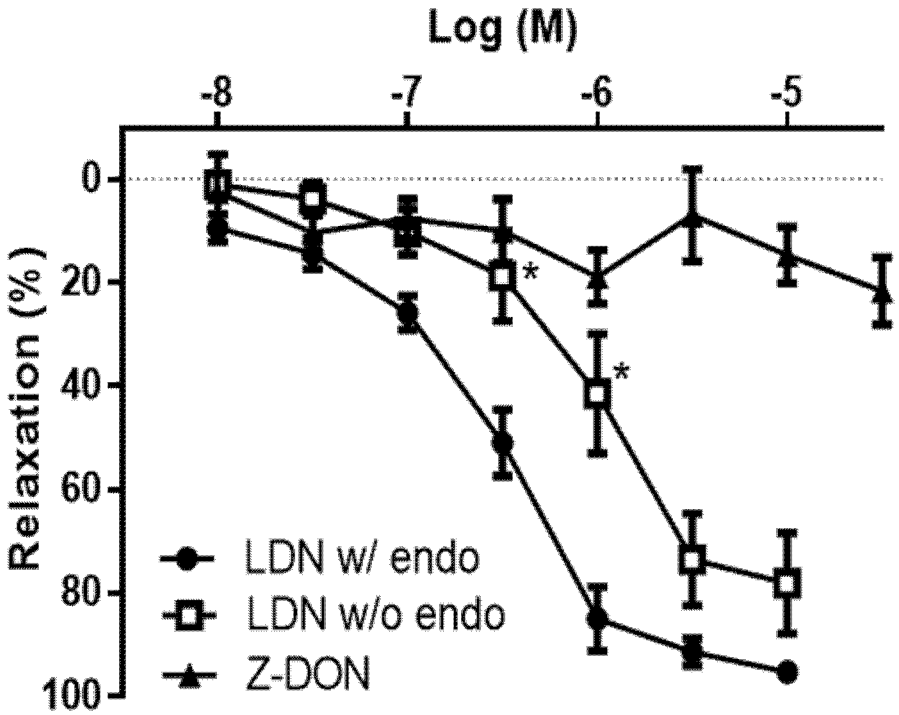
Log (M)
-8
-7
-6
-5
0
20
40
60
80
100
Relaxation (%)
*
*
LDN w/ endo
LDN w/o endo
Z-DON

Fig. 5A-5B

C)

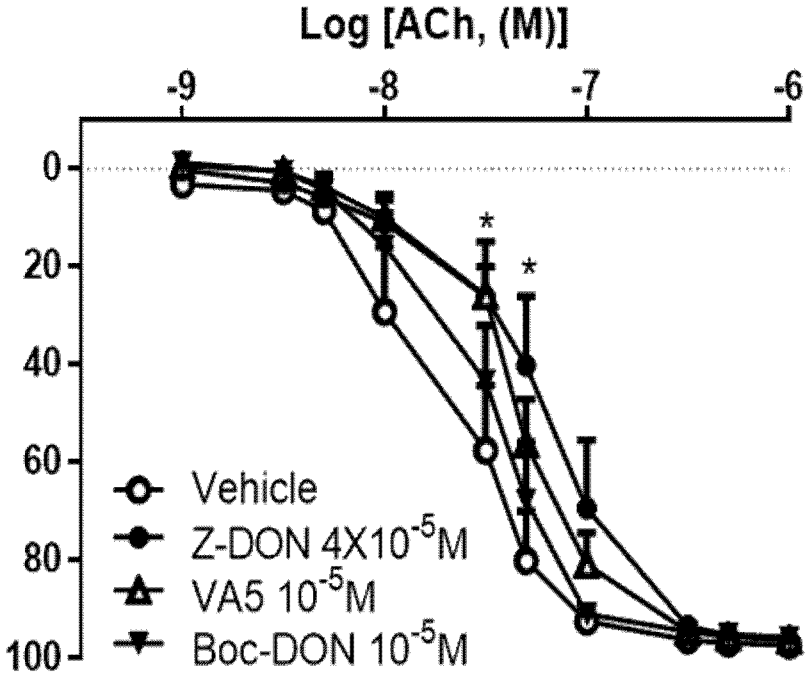
Log [ACh, (M)]
-9
-8
-7
-6
0
20
40
60
80
100
*
*
Vehicle
Z-DON 4X10-5M
VA5 10-5M
Boc-DON 10-5M

D)

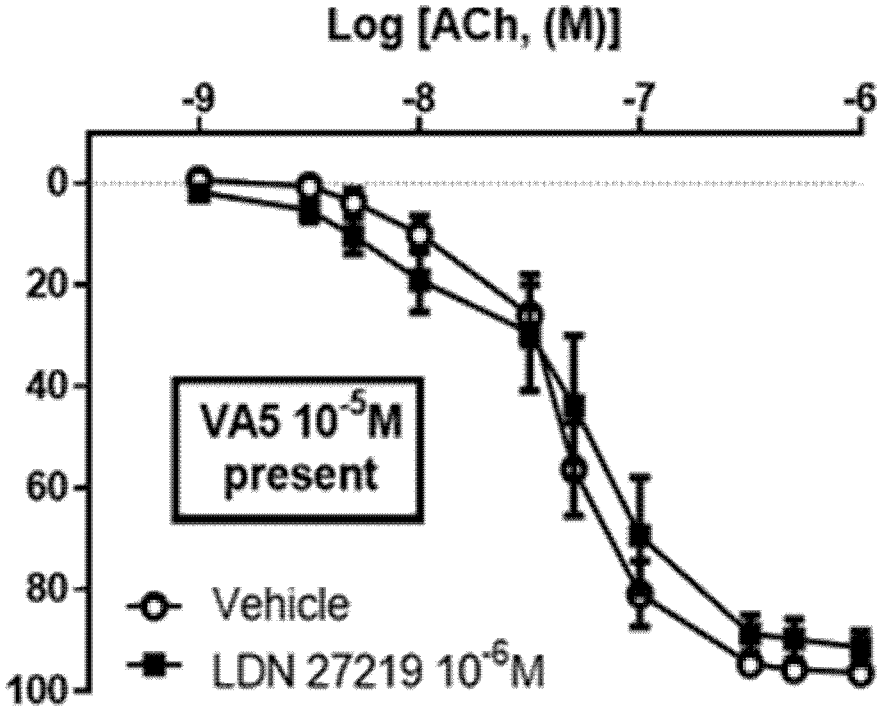
Log [ACh, (M)]
-9
-8
-7
-6
0
20
40
60
80
100
VA5 10-5M
present
Vehicle
LDN 27219 10-6M

Fig. 5C-5D

E)

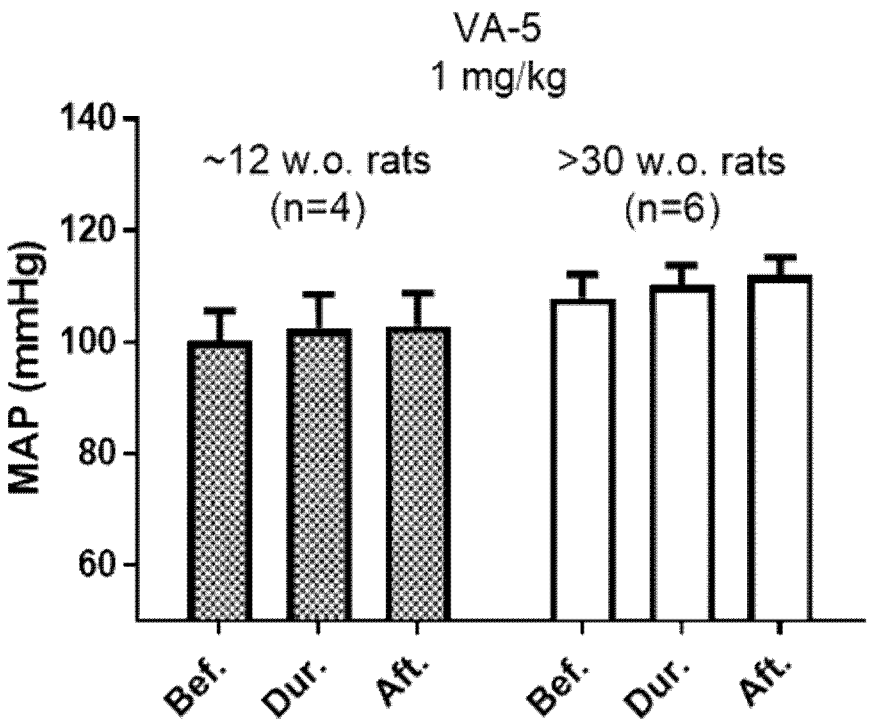
VA-5
1 mg/kg
~12 w.o. rats
(n=4)
>30 w.o. rats
(n=6)
MAP (mmHg)
140
120
100
80
60
Bef.
Dur.
Aft.
Bef.
Dur.
Aft.

Fig. 5E

A)

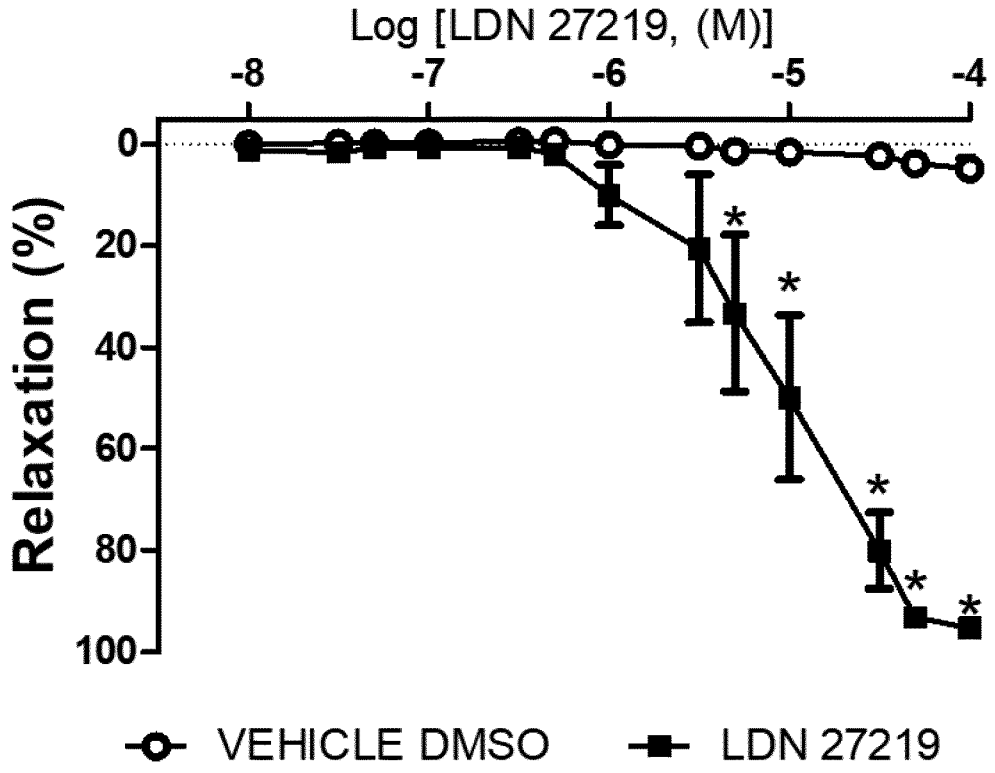
Log [LDN 27219, (M)]
-8
-7
-6
-5
-4
0
20
40
60
80
100
Relaxation (%)
*
*
*
*
*
VEHICLE DMSO
LDN 27219

B)

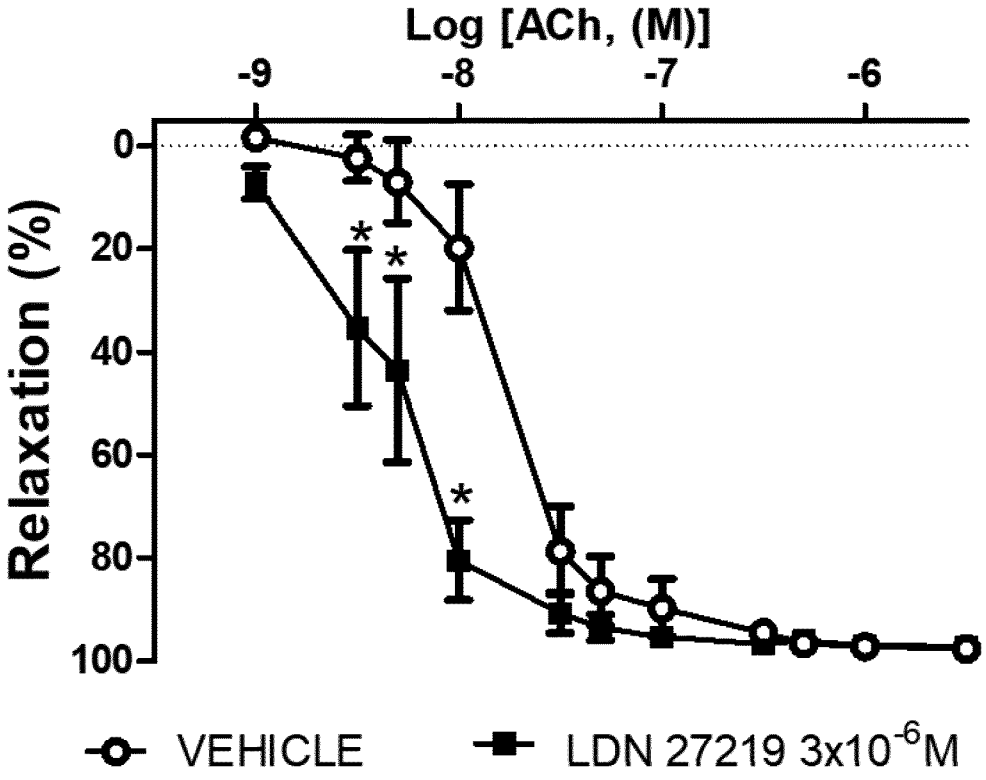
Log [ACh, (M)]
-9
-8
-7
-6
0
20
40
60
80
100
Relaxation (%)
*
*
*
VEHICLE
LDN 27219 3x10-6M

Fig. 6A-6B

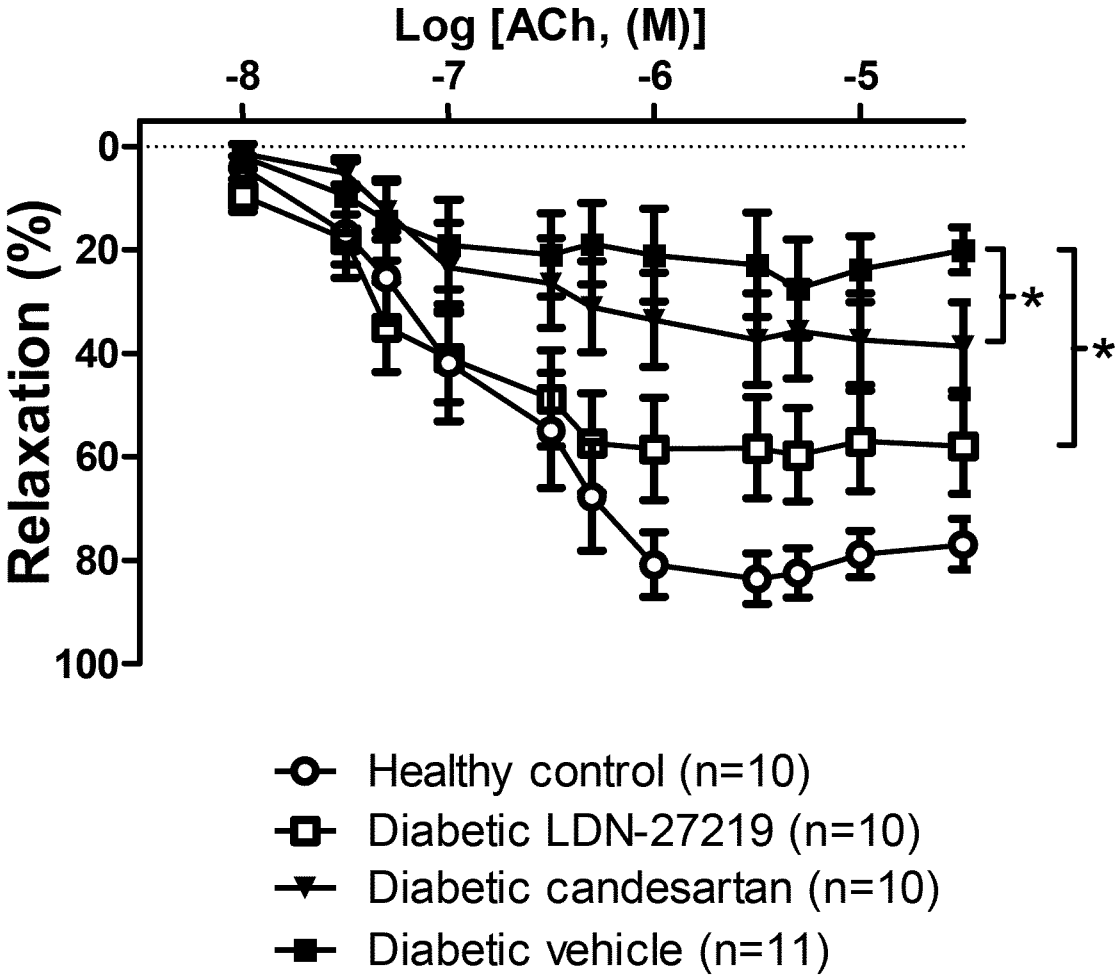
Log [ACh, (M)]
-8
-7
-6
-5
0
20
40
60
80
100
Relaxation (%)
*
*
Healthy control (n=10)
Diabetic LDN-27219 (n=10)
Diabetic candesartan (n=10)
Diabetic vehicle (n=11)

Fig. 7

# INTERNATIONAL SEARCH REPORT

International application No
PCT/EP2019/071134

A. CLASSIFICATION OF SUBJECT MATTER
INV. A61K31/519 A61P9/10 A61P9/14 A61P9/08 A61P9/12
ADD.

According to International Patent Classification (IPC) or to both national classification and IPC

B. FIELDS SEARCHED

Minimum documentation searched (classification system followed by classification symbols)
A61K A61P

Documentation searched other than minimum documentation to the extent that such documents are included in the fields searched

Electronic data base consulted during the international search (name of data base and, where practicable, search terms used)
EPO-Internal, WPI Data

C. DOCUMENTS CONSIDERED TO BE RELEVANT

| Category* | Citation of document, with indication, where appropriate, of the relevant passages | Relevant to claim No. |
|---|---|---|
| A | WO 2006/060702 A1 (BRIGHAM & WOMENS HOSPITAL [US]; STEIN ROSS L [US]; CASE APRIL [US]; YE) 8 June 2006 (2006-06-08) compounds of Fig. 2-4; claims, in particular claims 24, 29; p. 1, last ----- | 1-16 |
| A | MATLUNG HANKE L ET AL: "Transglutaminase activity regulates atherosclerotic plaque composition at locations exposed to oscillatory shear stress", ATHEROSCLEROSIS, vol. 224, no. 2, 2012, pages 355-362, XP028942294, ISSN: 0021-9150, DOI: 10.1016/J.ATHEROSCLEROSIS.2012.07.044 title, abstract ----- -/-- | 1-16 |

[X] Further documents are listed in the continuation of Box C.

[X] See patent family annex.

* Special categories of cited documents :

"A" document defining the general state of the art which is not considered to be of particular relevance

"E" earlier application or patent but published on or after the international filing date

"L" document which may throw doubts on priority claim(s) or which is cited to establish the publication date of another citation or other special reason (as specified)

"O" document referring to an oral disclosure, use, exhibition or other means

"P" document published prior to the international filing date but later than the priority date claimed

"T" later document published after the international filing date or priority date and not in conflict with the application but cited to understand the principle or theory underlying the invention

"X" document of particular relevance; the claimed invention cannot be considered novel or cannot be considered to involve an inventive step when the document is taken alone

"Y" document of particular relevance; the claimed invention cannot be considered to involve an inventive step when the document is combined with one or more other such documents, such combination being obvious to a person skilled in the art

"&" document member of the same patent family

| Date of the actual completion of the international search | Date of mailing of the international search report |
|---|---|
| 16 October 2019 | 29/10/2019 |

| Name and mailing address of the ISA/ | Authorized officer |
|---|---|
| European Patent Office, P.B. 5818 Patentlaan 2<br>NL - 2280 HV Rijswijk<br>Tel. (+31-70) 340-2040,<br>Fax: (+31-70) 340-3016 | Dahse, Thomas |

1

C(Continuation). DOCUMENTS CONSIDERED TO BE RELEVANT

| Category* | Citation of document, with indication, where appropriate, of the relevant passages | Relevant to claim No. |
|---|---|---|
| A | MORTEN ENGHOLM ET AL: "Involvement of transglutaminase 2 and voltage-gated potassium channels in cystamine vasodilatation in rat mesenteric small arteries : Vasoactive effects of cystamine", BRITISH JOURNAL OF PHARMACOLOGY, vol. 173, no. 5, 27 January 2016 (2016-01-27), pages 839-855, XP055551401, UK ISSN: 0007-1188, DOI: 10.1111/bph.13393 title, abstract<br>----- | 1-16 |
| A | H TATSUKAWA ET AL: "Transglutaminase 2 has opposing roles in the regulation of cellular functions as well as cell growth and death", CELL DEATH & DISEASE, vol. 7, no. 6, 1 June 2016 (2016-06-01), pages e2244-e2244, XP055552630, DOI: 10.1038/cddis.2016.150 introduction: first on p. 1; Fig. 1<br>----- | 1-15 |

1

# INTERNATIONAL SEARCH REPORT

Information on patent family members

International application No
PCT/EP2019/071134

| Patent document cited in search report | Publication date | Patent family member(s) | Publication date |
|---|---|---|---|
| WO 2006060702 A1 | 08-06-2006 | US 2006183759 A1 | 17-08-2006 |
| | | WO 2006060702 A1 | 08-06-2006 |